(12)

RADC-TR-82-260
Final Technical Report
October 1982



AD A123538

LIGHTWEIGHT ZERODUR MIRROR TECHNOLOGY

The Perkin-Elmer Corporation

Sponsored by
Defense Advanced Research Projects Agency (DOD)
ARPA Order No. 3503

DTIC
JAN 19 1983
D
H

APPROVED FOR PUBLIC RELEASE; DISTRIBUTION UNLIMITED

The views and conclusions contained in this document are those of the authors and should not be interpreted as necessarily representing the official policies, either expressed or implied, of the Defense Advanced Research Projects Agency or the U.S. Government.

DTIC FILE COPY

ROME AIR DEVELOPMENT CENTER
Air Force Systems Command
Griffiss Air Force Base, NY 13441

83 01 19 010

Best
Available
Copy

This report has been reviewed by the RADC Public Affairs Office (PA) and is releasable to the National Technical Information Service (NTIS). At NTIS it will be releasable to the general public, including foreign nations.

RADC-TR-82-260 has been reviewed and is approved for publication.

APPROVED: Doris Hamill

DORIS HAMILL, Capt, USAF
Project Engineer

APPROVED: Frank J. Rehm

FRANK J. REHM
Technical Director
Surveillance Division

FOR THE COMMANDER: John P. Huss

JOHN P. HUSS
Acting Chief, Plans Office

If your address has changed or if you wish to be removed from the RADC mailing list, or if the addressee is no longer employed by your organization, please notify RADC (OCSE) Griffiss AFB NY 13441. This will assist us in maintaining a current mailing list.

Do not return copies of this report unless contractual obligations or notices on a specific document requires that it be returned.

LIGHTWEIGHT ZERODUR MIRROR TECHNOLOGY

George J. Gardopee
Da-Wun Shen

Contractor: The Perkin-Elmer Corporation
Contract Number: F30602-81-C-0281
Effective Date of Contract: 17 September 1981
Contract Expiration Date: 15 May 1982
Short Title of Work: Lightweight Zerodur Mirror Technology
Program Code Number: 1L10
Period of Work Covered: 21 Sep 81 - 21 May 82

Principal Investigator: George Gardopee
Phone: 203-757-6171

Project Engineer: Doris Hamill, Capt, USAF
Phone: 315-330-3148

Approved for public release; distribution unlimited

This research was supported by the Defense Advanced Research Projects Agency of the Department of Defense and was monitored by Doris Hamill, Capt, USAF (OCSE) Griffiss AFB NY 13441, under Contract F30602-81-C-0281.

UNCLASSIFIED

SECURITY CLASSIFICATION OF THIS PAGE (When Data Entered)

REPORT DOCUMENTATION PAGE	READ INSTRUCTIONS BEFORE COMPLETING FORM
1. REPORT NUMBER RADC-TR-82-260	2. GOVT ACCESSION NO. AD-A123 538
	3. RECIPIENT'S CATALOG NUMBER
4. TITLE (and Subtitle) LIGHTWEIGHT ZERODUR MIRROR TECHNOLOGY	5. TYPE OF REPORT & PERIOD COVERED Final Technical Report 21 Sep 81 - 21 May 82
	6. PERFORMING ORG. REPORT NUMBER 15512
7. AUTHOR(s) George J. Gardopee Da-Wun Shen	8. CONTRACT OR GRANT NUMBER(s) F30602-81-C-0281
9. PERFORMING ORGANIZATION NAME AND ADDRESS The Perkin-Elmer Corporation 100 Wooster Heights Road Danbury CT 06810	10. PROGRAM ELEMENT, PROJECT, TASK AREA & WORK UNIT NUMBERS 62711E C5030111
11. CONTROLLING OFFICE NAME AND ADDRESS Defense Advanced Research Projects Agency 1400 Wilson Blvd Arlington VA 22209	12. REPORT DATE October 1982 13. NUMBER OF PAGES 290
14. MONITORING AGENCY NAME & ADDRESS(if different from Controlling Office) Rome Air Development Center (OCSE) Griffiss AFB NY 13441	15. SECURITY CLASS. (of this report) UNCLASSIFIED 15a. DECLASSIFICATION/DOWNGRADING SCHEDULE N/A
16. DISTRIBUTION STATEMENT (of this Report) Approved for public release; distribution unlimited	
17. DISTRIBUTION STATEMENT (of the abstract entered in Block 20, if different from Report) Same	
18. SUPPLEMENTARY NOTES RADC Project Engineer: Doris Hamill, Capt, USAF (OCSE)	
19. KEY WORDS (Continue on reverse side if necessary and identify by block number) Zerodur Lightweight Mirrors Mirror Blank Fabrication Frit Bonding	
20. ABSTRACT (Continue on reverse side if necessary and identify by block number) The manufacturing techniques applicable to the fabrication of lightweight passive mirror blanks from Zerodur glass-ceramic are demonstrated. The techniques include bending and welding Zerodur to form lightweight eggcrate cores and frit bonding thin facesheets to the cores. Physical property measurements show that the joints meet the requirements for a mirror blank design. The thermal performance of a lightweight Zerodur mirror is predicted analytically and is superior to the performance of conventional →	

DD FORM 1 JAN 73 1473 EDITION OF 1 NOV 65 IS OBSOLETE

UNCLASSIFIED

SECURITY CLASSIFICATION OF THIS PAGE (When Data Entered)

ULE mirrors. The cost and schedule for establishing a large mirror blank fabrication facility are estimated.

Accession For
NTIS GRA&I
DTIC TAB
Unannounced
Justification
By
Distribution/
Availability Codes
Dist | Avail and/or special
A

TABLE OF CONTENTS

Section	Title	Page
I	INTRODUCTION	1
II	BACKGROUND	2
III	PROGRAM OBJECTIVE	7
IV	MIRROR FABRICATION PROCESSES	9
	4.1 Core Making	10
	4.1.1 Rib Production	10
	4.1.2 Hex Forming	13
	4.1.3 Welding	14
	4.1.4 Welded Sample Properties and Evaluation	15
	4.1.5 Core Fabrication - Conclusions	22
	4.2 Facesheet Fabrication	26
	4.2.1 Stationary Casting	26
	4.2.2 Spin-Casting	27
	4.2.3 Slumping	30
	4.2.4 Facesheet Production - Conclusions	34
	4.3 Frit Bonding	34
	4.3.1 Frit Bonding - Physical Property Measurements	36
	4.3.2 Sample Production	37
	4.3.3 Sample Evaluation	37
	4.3.4 Frit Development - Proposed Future Effort	42
	4.3.5 Frit Bonding - State of the Art	42
	4.3.6 Mirror Fabrication Processes - Summary	44
V	PERFORMANCE ANALYSIS	46
	5.1 Analytical Method Development	46
	5.1.1 Structural Modeling Technique	46
	5.1.2 Thermal Performance Optimization Scheme	47
	5.2 General Survey of Zerodur Lightweight Mirror	50
	5.3 Performance Comparison Between ULE and Zerodur Mirrors	54
	5.4 Optimization Procedures and Performance of Optimum Zerodur Mirror Design	59
	5.5 Conclusions	65
VI	MANUFACTURING TECHNOLOGY/SCALE-UP STUDY	70
	6.1 Technology Development	71
	6.1.1 0.46 Meter Mirror Blank	71
	6.1.2 1.5 Meter Blank Fabrication Plan	72
	6.1.3 Alternative Approaches	74
	6.1.4 Schedule	75

TABLE OF CONTENTS (cont'd)

Section	Title	Page
VII	CONCLUSIONS	77
VIII	RECOMMENDATIONS FOR FUTURE WORK	78
APPENDICES		
A	MANUFACTURE OF ROLLED GLASS FOR THE HONEYCOMB SYSTEM OF ZERODUR LIGHTWEIGHT MIRRORS	A-i
B	WEIBULL STATISTICS FOR BREAKING STREGTHS OF WELDED ZERODUR SAMPLES AND MEASUREMENT OF THE COEFFICIENT OF THERMAL EXPANSION OF THE HEAT AFFECTED ZONE	B-i
C	PRODUCTION OF A CORE SECTION MADE BY THE WELDING PROCESS	C-i
D	SPIN-CASTING	D-i
E	REPORT OF FRIT DATA AND FINAL REPORT ON THE BONDING OF ZERODUR TO GLASS FRIT	E-i
F	STUDY FOR THE MANUFACTURE OF 1.5 METER LIGHTWEIGHT MIRRORS AND SCALE-UP TECHNOLOGY REPORT	F-i
G	COST AND TIME REQUIRED FOR THE MANUFACTURE OF TWO LIGHTWEIGHT MIRRORS, 0.46 METER DIAMETER	G-i
H	THERMAL MODELING	H-i
I	ZERODUR FRIT DEVELOPMENT OUTLINE OF WORK AND SCHEDULE	I-i

LIST OF ILLUSTRATIONS

Figure	Title	Page
1	Thermal Expansion Behavior of Zerodur, ULE, and Fused Silica	5
2	Rolling of Zerodur Sheet	12
3	Bending of Zerodur Plate	13
4	Welding of Zerodur Core	16
5	120° Bent and Welded Zerodur	19
6	Butt Welded Zerodur	19
7	Bent and Welded Zerodur	21
8	Welded Zerodur Core Sample	21
9	Core Welding Machine	23
10	Core Welding Machine (Side View)	24
11	Cell Welded Zerodur Core	25
12	Cell Welded Zerodur Core	25
13	Example of Glass Part made by Spin Casting	28
14	Spin-Casting Apparatus	29
15	Slumping Furnace	32
16	Slumped Zerodur Glass	33
17	Slumped Zerodur Glass	33
18	Thermal Expansion of Candidate Frits	38
19	Frit Bonded "L" Samples	39
20	Fritted Lap Shear Samples	39
21	0.3 meter Fritted Zerodur Blank	41

LIST OF ILLUSTRATIONS

Figure	Title	Page
22	Thermal Expansion Mismatch of Frit with Zerodur	41
23	Change of Tensile Stress in Zerodur with Temperature	43
24	Test Models, 60 Degree Symmetry	48
25	Various Surface Distortions	49
26	Mirror Configuration and Finite Element Model	51
27	Zerodur CTE Variations as Function of Temperature	53
28	Effect of Frit Bondline on Surface Thermal Distortion	53
29	Spatial Variation of α_{REF} for Zerodur (Typical)	55
30	Effect of CTE Spatial Variation of Surface Thermal Distortion	55
31	Surface Distortion for ULE and Zerodur Mirrors	56
32	CTE as a Function of Temperature	58
33	Temperature Gradient under Thermal Loading	58
34	Thermal Moment and Section Rigidity	60
35	Zerodur CTE and Thermal Strain	61
36	Four Meter Zerodur Mirror Thermal Performance Parametric Study (M_T/D vs. Faceplate and Backplate Thickness)	63
37	Four Meter Zerodur Mirror Thermal Performance Parametric Study (M_TD vs. Facesheet Thickness and Total Weight)	63
38	Four Meter Zerodur Mirror Thermal Performance Parametric Study (M_T/D vs. Faceplate Thickness and Core Density)	64
39	Four Meter Zerodur Mirror Thermal Performance Parametric Study (M_T/D vs. CTE_{REF})	64

LIST OF ILLUSTRATIONS

Figure	Title	Page
40	Mirror Configuration and Finite Element Model	66
41	Mirror Surface Thermal Distortions	67
42	Time Schedule for the Production of a Plane and a Spherical 1.5 m Light-Weight Mirror	76
43	Proposed Technology Development Schedule	80

LIST OF TABLES

Table	Title	Page
1	Properties of Zerodur and ULE	4
2	Zerodur Mirror Fabrication Process Outline	9
3	Bend Strength Summary	15
4	Breaking Strength Effects	36
5	Elastic Moduli of Schott Frits	36
6	Physical Properties	52
7	Thermal Performance of ULE and Zerodur Mirror	56
8	Four Meter Zerodur Mirror Thermal Performance Summary Optimum Mirror Configuration W_{Total} = 2500 lbs	68
9	Mirror Blank Manufacturing Process	73

SECTION I

INTRODUCTION

In design tradeoffs for large passive mirrors, Zerodur glass ceramic has been shown to be an attractive alternative to ULE because of its low coefficient of thermal expansion, greater homogeneity, and easier machinability and polishability. Zerodur was not selected as a candidate blank material because the technology for producing lightweight passive mirrors from Zerodur did not exist.

Perkin-Elmer has been working closely with Schott Glaswerke for several years and has been instrumental in instigating technology developments that have made Zerodur a candidate material for several applications. In response to inquiries by Perkin-Elmer, Schott began developing the technology required for the fabrication of lightweight Zerodur mirror blanks. They produced a number of samples that demonstrated the feasibility of bending, welding, and fritting Zerodur to produce large egg-crate core mirror blanks.

Perkin-Elmer planned and executed a program designed to evaluate these new fabrication processes for the production of mirror blanks suitable for use in various applications. As part of this program, a subcontract was awarded to Schott consisting of tasks for (1) the documentation of state-of-the-art manufacturing techniques, (2) the preparation and evaluation of samples (including property measurements), and (3) the estimation of the cost and schedule for completion of technology development and the establishment of a facility for the production of large lightweight Zerodur mirrors. Perkin-Elmer evaluated Schott's proposed manufacturing process and completed a design study and thermal performance analysis of a 4 meter Zerodur mirror.

This document constitutes the Final Report for the Lightweight Zerodur Mirror Technology Study.

SECTION II

BACKGROUND

Until recently, many designs for large beam expander systems included passive, monolithic mirrors up to 4 meters in diameter. Weight limitations dictated the use of structures consisting of relatively thin facesheets attached to a lightweight eggcrate-type core. Because the mirrors must retain a very precise optical figure under high thermal loading, only those materials having very low coefficients of thermal expansion (CTE) can be considered.

Only one material which meets these requirements is currently available in the form of large lightweight monolithic mirror blanks. Corning Glass Works manufactures mirror blanks of ULE(TM) ultra low expansion titania-silica glass. Corning's technology has produced lightweight blanks up to 96 inches in diameter.

ULE is produced by a hydrolysis process in which a soot of titania-silica glass is deposited in a furnace to form a solid 60 inch diameter boule. The boules are machined into the various core components which are then welded to form a lightweight eggcrate core. Other boules are "flowed out" in a furnace to form the pieces from which the facesheets are machined. The facesheets and core are fused and simultaneously slumped to an approximate curvature in another furnace operation. More recent developmental programs have examined the possibility of fabricating mirror blanks of lower weights by frit bonding the facesheets to the core structure.

Corning's process for fabricating ULE mirror blanks does not efficiently utilize the raw material. At least 10,000 pounds of glass must be produced to fabricate a 1000 pound mirror blank. At this time, production of the large ULE boules is limited to four boules or approximately 5000 pounds of glass per month. The process of machining the mirror components and assembling the blank requires several more months to complete.

As of late 1979, projected requirements for large lightweight mirrors exceeded Corning's manufacturing capacity. It was apparent that a second supplier was required to fulfill the anticipated need for large mirror blanks.

One promising material for fabricating lightweight mirror blanks is Zerodur. This material is a low expansion glass-ceramic produced by Schott Glaswerke in Mainz, FRG. Zerodur is made by melting the component oxides in a platinum-lined furnace. The molten glass is homogenized and subsequently cast into metal molds to form the required shapes and sizes. The glass blanks are annealed to relieve stress and are subjected to heat treatment process referred to as "ceramization". During this ceramization step, crystallites are nucleated in the glass and grow to a size of several hundred angstroms. The crystalline phase has a negative coefficient of thermal expansion while the parent glass has a positive thermal expansion. Careful control of the proportion of crystalline phase to residual glass results in a glass-ceramic material having a nominal CTE of zero.

Schott Glaswerke has been producing Zerodur for more than 10 years for a variety of applications where stability is a necessity. Mirror blanks for astronomical telescopes up to 4 meters in diameter have been successfully produced from Zerodur.

Perkin-Elmer has been a major user of Zerodur for many years. The primary mirrors and other optical components in the Micralign(TM) mask alignment projection system are made from Zerodur. Zerodur is the only material that can meet the stringent requirements for homogeneity, low expansion and high optical quality imposed by the Micralign system.

The potential of Zerodur as a material for large lightweight mirrors has been examined in earlier design tradeoff studies for beam expander systems. Table 1 contains a comparison of the properties of Zerodur and ULE. The specific stiffness of Zerodur (E/ρ) is approximately 20% higher than that of ULE. The higher thermal conductivity and heat capacity of Zerodur would be an advantage for this application.

TABLE 1. PROPERTIES OF ZERODUR AND ULE

	ZERODUR	ULE
E	13.6×10^6 PSI	9.8×10^6 PSI
ρ	0.091 lbs/in^3	0.080 lbs/in^3
K	0.96 Btu/hr-ft-°F	0.76 Btu/hr-ft-°F
Cp	0.194 Btu/lb-°F	0.183 Btu/lb-°F
α_o-50 °C	0 ± 28 ppb/°F	0 ± 17 ppb/°F
ν	0.24	0.17

The thermal expansion behavior of Zerodur, ULE, and fused silica is shown in Figure 1. Note that the CTE of a typical Zerodur sample is negative over the range from -200 °C to +100 °C.

Zerodur is a very homogeneous material with respect to coefficient of thermal expansion. Large blocks of Zerodur have been produced which have a variability in CTE of only a few parts per billion. The glass-ceramic can be machined more easily than glass and the lower incidence of bubbles and inclusions results in an optically polished surface superior to that achievable with ULE. A significant advantage of Zerodur is that it is already available in sizes up to 4 meters in diameter. Schott has considerable experience with producing large mirror blanks for ground-based telescopes.

The coefficient of thermal expansion of Zerodur can be tailored, within limits, by varying the ceramization heat treatment. The CTE of Zerodur is usually slightly negative, but additional heat treatment will drive the CTE in the positive direction. This capability can be used to tailor the CTE of Zerodur to optimize mirror performance for applications in which thermal stability is critical.

The most significant disadvantage with Zerodur is that prior to this program, lightweighting of a Zerodur mirror could only be accomplished by machining a solid blank. This method uses material inefficiently and is a high-risk process for large mirror blanks.

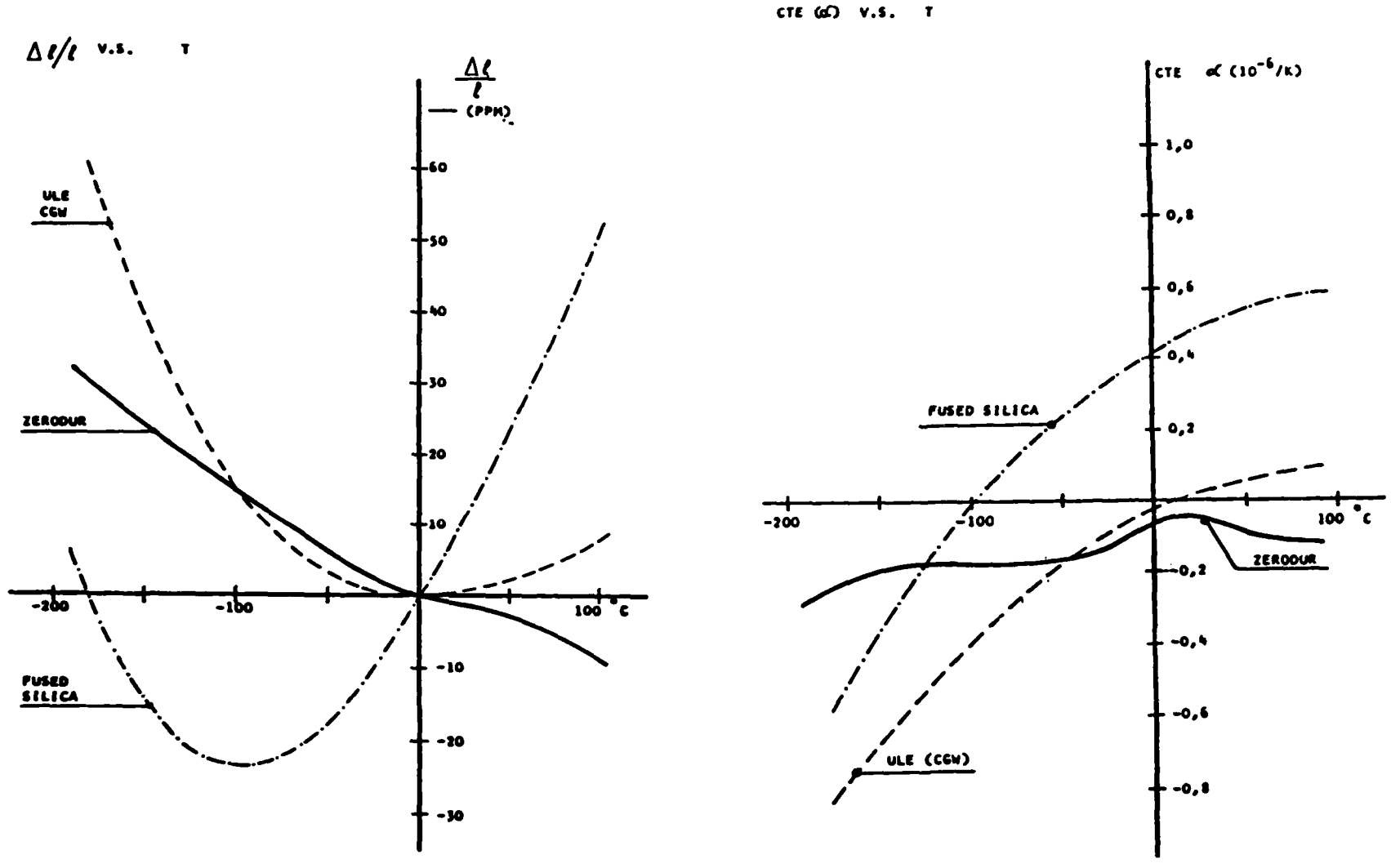


Figure 1. Thermal Expansion Behavior of Zerodur, ULE, and Fused Silica

In response to inquiries by Perkin-Elmer, Schott embarked on a program to investigate more efficient techniques for fabricating lightweight passive mirrors. Schott developed techniques for (1) producing core components by casting and bending, (2) assembling the core components by welding, (3) forming facesheets by casting or slumping, and (4) frit bonding facesheets to the core. These techniques had potential for use in fabricating large passive lightweight mirrors from Zerodur.

The purpose of this program was to document the state-of-the-art of Schott's techniques and to evaluate these processes in terms of manufacturability and scale-up to the production of 4 meter mirror blanks.

SECTION III

PROGRAM OBJECTIVE

The five specific objectives in this program were as follows: 1) Demonstrate the required technologies for fabricating mirror blanks, 2) Obtain data on the properties of bent and welded Zerodur and frit bonded Zerodur joints, 3) Investigate manufacturing processes applicable to the production of lightweight mirror blanks, 4) Analytically predict the performance of a large lightweight Zerodur mirror under high front surface thermal loading, 5) Identify areas requiring further development effort.

Schott Glaswerke had produced a limited number of welded and fritted Zerodur during their own development efforts. Under subcontract in this program, Schott produced samples for systematic evaluation and property measurement. The number of samples was selected to provide some statistical basis for the property data and to demonstrate reproducibility of the processes. The sizes of some of the samples were intended to demonstrate the applicability of these techniques to the production of real mirror structures.

Schott also performed engineering studies that were directed towards evaluating the various techniques in terms of scaling up the processes for the manufacture of large mirrors. This evaluation included the selection of the optimum techniques, preliminary engineering designs of the required equipment, and cost and schedule estimates for the establishment of a facility capable of producing mirrors up to 4 meters in diameter.

Analyses were performed to predict the performance of a Zerodur mirror under high front surface thermal loading. Detailed thermal analysis provided temperature distributions in the mirror as a function of irradiation time. Mirror distortions were calculated using finite element methods. A comparison between a Zerodur mirror and a ULE mirror were made. For this analysis, actual measured properties of Zerodur and the bonding frit were used.

The last objective of this program was the identification of areas requiring further effort to complete the technology development. Schott has estimated the cost and schedule to complete the technology portion of their effort.

The overall goal of this program was to assess the potential of Zerodur for use as a large lightweight mirror material in terms of properties, producibility, and performance.

SECTION IV

MIRROR FABRICATION PROCESSES

Schott has developed and evaluated several techniques that are applicable to the production of large lightweight passive mirrors from Zerodur glass-ceramic. An outline of the fabrication process appears in Table 2. The following sections discuss the details of the various steps in the process and include the results of the sample production and testing program.

TABLE 2. ZERODUR MIRROR FABRICATION PROCESS OUTLINE

I. CORE MAKING

- Rib Forming
- Bending to Form Half-Hexagons
- Welding Half-Hexagons to Build Up Core
- Anneal and Ceramize Core
- Generate Curvature

II. FACESHEET FABRICATION

- Cast Zerodur Glass to Form Large Block
- Wiresaw into slabs, Grind and Polish Plano
- Slump into Polished Metal Mold and Ceramize
- Generate if necessary

III. BONDING FACESHEETS TO CORE

- Apply Frit/Vehicle Paste to Core
- Assemble Facesheets to Core
- Frit Bond in Ceramizing Furnace

IV. BLANK FINISHING

- Grind to Finished Dimensions

4.1 CORE MAKING

Several alternative manufacturing processes for producing lightweight eggcrate-type cores from Zerodur were investigated by Schott both before and during this program. Consideration was given to casting partially lightweighted cores by pouring Zerodur glass into a brick mold machined to resemble a negative of the desired core structure. Further machining would be required to complete the lightweighting. This process was eliminated from consideration due to its lack of efficiency, the difficulty of making such a mold, and the extensive machining and risk in the finishing process.

The potential of spin casting one piece cores was evaluated. The advantages are the lack of joints and the near net shape of the spin cast piece. Schott's engineering calculations indicated that the temperature/viscosity relationship in Zerodur glass precluded the flow of glass into the narrow channels that define the cell walls. This alternative was also eliminated.

The two remaining processes are: 1) continuous casting of flat sheet, and 2) cut and grind ribs from block. Both processes are followed by a bending process to form half-hexagons and a welding process where the glass hexagons are fused together to form a core. The welded core is then annealed and ceramized.

The selection of either continuous casting or cutting and grinding is dependent on the number of pieces to be produced. Fabrication of a small number of mirrors favors cutting and grinding, while large volumes of ribs may be produced quickly and more cheaply by continuous casting. The following sections detail the development work, sample fabrication and testing performed by Schott Glaswerke.

4.1.1 Rib Production

Core fabrication begins with the production of flat ribs. Presently all core ribs are produced by sawing slabs from Zerodur glass blocks and grinding the slabs to finished dimensions. Final surface grinding is

performed with 320 grit abrasive. After grinding, a small hole is bored in the center of the plates for venting purposes. All samples produced by Schott during this program were prepared in this fashion.

The major advantage of this process is that no extension of technology is required. Almost no capital equipment is required if the volume of parts to be produced is not large. The disadvantage of this process is realized if large numbers of ribs are required (i.e., fabrication of many large cores). The sawing and grinding processes are relatively slow and inefficient for the production of many parts.

An attractive alternative for forming the core ribs is continuous casting. In this process, Zerodur glass is drawn from the melting furnace and rolled to the required thickness between water cooled rollers. The continuous ribbon on glass is annealed, inspected, then cut to size when cool. A diagram of the process is shown in Figure 2.

Schott employs rolling to form sheets of both glass and technical glass ceramic. A material very similar to Zerodur is rolled to form stove tops measuring 31" x 24" x 0.12". Schott has evaluated this process with respect to the production of Zerodur and has identified no technical difficulties. The physical properties of Zerodur glass are actually more favorable for rolling than are those of the stove top material. At the present time, Schott has no experience with rolling plates less than 0.12" thick. A 4% core requires a core plate approximately 0.080" thick. Experiments can determine if the rolling process produces this thickness plate. If not, grinding might be employed to reach final thickness.

Schott has performed a cost analysis to determine the most efficient process for producing plates. Appendix A is a summary of Schott's evaluation. The choice of process is dependent on the number of mirrors to be produced. The graph on Page 3 of Appendix A shows qualitatively the relationship between fixed and variable costs and mirror quantities. The fixed costs are mainly those incurred in start-up. Each of the three production lines have furnaces that must be purged with Zerodur glass prior

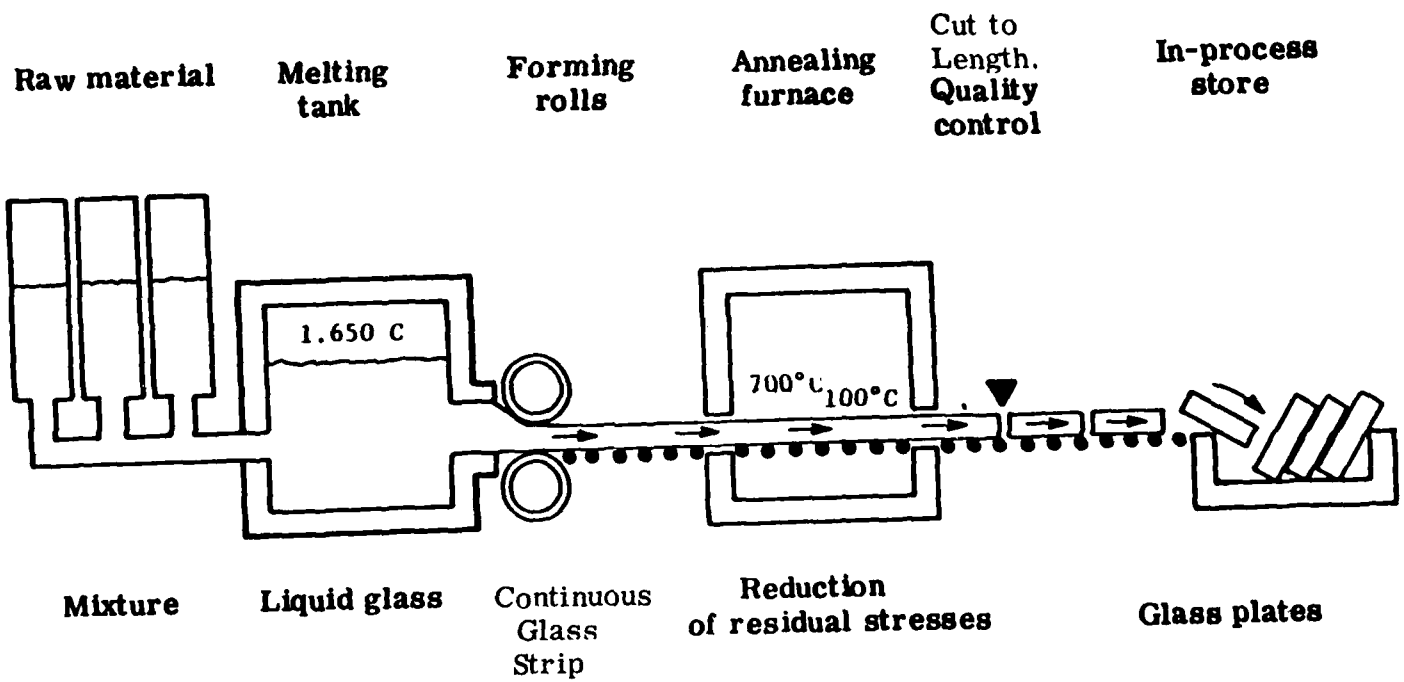


Figure 2. Rolling of Zerodur Sheet

to the start of rolling. Because the furnaces are different sizes, the amount of glass to be melted and discarded varies. The Ceran technology, for example, has the largest furnace and thus the greatest start-up costs. The proportional costs of rolling Zerodur on the Ceran line is lower, however, due to greater production rates.

No new technology is required to produce core plates by rolling Zerodur. All the required equipment currently exists at Schott. Based on current production rates, all of the plates required for a 4 meter mirror could be produced in a few hours. Rolling is, however, a high volume process. The core plates for the first mirrors would probably be made by cutting and grinding from blocks. Transition to rolling could occur if and when the volume justifies the setup costs.

4.1.2 Hex Forming

The next step in the core building process, shown in Figure 3, is the bending of the core plates to form the half-hexagons. Prior to bending, a vent hole is drilled in the center of each plate. The process as developed and tested by Schott consists of the following steps:

1) preheat Zerodur glass plates in oven
2) transfer preheated plates to clamping fixture
3) heat areas to be bent with gas-oxygen burners ($\sim$ 6 seconds)
4) bend plate against mechanical stops to form half hexagon
5) unclamp plate and return to annealing oven
6) after annealing, grind mating edges to precise dimensions (if required).

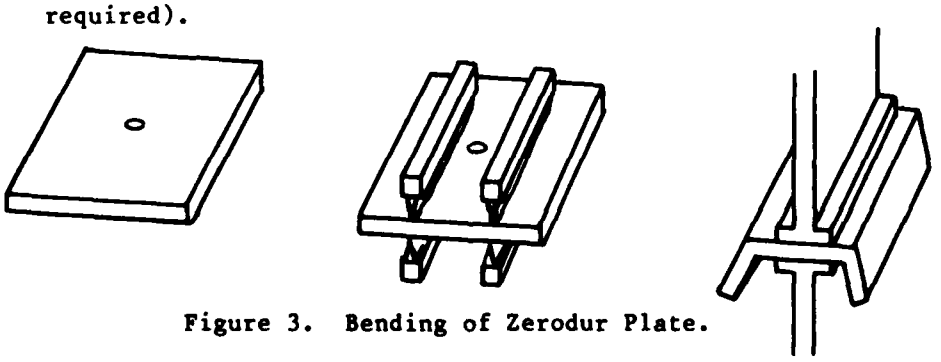


Figure 3. Bending of Zerodur Plate.

Schott built and tested a semiautomatic machine for bending Zerodur plates. Handling of the plates before and after bending was performed manually. All of the bent samples produced on this program for welding experiments were made on this machine. A more detailed discussion of the bending process and the effect of the bending on strength and CTE can be found in Appendix B.

Based on their experiments, Schott has concluded that the bending technology is completely developed. Preliminary designs for fully automatic equipment to produce the half-hexes have been prepared (see Appendix F). According to Schott's engineering estimates, all of the half hexes for a 4 meter mirror could be prepared on the automatic equipment in approximately 8 hours. Cost estimates for this equipment are discussed in Section 6.

4.1.3 Welding

Joining the half-hexagons together to build a lightweight core is accomplished by a welding technique developed by Schott. The process consists of the following steps:

1) Preheat half-hexes in oven
2) Load half-hexes into ceramic fixtures
3) Heat mating surfaces with gas-oxygen linear burners
4) Push mating surfaces together to fuse
5) Remove fixtures and index welded core into furnace
6) Anneal and ceramize welded core.

The Schott welding process differs from that used to weld ULE in several respects. The welding of the Zerodur is performed prior to the ceramizing step. At this point, the material does not yet have a low coefficient of thermal expansion. For this reason, the welding cannot be performed at room temperature as thermal shocking of the glass would occur on application of the burners. To avoid this problem, the half-hexagons are preheated to around 650° C and are maintained at this temperature throughout the process. The welding takes place at the entrance of an annealing

furnace in which the previously welded rows of hexagons are kept at around 600° C. After each row of half hexagons is added, the core is indexed into the furnace. A diagram of the process appears in Figure 4.

After the core is built up to the required size, the core is annealed and ceramized to develop Zerodur's characteristically low CTE.

4.1.4 Welded Sample Properties and Evaluation

Schott prepared welded samples for strength testing in several configurations. Their testing included: 1) 90° "L" samples, 2) 120° samples in which one part was bent and the second part was welded to the area of the bend, and 3) butt welded samples. Details of the sample preparation and configuration appear in the Schott report in Appendix B.

4.1.4.1 Welded Joint Strength

Schott performed bending strength testing on bent and welded samples of Zerodur. Testing of Zerodur samples without welds was supplied for comparison. Details of their testing and raw data appear in Appendix B. Table 3 summarizes the results of bend strength testing of these samples.

TABLE 3. BEND STRENGTH SUMMARY

SAMPLE TYPE	N	$\bar{x}$ (PSI)	STD DEV	LOW(PSI)	HIGH(PSI)
120° bent and welded	20	3477	563	2517	4267
90° welded	20	2015	103	1782	2137
180° butt welded	14	5550	603	4557	6413
180° butt welded, ground	15	5893	987	3880	7349
Flat sheet, no weld	19	7476	858	5917	8891
Flat sheet, ground	19	9386	824	8013	11,177

Schott's report indicates that failure was a function of the geometry of the notches adjacent to the welded region. In the 120° samples, for example, no failure occurred in the weld itself. An attempt was made to

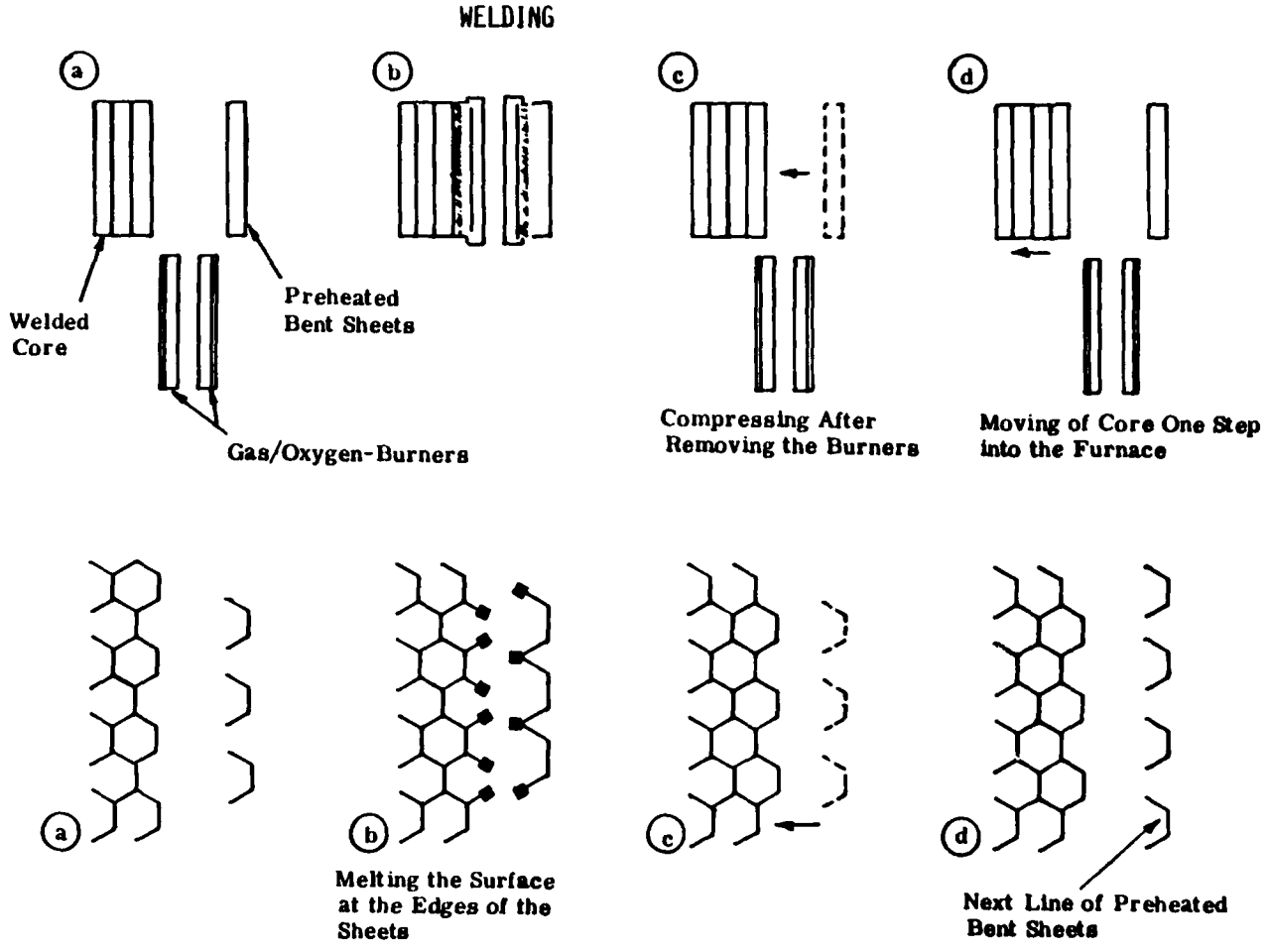


Figure 4. Welding of Zerodur Core

determine the influence of the geometry of the bulges and notches adjacent to the weld by grinding the welded area of the butt samples flat before testing. The grinding of the weld opened up the bubbles in the weld and the fractures all originated in the welded seam. The strengths did not change, however, from the values obtained on unground samples.

The conclusion reached from this testing is that the strength of the bent and welded joints is adequate for the production of lightweight Zerodur cores.

4.1.4.2 Influence of Bending and Welding on CTE

Heat treatment influences the coefficient of thermal expansion of Zerodur. A testing program was performed by Schott to determine the influence of the bending and welding process on the CTE of Zerodur. Although the bending and welding processes are employed while the Zerodur is still in the glassy state, there was concern that the application of heat to the bent and welded areas would change the thermal expansion behavior of those areas.

Schott resolved this issue by cutting test rods from 120° welded samples for thermal expansion measurements. Samples were taken from the bent and welded zone, areas adjacent to the weld, and from the material unaffected by the bending and welding process. The results show that the welded region, as expected, has a higher (less negative) coefficient of thermal expansion in the temperature range from 0 to 50° C. The differences, however, are the same order of magnitude as the repeatability of the measurement ($\pm$ 0.005 x 10^{-6}/° K). Details of these measurements appear in Appendix B. The conclusion reached is that the bending and welding of Zerodur to form a core structure does not significantly affect the thermal expansion properties of the material.

4.1.4.3 Evaluation of Welded Samples

Perkin-Elmer obtained several samples of 120° bent and welded and butt welded Zerodur parts for examination and testing. Figure 5 shows the

120° samples and Figure 6 the butt welded samples. These samples were examined for workmanship, uniformity, cracks, inclusions, and residual stresses. The butt welded samples were tested to obtain the tensile strength of the weld. These samples were prepared using the same techniques as the samples evaluated by Schott.

- o 120° Sample Evaluation
  - Appearance: All samples appeared to have very uniform welds and bends. The surface of the parts had a ground finish except in the bent and welded regions where some firepolishing was evident. The bulges and notches referred to in the strength testing section can be seen clearly in Figure 7. These features are the result of upsetting the mating surfaces during the welding process. Examination of the welded samples revealed the presence of bubbles in the weld. No cracks, tears, or inclusions were evident. A black deposit appeared on some of the samples. The deposit was, most likely, soot from the gas/oxygen burners.
  - Residual Stress: Birefringence measurements were performed on the welded samples. In all cases, less than 100 psi residual compression was detected in the Zerodur. It should be noted here that the ceramization heat treatment results in residual compression in the samples. There was no evidence of residual stress induced as a result of the bending or welding processes.
- o 90° Butt Sample Evaluation
  - Appearance: Same comments as for the 120° samples.
  - Residual Stress: Less than 100 psi compression.
  - Strength Testing: Tensile testing was performed on seven of the butt welded samples. Steel fixtures were epoxied to the ends of the samples to enable the parts to be gripped using a clevis pin fixture. The mean tensile strength of the butt welded joints was 1871 psi with a standard deviation of 536

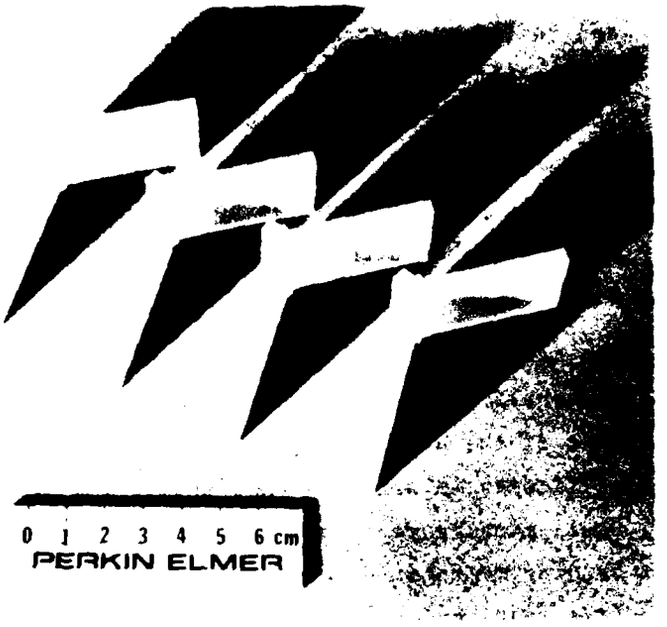


Figure 5. 120° Bent and Welded Zerodur

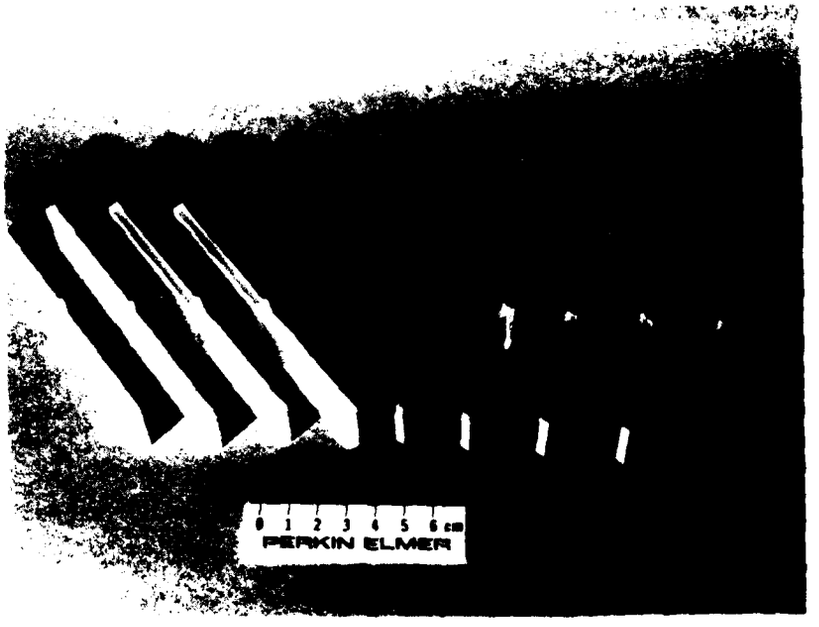


Figure 6. Butt Welded Zerodur

psi. One of the seven was grossly misaligned during the test and failed at a stress of 961 psi due to bending. Elimination of the sample from the set results in a mean tensile stress of 2022 psi with a standard deviation of 389 psi. The stress was calculated based on the cross section of the bars. The area of the bulge at the weld was not measured. Four of the seven failed at the notch adjacent to the weld and three failed in the welded seam.

The mean failure stress in tension for these samples was less than half of the measured bending strength in the Schott data. Most of the discrepancy is believed to be related to the difficulty in aligning the tensile samples during testing. Small misalignments during tensile testing result in large bending moments in the samples. The clevis pin fixtures used in this test would not eliminate these unwanted bending moments.

4.1.4.4 Welded Core Sample

In order to demonstrate the applicability of the bending and welding processes to the fabrication of lightweight cores, Schott fabricated a sample core section consisting of four complete hexagonal cells. The inside dimension of the cells (flat to flat) was approximately 3.5 inches. Cell walls were 0.164 inches thick. Overall core height was 3.9 inches. The core density was 8.75%. Figure 8 is a photograph of this core section.

In order to fabricate this core section, Schott constructed a semiautomatic welding machine (a detailed description of the operation of this machine is included in Appendix C). The ceramic fixtures that hold the half-hexagons are loaded manually and are preheated to around 650° C. The heated hexes and fixtures are manually transferred onto the welding machine. From this point on, the process is automatic. The pneumatically controlled machine moves the half-hexes into position, raises the gas-oxygen burners to heat the mating surfaces, and subsequently pushes the mating surfaces together. After the fusion is completed, the core is automatically pulled

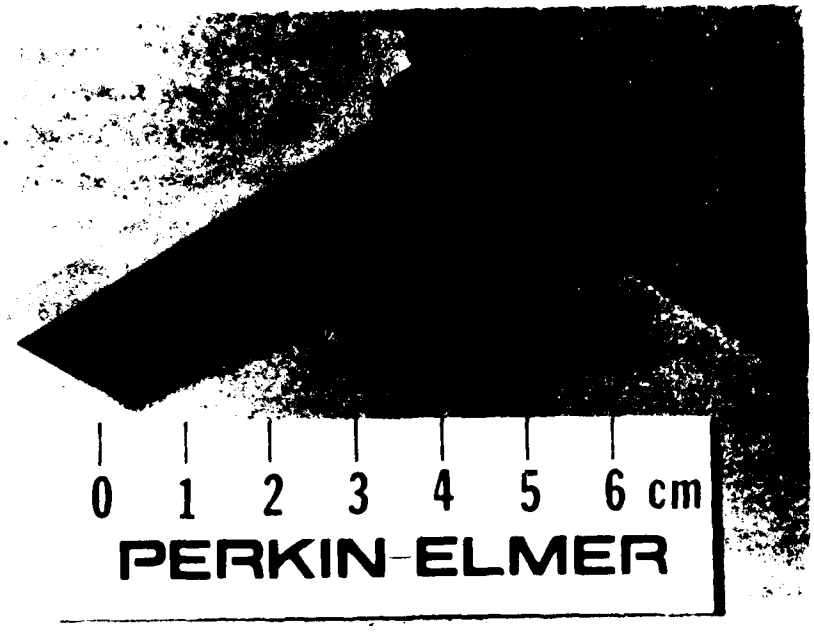


Figure 7. Bent and Welded Zerodur

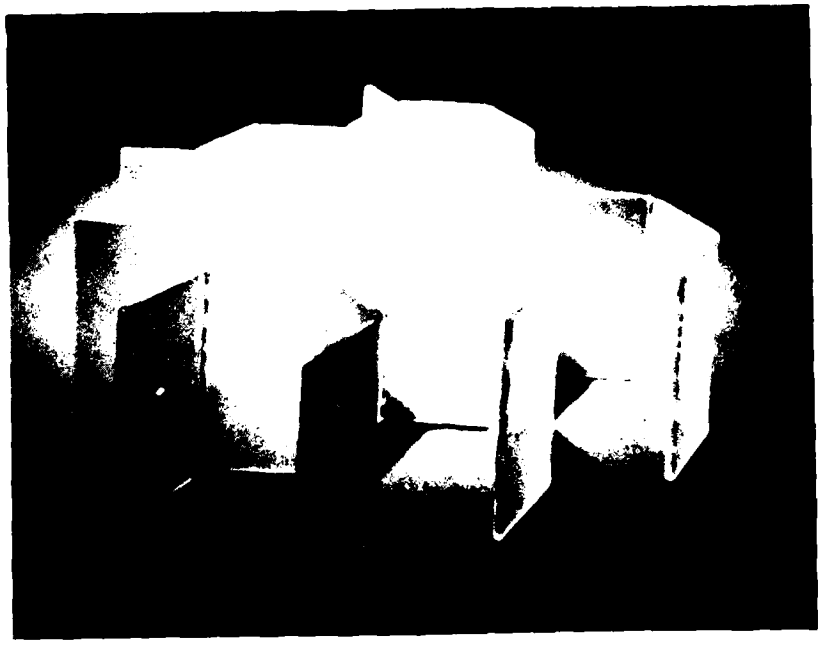


Figure 8. Welded Zerodur Core Sample

into the furnace. The process is repeated for each row of hexagons added to the core. Figure 9 is a sketch of the welding machine showing a row of half-hexes about to be added to the core in the annealing furnace. Figure 10 is a side view of the welding machine showing the lowered gas-oxygen burners. The partially completed core in Figure 10 is shown at the furnace opening. The transport system on the right automatically indexes the core into the furnace as each row is added. Photographs of the welding machine are included in Appendix C.

4.1.4.4.1 Core Sample Evaluation -- The four cell core sample was delivered to Perkin-Elmer for evaluation. The joints all appeared to be completely fused. Uniformity of the welds was good within each weld but the size of the bulges formed adjacent to the welds varied from weld to weld. Black deposits in some of the welds again indicated improper gas-oxygen mixture in the burners. As in the smaller samples discussed in the previous section, bubbles were visible in the welded areas but none were open to the surface. Cracks were found in one welded seam.

The core sample was geometrically uniform with the inside dimension of the hexagonal cells (flat to flat) varying by no more than about 0.08 inches.

Schott continued to experiment with the welding machine after fabrication of the four cell sample. Several large cores were built using both Robax (a technical glass ceramic similar to Zerodur) and Zerodur. Figures 11 and 12 are photographs of one of the 7 cell core sections built on the welding machine. Examination of these cores showed considerable improvement in Schott's control of the welding process. The uniformity of the welds was much better and no black soot deposits were visible.

4.1.5 Core Fabrication - Conclusions

The construction and testing of the semiautomatic core welding machine completed the technology development effort in the area of lightweight core fabrication. Schott has concluded that the production of

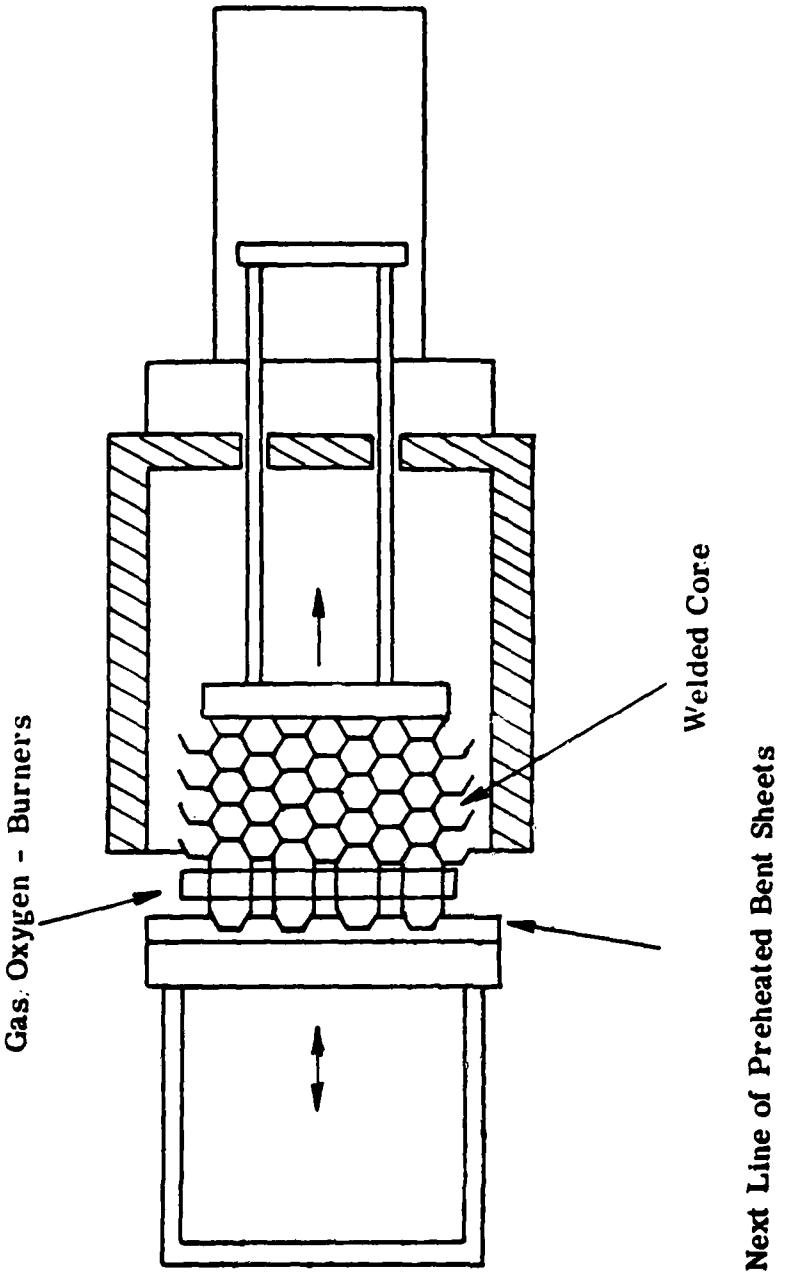


Figure 9. Core Welding Machine

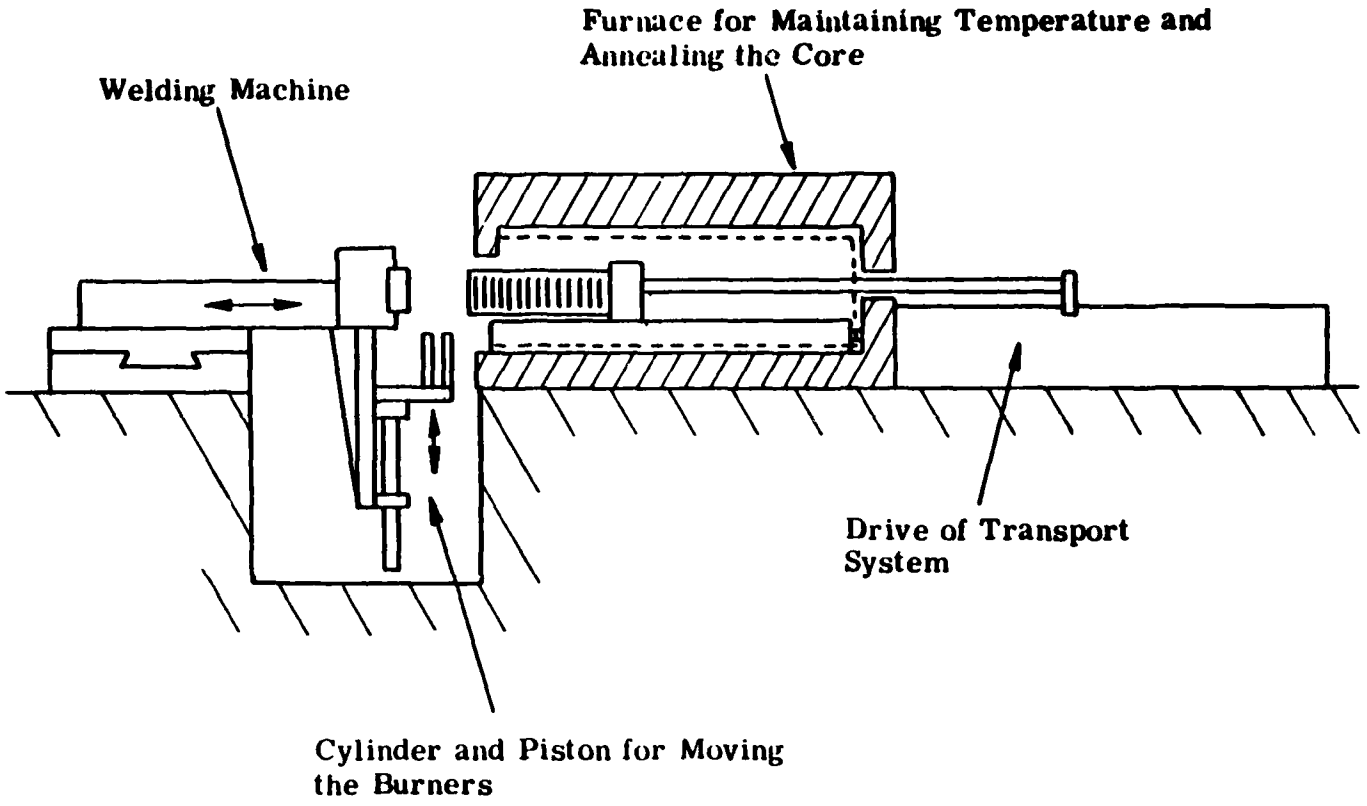


Figure 10. Core Welding Machine (Side View)

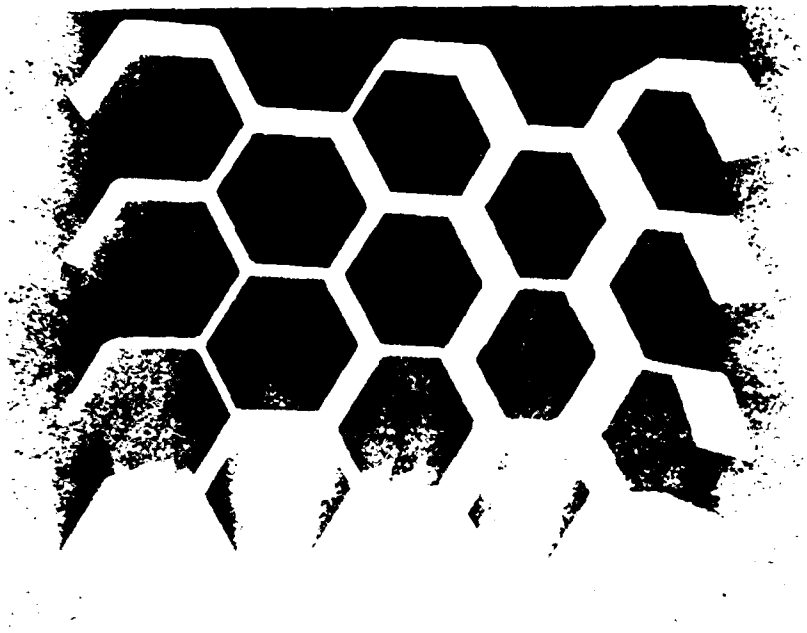


Figure 11. 7 Cell Welded Zerodur Core



Figure 12. 7 Cell Welded Zerodur Core

full scale lightweight cores requires only the establishment of a facility and the acquisition of the necessary equipment. According to Schott's engineering estimates, the production of bent core plates and the welding of the half-hexes to form a core for a 4 meter mirror would take about 2 days (not including annealing and ceramizing). Schott has completed the preliminary design and cost estimates for the fabrication of the required equipment. The cost estimates are discussed in more detail in Section VI).

4.2 FACESHEET FABRICATION

Prior to this study, the only practical method for forming thin curved facesheets from Zerodur was to machine the facesheet from a large block of the glass-ceramic. It is not possible to hot-form Zerodur after ceramization without changing the thermal expansion characteristics. Machining a large facesheet from a solid Zerodur block is inefficient in terms of material utilization. The manufacture of a typical 4 meter diameter facesheet weighing about 900 pounds would waste approximately 15,000 pounds of Zerodur. During this program, Schott studied the feasibility of several techniques for the more efficient production of thin curved facesheets.

These processes considered were: 1) stationary casting to final curvature on one surface, 2) spin casting, and 3) slumping.

4.2.1 Stationary Casting

This method improves material utilization by casting blanks having a curvature on one side. A mold is shaped to an approximate curvature on the bottom. The Zerodur glass is cast into the mold from the melting furnace. After cooling, annealing and ceramizing, the final shape is generated. This technique reduces the amount of Zerodur wasted by nearly half.

Schott has indicated that the homogeneity of the thermal expansion properties depend, to some extent, on the thermal conditions during casting and annealing. Schott scientists believe that the uneven cooling rates experienced by a non-uniform thickness blank would adversely impact the

homogeneity of the coefficient of thermal expansion. For this reason, Schott has recommended that this technique not be considered further.

4.2.2 Spin-Casting

Schott has for many years employed spin-casting to fabricate a number of technical glass products. In this process, molten glass is cast into a mold which is then rotated. Centrifugal forces distribute this viscous glass in the mold and maintain the desired shape until the glass cools and becomes rigid. Large glass vessels for commercial/chemical manufacture are produced using spin casting. Figure 13 is a sketch of a typical part produced by this process.

Schott studied the potential of spin casting for the production of large curved facesheets for lightweight mirrors. A sketch of the apparatus designed by Schott for spin-casting facesheets appears in Figure 14. The molten Zerodur glass is fed into the preheated, rotating mold. The rotation causes the molten glass to be distributed in the mold. The rotation of the mold continues until the glass becomes rigid. The blank is then transferred into an annealing and ceramizing furnace. Using this technique, blanks may be produced having near net curvature on both sides, thus greatly reducing the amount of material removed during generation.

A more detailed description of this process is included in Schott's Spin-Casting Report (Appendix D). In this report, Schott estimates the cost and time required for the design, construction, and testing of a spin-casting facility. The only development effort required involves the design of a molten glass feeder capable of the high rates required for the casting of a large facesheet blank. Engineering drawings of the spin-casting equipment are included in Appendix D. Schott has estimated a cost of about $2.0M and three years for the construction and testing of a spin casting unit and the production samples up to 2 meters in diameter. Schott has estimated that scaling up to the production of 4 meters diameter plates would cost an additional $650K to $870K.

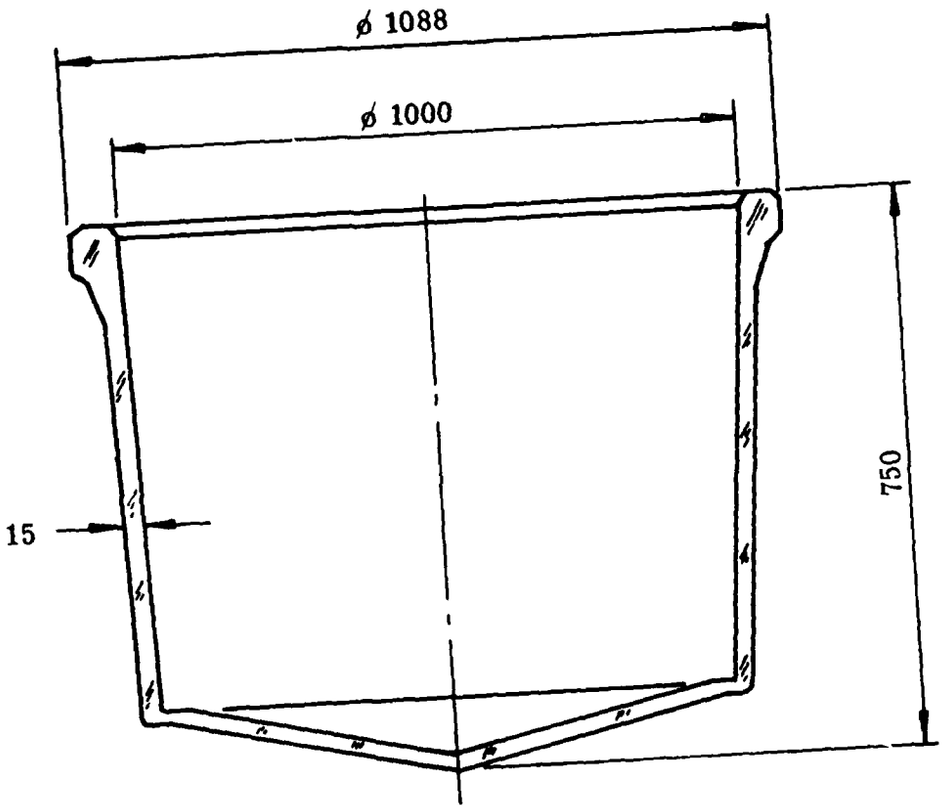


Figure 13. Example of Glass Part made by Spin Casting
(Dimensions in Millimeters)

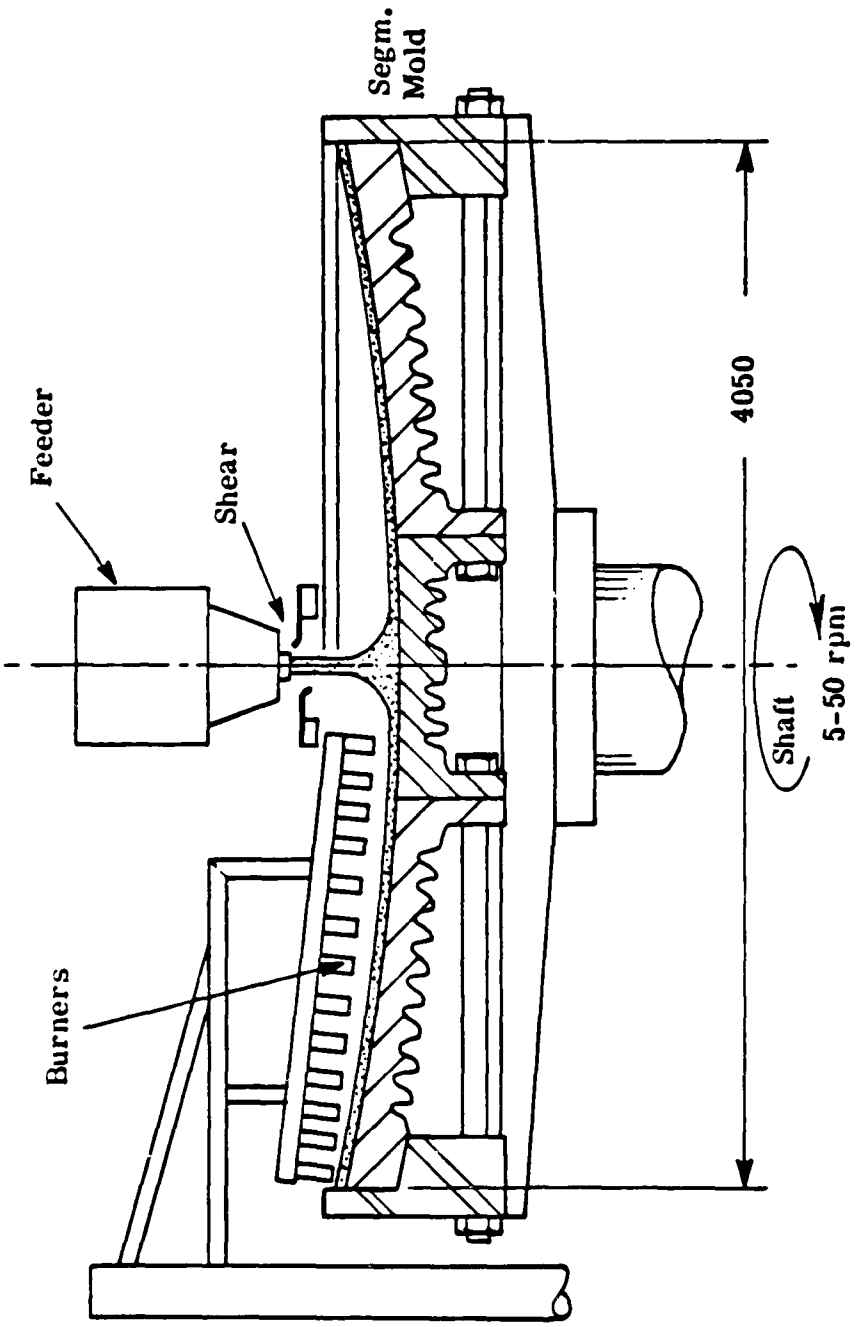


Figure 14. Spin-Casting Apparatus

Spin-casting is considered to be a viable process for the efficient production of large curved facesheets. The technology already exists at Schott and needs only to be adapted for use with Zerodur.

The large initial costs indicate that the selection of spin-casting for the manufacture of facesheets depends on the number of facesheets required. Machining from a solid blank is more cost-effective if only a limited number of facesheets were required.

4.2.3 Slumping

Schott's experience with spin-casting has shown that the process is more effective for the production of shapes with steeply curved sides (for example, see Figure 13). The facesheets for a beam expander mirror, however, are relatively flat in comparison. Schott continued to investigate alternative fabrication techniques and developed a slumping process with the potential for fabricating Zerodur facesheets.

Although it is not possible to slump Zerodur after ceramizing, Schott has discovered that Zerodur may be hot-formed while in the glassy state. A very limited number of laboratory-scale specimens have been produced using this new process. The samples were made by cutting disks of Zerodur glass from a solid block. The cut disks were placed on a curved metal mold in a small furnace. The furnace was heated and the disks were mechanically deformed to the shape of the metal mold. The disks were then annealed and ceramized.

Production of Zerodur facesheets using the slumping process consists of the following steps:

1) melt oxides
2) cast large circular blank
3) anneal blank
4) wire saw into thin slabs
5) grind plano
6) slump in metal molds

7) anneal and ceramize

8) generate rough curvature by grinding.

Figure 15 is a sketch of a slumping furnace. The glass block is heated and softens as the furnace temperature is raised. Ports in the metal mold are connected to a vacuum pump to provide the pressure required to force the glass into the mold. Compressed air may be provided through the same ports during heat-up to support the glass.

There are seveal differences between the slumping of Zerodur and the slumping of ULE. Zerodur glass is slumped at a temperature of around 800 ° C as compared to 1500 ° C for ULE. The lower temperature used for Zerodur makes possible the use of metal molds instead of firebrick molds. Preliminary experiments indicate that the lower temperatures and the use of metal molds greatly reduces the extent of surface damage and contamination of the slumped pieces.

Figures 16 and 17 are photographs of a sample of slumped Zerodur glass. This piece was ground and polished plano prior to slumping. The surfaces shown in the photographs are the as-slumped surfaces; no subsequent grinding or polishing has been performed. Close inspection of this part revealed no visible surface contamination or cracks. Machining marks in the metal mold were replicated in the glass. This lack of surface damage and contamination constrasts with the requirement to remove at least ¼" per surface from a slumped ULE plate.

Development of the slumping process has a number of distinct advantages over the other techniques considered. The ability to form a curved facesheet by slumping wastes a minimal amount of material. Capital investment is considerably lower than spin-casting since no complicated rotating equipment is needed. If large facesheets can be slumped to near net shape and thickness, the time and cost for generating the surfaces would be greatly reduced. The retention of polished surfaces during the slumping operation would facilitate inspection for inclusions, bubbles and striae after slumping.

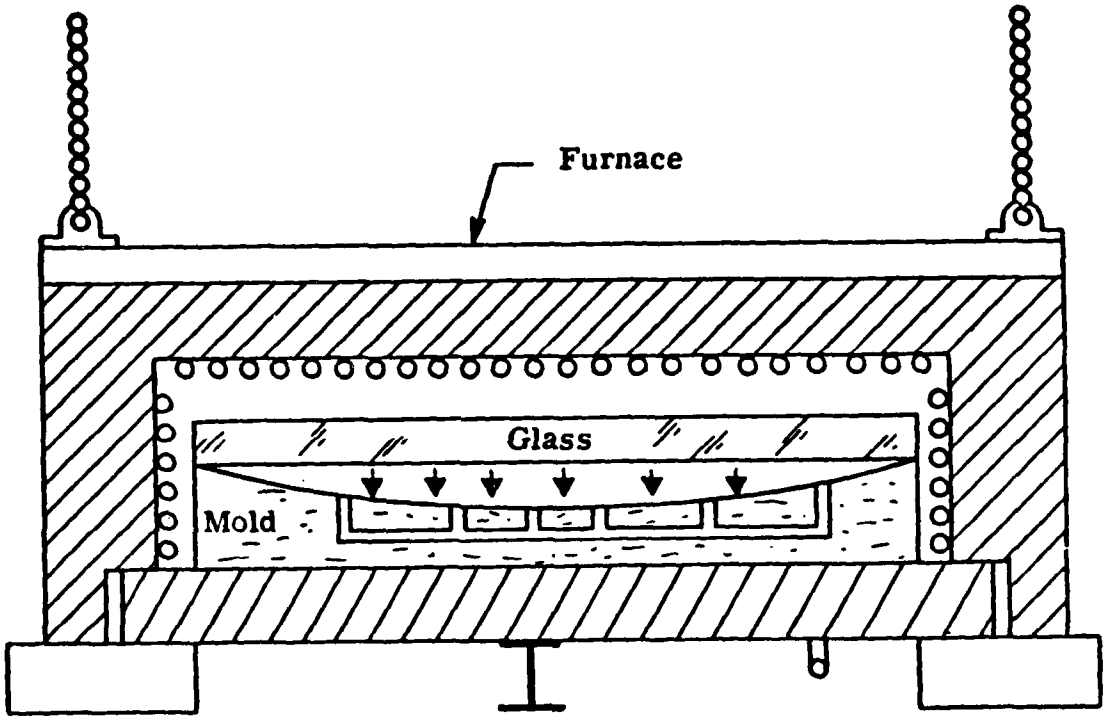


Figure 15. Slumping Furnace

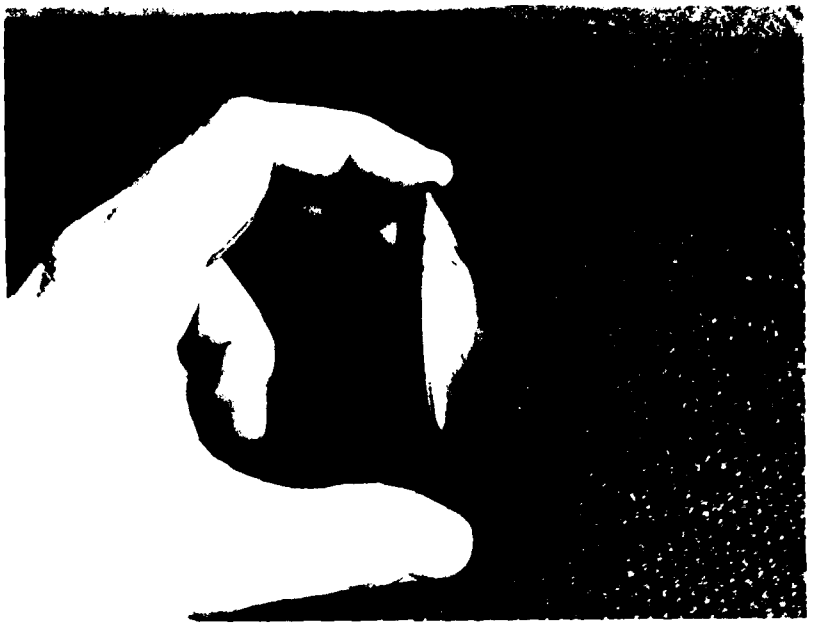


Figure 16. Slumped Zerodur Glass

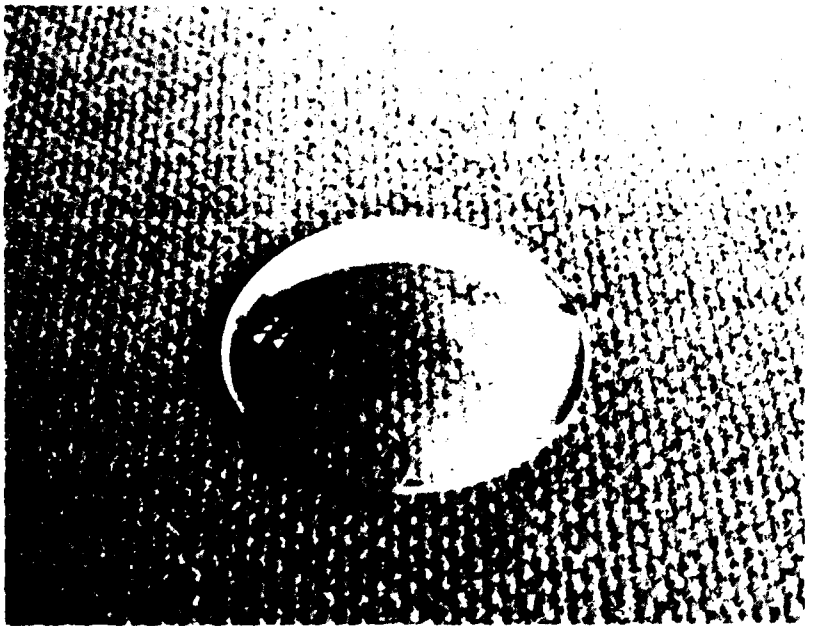


Figure 17. Slumped Zerodur Glass

A one year program to fully develop the slumping technology has been proposed by Schott and Perkin-Elmer. The program includes all laboratory experimentation to optimize the process parameters and the production of samples for evaluation. Successful completion of the proposal program would enable the production of Zerodur facesheets up to 2 meters in diameter. The process is expected to be scaleable to larger sizes. A more detailed discussion of this proposed program is included in Section VIII.

4.2.4 Facesheet Production - Conclusions

Both spin-casting and slumping have potential for the production of Zerodur facesheets for large mirrors. Spin-casting is an established technology and requires very little development to apply the process to Zerodur. The slumping process requires more development but may be more efficient for the manufacture of the thin, relatively flat facesheets required for large mirrors. Perkin-Elmer and Schott have concluded that the slumping process is the first choice for the production of facesheets. Spin-casting is a viable alternative which could be pursued if required.

4.3 FRIT BONDING

After fabrication of the lightweight core by welding and the facesheets by slumping, the facesheets must be bonded to the core. For ULE mirrors of conventional design, the bonding of facesheets to the core is accomplished by a high temperature fusion process. A fusion process cannot be performed on the ceramized Zerodur mirror part because the high temperature required destroys the low coefficient of thermal expansion. An alternative to fusion is using a frit as a bonding agent between the core and the facesheets.

A frit is a finely ground glass that fuses and forms a bond between parts when heated. Frits are used in a wide range of joining and sealing operations such as electronic packaging and glass-to-metal seals. Frits are generally low melting point glasses designed to soften and flow at relatively low temperatures.

A frit suitable for joining components for a lightweight mirror must meet several requirements not normally fulfilled by conventional glass frits. The requirement for low thermal expansion is perhaps the most difficult to satisfy. Glass frits are generally formulated to melt at low temperatures. The additives used to lower the melting point usually increase the coefficient of thermal expansion. In the case of a frit suitable for use with Zerodur, the fritting temperature must be below approximately 800° C to avoid further crystallization of the Zerodur, thereby increasing the thermal expansion coefficient.

The thermal expansion of the frit must closely match the expansion of the Zerodur in the operating temperature range of the mirror. Any mismatch may result in distortions as the temperature changes during use. The expansion of the frit must also be similar to that of the Zerodur from the fritting temperature to room temperature to avoid residual stress in the bonded joints.

Another requirement is that the strength of the fritted joints be adequate to permit the handling, figuring, launch, and operation of the mirror. Allowable stresses in glass mirrors are frequently set at 1000 psi. This establishes a lower limit for the strength of a fritted joint.

Prior to this program, Schott Glaswerke had developed three frit compositions with potential for use in bonding Zerodur to Zerodur. Two of the frits are devitrifying, i.e., the glass frit flows to and forms a bond when heated but subsequently crystallized. The crystalline phase has a low thermal expansion. The third frit is a "composite" frit. This frit is composed of a mixture of low CTE crystals and a low melting point glass. Details of the composition and processing of the frit are considered to be proprietary by Schott. During this program, Schott performed property measurments of their frits and fabricated several samples for evaluation. The following sections summarize this activity.

4.3.1 Frit Bonding - Physical Property Measurements

Schott measured the bond strength, the coefficient of thermal expansion, and elastic moduli of the three frits. The details of their measurement program appear in Appendix E.

Breaking Strength: The strength of frit bonded "L" samples was measured for the three frits. The effect of particle size and frit layer thickness was studied. Table 4 summarizes the results.

TABLE 4. BREAKING STRENGTH EFFECTS

	Layer Thickness (in)	Mean Strength (psi)
GM 31615	0.12 - 0.16	1976 - 2192
GM 31811	0.12 - 0.16	1977 - 2546
GM 31811	0.04	2559
13 - 51	0.12 - 0.16	2098
13 - 51	0.04	3406

In all cases the bonding strengths of the frits exceed the goal of 1500 psi that was established at the start of the program. All of the raw data and the Weibull analyses are given in Appendix E.

Elastic Modulus: The elastic moduli of the three frits were measured on sintered stacks. The frits require application of pressure during sintering. Modulus measurements were made on samples prepared with and without applied pressure (Table 5).

TABLE 5. ELASTIC MODULI OF SCHOTT FRITS

Frit	Pressure	Modulus (psi)
13-51	no	1.28×10^6
13-51	yes	1.22×10^6
GM 31615	no	3.41×10^6
GM 31811	no	3.34×10^6
GM 31811	yes	2.17×10^6

Coefficient of Thermal Expansion: The thermal expansion behavior of the three frits was measured on sintered stacks over the range from room temperature to 600° C. Figure 18 is a copy of the plot in Appendix E showing the results of these measurements. It can be seen that the expansion behavior of the frits varies tremendously. Frit GM 31811 appears to be the best match for Zerodur in the vicinity of room temperature. More detail on the thermal expansion measurement program is given in Appendix E.

Based on the physical property measurements, frit GM 31811 was judged to have the best properties of the three frits. This frit was used in the production of samples for evaluation and further property determination.

4.3.2 Sample Production

Frit GM 31811 was prepared as a paste by mixing the powdered glass with an organic vehicle. The paste was applied to the samples in 0.012" layers. The bonding operation was performed in a furnace while applying a pressure of about 7 psi to the parts. "L" samples were prepared for strength testing by Schott. Lap shear samples were prepared and shipped to Perkin-Elmer for testing. Frit bonded stacks of Zerodur were made for thermal expansion measurements.

4.3.3 Sample Evaluation

"L" Samples: Figure 19 is a photograph of the "L" samples received from Schott. The bondlines appear between 0.004" and 0.010" thick. One of the three bondlines is wedge shaped due to improper alignment of the pieces during bonding. One of the samples contains shrinkage cracks in the bondline. Birefringence measurements indicated a residual stress between 170 and 250 psi.

Samples similar to these were made by Schott for measurement of the bend strength of the fritted joints.

Lap Shear Samples: Six lap shear samples were received by Perkin-Elmer for evaluation. These samples are shown in Figure 20. The bondlines

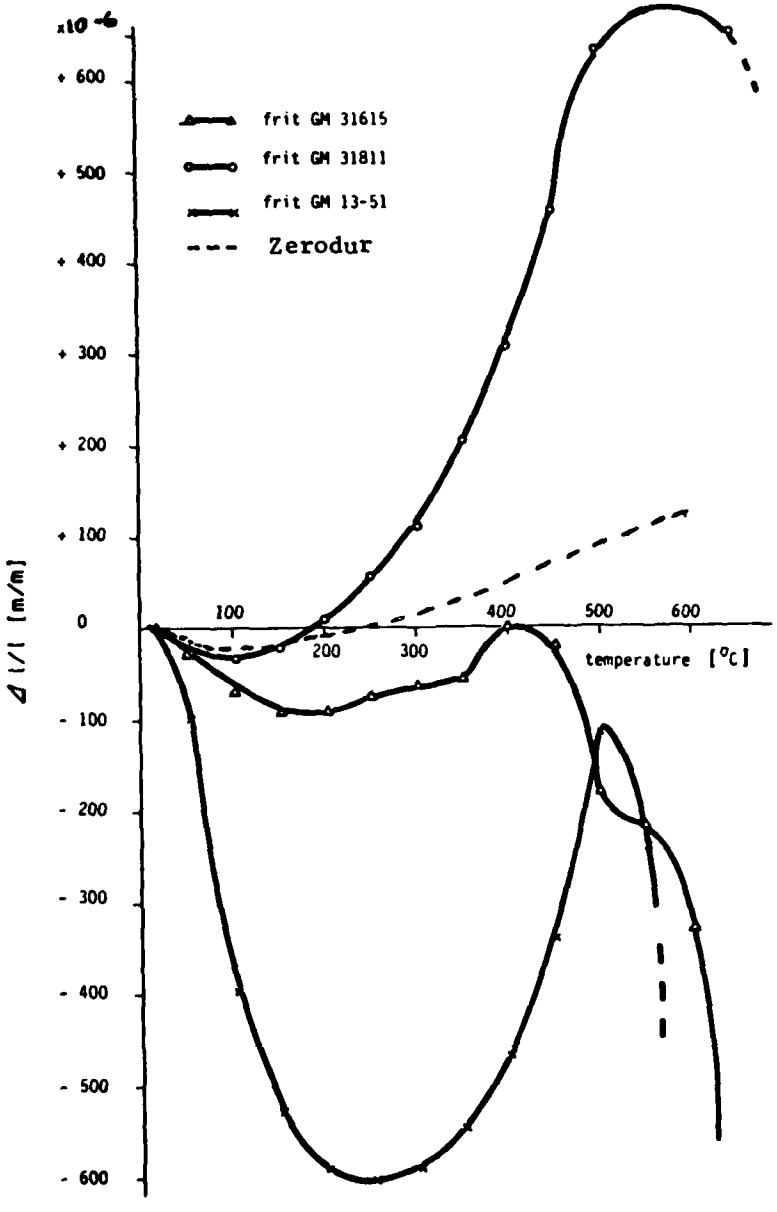


Figure 18. Thermal Expansion of Candidate Frits

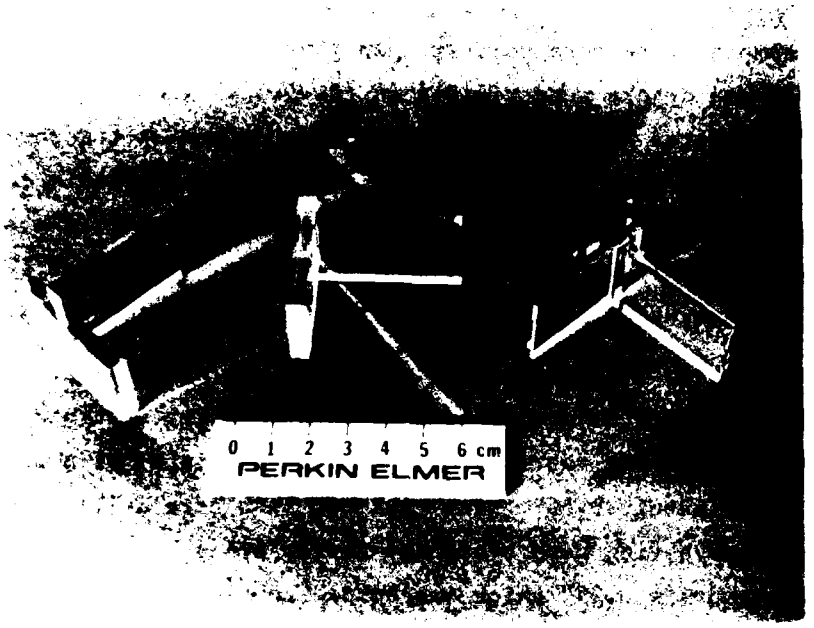


Figure 19. Frit Bonded "L" Samples

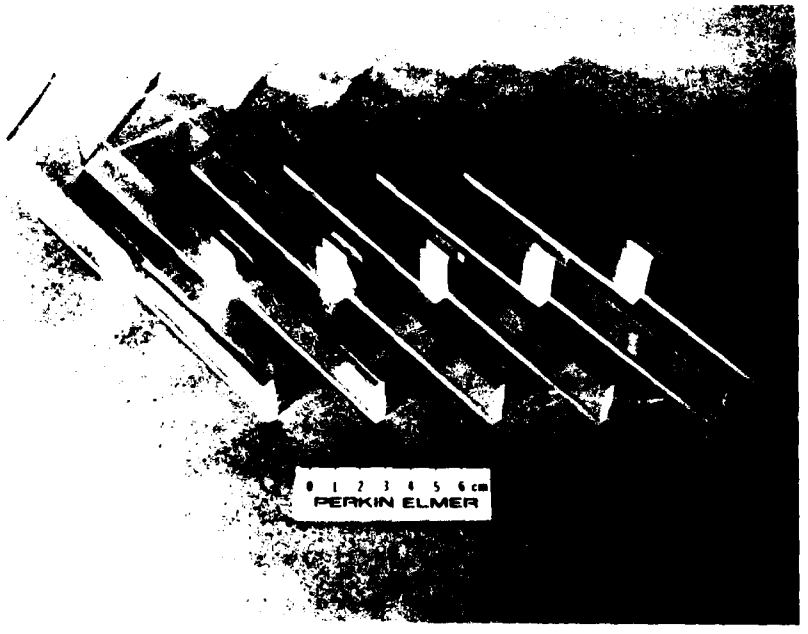


Figure 20. Fritted Lap Shear Samples

in these samples were more uniform than those of the "L" samples. A few small shrinkage cracks were visible in the frit. These samples were epoxied into steel fixtures and tested in tension to determine the shear strength of the bondline. On five of the six samples, the glass-ceramic coupons failed in bonding. One of the samples failed in the bondline from a shock load applied accidentally during mounting. The shear strength of the bondline cannot be determined from the testing of single lap shear samples.

In order to demonstrate the applicability of this frit to bonding a Zerodur facesheet to a core, a plano blank measuring approximately 0.3 meters in diameter was fabricated. The core consisted of a solid blank of Zerodur approximately 0.55" thick that has been core drilled to create a bonding surface having both broad and narrow areas. A planar solid facesheet measuring 0.25" thick was bonded to the core using frit GM 31811. The process used was identical to that employed in the production of the "L" and lap shear samples. A photograph of this blank appears in Figure 21.

The bondline in this sample was very uniform in thickness. The cracks apparent in this sample were the result of the shrinkage of the frit/organic vehicle paste during drying. The appearance of the bondline did not vary between the narrow and broad areas.

4.3.3.1 Residual Stress in Fritted Joints

Schott has made an extensive study of the magnitude and origin of the residual stresses measured in the bonded Zerodur pieces. Figure 22 is a plot of the difference in thermal expansion between the frit and the Zerodur. On cooling from the fritting temperature, the frit shrinks more than the Zerodur, creating a small compressive stress in the Zerodur. Schott has determined, however, that a chemical ion exchange takes place between the frit and the Zerodur that creates very large compressive stresses in the surface of the Zerodur. These stresses generate smaller tensile stresses in the bulk of the Zerodur piece. The magnitude of these stresses depends on the relative thickness of the frit layer and the Zerodur parts. Schott has reported good correlation between the stress measured by

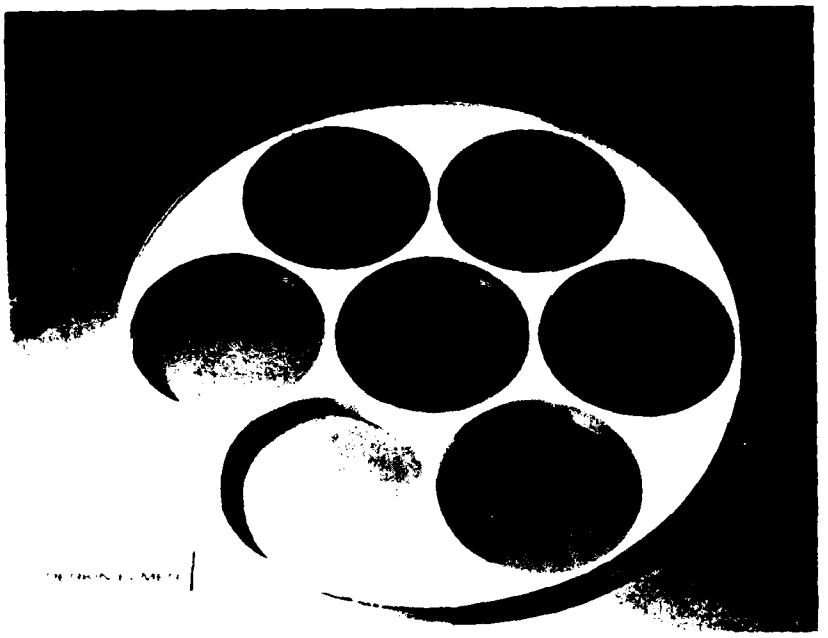


Figure 21. 0.3 meter Fritted Zerodur Blank

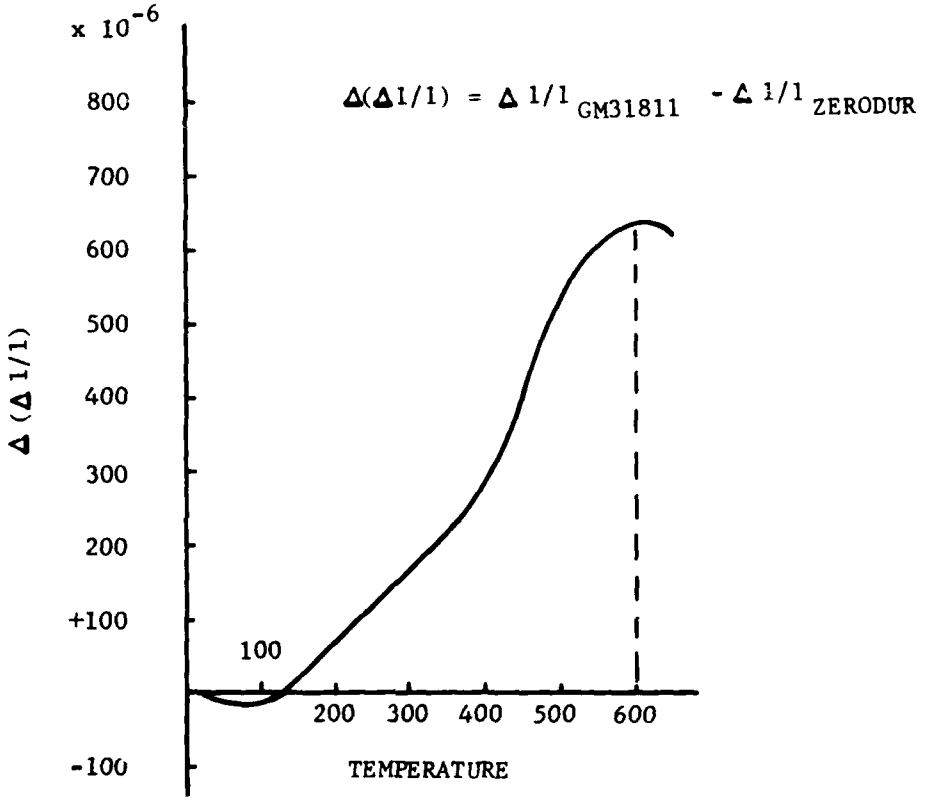


Figure 22. Thermal Expansion Mismatch of Frit with Zerodur

birefringence and the stress calculated from the mismatch of the thermal expansion between the Zerodur and the frit. Techniques have been developed to eliminate the compressive layer generated by the ion exchange.

Schott has measured the change in stress birefringence in fritted samples in the temperature range from room temperature to 200° C. Figure 23 shows the results of their measurements. The change in stress is relatively small for the thicker frit layers and is in agreement with the behavior predicted from the thermal expansion data. The actual mismatch of the thermal expansion of the frit and Zerodur was used in the Performance Analysis Task (Section V).

4.3.4 Frit Development - Proposed Future Effort

The development of a frit suitable for use for bonding Zerodur facesheets to lightweight cores is in the early stages. Schott has prepared an outline of the required technology development prior to production of lightweight mirrors. Schott's proposed program for the technology development is included in Appendix E. The effort is divided into two main areas. The first is concerned with the development, characterization, and understanding of the frit. This work includes compositional studies, development of techniques for property measurement, and a study of the influence of the various parameters on the physical properties of the fritted joints. The second area is the development of techniques and processes for preparing and applying the frit to cores and facesheets, determining the optimum drying and firing conditions, and developing the necessary equipment used to frit bond large mirrors. The cost and schedule to complete this work is included in Appendix E.

4.3.5 Frit Bonding - State of the Art

Schott has continued their own development work on the frit since the completion of their subcontract. They have developed a new application technique that allows the frit thickness to be accurately controlled between 0.002 and 0.010". Additional strength testing has shown that the strength of the joints is not strongly dependent on bondline thickness.

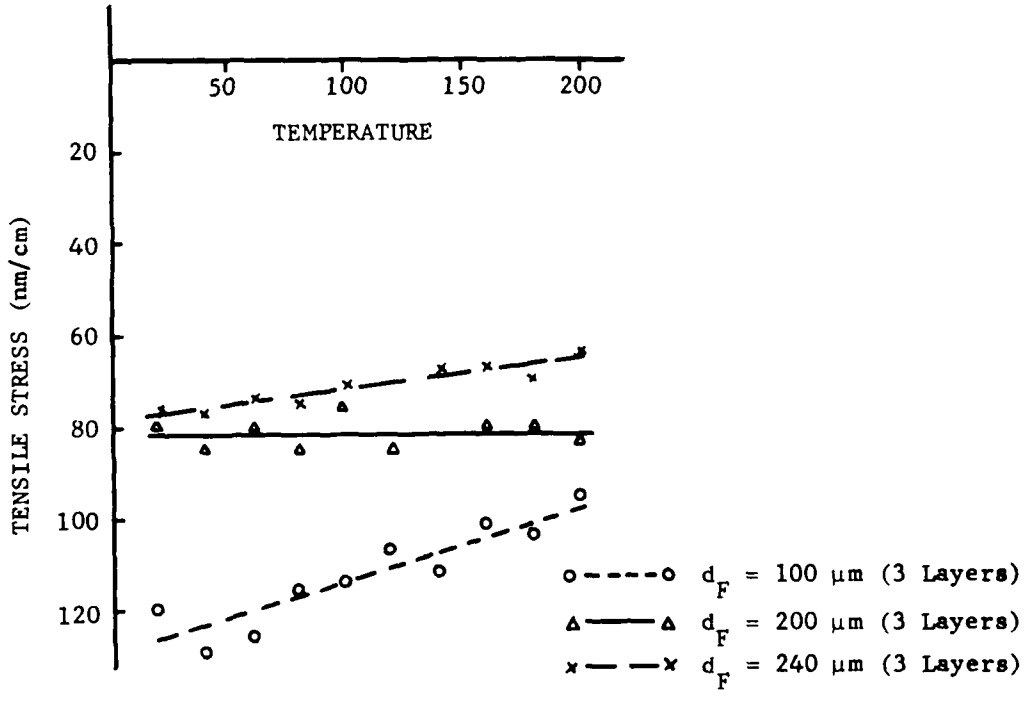


Figure 23. Change of Tensile Stress in Zerodur with Temperature

This insensitivity of the joint strength to bondline thickness may be an asset in the manufacture of lightweight mirrors. The tolerances for generating the curvatures on the mating surtaces of the cores and facesheets may be relaxed, resulting in a savings of time and a reduction in cost. A determination of the tolerance on the machining of the mating surfaces would be made as part of the Frit Development Program.

Schott has also developed and tested a technique for applying the required 7 to 8 psi pressure to the parts during the bonding process.

Although more effort is required to reduce the frit process to engineering practice, it is apparent that fritting has demonstrated potential for the bonding of Zerodur facesheets to lightweight cores. The performance analysis section will show that excellent performance can be expected of a Zerodur mirror made using the frit in its current state of development. Schott is confident that the properties of the frit can be further improved and that processes for applying this technology to the fabrication of large lightweight mirrors can be developed.

4.3.6 Mirror Fabrication Processes - Summary

Schott has developed processes with potential for fabricating lightweight mirrors from Zerodur. A thorough engineering study and evaluation has been performed to select the most suitable processes for the efficient production of large mirror blanks.

The technology development for core fabrication is complete. All the component techniques have been demonstrated in sizes adequate to give confidence in the scaleability of the process. The cost and schedule for the establishment of the capability to produce cores up to 4 meters in diameter has been estimated (see Appendix F). Analysis of the properties of the core components fabricated using these techniques has been performed. All properties of the welded core components are more than adequate for the construction of a lightweight Zerodur mirror.

Schott has investigated several techniques for the efficient manufacture of curved facesheets from Zerodur. Slumping appears to be the most promising and a proposal has been submitted for a program to complete the technology development. Spin casting has been judged to be a viable technique as an alternative/backup to slumping. The cost and schedule to complete the spin casting development has been estimated.

Analysis and testing of the properties of bonding frits have been performed and have demonstrated the potential of frit bonding for the joining of facesheets to lightweight cores. The details of a program to complete the technology development, including cost and schedule, have been prepared by Schott.

The following section contains the results of an analytical prediction of the performance of lightweight Zerodur mirror designs subjected to thermal loading. In this analysis, the actual measured properties of the Zerodur and the fritted and welded Zerodur joints were used. The results show that excellent performance can be obtained from a lightweight Zerodur mirror fabricated using the techniques demonstrated during this program.

SECTION V

PERFORMANCE ANALYSIS

The objective of the performance analysis task is to evaluate the overall performance of lightweight Zerodur mirror blanks when subjected to high front surface thermal loadings. Advantages and disadvantages of Zerodur as a large lightweight mirror building material and the adequacy of current manufacturing technology will be identified and, thereafter, the direction for future technology development can be set. The performance evaluation procedure is two-staged. One criterion is the relative performance measured against a lightweight ULE mirror under parallel standards. The second criterion is the absolute optimum performance a Zerodur mirror can achieve under certain weight limitations. The baseline mirror under consideration is 4 meters (or approximately 160 inches) in diameter.

The analysis is divided into the following four categories: 1) Analytical Method Development, 2) General Survey of Zerodur Lightweight Mirror, 3) Performance Comparison Between ULE and Zerodur Mirrors, 4) Optimization Procedures and Performance of Optimum Zerodur Mirror Design.

5.1 ANALYTICAL METHOD DEVELOPMENT

Two major analytical methods must be developed before the actual mirror analysis can begin. The first is to devise an accurate and economical finite element structural modeling technique; the second is to derive a thermal performance optimization scheme.

5.1.1 Structural Modeling Technique

Since sensitive subjects such as the impact of bondline frit stiffness, or spatial variations of CTE_{REF} on the mirror surface distortions will be investigated, the basic structural analytical model is necessary to

generate results with a high degree of accuracy. However, in order to put the available resource to best useage so that a broad range of issues can be addressed, the modeling technique has to be economical. To satisfy both constraints, the so-called "simplified 3-D" finite element model has been developed for the purpose of this study. This "3-D" technique conducts detailed modeling of the front and back faceplates and the character of the bondline between faceplates and core. The only part of the mirror structure that is simplified in modeling is the core structure. This is achieved with orthotropic continuum elastic media instead of a large number of plates. The attempt is, then, to validate the "simplified 3-D" model by comparing its results with that of the detailed core structure in the "detailed 3-D" model.

A 24.75 inch lightweight mirror with a 2.75 inch cell pocket (pitch) is modeled using both techniques. These test models are shown in Figure 24. When subjected to various thermal loadings, the surface distortions predicted by the two models are plotted as in Figure 25.

The two sets of results correlate extremely well for all three thermal loading cases. The results indicate that the core structure, though discrete in nature, behaves in fact like a layer of continuum media. For a mirror with a larger mirror diameter/cell size ratio, the results should be even closer. Therefore, the simplified 3-D model is a valid structural analytical tool for the lightweight mirror structure under consideration.

5.1.2 Thermal Performance Optimization Scheme

The deformation of a structure under certain boundary conditions is totally dependent upon the load applied and the stiffness of the structure itself. With lightweight mirror structures under front surface thermal loading, the predominant factor determining the mirror distortion is the parameter M_T/D, thermal moment/section rigidity. Based on this, the method developed to derive the optimum mirror configuration minimizes the parameter M_T/D instead of directly optimizing the surface distortion. The latter approach, understandably, is much more time consuming and expensive.

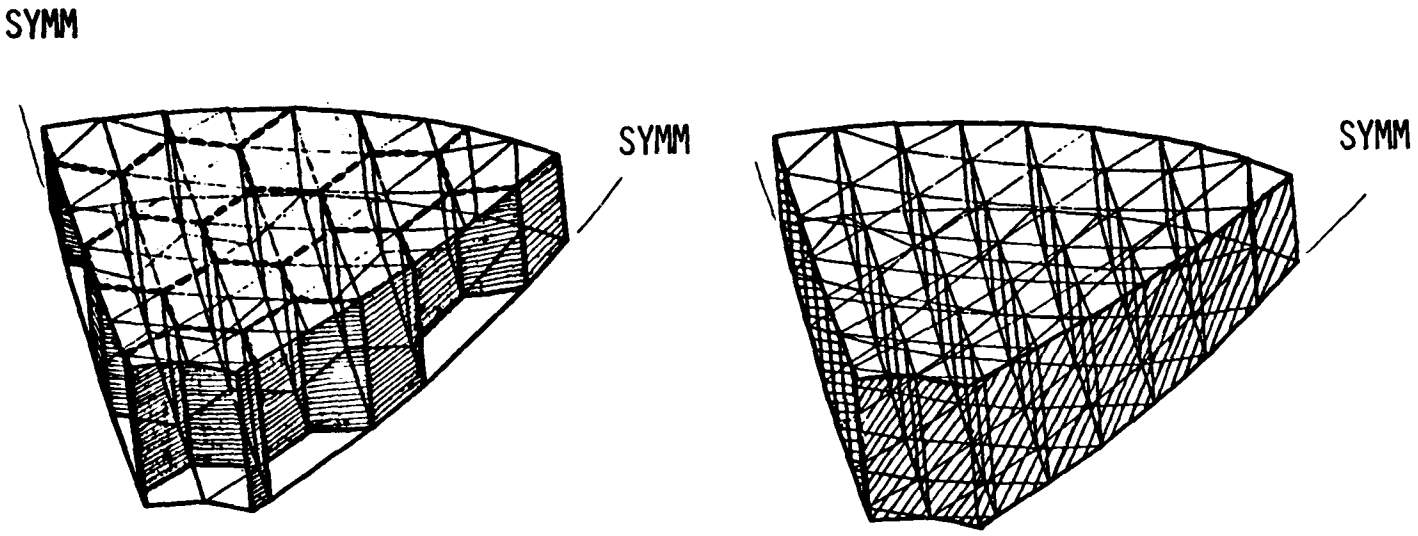


Figure 24. Test Models, 60 Degree Symmetry

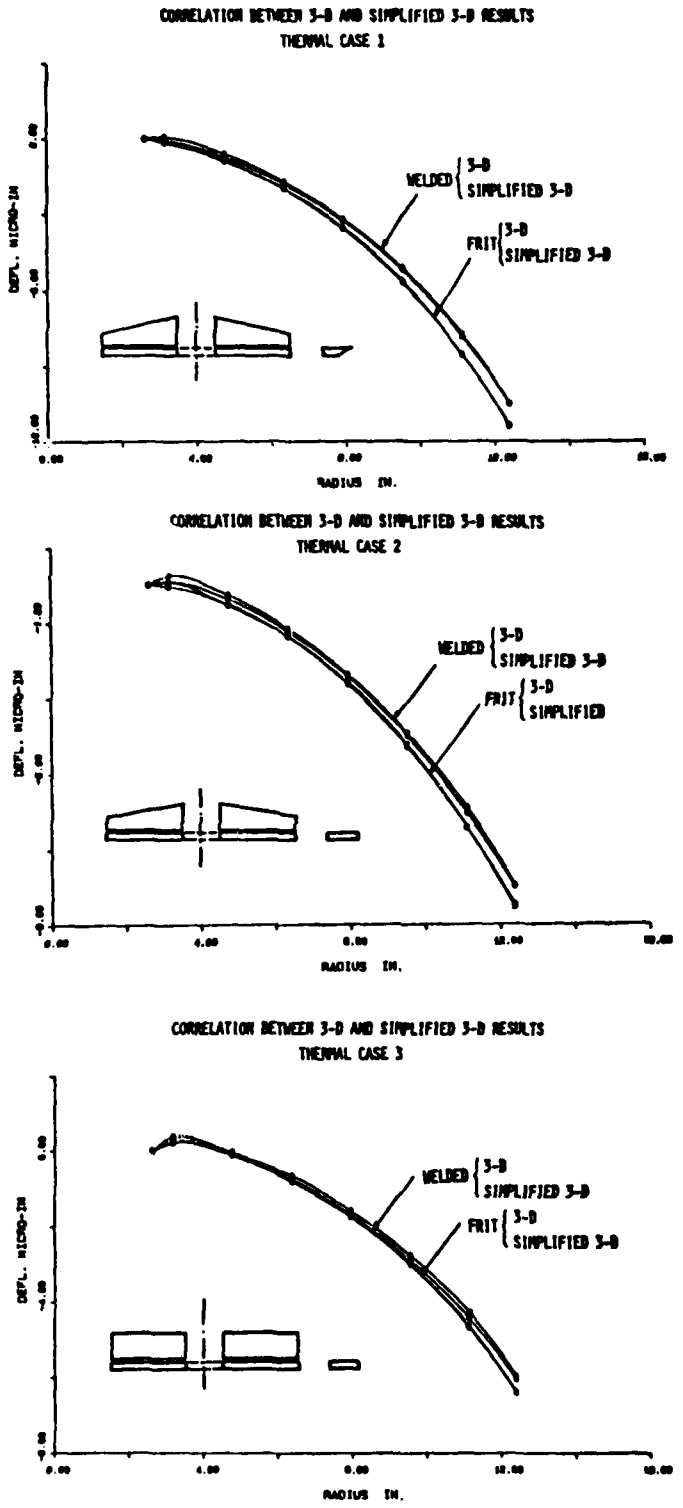


Figure 25. Various Surface Distortions

An algorithm for the optimization purpose has been developed. It can examine the M_T/D parameter for various faceplate thicknesses, core density, mirror weight, material CTE and heat input. With this analytical capability, a parametric analysis is performed and, based on the results, an optimum mirror design is derived. The parametric analysis and the selection of an optimum mirror configuration will be described in detail in Section 6.4.

5.2 GENERAL SURVEY OF ZERODUR LIGHTWEIGHT MIRROR

This section examines the various factors that affect the performance of a Zerodur mirror. These factors include the thermal and structural characteristics of Zerodur and manufacturing factors. The mirror design used as the basis for this purpose has the geometric configuration identical to that of a fritted ULE mirror design proposed by Kodak in RADC Technical Report No. RADC-TR-81-226. The finite element model and essential geometric parameters are as shown in Figure 26. The thermal loading under consideration has a 2:1 frustrum distribution and up to 100 seconds exposure time.

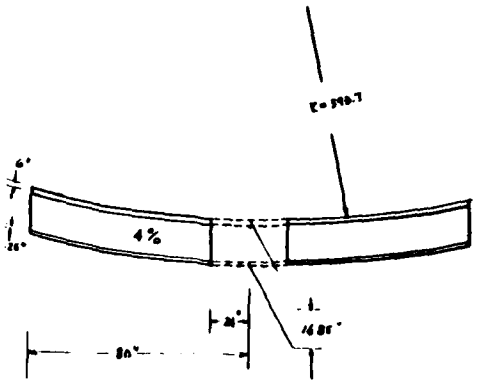
An improved algorithm for calculating temperature distributions in passive, eggcrate type mirrors exposed to high front surface thermal loading was developed. A detailed discussion of this algorithm is given in Appendix H.

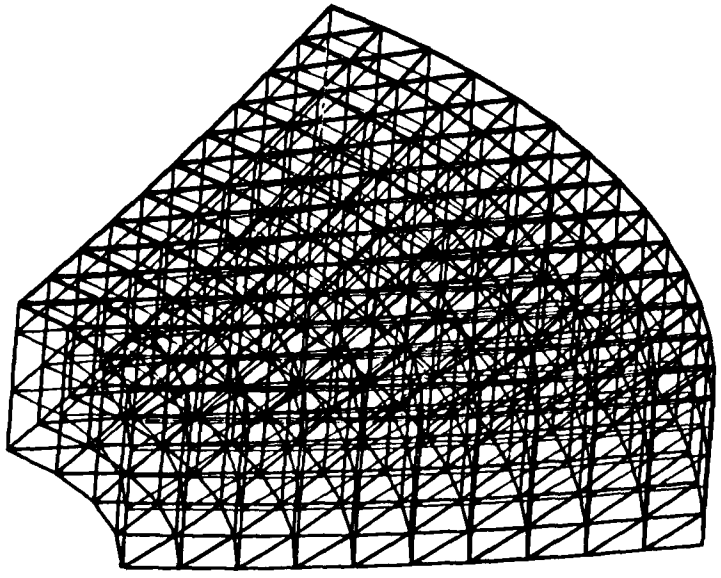
A physical properties of Zerodur and the frit-bonded joints and welded joints used in this analysis were those obtained from Schott's measurement program. The properties appear in Table 6.

660 GRID POINTS, 2640 DOF

360 PLATE ELEMENTS

540 SOLID ELEMENTS





ROC = 393.7 "

OD = 160.0 "

ID = 48.0 "

h = 16.85"

t_f = 0.6 "

t_b = 0.25"

n = 4%

Figure 26. Mirror Configuration and Finite Element Model (60 Degree Symmetry)

TABLE 6. PHYSICAL PROPERTIES

Zerodur	
Young's Modulus	13.6×10^6 psi
Density	0.091 lbs/in^3
Thermal Conductivity	0.96 BTU/hr ft ° F
Heat Capacity	0.194 BTU/lb ° F
Frit	
Young's Modulus	2.2×10^6 Psi
thermal strain mismatch with Zerodur	25 ppm maximum (0 - 50 ° C)

The Zerodur thermal expansion characteristics are identified from the material property study task. The family of parallel curves in Figure 27 demonstrates that variations in Zerodur's CTE is a function of temperature. For convenience, a specific curve will be identified by referring to its CTE_{REF}, i.e., CTE at reference temperature. By the use of two of the curves, CTE_{REF} -22.5 ppb/ ° C and 0.0 ppb/ ° C, the surface distortions of the mirror are examined to identify the impact of material CTE_{REF}. The analytical results are summarized in Figure 28. The maximum distortion for the mirror with CTE_{REF} -22.5 ppb/ ° C is almost five times larger than the one with CTE_{REF} 0.0 ppb/ ° C. Therefore, the CTE_{REF} of the material is an important parameter in determining the thermal performance.

The relatively low Young's Modulus of the frit material currently available for bonding the mirror blank (2.2×10^6 psi compared with 13.1×10^6 psi for the parent Zerodur material) causes additional shearing deformation of the mirror. Nevertheless, the figure shows this effect is insignificant, due to the fact that the bondline thickness is extremely small (0.004 inch).

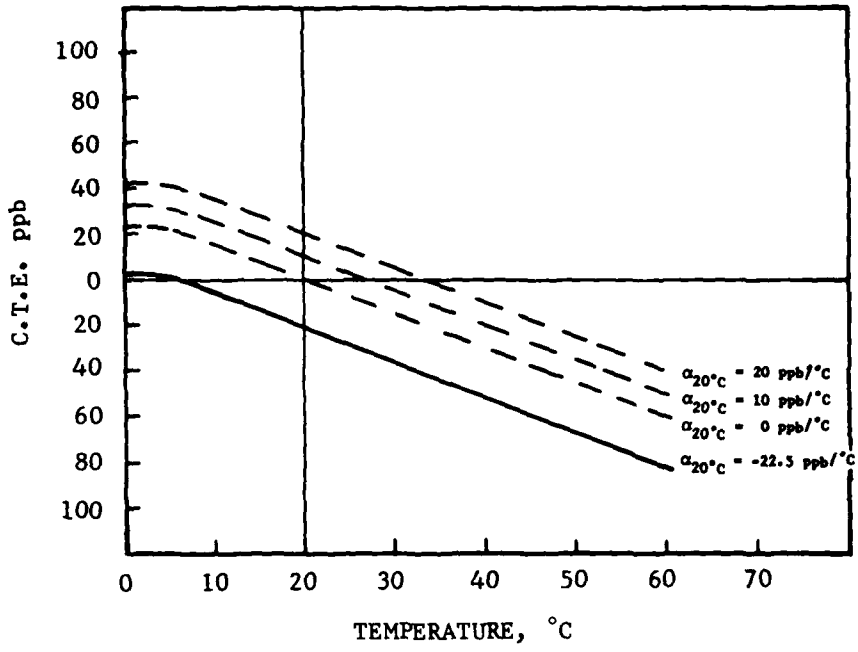


Figure 27. Zerodur CTE Variations as Function of Temperature

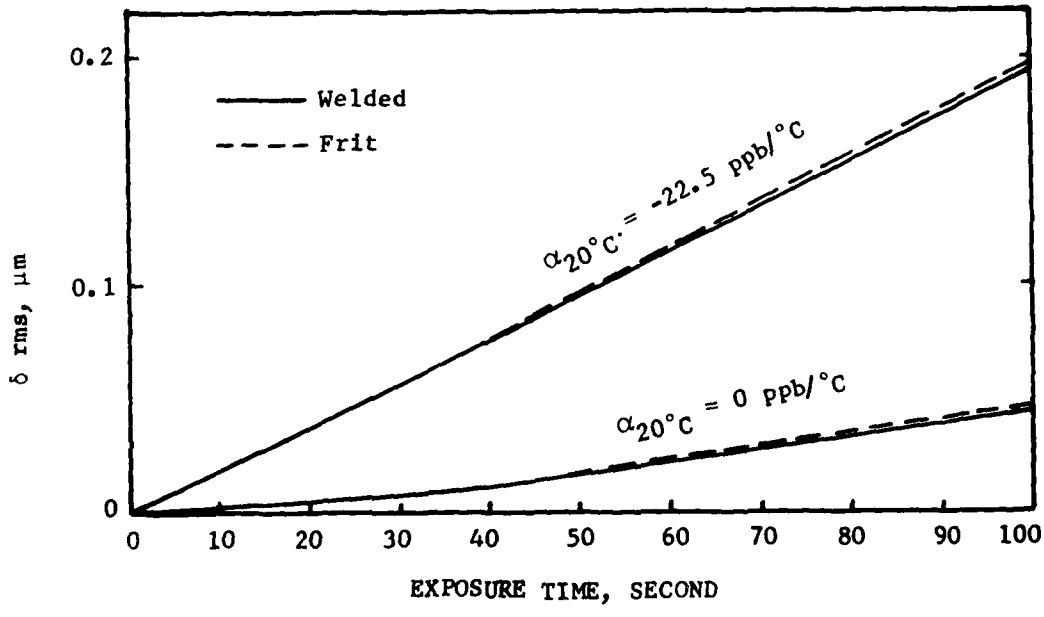


Figure 28. Effect of Frit Bondline on Surface Thermal Distortion

Another important factor that affects surface quality is the spatial variation of the CTE. Figure 29 plots a typical CTE spatial change pattern of a Zerodur blank. The maximum deviation is about 8 ppb from center to outer edge. This variation in CTE produces substantially larger distortions at the mirror surface as shown in Figure 30.

The mirror surface distortions due to the properties of the fritted and welded joints were calculated separately. The contribution of each of these factors are as follows:

Frit bondline thermal strain differential	δ_{pp} = 0.0038 um
Welded bondline thermal strain differential	δ_{pp} = 0.0013 um
Thermal Quilting	δ_{pp} = 0.0194 um
Thermal Growth	δ_{pp} = 0.0025 um

These values indicate that the differences between the properties of the fritted and welded areas and the Zerodur glass-ceramic have a negligible impact on the thermal performance of the mirror.

The total weight of the mirror for this configuration is 3180 pounds.

5.3 PERFORMANCE COMPARISON BETWEEN ULE AND ZERODUR MIRRORS

This comparison between ULE and Zerodur mirrors is based on the performance of two mirrors that are identical in geometric configuration and subjected to the same thermal loading conditions as described in Section 5.2. Approached in this way, the differences reflect only the influences caused by the material properties while neutralizing those by the cross-sectional properties. First a final performance comparison will be made, then, the individual contributing items will be examined.

Figure 31 plots the surface rms distortions as a function of exposure time for ULE and Zerodur mirrors. When comparing the curves, it is clear that the Zerodur mirror consistently performs better than the ULE mirror when the two mirrors have comparable CTE_{REF}. The detailed numerical data of the surface distortions are given in Table 7.

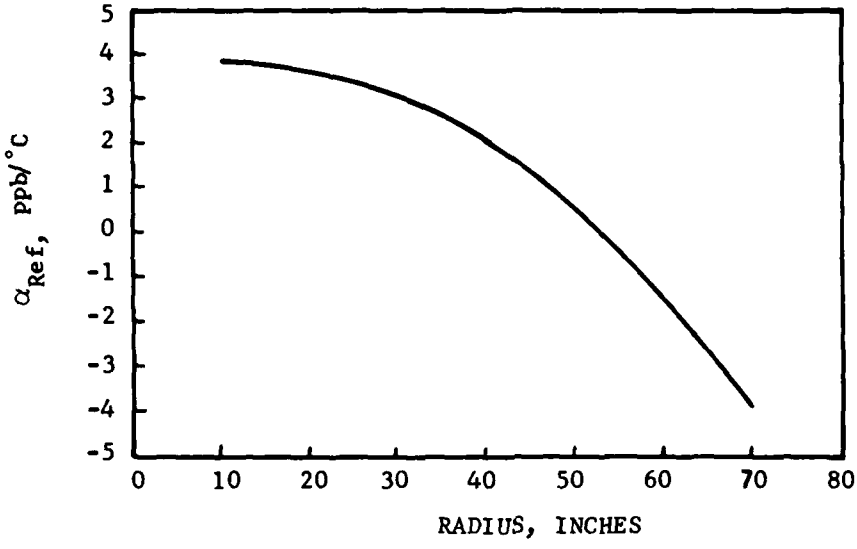


Figure 29. Spatial Variation of α_{REF} for Zerodur (Typical)

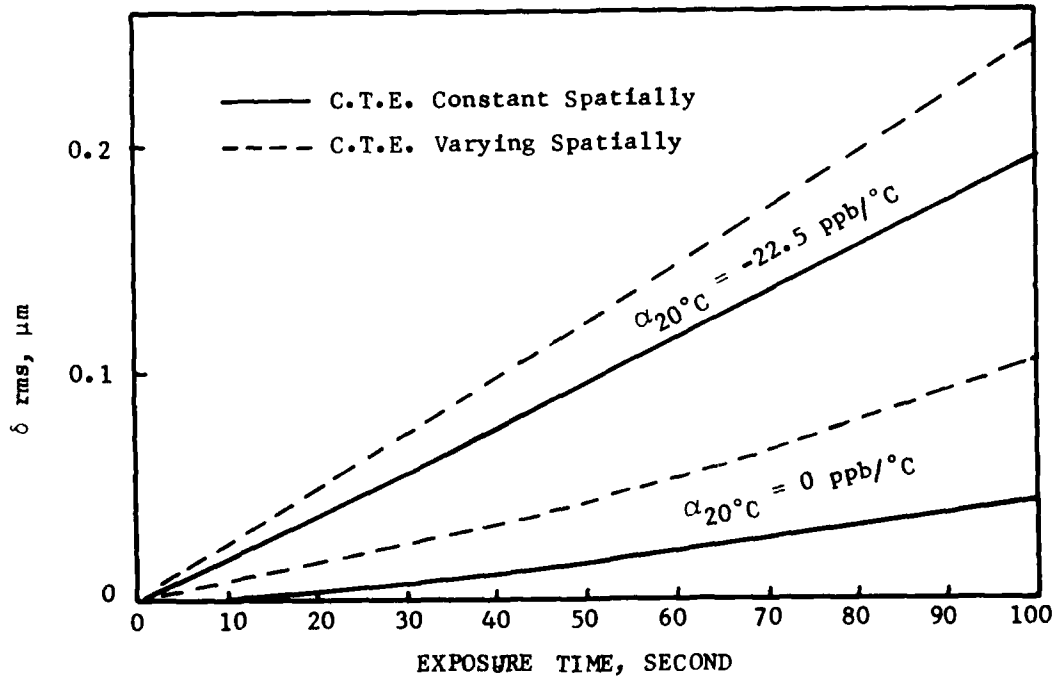


Figure 30. Effect of CTE Spatial Variation of Surface Thermal Distortion

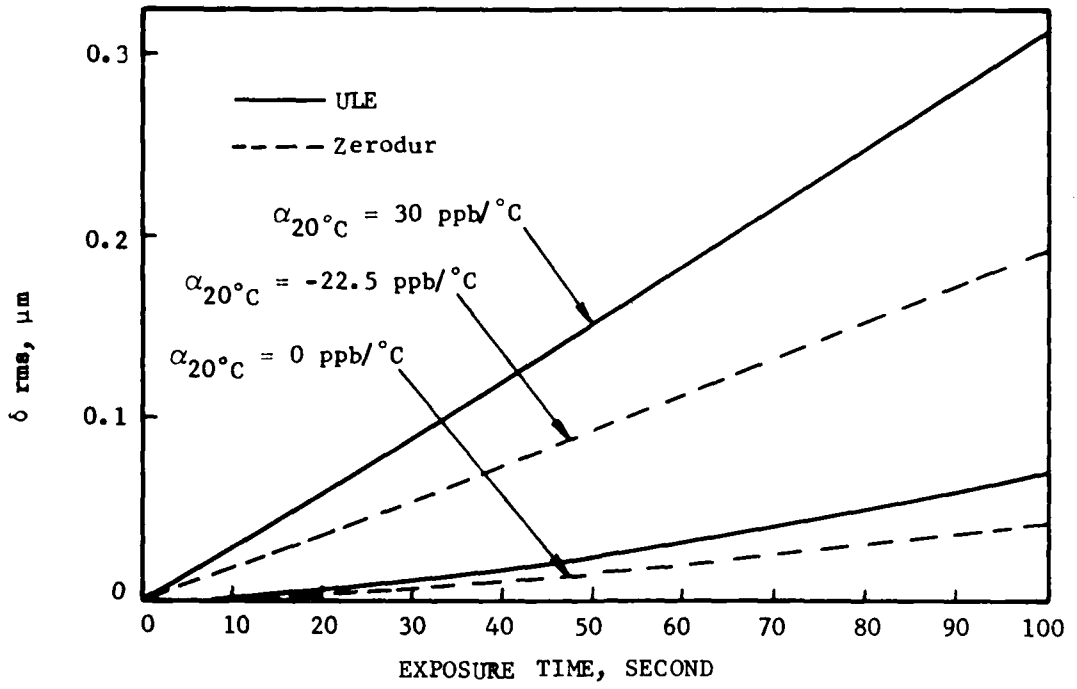


Figure 31. Surface Distortion for ULE and Zerodur Mirrors

TABLE 7. THERMAL PERFORMANCE OF ULE AND ZERODUR MIRROR

MATERIAL	CTE	EXPOSURE TIME SEC	WITHOUT FOCUS CORP. δ_{pp}	WITHOUT FOCUS CORP. δ_{rms}	WITH FOCUS CORP. δ_{pp}	WITH FOCUS CORP. δ_{rms}	CHANGE IN RADIUS OF CURVATURE μIN
ULE (2780 lbs)	Const. in R $\alpha_{20°C}$=30 ppb/°C	20	λ/3.11	λ/10.6	λ/48.3	λ/268	492
		40	λ/1.55	λ/5.25	λ/27.4	λ/155	998
		100	λ/0.60	λ/2.02	λ/13.1	λ/75.7	2582
	Const. in R $\alpha_{20°C}$=0 ppb/°C	20	λ/28.1	λ/95.9	λ/309	λ/2170	55
		40	λ/10.6	λ/35.9	λ/127	λ/889	146
		100	λ/2.67	λ/8.93	λ/40.8	λ/277	587
Zerodur (3180 lbs)	Const. in R $\alpha_{20°C}$= -22.5 ppb/°C	20	λ/5.04	λ/17.1	λ/75.9	λ/422	-305
		40	λ/2.48	λ/8.46	λ/42.4	λ/240	-619
		100	λ/0.96	λ/3.25	λ/20.6	λ/120	-1607
	Const. in R $\alpha_{20°C}$=0ppb/°C	20	λ/47.6	λ/162	λ/498	λ/3518	-127
		40	λ/17.2	λ/58.1	λ/196	λ/1378	-90
		100	λ/4.31	λ/14.4	λ/62.3	λ/427	-364

Note: λ = 0.6328 μm

It should be noted that in both mirrors, the spatial variations of CTE are not accounted for. This is due to the lack of ULE CTE data for the boule size under consideration. Nevertheless, from past experience, the ULE CTE spatial variations for smaller size boules generally exceed 8 ppb measured in Zerodur boules. On the other hand, with identical geometric configurations, the weight of the Zerodur mirror is substantially higher (3180 pounds compared to 2780 pounds for the ULE mirror). This increase in weight is certainly a disadvantage for Zerodur when total weight is critical to a mirror's design.

To understand these results further, we trace back to various properties that contribute to the final performance.

In Figure 32, the CTEs for Zerodur and ULE are plotted as a function of temperature. Though the slopes of the two families of curves are opposite in sign, the absolute magnitudes are close. This indicates that CTE contributions to the distortions of the mirror surface are not significantly different for the two materials as long as their CTE_{REF}s are comparable.

Figure 33 describes the temperature gradient along the thickness of the mirror for the two materials. Interestingly, the temperature rise for ULE is about 20% higher than that for Zerodur. This is attributable to the superior material thermal characteristics of Zerodur, namely, high conductivity, specific heat, and mass denisty.

The smaller temperature change of Zerodur produces less thermal moment, and therefore results in smaller thermal distortions.

The Young's Modulus of Zerodur is higher than that of ULE (13.1×10^6 psi to 9.8×10^6 psi). The high Young's Modulus generally creates higher structural stiffness, hence, the smaller distortions. In this case, however, the thermal moment produced by temperature change is also dependent on Young's Modulus. Therefore, considering only the thermal loading cases, the advantage of having a higher Young's Modulus cannot be realized.

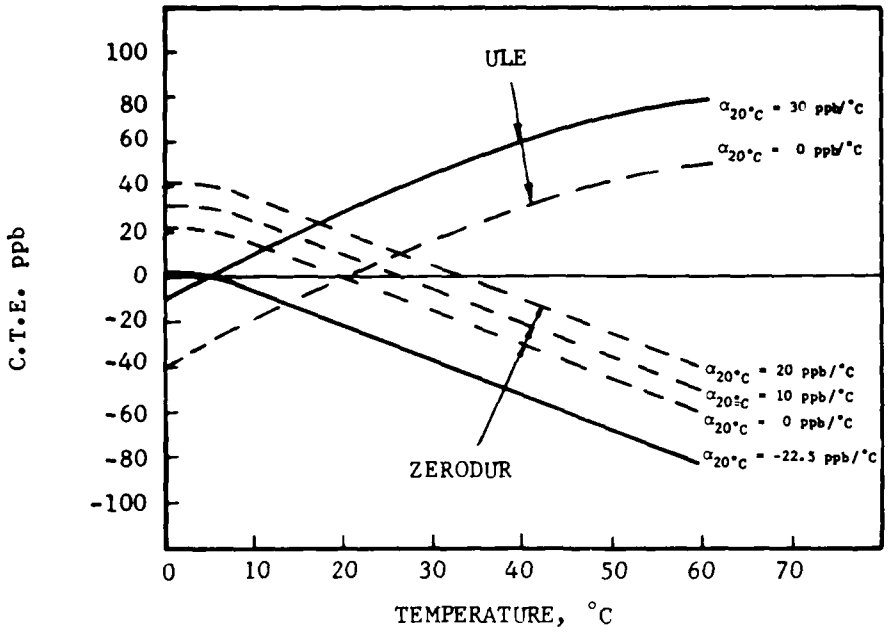


Figure 32. CTE as a Function of Temperature

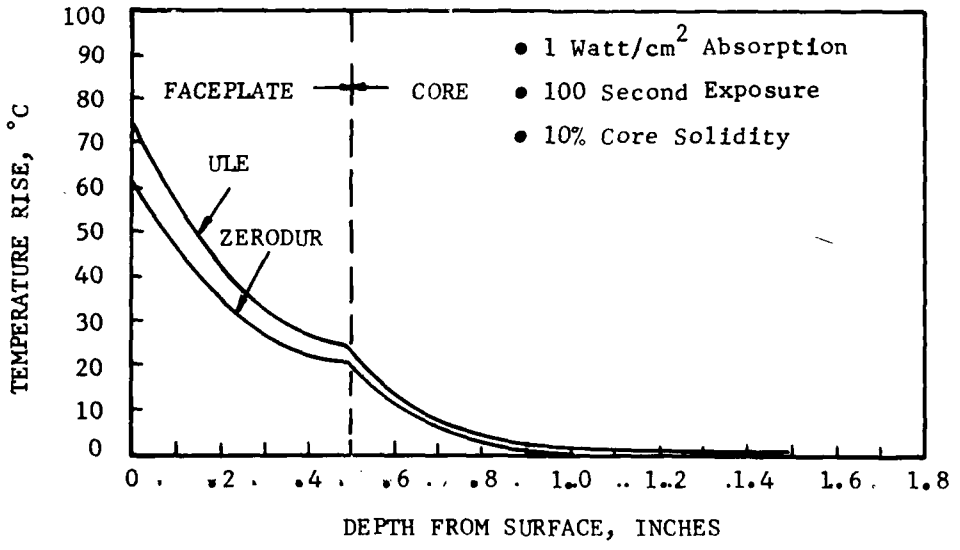


Figure 33. Temperature Gradient under Thermal Loading

In summary, the superior thermal properties of Zerodur leads to better thermal performance. The higher material density, however, puts Zerodur in a disadvantageous position in manufacturing a lightweight mirror, compared to ULE. Nevertheless, it will be shown later in the report that by optimizing the section geometry, the weight can be greatly reduced.

5.4 OPTIMIZATION PROCEDURES AND PERFORMANCE OF OPTIMUM ZERODUR MIRROR DESIGN

Mirror design optimization can be approached in two ways: 1) by achieving maximum peformance for a given weight limit, and 2) by meeting certain performance requirements with minimum weight. However, for the current study program, no definite criterion is imposed. Consequently, our optimization approach is to use the results presented in Section 6.2 as a basis and reduce further the total mirror weight and concurrently upgrading performance.

The procedure consists of two steps: optimization of the cross-section geometry, and optimization of the thermal property CTE. In order to do so, an extensive parametric analysis is performed to investigate the trade-offs of each of the independent parameters. These parameters include front and back plate thicknesses, core density, total mirror weight and material CTE. The inter-relations between the dependent parameters (section stiffness, temperature gradient, thermal strain and thermal moment) and independent parameters are schematically illustrated in Figure 34. For a selected section geometry, the section rigidity, D, is determined. The temperature gradient, T(z), along the mirror thickness is obtained based on the thermal dynamics formulation described and detailed in Appendix H. The thermal strain E_T derived for the temperature change is based on the material CTE curve, as explained in Figure 35. Finally, the thermal moment M_T is calculated by integrating E_T along the entire cross-section with respect to the section neutral axis.

With these understandings in mind, the parametric analysis starts out by varying the front and back plate thicknesses, denoted by t_f and t_b, re-

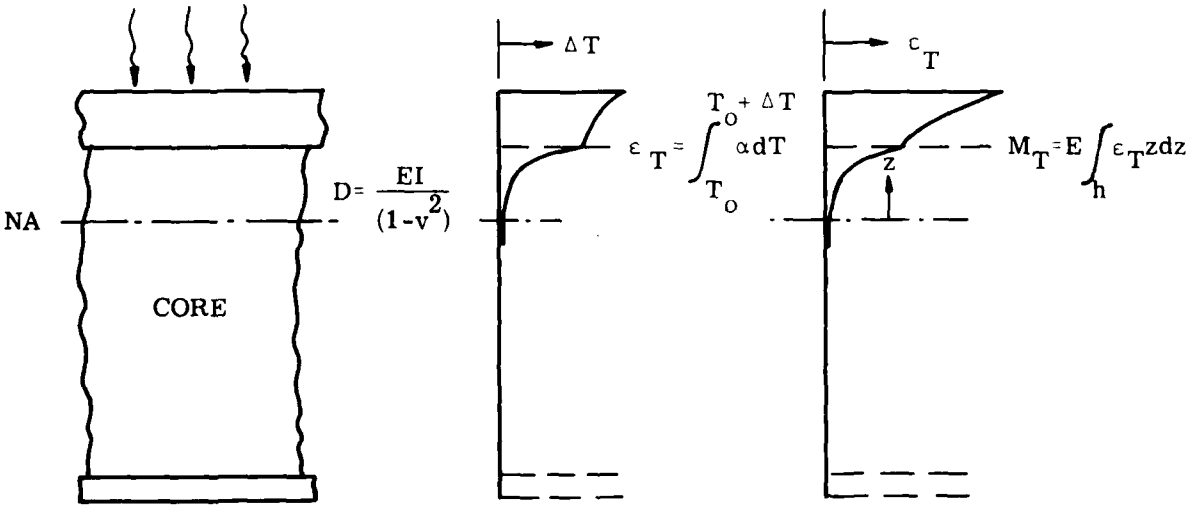


Figure 34. Thermal Moment and Section Rigidity

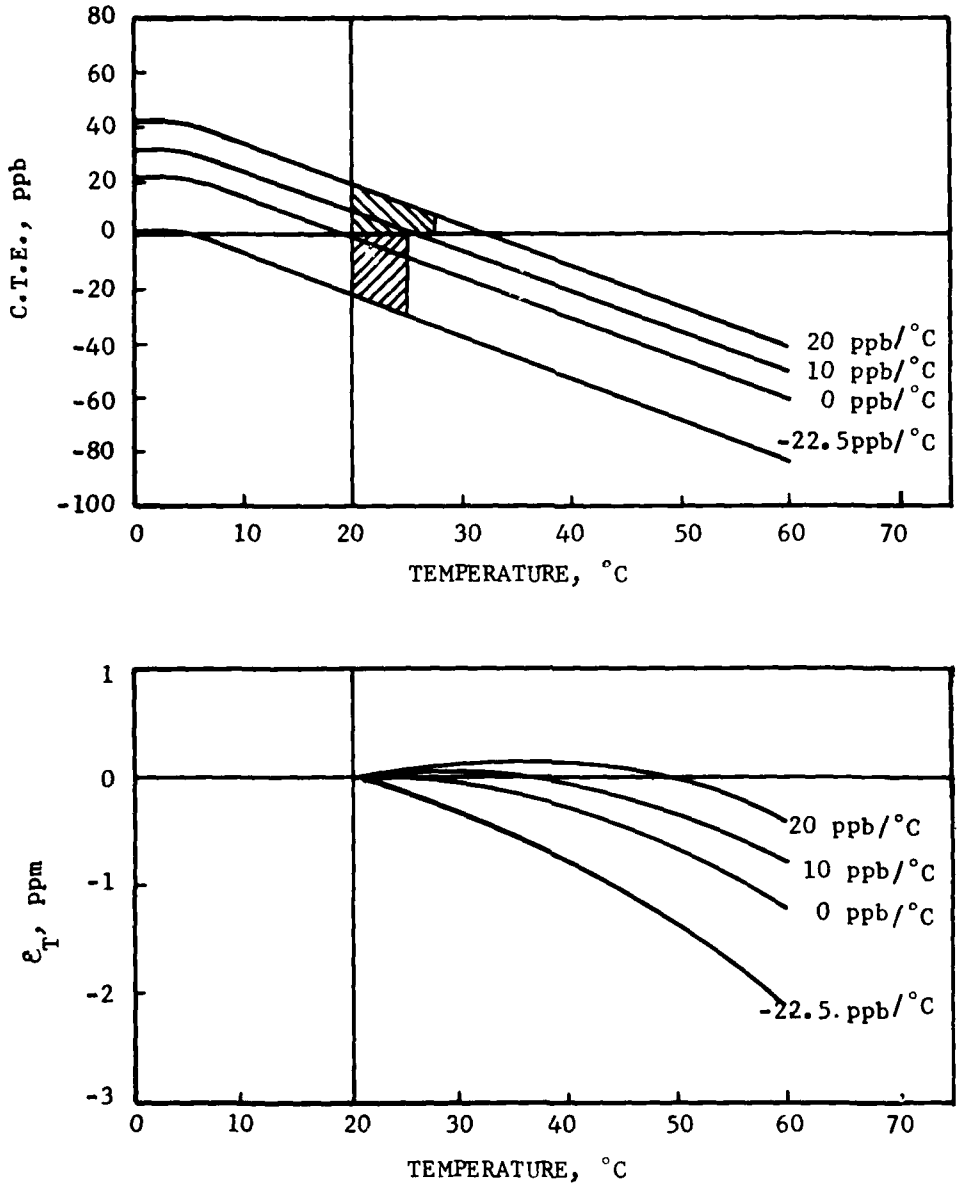


Figure 35. Zerodur CTE and Thermal Strain

spectively. As shown in Figure 36, the parameter $M_T D/$ is plotted by varying t_f from 0.2" to 1.0" and t_b from 0.2" to 0.5" for given weight, W, and core density η. These curves demonstrate that M_T/D becomes smaller as back plate thickness decreases. This phenomenon is understandable because the decrease of back plate thickness moves the relative neutral axis location closer to the front surface, thus reducing the thermal moment arm. However, the rate of decrease in M_T/D slows down noticably as the section approaches open back rib structure. By taking into consideration the possible mounting mechanism and mechanical stresses, a back plate thickness of 0.25" is selected for the design. For this back plate thickness, the front plate thickness corresponding to the minimum M_T/D is 0.6".

The weight impact on surface performance ranges from 2250 pounds to 3000 pounds, as shown in Figure 37. It is self-evident that a higher weight achieves better performance. Nevertheless, this graph helps us determine the weight target for the design. After examining the performance level (M_T/D level) and the weight of the mirrors discussed in Section 63, the baseline weight for this Zerodur mirror design is chosen at 2500 pounds.

The core density is an important parameter for the optimum design. The 4% core structure currently proposed reduces the thermal distortion two to three times compared to the conventional core design of 8 to 12%. These data are shown in Figure 38.

Based on these results, the optimum parameters of the configuration are summarized as follows:

Shape:	Meniscus
Radius of Curvature	393.7"
Outer Radius	160.0"

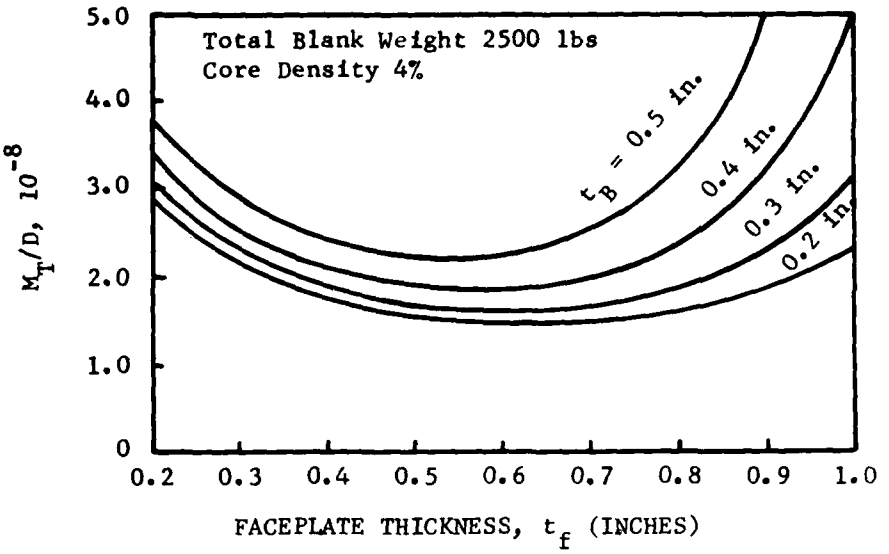


Figure 36. Four Meter Zerodur Mirror Thermal Performance Parametric Study (M_T/D vs. Faceplate and Backplate Thickness)

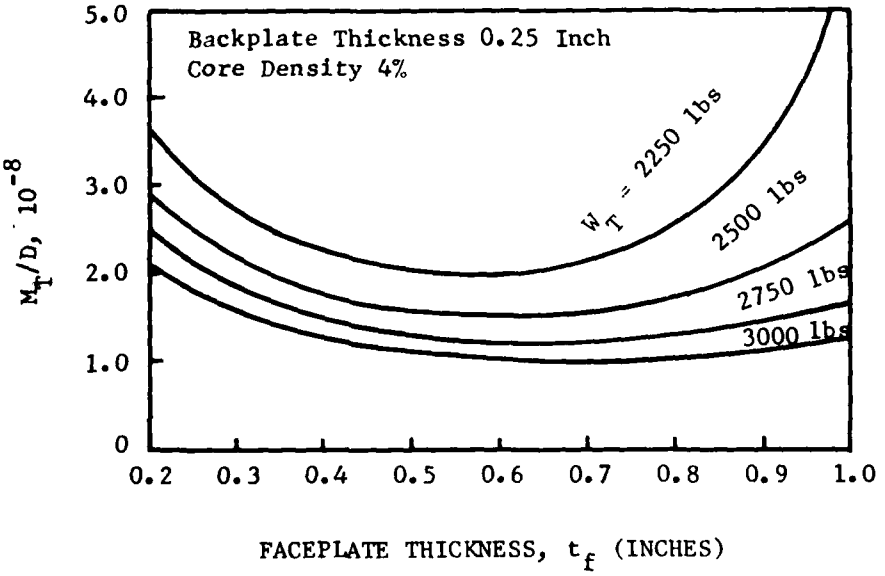


Figure 37. Four Meter Zerodur Mirror Thermal Performance Parametric Study ($M_T D$ vs. Facesheet Thickness and Total Weight)

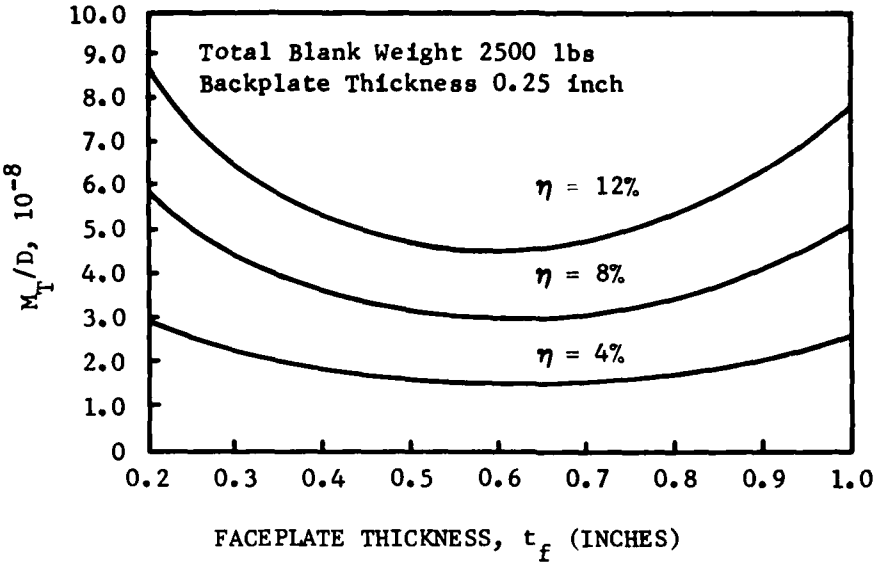


Figure 38. Four Meter Zerodur Mirror Thermal Performance Parametric Study (M_T/D vs. Faceplate Thickness and Core Density)

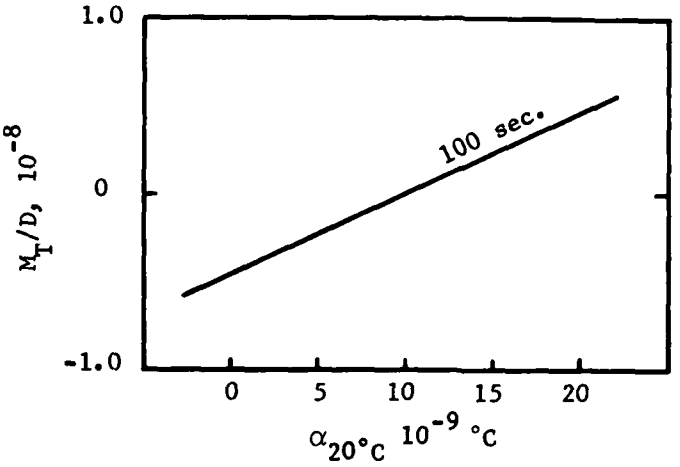


Figure 39. Four Meter Zerodur Mirror Thermal Performance Parametric Study (M_T/D vs. CTE_{REF})

Inner Radius	48.0"
Section Height	16.85"
Front Plate Thickness	0.6"
Back Plate Thickness	0.25"
Core Density	4%
Total Weight	2500 pounds

To optimize the material CTE, the M_T/D versus CTE_{REF} curve is plotted for an exposure time of 100 seconds, as shown in Figure 39. The minimum absolute value of M_T/D, zero, occurs at CTE_{REF} 10 ppb/°C. Taking into consideration the spatial variation of CTE, the optimum CTE_{REF} is estimated between 10 and 20 ppb/°C.

Up to this point, we have optimized the mirror design. To verify the design and conduct detailed evaluation of the surface performance, a simplified 3-D finite element is constructed as shown in Figure 40. The thermal loading case used is the same as prescribed in Section 6.2.

The surface distortions, along with some results obtained from previously analyzed mirror designs, are plotted in Figure 41. These curves highlight the improvement of the thermal performance achieved by the Zerodur mirror optimum design. Curves 1 and 2 are the distortion levels of the ULE and Zerodur mirror designs discussed in Section 6.3. By cross-section optimization, the mirror weight reduces to 2500 pounds while maintaining the distortion level as indicated in Curve 3. Curves 5 and 6 display the distortion results when the material CTE is further optimized. The numerical data of these surface distortions are summarized in Table 8. The best surface qualities achieved are, at 100 seconds exposure time, $\lambda/29$ and $\lambda/314$ before and after the focus correction, respectively (λ = 0.6328 μm).

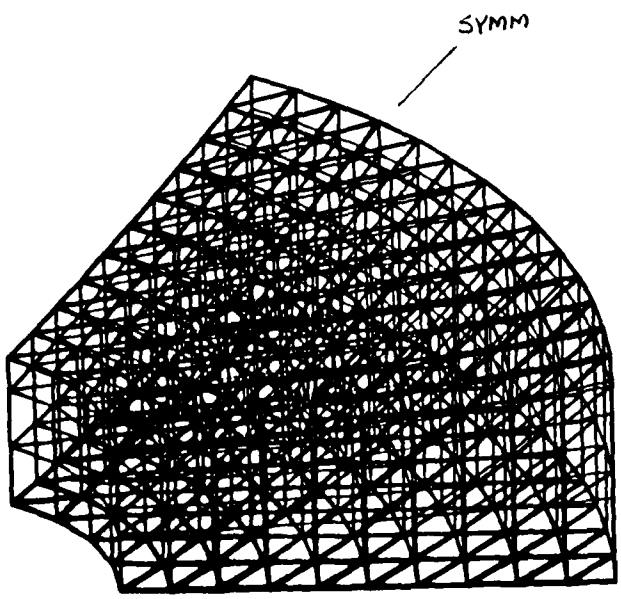
5.5 CONCLUSIONS

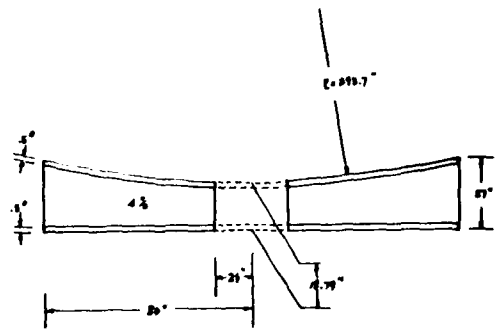
Four important conclusions from the results of the performance analysis follow:

660 GRID POINTS, 2640 DOF

360 PLATE ELEMENTS

540 SOLID ELEMENTS





ROC	=	393.7"
OD	=	160.0"
ID	=	48.0"
h_{od}	=	27.0"
h_{id}	=	18.8"
t_f	=	0.5"
t_B	=	0.5"
η	=	4%

Figure 40. Mirror Configuration and Finite Element Model (60 Degree Symmetry)

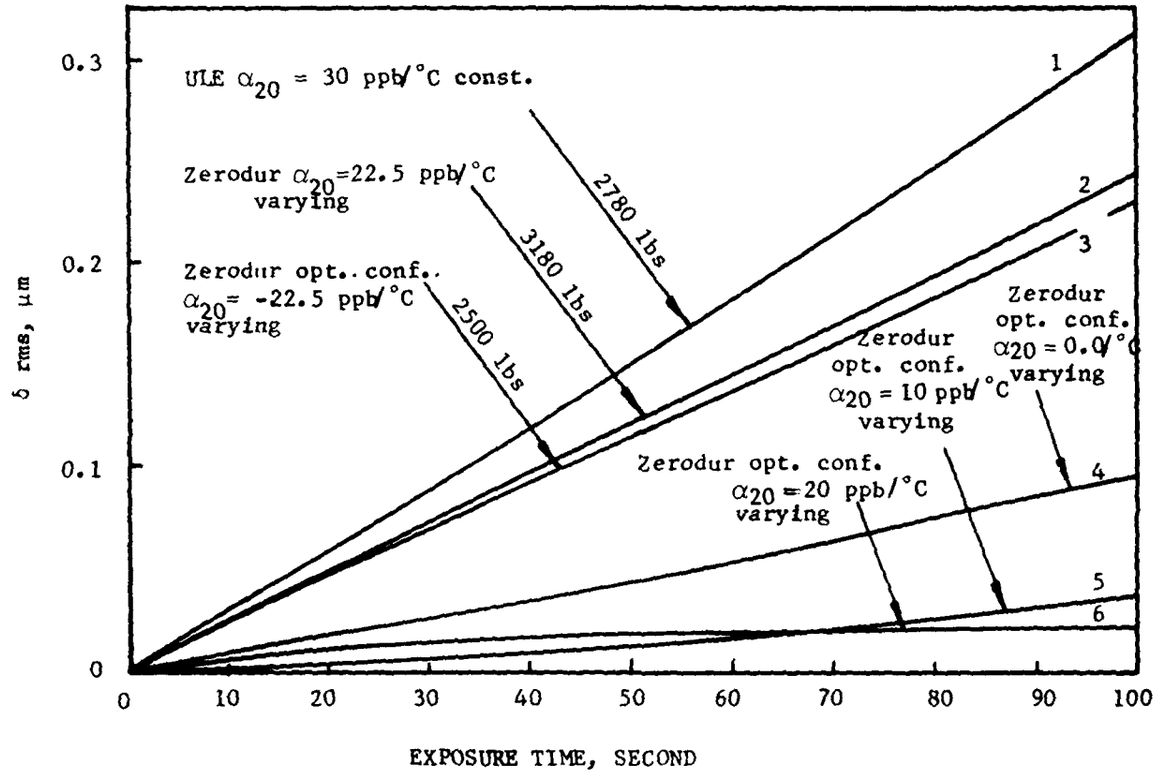


Figure 41. Mirror Surface Thermal Distortions

TABLE 8. FOUR METER ZERODUR MIRROR THERMAL PEROFRMANCE SUMMARY
OPTIMUM MIRROR CONFIGURATION W_{TOTAL} = 2500 lbs

MATERIAL	CTE	EXPOSURE TIME SEC	WITHOUT FOCUS CORP. δ_{pp}	WITHOUT FOCUS CORP. δ_{rms}	WITH FOCUS CORP. δ_{pp}	WITH FOCUS CORP. δ_{rms}	CHANGE IN RADIUS OF CURVATURE μIN.
	$\alpha_{20°C}$= -2.25x10^{-8}/°C at Center	20	λ/3.68	λ/12.7	λ/62.8	λ/294	-410
		40	λ/1.99	λ/6.87	λ/37.0	λ/170	-762
		100	λ/0.80	λ/2.74	λ/17.9	λ/81.6	-1901
Zerodur α varying spatially	$\alpha_{0°C}$=0.0/°C at Center	20	λ/10.1	λ/36.3	λ/116.7	λ/579	-144
		40	λ/5.16	λ/18.3	λ/67.5	λ/332	-286
		100	λ/1.87	λ/6.54	λ/32.1	λ/154	-799
	$\alpha_{20°C}$=1.0x10^{-8}/°C at Center	20	λ/45	λ/203	λ/171.6	λ/847	-25
		40	λ/17.4	λ/69.8	λ/106.2	λ/495	-74
		100	λ/4.60	λ/16.9	λ/48.3	λ/232	-310
	$\alpha_{20°C}$=20x10^{-8}/°C at Center	20	λ/17.2	λ/55.8	λ/135.5	λ/916	93.
		40	λ/11.9	λ/38.2	λ/85.3	λ/577	137
		100	λ/9.37	λ/29.0	λ/49.7	λ/314	180

Note: λ = 0.6328 μm

1) For the same geometric configuration, the Zerodur mirror has a better thermal performance than the ULE mirror due to its superior material thermal conductivity and specific heat. Nevertheless, the Zerodur mirror is heavier due to higher mass density.

2) By selecting the proper lightweight section design, the mirror weight can be sufficiently reduced while maintaining the thermal performance level.

3) Material CTE is essential in determining the thermal performance. Selecting the desired CTE property can further improve the performance.

4) The currently available frit is adequate for its stiffness, strength, and thermal properties.

SECTION VI

MANUFACTURING TECHNOLOGY/SCALE-UP STUDY

The mirror blank fabrication processes have been evaluated with respect to the manufacture of large diameter lightweight mirrors. An important aspect of this evaluation is the assessment of the scaleability of the fabrication techniques. Schott has performed the engineering study of the scaleability of these processes. Appendix F is Schott's report of this effort. This report contains a detailed process description of the proposed manufacturing process and includes the preliminary design drawings of the necessary equipment. The report also discusses a breakdown of the costs and an estimate of the schedule for the establishment of a facility for the production of 4 meter lightweight mirrors.

The basis for the plan includes several preconditions and assumptions. The first and most important precondition is that the frit development be completed prior to the manufacture of lightweight mirror blanks. As discussed in Section IV, additional development work to optimize the frit and to establish the process for frit bonding cores and facesheets is required. Slumping technology must also be developed before large facesheets can be made efficiently.

The stages in the scale-up to 4 meters have been established. The first mirror blanks to be built would be a 0.46 meter diameter flat and a 0.46 meter sphere. Successful fabrication of the 0.46 meter blanks would be followed by the production of 1.5 meter demonstration blanks. The process would then be scaled up to the production of 4 meter blanks.

Section 7 of Appendix F deals with alternatives to the selected processes in the event technical obstacles are encountered. The cost and schedule impact of these alternatives is discussed.

The following sections summarize the important aspects of this study.

6.1 TECHNOLOGY DEVELOPMENT

A precondition to the manufacture of lightweight mirrors from Zerodur is the completion of the technology development programs in the areas of frit bonding and facesheet production. The frit development work at Schott has been discussed in Section IV. Further details and a firm price for this effort appears in Appendix E. Successful completion of this program would provide a frit having the required properties and the technology for applying the frit and forming a good bond between facesheets and lightweight cores.

The second area requiring further development work is facesheet fabrication technology. For smaller mirror blanks, facesheets may be machined from larger blocks. This may even be the recommended approach for the 1.5 meter demonstration mirror. Fabrication of 4 meter facesheets is, however, inefficient by machining. The slumping process is the most promising of the alternatives. Development of the slumping process should be completed prior to the manufacture of 4 meter mirrors.

Schott has proposed a program that includes laboratory study of the slumping process and the production of slumped samples up to 1.3 meters in diameter. This proposal is discussed in more detail in Section VIII.

Schott's firm prices for this development work are as follows:

Frit Development	$475 K
Facesheet Slumping	$220 K
Total	$705 K

6.1.1 0.46 Meter Mirror Blank

The first demonstration blanks to be built by Schott would be one 0.46 meter diameter flat followed by a 0.46 meter diameter sphere. These mirror blanks could be produced in existing facilities at Schott. The core plates would be made by cutting and grinding glass block. The core plates would be bent and welded on the automatic welding machine used to produce

the core samples shown in Figures 11 and 12. Cover sheets would be machined from Zerodur blocks. Manufacture of these mirror blanks requires the successful completion of the frit development discussed in Section 5.1. Schott has quoted a firm price of $220,000 for the fabrication of these two mirrors. More details and Schott's estimate of the schedule are given in Appendix C.

6.1.2 1.5 Meter Blank Fabrication Plan

The next step in the scale-up to 4 meters is the fabrication of 1.5 meter diameter mirror blanks. Schott has no equipment or facilities that could be used for this effort. Their plan includes the construction of a facility and the fabrication of the necessary furnaces and processing equipment. A detailed description of the manufacturing process is given in Appendix F, Sections 2 and 3. An outline of the recommended process is given in Table 9. Because the frit bonding technology is not fully developed, a complete description of the fritting process could not be given. Section 4 of Appendix F discusses some of the considerations involved in a frit bonding process and gives a description of Schott's best prediction of the required steps to frit-bond facesheets to a lightweight core.

The cost estimates made by Schott include the construction of a mirror blank fabrication facility. Schott has sized the facility and the equipment for the eventual production of 4 meter mirrors. All furnaces, handling equipment, and processing machines will be capable of accommodating 4 meter mirror blanks. The only exception to this is the welding machine. The welding machine is initially sized for 1.5 meter diameter mirrors but is designed to be expanded at a later date. Schott has indicated that this approach to facility design reduces the cost and time required to scale-up to 4 meters. Designing and building a facility sized for a maximum mirror blank diameter of 1.5 meters would not be appreciably cheaper and would greatly increase the ultimate cost of scaling to 4 meters.

TABLE 9. MIRROR BLANK MANUFACTURING PROCESS

Proposed Mirror Blank Fabrication Process

Core Rib Forming

- Continuous Rolling or Cut from Block
- Grind to Required Thickness

Rib Bending

- Automated System for Preheating, Handling, Bending, and Annealing
- Automated Grinding on Edges

Core Welding

- Manually Load Ceramic Fixtures with Half-Hexes
- Automated Preheating and Welding of Half-Hexes to Form Core
- Annealing and Ceramizing of Welded Core

Generation of Core

- Rough Working at Schott
- Fine Grinding at Zeiss

Facesheet Production

- Glassy Zerodur Plates Slumped into Mold
- Slumped Plates Ceramized
- Rough Generation Performed by Schott, Fine Grinding at Zeiss

Frit Bonding Core and Facesheets

- Frit with Vehicle Applied to Core
- Both Facesheets Contacted to Core and Clamped in Fixture
- Weights or Vacuum Applied
- Bonding Performed in Ceramizing Furnace

Rough Working of Bonded Blank

- Facesheets Generated to Nominal Thickness after Bonding by Schott

The following summarizes the total costs for this program up to the fabrication of 1.5 meter demonstration blanks. The cost of optical finishing and testing of these blanks is not included.

1.5 METER BLANK FABRICATION COSTS

Technology	
Frit Development	$ 195 K
Frit Application + Soldering Technology	280
0.46 M Demonstration	220
Slumping	230
	$ 925 K
4 M Facility Inc. 1.5 M Samples	
Building	$ 2,556 K
Core Bulding Equipment	2,692
Facesheet Slumping	162
Soldering Equipment	325
Glass Costs	1,848
Rough Grind Costs (Zeiss) (1 plane, 1 sphere)	188
Fuel + Maintenance (8 years)	979
Personnel	1,957
	$ 11,632 K
Fine Grind cost for Core, Facesheets	2,025
	$ 13,657 K

6.1.3 Alternative Approaches

Section 7 of Appendix F discusses several alternative approaches and provides some back-up processes in the event technical obstacles are encountered. Also covered in this section are the cost impacts of certain scheduling uncertainties such as the unavailability of a Zerodur tank for

rolling experiments. The cost and schedule for spin-casting development and testing as a back-up to the slumping process is discussed in Section 7.4 of Appendix F. Section 8 of Appendix F contains the cost of fine grinding the mating surfaces of the cores and cover sheets.

6.1.4 Schedule

Schott's estimate of the schedule for the establishment of a 4 meter mirror facility and the fabrication of 1.5 meter demonstration blanks is shown in Figure 42. The schedule includes 2 years for the design and construction of the facility and equipment. The first 1.5 meter mirror would be produced approximately 4½ years from the start of the program.

Schott considers this plan to be the minimum cost and minimum technical risk. Schott personnel have indicated that alternative approaches may abbreviate the schedule at higher cost and technical risk.

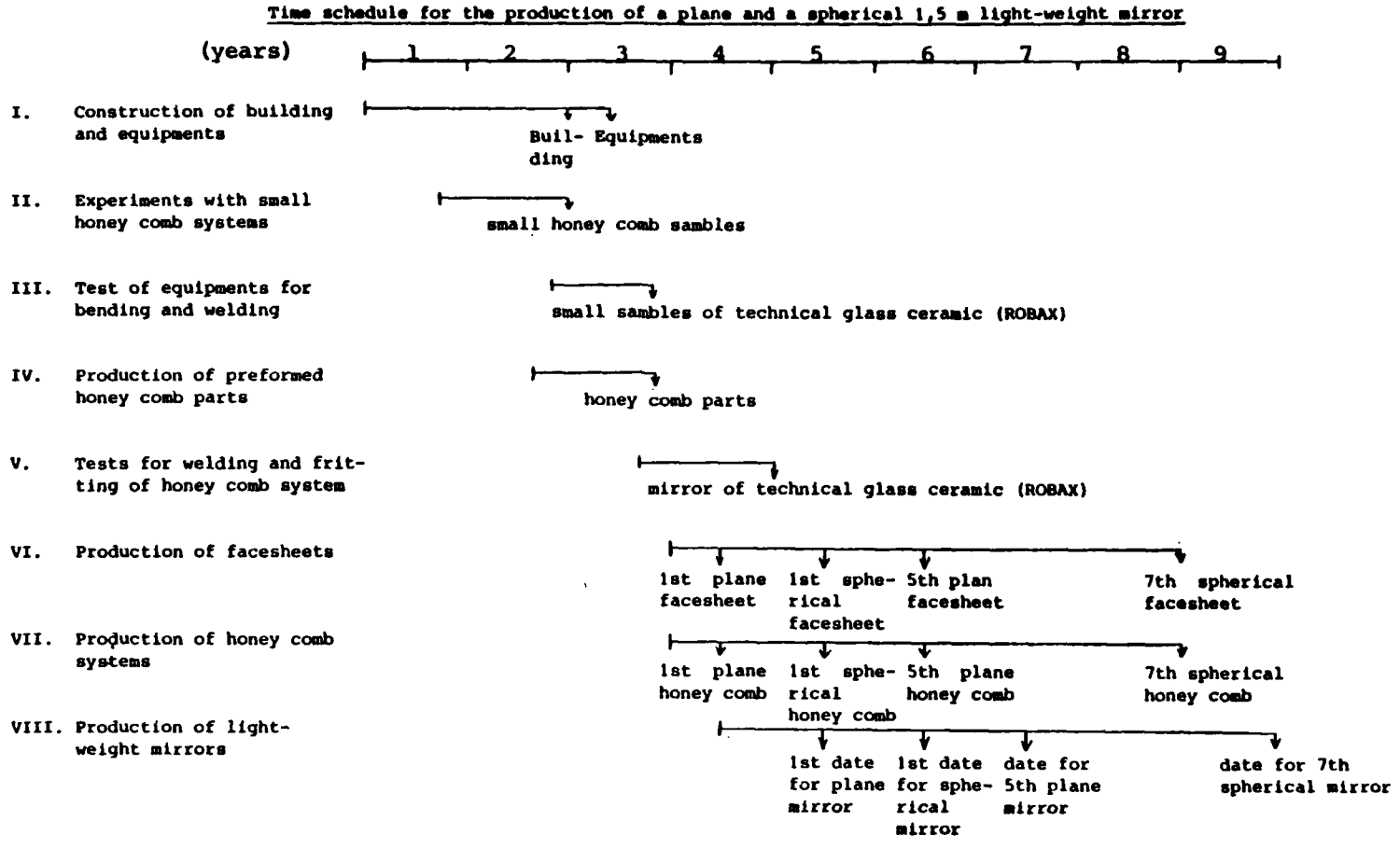


Figure 42. Time Schedule for the Production of a Plane and a Spherical 1.5 m Light-Weight Mirror.

SECTION VII

CONCLUSIONS

The potential of all of the technologies required for fabricating lightweight passive Zerodur mirror blanks has been demonstrated during this program. The core fabrication processes are now fully developed. Facesheet slumping and frit-bonding will require additional effort to bring these techniques to maturity.

All of the processes developed by Schott are scalable to the production of 4 meter mirror blanks. The cost and time required to establish this capability have been estimated.

Measurements of the physical properties of Zerodur subjected to the mirror fabrication processes have been made. Evaluation of the properties has shown that the processes are suitable for the fabrication of large lightweight mirror blanks.

The performance of a lightweight Zerodur mirror under high front surface thermal loading has been analytically predicted. The Zerodur mirror was shown to have superior performance to a ULE mirror of the same design. The Zerodur mirror was heavier due to the higher density of the material. The analysis proved that this level of performance could be retained while decreasing the weight of the mirror by optimizing the mirror design.

The cost and schedule to resolve the remaining technology issues have been estimated. Preliminary design of a 4 meter blank fabricating facility has been completed. The cost and schedule to establish this facility and to fabricate demonstration blanks has been estimated.

The Zerodur process is a viable option for the production of large passive lightweight mirrors.

SECTION VIII

RECOMMENDATIONS FOR FUTURE WORK

As a result of this program, two areas of technology have been identified that require additional development effort before the fabrication of large lightweight Zerodur mirrors can be undertaken. The two technologies requiring further effort are frit bonding and facesheet slumping. Successful completion of these developments will resolve all the remaining technical uncertainties of the manufacturing process. Establishment of a 4 meter mirror facility and the fabrication of large mirror blanks will then require engineering scale-up only.

A program has been proposed by Schott and Perkin-Elmer that includes process development, laboratory demonstration, and the production of slumped Zerodur samples up to 1.3 meters in diameter. Schott has successfully performed some preliminary slumping experiments on a laboratory scale. There is a high probability of success for the slumping program. Completion of this program will result in the establishment of the capability to produce slumped facesheets up to 2 meters in diameter. At the present time there are no known technical obstacles in scaling up this process to 4 meter diameter facesheets.

This development work, although not critical to the fabrication of Zerodur and lightweight mirrors, has the potential for the greatest positive impact on large mirror fabrication technology. The slumping process could be used to fabricate thin shell facesheets for active mirrors. These facesheets would have certain advantages as compared to ULE for many applications:

- superior cosmetics
- near net shape fabrication
- tunable CTE
- larger sizes
- greater homogeneity
- simplified inspection (due to retention of polished surfaces)

It is particularly important that Zerodur is already manufactured in sizes up to 4 meters. Monolithic, homogeneous facesheets as large as 4 meters could be made using the slumping technique. No piecing together of smaller hexagons would be required.

It is recommended that the facesheet development program be continued at Schott. The technology has wide applicability to the fabrication of both active and passive mirrors.

The second area requiring additional development work is frit bonding. Schott has proposed a program that will (1) complete the development and characterization of frit, and (2) develop the process and parameters for using this frit to bond facesheets to lightweight cores. An outline of the proposed program is included in Appendix I. Completion of the composition and processing studies and measurement of physical properties is estimated to be a one year program. The engineering study of techniques to apply the frit to the cores, construction of the required equipment, and determination of the techniques and process for performing the frit bonding under pressure would require 2 years. The programs would run concurrently. Schott's schedule for this program appears in Appendix I.

The completion of the frit development is critical to the fabrication of lightweight passive mirrors. Schott has stated that the frit glass development must precede the construction of lightweight demonstration blanks. The engineering study of the frit bonding process could run concurrently with the 1.5 meter scale-up program.

Completion of the frit development program will enable the fabrication of the 0.46 meter demonstration blanks. Fabrication of these blanks is the first step in the scale-up program proposed by Schott. Appendix G is an outline of Schott's proposal for the 0.46 meter demonstration blank program. A significant issue is that the fabrication of these blanks requires no additional facilities at Schott. The existing welding machine can be used to build cores for these two mirrors. Delivery of the mirrors would require approximately 16 months. Although the fabrication of these mirrors requires

the completion of the frit development, the program could be phased to minimize total delivery time by initiating the core and facesheet fabrication concurrently with the frit development program. A possible schedule for the frit development program and the 0.46 meter blank fabrication program is shown in Figure 43. The phasing of the two programs insures that the frit development is essentially complete in time to perform the fritting operation on the 0.46 meter blanks. The slumping program is not shown in this schedule as its execution is entirely independent of both the frit development and the 0.46 meter demonstration blanks. The performance of these programs would complete the lightweight mirror technology development and would demonstrate the fabrication of mirror blanks with the lowest technical risk and cost.

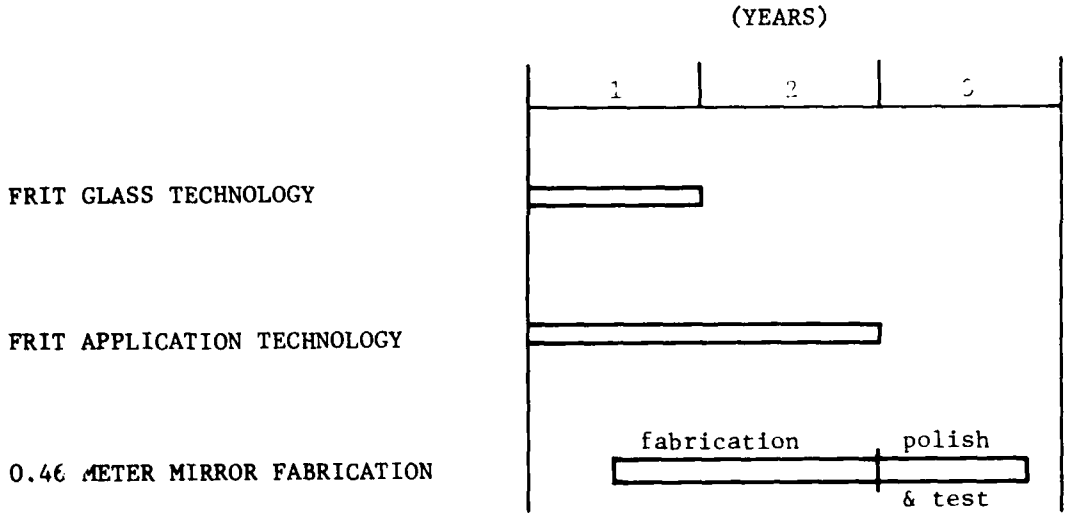


Figure 43. Proposed Technology Development Schedule

Although the techniques demonstrated during this program were designed for use in the fabrication of lightweight passive mirrors, these techniques would have wider applicability if fully developed. As previously discussed, the slumping of zerodur could be employed for the production of high quality facesheets for use as thin shell mirrors. The core making processes could be modified for the production of shallow eggcrate structures for stiffening of the thin active facesheets. Completion of the

frit development program would provide a method for bonding the shallow egg-crate ribs to the thin active facesheets. Completion of these technology developments would make possible the use of Zerodur in the production of both active and lightweight passive mirror blanks.

APPENDIX A

SCHOTT REPORT

"Manufacture of Rolled Glass for the

Honeycomb System of Zerodur Lightweight Mirrors"

Manufacture of rolled glass for the honeycomb system of Zerodur lightweight mirrors.

1. Objective

Glass plates are required for the honeycomb system of Zerodur lightweight mirrors which meet the following specifications:

Dimensions:	length:	(750 ± 1) mm
	width:	(200 ± 0,2) mm
	thickness:	(4 ± 0,1) mm
Surface:	Rolled or processed using SiC with 600 grain, plane.	
Optical properties:	No special demands, standard Zerodur quality according to our delivery terms.	

2. Manufacturing technology

Plates with the dimensions required and in the necessary quantities can be conveniently produced using rolled glass. The following will describe Schott's experience in the field of rolled glass manufacture and to what extent this experience can be applied to the production of Zerodur rolled glass.

2.1 Ceran technology

Using a rolled glass technology, Schott produces plates of glass ceramics which are known throughout the world under the trade names Ceran, Cerax and Robax. This technology makes it possible to manufacture plates of 3 to 5 mm thickness measuring up to 790 x 620 mm in size. More than 1 million Ceran cooktops are proof of the capability of this process.

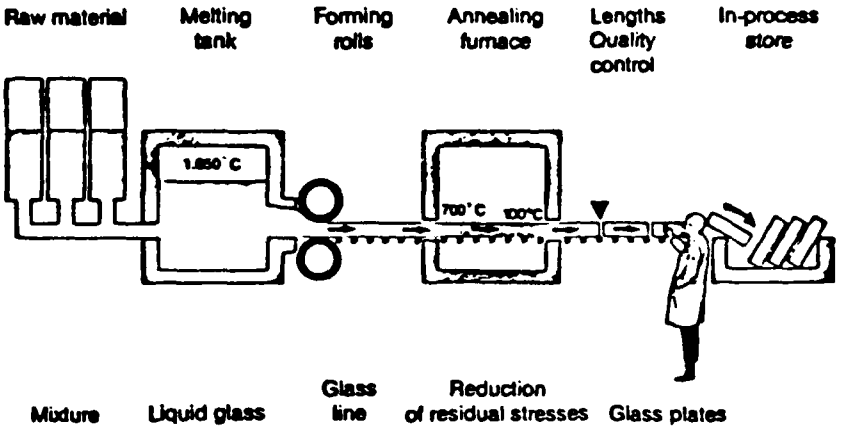


Fig. 1 Ceran technology

In the manufacture of Ceran and similar glass ceramics, the problems arising form the extreme process temperatures are of major importance. In the case of Zerodur, as compared to Ceran, these are more favourable and no problems are expected from the point of view of Zerodur production.

2.2 Optics technology I

The capability of this technology can be seen from the fact that heat absorbing and optical glass types have been produced for years using this rolling technology. Rolled Zerodur glass has also been manufactured using this process. Our experience is, however, limited to thicknesses of = 6 mm at a width of approx. 220 mm so that further processing is necessary.

2.3 Optics technology II

This technology is basically a modification of the technology described above. Using this technology it is possible to roll plates of 4 mm thickness. We have no experience of using Zerodur in this technology but do not expect to run into any difficulties in rolling Zerodur plates of 4 mm thickness. Tests are, however, necessary.

3. Cost comparison

The fix and proportional costs of the individual processes are variable. This follows that according to the production quantities one of the processes is more favourable.

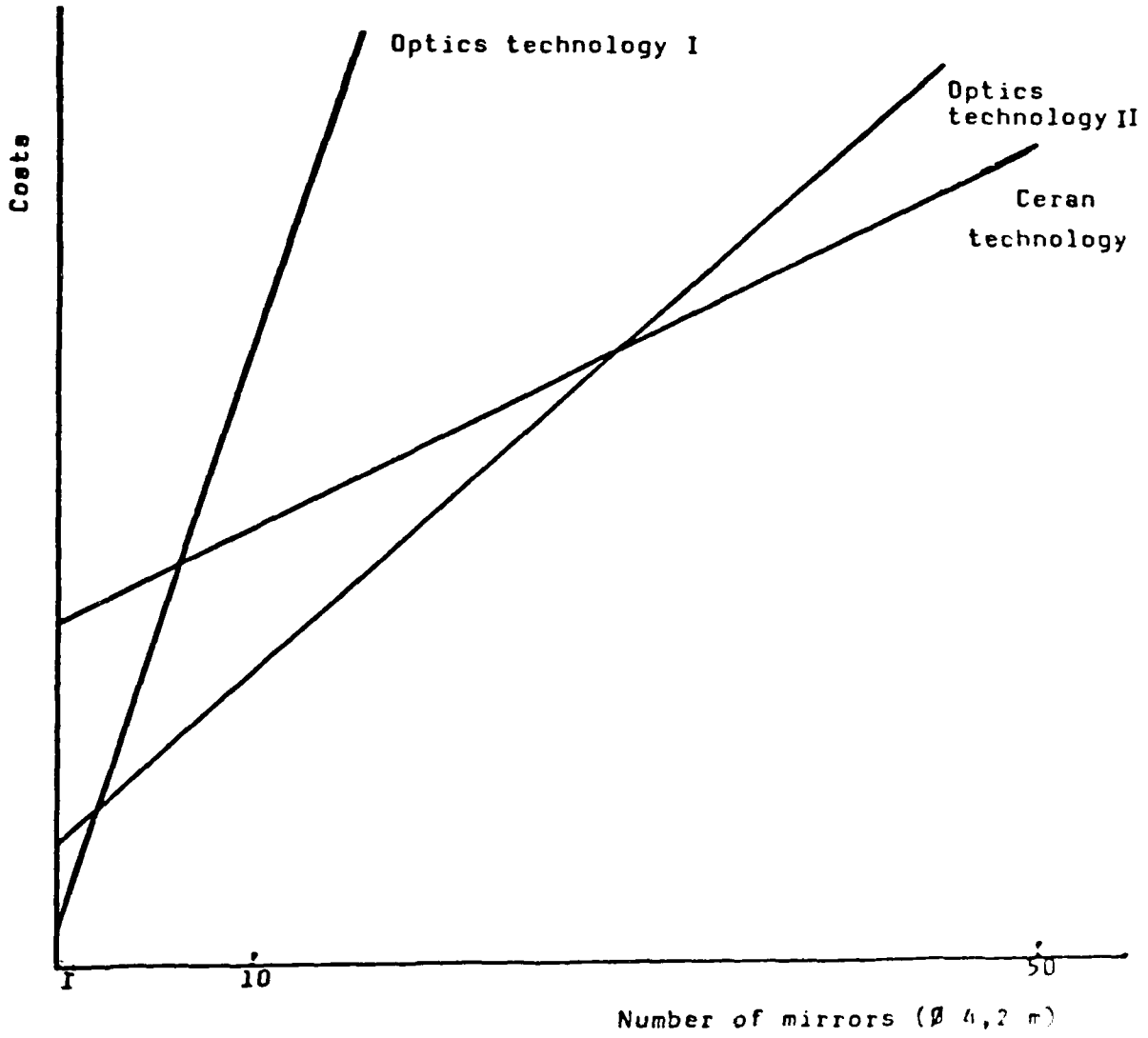


Fig. 2 Cost comparisation

In respect to the comparison of costs shown in Fig. 2, the following points should be noted:

- The comparison of costs was based on:
  - Ceran technology,
  - Optics technology I (6 mm)
  - Optics technology II(4 mm).
- The fix costs contain principally those costs occuring during the starting and melting process.
- The fix costs of Optics technology I and Optics technology II differ in the amount necessary for the tests (see Par. 2.3).
- The proportional costs for Optics technology II as opposed to Optics technology I are lower (by the amount necessary for further processing).
- The proportional costs for the Ceran technology are more favourable than those of the optics technologies as a result of the shorter production time.
- Output reduction due to spoilage was taken into consideration when calculating the proportional costs.

4. Summary

As described, Schott posesses extensive experience in the manufacture of rolled glass. There are 3 technologies available for the production of rolled Zerodur glass and each of these technologies is suitable. The decision as to which processing method is used will, therefore, mainly depend upon the production quantity involved.

APPENDIX B

SCHOTT REPORT

Weibull Statistics for Breaking Strengths of Welded Zerodur Samples and Measurement of the Coefficient of Thermal Expansion of the Heat-Affected Zone"

REPORT

on

Weibull statistics for breaking strength of welded Zerodur samples and unbonded Zerodur samples for comparison, as well as coefficient of thermal expansion (CTE) of the heat-affected zone of welded Zerodur samples,

process parameter statistics for bending and welding of the Zerodur samples.

(Referring to paragraphs 3.1.1.1, 3.1.1.2, 3.1.3, 3.1.4 of the contract)
Samples were sent to PE on January 22, 1982.

1. Production of the samples

Casting of Zerodur glass blocks 180 mm x 180 mm x 160 mm;

annealing of the blocks within 6 h;

sawing into rectangular plates;

grinding the plates at all surfaces, with grain 320, to the dimensions 170 mm x 100 mm x 4,1 mm.

1.1 Bending

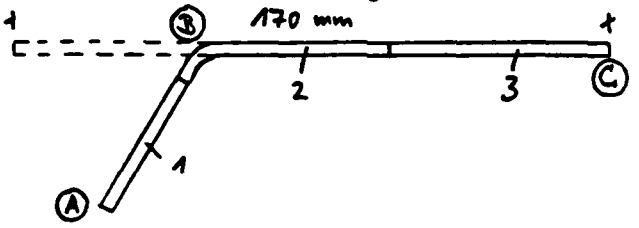
Preheating each plate individually within a time of 5 min, one plate every 7 min, in a laboratory oven, which is heated up to 660 °C; transposing the preheated plate into the bending apparatus within 5 s, including positioning and fixing; parts of the bending apparatus coming into contact with the plate and the plate itself are kept at about 600 - 650 °C with gas/air-burners to avoid breakage; heating up the bending zone with two special gas/oxygen-burners, one at each side of the plate, within 6 s; pressures of gas and oxygen, as well as their flow rates, adjusted to and kept constant at values which gave enough energy to allow the short heating-up time; all samples produced under the same conditions of time, temperature and geometry, which are applied later on, to produce the bent plates for the core section, too; immediately pushing down with a stick the free part of the plate (length 53 mm) to a stop for reaching the angle of 120 ° (as necessary in the honeycomb system); after another time of about 5 s, in which cooling-down of the bending zone takes place,

transposing the bent plate into another laboratory oven which is at 600 °C; filling theoven with 20 bent plates; heating up the filled oven to 650 °C and then switching off to cool down with door closed; taking out the 20 annealed bent plates next morning.

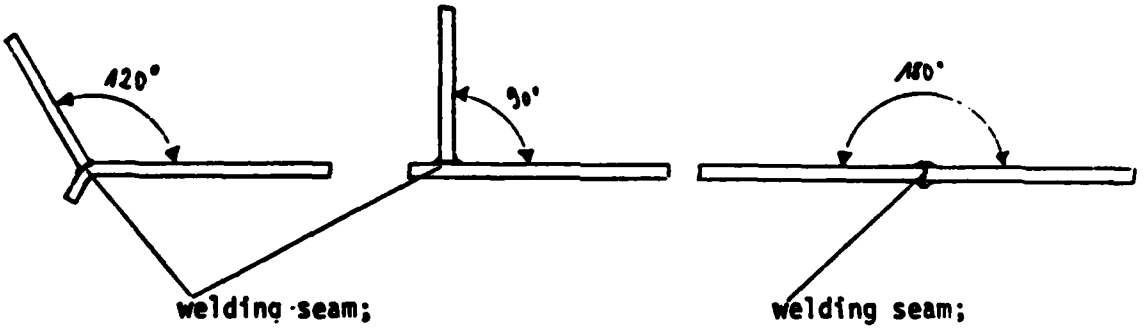
In the case of some plates, after heating up the bending zone, we do not push down the free part in order to produce 90 °-samples by welding, which can directly be compared with the frit-bonded samples; all other conditions of time, temperature and geometry were equal to the 120 °-samples.

1.2 Welding

Before carrying out the welding process, the bent plates were cut into three parts and ground at the sections with grain 320;



part 1 is to be welded with edge (A) to edge (B) of part 2 (120 °-samples and 90 °-samples); two parts 3 are to be welded together at their edges (C) (butt samples).



welding seam;

surrounding material is heat-affected by the bending process as well as by the welding process

welding seam;

surrounding meterial is only heat-affected by the welding process

Run of the welding process:

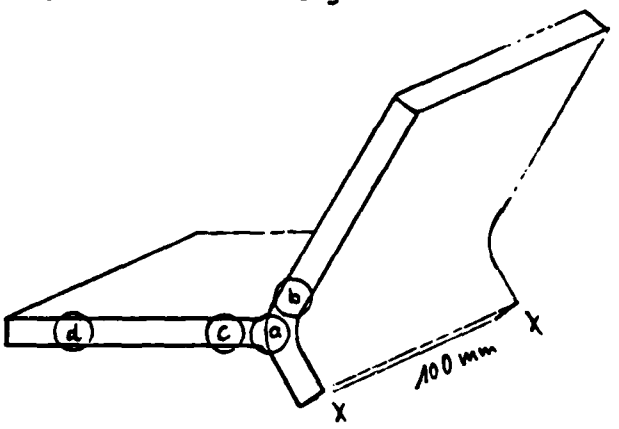
Preheating simultaneously the two parts to be welded within a time of 5 min in a laboratory oven, which is heated up to 660 °C; transposing the preheated parts into the welding apparatus within 5 s, including positioning and fixing; parts of the welding apparatus coming into contact with the plates, and the plates themselves are kept at about 600 - 650 °C with gas/air-burners to avoid breakage; heating up the above-mentioned edges Ⓐ and Ⓑ and Ⓒ, respectively, with 2 gas/oxygen-burners within 5 s; pressures of gas and oxygen, as well as their flow rates, adjusted to and kept constant at values which gave enough engergy to allow the short heating-up time; all samples produced under the same conditions of time, temperature and gemometry, which will be applied later on to weld the core section, too; removing the burners and immediately compressing the two edges; after another time of about 5 s, in which cooling-down of the welding zone takes place, transposing the welded sample into another laboratory oven, which is at 650 °C; filling the oven with 20 - 25 samples, one sample every 7 min; heating up the filled oven to 700 °C and then switching off for cooling-down with door closed; taking out the annealed samples next morning.

1.3 Ceramizing

The welded samples (90 °, 120 ° and 180 ° = butt samples) as well as unbent and unwelded plates are ceramized in 2 laboratory ovens of the same type with the same time-temperature-program within 10 days. This is shorter than is normally the case for Zerodur, so that CTE is negative; but this time is long enough to equalize the properties in the ceramized state, which are not equal in the glassy state because of heat action during bending and welding; this time is also long enough to reach sufficient strength. All properties can only become better and more equal if the ceramizing program is extended, for example 20 - 30 days as is necessary for greater cores. The value of CTE can be controlled by the ceramizing program.

2. Measurement of CTE (0 - 50 °C)

Measurements were only done with 120 °-samples (corresponding to the core to be welded). From each of the two ovens, we took 3 samples, and from each sample we took 4 rods of 95 mm in length and 4 - 5 mm in diameter for the measurements:



a) including the welding seam

b) near-by the welding seam, in the zone which was heat-affected by the bending process

c) near-by the welding seam, in the zone which was heat-affected only by the welding process

d) zone heat-affected neither by bending nor by welding, only by twofold preheating and annealing

The deviation in repetition lies at 0,005 x 10^{-6}/K. The results are summerized in the following table:

oven No.	120 °-sample No.	CTE (0 - 50 °C) · 10^6 K			
		rod a	rod b	rod c	rod d
1	1	- 0,100	- 0,104	- 0,103	- 0,102
	2	- 0,108	- 0,111	- 0,110	- 0,110
	3	- 0,100	- 0,102	- 0,106	- 0,108
2	4	- 0,093	- 0,101	- 0,101	- 0,105
	5	- 0,101	- 0,103	- 0,102	- 0,101
	6	- 0,096	- 0,103	- 0,102	- 0,104
1 + 2	1 - 6	- 0,100	- 0,104	- 0,104	- 0,105

The welding seam itself has, as expected, a CTE little bit higher than the other parts of the welded samples; the difference between the highest and the lowest value (- 0,093 and - 0,111), which is 0,018 · 10^{-6}/K, is low enough for the assigned purpose.

3. Measurement of breaking strength at room temperature

3.1 Kinds of samples and carrying-out of tests

These measurements were done with samples having a width of 20 mm, produced by cutting the original welded samples (width 100 mm) into 4 pieces and grinding the sections with grain 320.

Measurements were done with 6 different kinds of samples:

A) welded 120 °-samples (geometry of the core)

B) welded 90 °-samples (for comparison with frit-bonded samples)

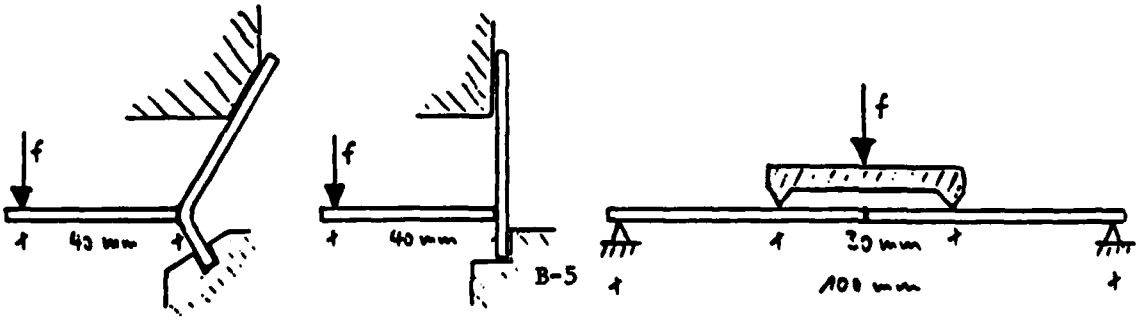
C) welded 180 °-samples (butt samples)

D) welded 180 °-samples (butt samples), tension side ground with grain 320 after ceramizing, in order to remove the welding bulge

E) flat samples, not welded, only twice preheated/annealed and then ceramized (for comparison with C)

F) as E), but ground after ceramizing with grain 320 at the tension side (for comparison with D)

Geometry in the testing machine was as follows: (f = bending force)



All samples lie in water at room temperature for about 1 day before being tested. All measured single values were evaluated and plotted by a computer; the results are given in the enclosed tables/diagrams ① to ⑳.

3.2 Comments on the results

A) 120 °-samples (tables/diagrams ① to ④)
The breaking strengths are calculated from breaking force and geometry of the sample without consideration of geometrical deviations as bulges and notches. But especially the notches define the breakage, so that the calculated values cannot be regarded as material values for the welding seam under the represented test conditions.

The worst geometry of the welding zone is case b) (see ④); the 6 smallest values belong to this kind of breakage.

The welding seam itself was never the surface of fracture.

B) 90 °-samples (tables/diagrams ⑤ to ⑦)
Fundamentally, the same remarks as were made for 120 °-samples are valid. The Weibull-plot shows two characeristics which are not analyzed in detail. The lower aggregate is regarded to be the crucial one. Only with one sample, the welding seam itself was the surface of fracture.

Comparing these values with those of frit bonding, we can see that only the frit GM 31811 is a little bit better (see earlier report).

C) 180 °-samples, butt-samples (tables/diagrams ⑧ to ⑩)
Distribution and height of the values are fully satisfactory. Only with two samples, the welding seam itself was the surface of fracture. Only in one case, the origin of fracture was at the edge of the sample, otherwise in the area.

D) 180° -samples (butt samples), ground after ceramizing (tables/diagrams ⑪ to ⑬)
Because of the opening of the bubbles in the welding seam upon the grinding of the whole tension side, the origin of fracture, as well as the surface of fracture, lies in the welding seam itself with all samples. Distribution and height of the values are, nevertheless, satisfactory, and the difference to C) is inconsiderable.

E) Flat samples, not welded (tables/diagrams ⑭ to ⑯)
As expected, the values lie higher than those of C). All origines of fracture lie in the areas, not at the edges of the samples.

F) Flat samples, not welded, ground after ceramizing (tables/diagrams ⑰ to ⑲)
Distribution and height of the values are better than those of samples E); that is not understandable at all, but we have had comparable results with other glasses.

Diagram 20 shows all Weibull straight lines for the samples A, B, C, D, E, F to allow a better comparison. We can say, that the breaking strength of 120 °-samples is good enough for the assigned purpose.

Glas:	Name	:Zerodur
-----	Nummer	:-
	Artikel,Anzahl	:120 Grad Schweisspr.
	Datum des Probeneingangs	:5.1.82
Prüfung:	Maschine	:1
--------	Kraftanzeige der Maschine N oder kp	:kp
	Probenlänge mm	:-
	Ls	:87.2
	La	:0
	Messgeschirr Nr.	:-
Vorbehandlung,Oberflächenzustand der Probe		:Kanten 320er Korn

A

Datum Prüfbeginn	:15.1.82
Datum Prüfende	:20.1.82
Prüfungsart	:nass

Ergebnisse für die Werte von Rang 1 bis Rang 20

Mittelwert	N/mm^2	: 23.98
Standartabweichung		: 3.88
Weibullfaktor		: 6.83
charakteristische Festigkeit		: 25.64
kleinster Wert		: 17.36
grösster Wert		: 29.43
Korrelationskoeffizient		: 0.9637

(1)

120°- Proben

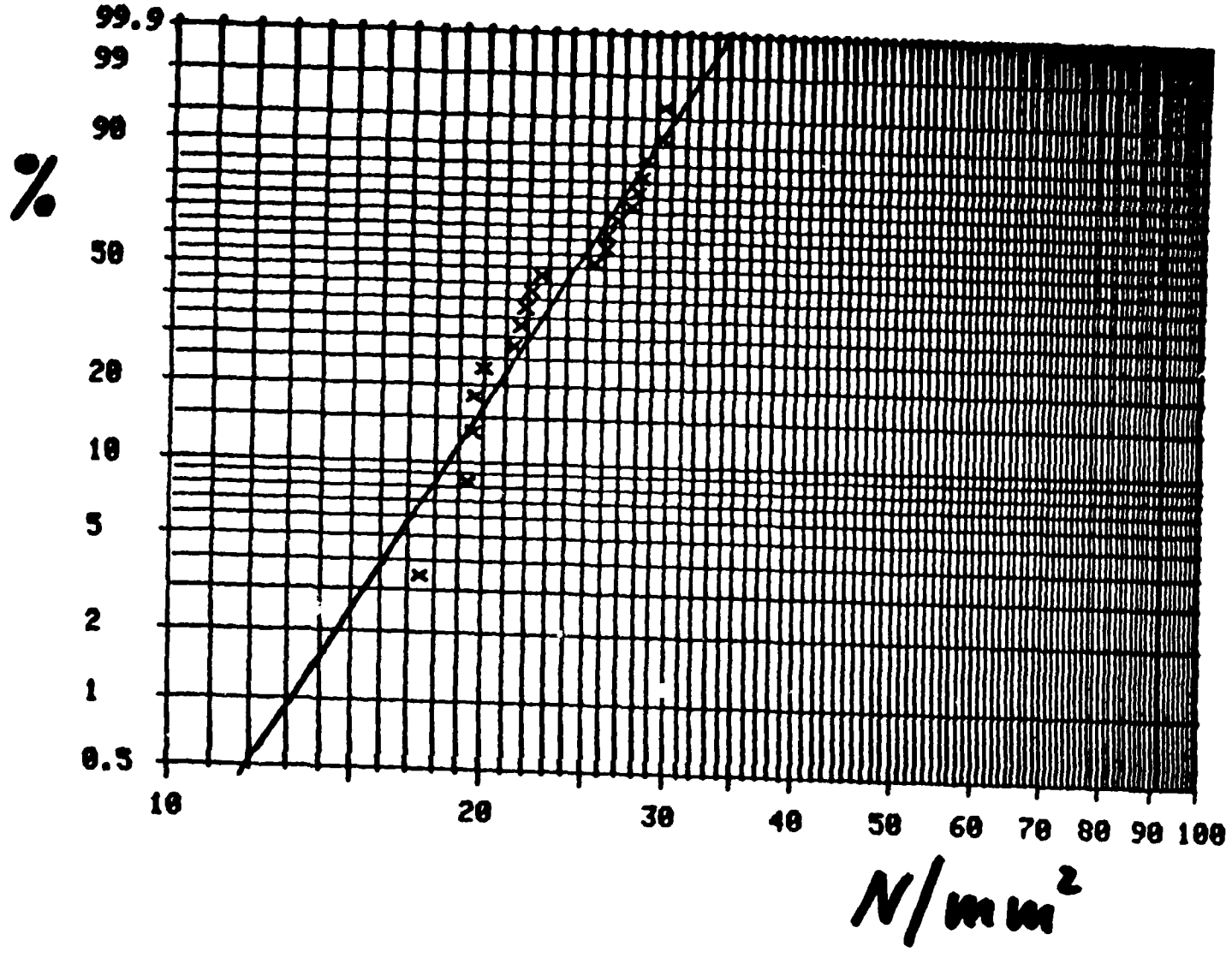
A

Rang	Bruchsp.		Median Rank	Kraft	Zeit	Dicke	Breite	Rate
	N/mm^2		%	N	s	mm	mm	N/mm^2s
1	17.36	b	3.43	44.64	19	4.09	20.10	0.91
2	19.27	b	8.33	49.05	21	4.07	20.10	0.92
3	19.47	b	13.24	49.54	20	4.09	19.90	0.97
4	19.53	b	18.14	50.42	22	4.12	19.90	0.89
5	19.89	b	23.04	52.39	22	4.15	20.00	0.90
6	21.29	b	27.94	56.90	21	4.17	20.10	1.01
7	21.60	c	32.84	54.45	20	4.07	19.90	1.08
8	21.84	b	37.75	58.37	22	4.17	20.10	0.99
9	22.08	a	42.65	55.92	25	4.07	20.00	0.88
10	22.57	c	47.55	58.86	26	4.13	20.00	0.87
11	25.33	b	52.45	64.16	26	4.07	20.00	0.97
12	26.01	a	57.35	66.22	25	4.07	20.10	1.04
13	26.03	b	62.25	66.90	25	4.10	20.00	1.04
14	26.71	a	67.16	71.02	28	4.16	20.10	0.95
15	27.50	b	72.06	71.02	27	4.12	19.90	1.02
16	27.88	b	76.96	72.01	28	4.12	19.90	1.00
17	28.10	a	81.86	73.20	27	4.13	20.00	1.04
18	28.33	a	86.76	72.10	28	4.08	20.00	1.01
19	29.37	c	91.67	74.75	28	4.08	20.00	1.05
20	29.43	b	96.57	76.03	32	4.10	20.10	0.92

(2)

120°- Proben

Geerade für die Messuerte Rang :1 bis Rang :20
Sollen andere Messuerte verwendet werden? :

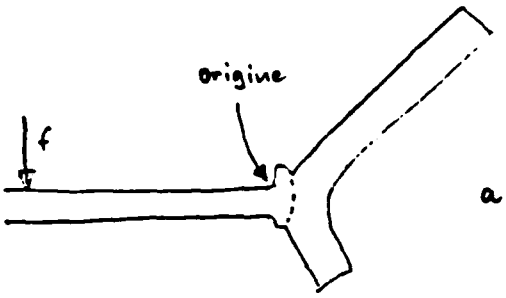


A

B-10

(3)

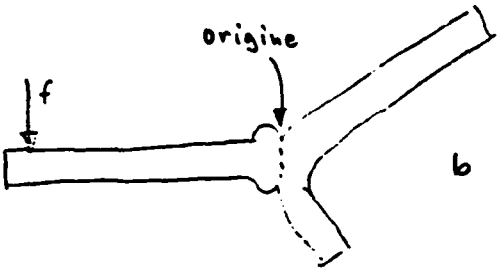
Welded 120°-samples, types of breakage



a

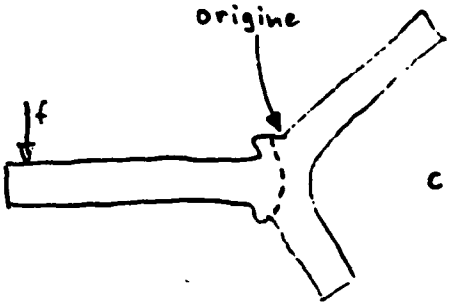
range No.

9
12
14
17
18



b

1
2
3
4
5
6
8
11
13
15
16
20



c

7
10
19

Glas:	Name	:Zerodur
-----	Nummer	:-
	Artikel,Anzahl	:90 Grad Schweisspr.
	Datum des Probeneingangs	:5.1.82
Prüfung:	Maschine	:1
--------	Kraftanzeige der Maschine N oder kp	:kp
	Probenlänge mm	:-
	Ls	:137.6
	La	:0
	Messgeschirr Nr.	:-
Vorbehandlung,Oberflächenzustand der Probe		:Kanten 320er Korn

---

Datum Prüfbeginn	:15.1.82
Datum Prüfende	:20.1.82
Prüfungsart	:nass

Ergebnisse für die Werte von Rang 2 bis Rang 12

Mittelwert	N/mm↑2	: 13.90
Standartabweichung		: 0.71
Weibullfaktor		: 13.37
charakteristische Festigkeit		: 15.02
kleinster Wert		: 12.29
grösster Wert		: 14.74
Korrelationskoeffizient		: 0.9688

B

90°-Proben

B

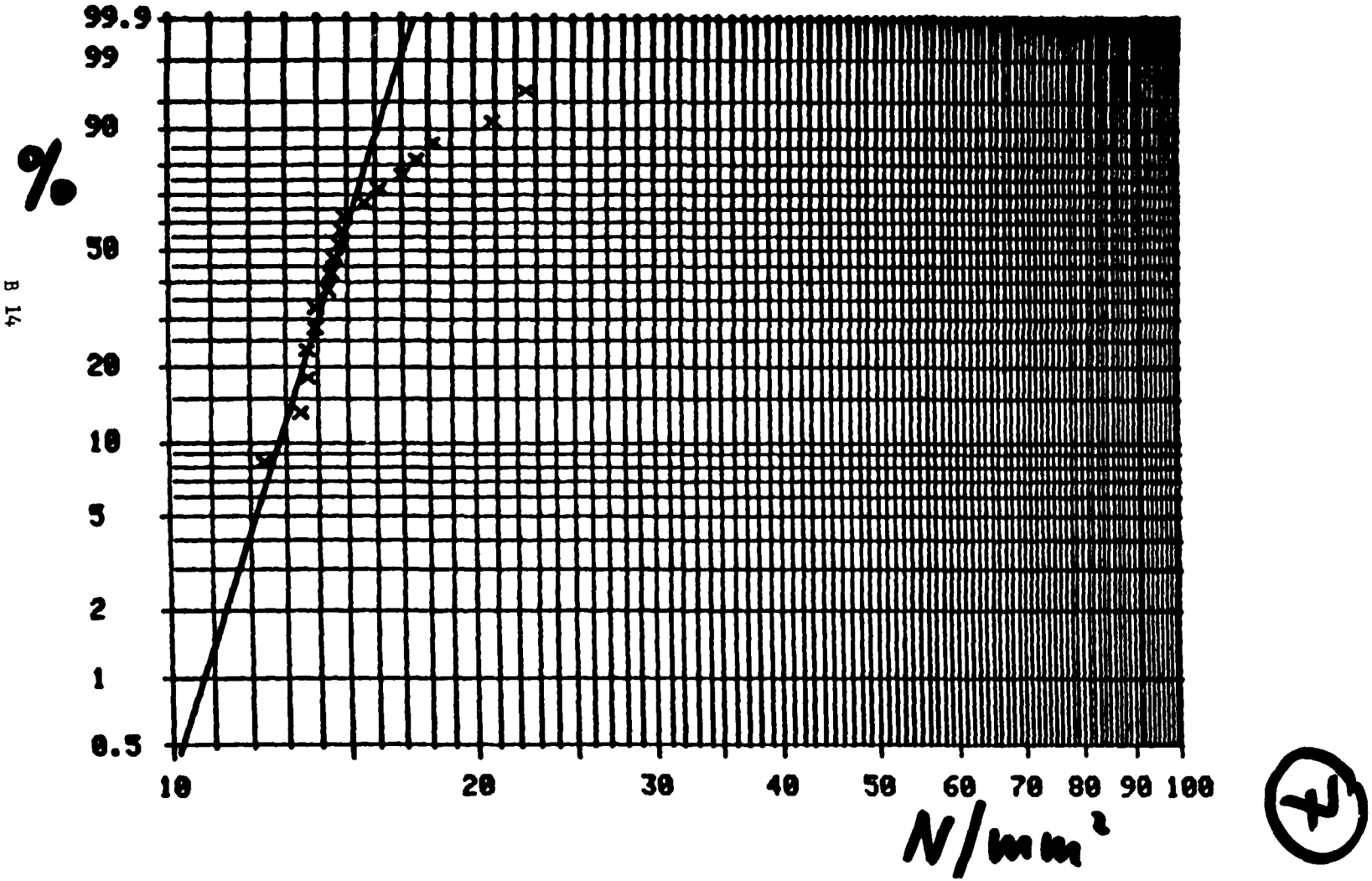
Rang	Bruchsp.	Median Rank	Kraft	Zeit	Dicke	Breite	Rate
	N/mm†2	%	N	s	mm	mm	N/mm†2s
1	X 7.49	3.43	12.75	7	4.14	20.50 !	1.07
2	12.29	8.33	20.60	8	4.16	20.00	1.54
3	13.35	13.24	22.07	12	4.13	20.00	1.11
4	13.58	18.14	22.56	10	4.13	20.10	1.36
5	13.59	23.04	22.56	10	4.14	20.00	1.36
6	13.81	27.94	23.05	9	4.14	20.10	1.53
7	13.84	32.84	21.78	9	4.03	20.00	1.54
8	14.22	37.75	23.05	9	4.09	20.00	1.58
9	14.33	42.65	23.35	10	4.09	20.10	1.43
10	14.47	47.55	24.03	10	4.14	20.00	1.45
11	14.67	52.45	23.54	10	4.06	20.10	1.47
12	14.74	57.35	23.54	11	4.05	20.10	1.34
13	14.81	62.25	23.54	10	4.04	20.10	1.48
14	15.51	67.16	24.53	10	4.04	20.00	1.55
15	16.04	72.06	26.00	13	4.08	20.10	1.23
16	16.91	76.96	27.27	13	4.07	20.10	1.30
17	17.46	81.86	28.45	14	4.09	20.10	1.25
18	18.16	86.76	29.43	13	4.09	20.00	1.40
19	20.80	91.67	33.55	13	4.08	20.00	1.60
20	22.44	96.57	37.28	15	4.13	20.10	1.50

6

90°-Proben

Gerade für die Messwerte Rang :2 bis Rang :12
Sollen andere Messwerte verwendet werden? :

B



B 14

4

Glas:	Name		:Zerodur
-----	Nummer		:-
	Artikel,Anzahl		:Staebe mit Schweissnaht
	Datum des Probeneingangs		:5.1.82
Prüfung:	Maschine		:1
--------	Kraftanzeige der Maschine N oder kp		:kp
	Probenlänge	mm	:110
	Ls		:100
	La		:20.8
	Messgeschirr Nr.		:-
Vorbehandlung,Oberflächenzustand der Probe			:Schweissnaht Original

---

Datum Prüfbeginn		:15.1.82
Datum Prüfende		:20.1.82
Prüfungsart		:nass

Ergebnisse für die Werte von Rang 1 bis Rang 14

Mittelwert	N/mm↑2	: 38.28
Standartabweichung		: 4.16
Weibullfaktor		: 10.02
charakteristische Festigkeit		: 40.16
kleinster Wert		: 31.43
grösster Wert		: 44.23
Korrelationskoeffizient		: 0.9710

Flachproben mit Original Schweißnaht

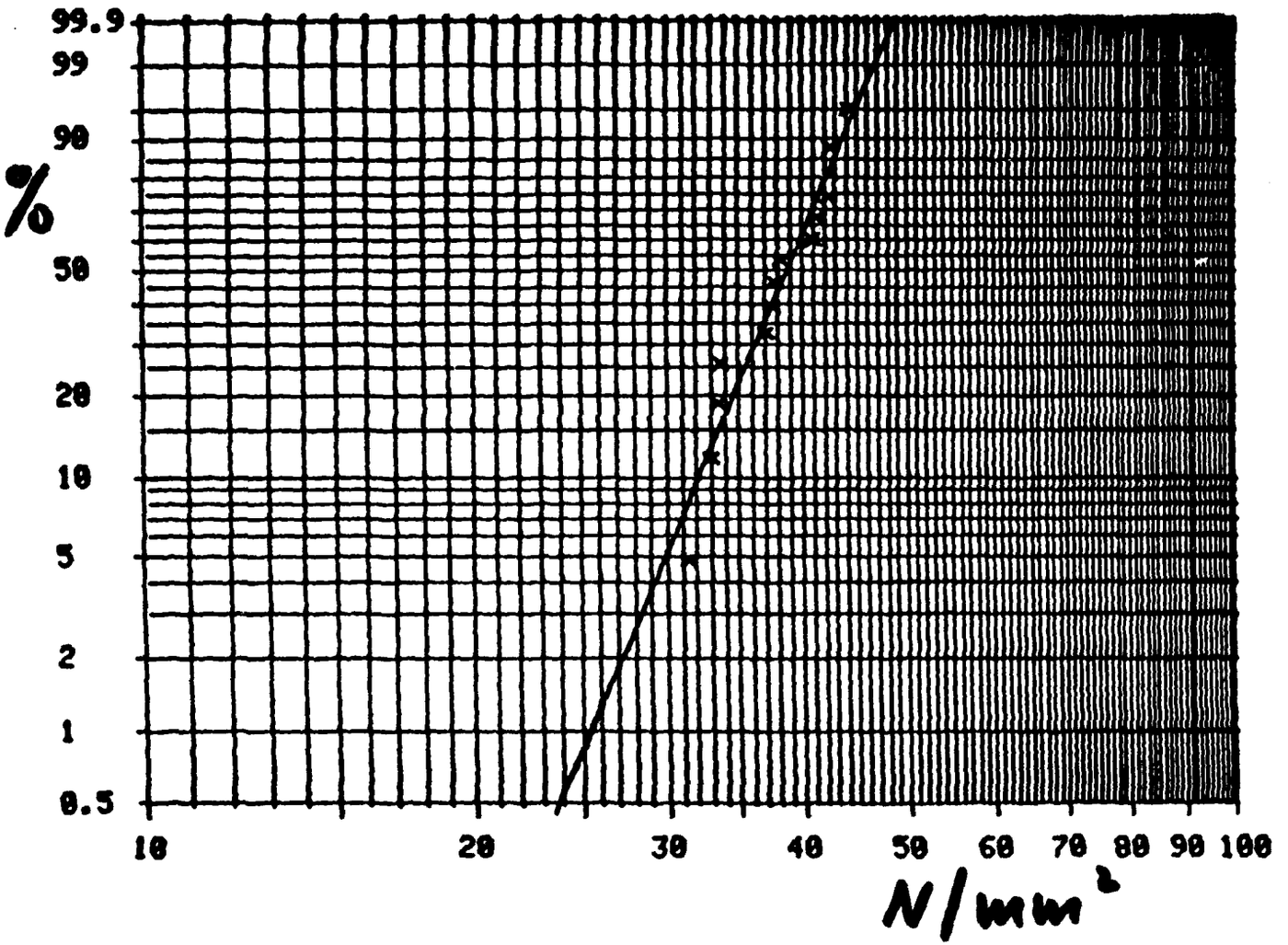
G

Rang	Bruchsp.	Median Rank	Kraft	Zeit	Dicke	Breite	Rate
	N/mm↑2	%	N	s	mm	mm	N/mm↑2s
1	31.43	4.86	90.25	27	4.13	20.00	1.17
2	32.98	11.81	95.16	32	4.14	20.00	1.03
3	33.47	18.75	95.16	41	4.12	19.90	0.82
4	33.64	25.69	96.14	34	4.11	20.10	0.99
5	37.07	32.64	105.95	38	4.11	20.10	0.98
6	37.56	39.58	108.40	32	4.13	20.10	1.17
7	37.76	46.53	107.91	31	4.12	20.00	1.22
8	38.28	53.47	109.38	31	4.13	19.90	1.23
9	40.93	60.42	118.70	38	4.13	20.20	1.08
10	41.34	67.36	118.70	34	4.14	19.90	1.22
11	42.29	74.31	119.68	34	4.10	20.00	1.24
12	42.50	81.25	119.68	48	4.09	20.00	0.89
13	42.50	88.19	119.68	48	4.09	20.00	0.89
14	44.23	95.14	127.04	40	4.10	20.30	1.11

(9)

Flachproben m. Original Schweißnaht G

Gerade für die Messwerte Rang :1 bis Rang :14
Sollen andere Messwerte verwendet werden? :



Glas:	Name	:Zerodur
-----	Nummer	:-
	Artikel,Anzahl	:Staebe m. Schweissn. 15
	Datum des Probeneingangs	:5.1.82
Prüfung:	Maschine	:1
--------	Kraftanzeige der Maschine N oder kp	:kp
	Probenlänge mm	:110
	Ls	:100
	La	:20.8
	Messgeschirr Nr.	:-
Vorbehandlung,Oberflächenzustand der Probe		:Schweissnaht mit 320er Korn
n----------		

	Datum Prüfbeginn	:15.1.82
	Datum Prüfende	:20.1.82
	Prüfungsart	:nass

Ergebnisse für die Werte von Rang 1 bis Rang 15

Mittelwert	N/mm^2	: 40.64
Standartabweichung		: 6.81
Weibullfaktor		: 6.39
charakteristische Festigkeit		: 43.58
kleinster Wert		: 26.76
grösster Wert		: 58.68
Korrelationskoeffizient		: 0.9850

Schweißnaht plan geschliffen 320 Korn

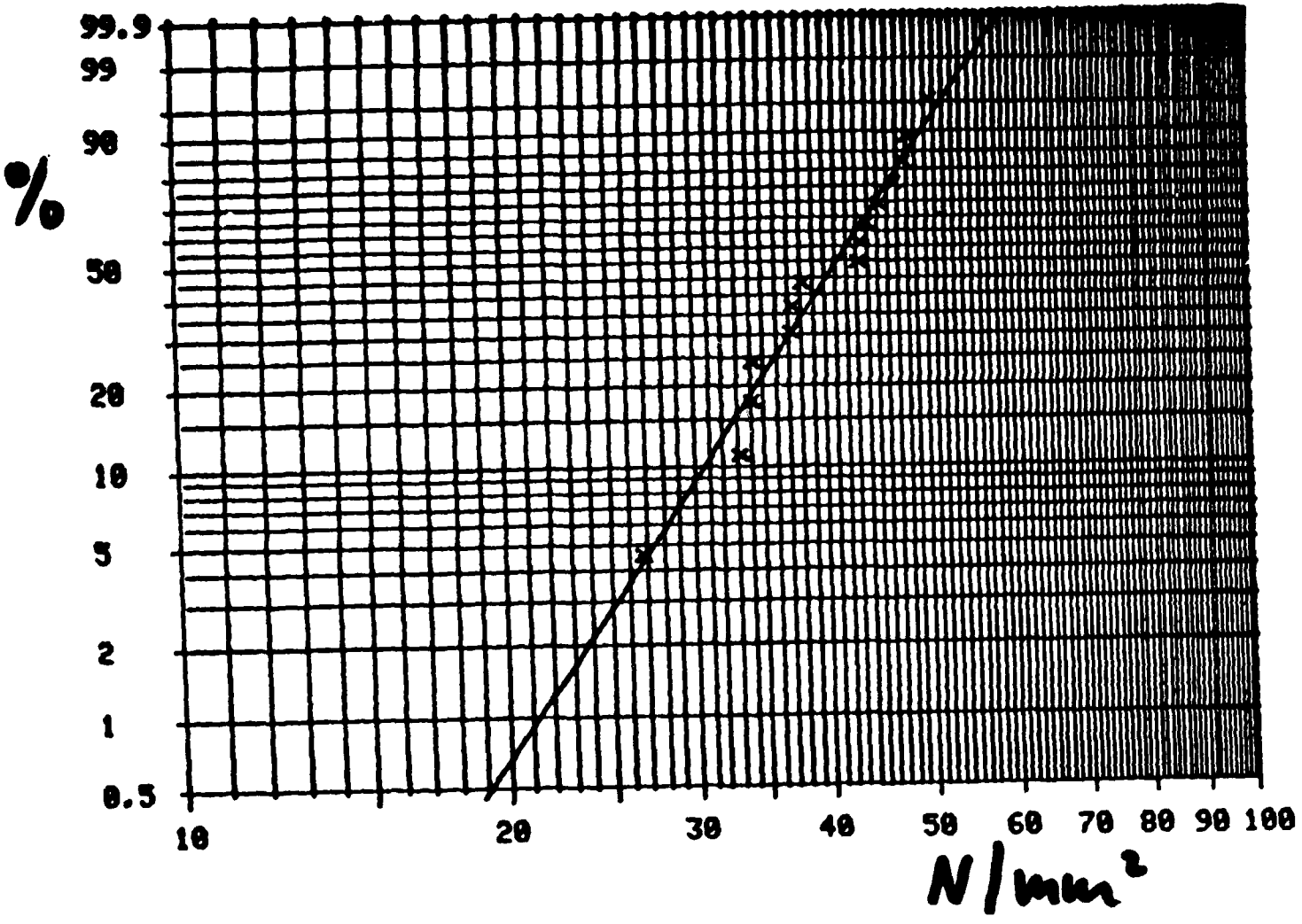
D

Rang	Bruchsp.	Median Rank	Kraft	Zeit	Dicke	Breite	Rate
	N/mm^2	%	N	s	mm	mm	N/mm^2s
1	26.76	4.55	70.63	25	3.94	20.20	1.07
2	33.19	11.04	85.84	25	3.91	20.10	1.33
3	34.08	17.53	86.82	28	3.89	20.00	1.22
4	34.18	24.03	89.76	28	3.94	20.10	1.22
5	37.17	30.52	96.14	25	3.91	20.10	1.49
6	37.33	37.01	101.04	31	4.00	20.10	1.20
7	38.12	43.51	98.10	30	3.90	20.10	1.27
8	43.09	50.00	117.23	36	4.01	20.10	1.20
9	43.35	56.49	109.87	36	3.88	20.00	1.20
10	43.99	62.99	119.68	38	4.02	20.00	1.16
11	45.20	69.48	109.87	34	3.80	20.00	1.32
12	46.66	75.97	129.49	40	4.05	20.10	1.17
13	47.72	82.47	130.47	41	4.02	20.10	1.16
14	48.07	88.96	129.49	40	3.99	20.10	1.20
15	50.68	95.45	132.44	39	3.94	20.00	1.30

(12)

Schweißnaht plan geschliffen 320 Korn D

Gerade für die Messwerte Rang :1 bis Rang :15
Sollen andere Messwerte verwendet werden? :



B-20

(13)

Glas:	Name	:Zerodur
-----	Nummer	:-
	Artikel,Anzahl	:Staebe19
	Datum des Probeneingangs	:5.1.82
Prüfung:	Maschine	:1
--------	Kraftanzeige der Maschine N oder kp	:kp
	Probenlänge mm	:110
	Ls	:100
	La	:20.8
	Messgeschirr Nr.	:-
Vorbehandlung,Oberflächenzustand der Probe		:Anlieferungszustand
----------		
	Datum Prüfbeginn	:15.1.82
	Datum Prüfende	:20.1.82
	Prüfungsart	:nass

E

B-21

Ergebnisse für die Werte von Rang 1 bis Rang 19

Mittelwert	N/mm↑2	: 51.56
Standartabweichung		: 5.92
Weibullfaktor		: 9.91
charakteristische Festigkeit		: 54.13
kleinster Wert		: 40.81
grösster Wert		: 61.32
Korrelationskoeffizient		: 0.9820

(14)

Flachproben Anlieferung, ohne Schweißnaht. E

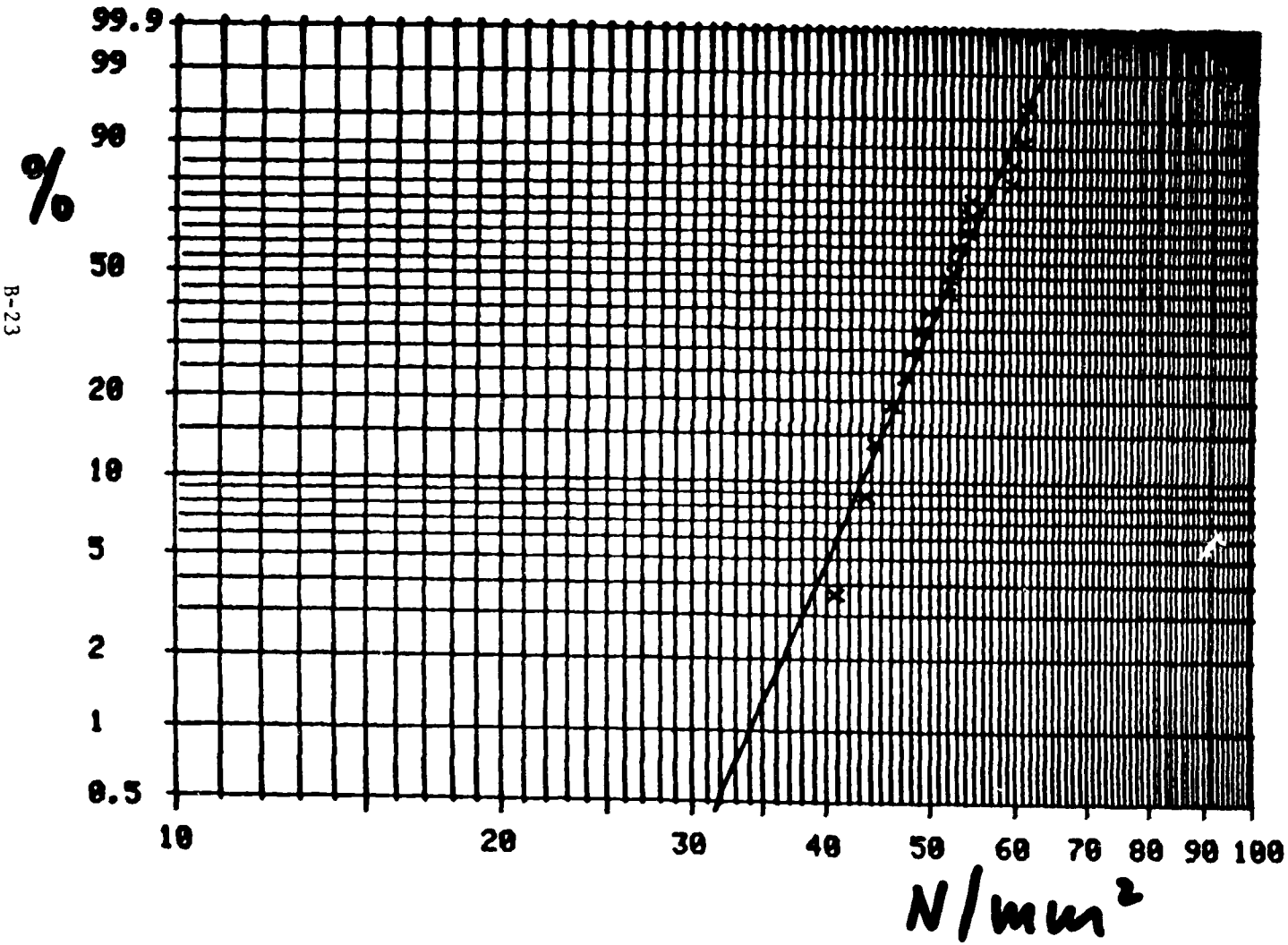
Rang	Bruchsp.	Median Rank	Kraft	Zeit	Dicke	Breite	Rate
	N/mm^2	%	N	s	mm	mm	N/mm^2s
1	40.81	3.61	113.80	36	4.07	20.00	1.13
2	43.47	8.76	123.61	36	4.12	19.90	1.21
3	44.38	13.92	125.57	38	4.11	19.90	1.17
4	45.89	19.07	130.47	38	4.12	19.90	1.21
5	47.26	24.23	134.40	43	4.11	20.00	1.10
6	47.73	29.38	134.40	42	4.10	19.90	1.14
7	48.82	34.54	138.81	44	4.12	19.90	1.11
8	49.68	39.69	141.26	45	4.12	19.90	1.10
9	51.66	44.85	146.17	44	4.11	19.90	1.17
10	51.74	50.00	147.15	58	4.11	20.00	0.89
11	52.51	55.15	147.15	41	4.08	20.00	1.28
12	52.78	60.31	150.09	40	4.11	20.00	1.31
13	53.91	65.46	151.07	45	4.08	20.00	1.20
14	54.08	70.62	151.56	40	4.08	20.00	1.35
15	54.35	75.77	153.04	40	4.10	19.90	1.36
16	59.29	80.93	167.75	44	4.11	19.90	1.35
17	59.40	86.08	169.71	44	4.13	19.90	1.35
18	60.67	91.24	171.68	41	4.11	19.90	1.48
19	61.32	96.39	172.66	43	4.10	19.90	1.43

(45)

Flachproben Anlieferung (ohne Schweißnaht)

E

Gerade für die Messwerte Rang :1 bis Rang :19
Sollen andere Messwerte verwendet werden? :



B-23

(91)

Glas:	Name	:Zerodur
-----	Nummer	:-
	Artikel,Anzahl	:Staebe,15
	Datum des Probeneingangs	:5.1.82
Prüfung:	Maschine	:1
--------	Kraftanzeige der Maschine N oder kp	:kp
	Probenlänge mm	:110
	Ls	:100
	La	:20.8
	Messgeschirr Nr.	:-
Vorbehandlung,Oberflächenzustand der Probe		:320er Korn

F

	Datum Prüfbeginn	:15.1.82
	Datum Prüfende	:20.1.82
	Prüfungsart	:nass

Ergebnisse für die Werte von Rang 1 bis Rang 15

Mittelwert	N/mm↑2	: 64.73
Standartabweichung		: 5.68
Weibullfaktor		: 12.86
charakteristische Festigkeit		: 67.25
kleinster Wert		: 55.26
grösster Wert		: 77.08
Korrelationskoeffizient		: 0.9709

Flachproben ohne Schweißnaht, mit 320er Korn

F

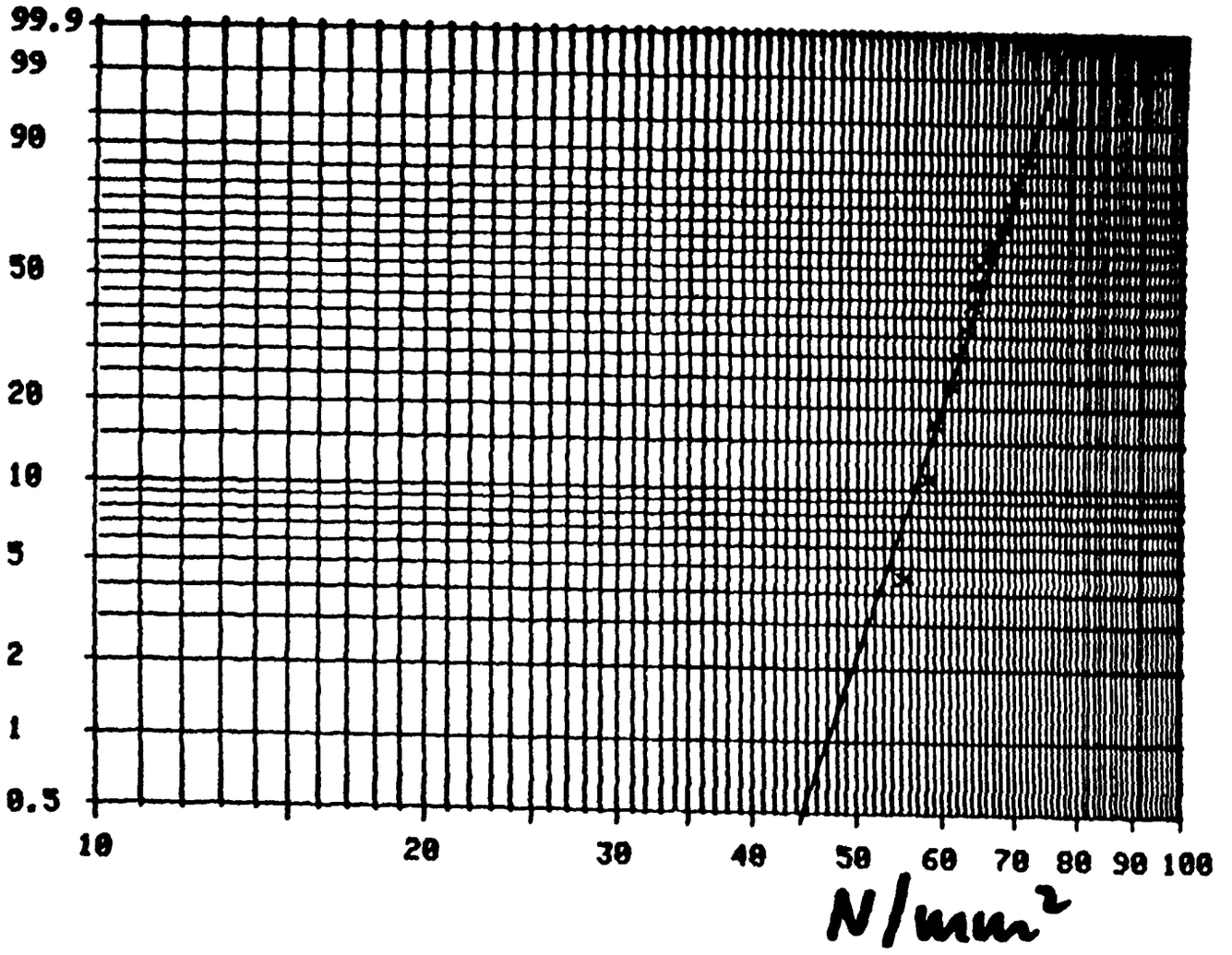
Rang	Bruchsp.	Median Rank	Kraft	Zeit	Dicke	Breite	Rate
	N/mm^2	%	N	s	mm	mm	N/mm^2s
1	55.26	4.55	151.07	26	4.04	19.90	2.13
2	58.12	11.04	155.00	30	3.99	19.90	1.94
3	58.94	17.53	166.77	63	4.11	19.90	0.94
4	60.81	24.03	168.73	32	4.07	19.90	1.90
5	61.76	30.52	175.60	33	4.12	19.90	1.87
6	62.71	37.01	176.58	47	4.10	19.90	1.33
7	63.50	43.51	177.07	38	4.08	19.90	1.67
8	63.93	50.00	180.01	55	4.10	19.90	1.16
9	64.63	56.49	181.98	32	4.10	19.90	2.02
10	66.05	62.99	181.49	51	4.05	19.90	1.30
11	67.86	69.48	187.37	39	4.06	19.90	1.74
12	68.96	75.97	192.28	38	4.08	19.90	1.81
13	69.94	82.47	189.33	36	4.02	19.90	1.94
14	71.40	88.96	194.24	32	4.03	19.90	2.23
15	77.08	95.45	213.86	34	4.08	19.80	2.27

(18)

Flachproben ohne Schweißnaht, mit 320er Korn nachbearb.

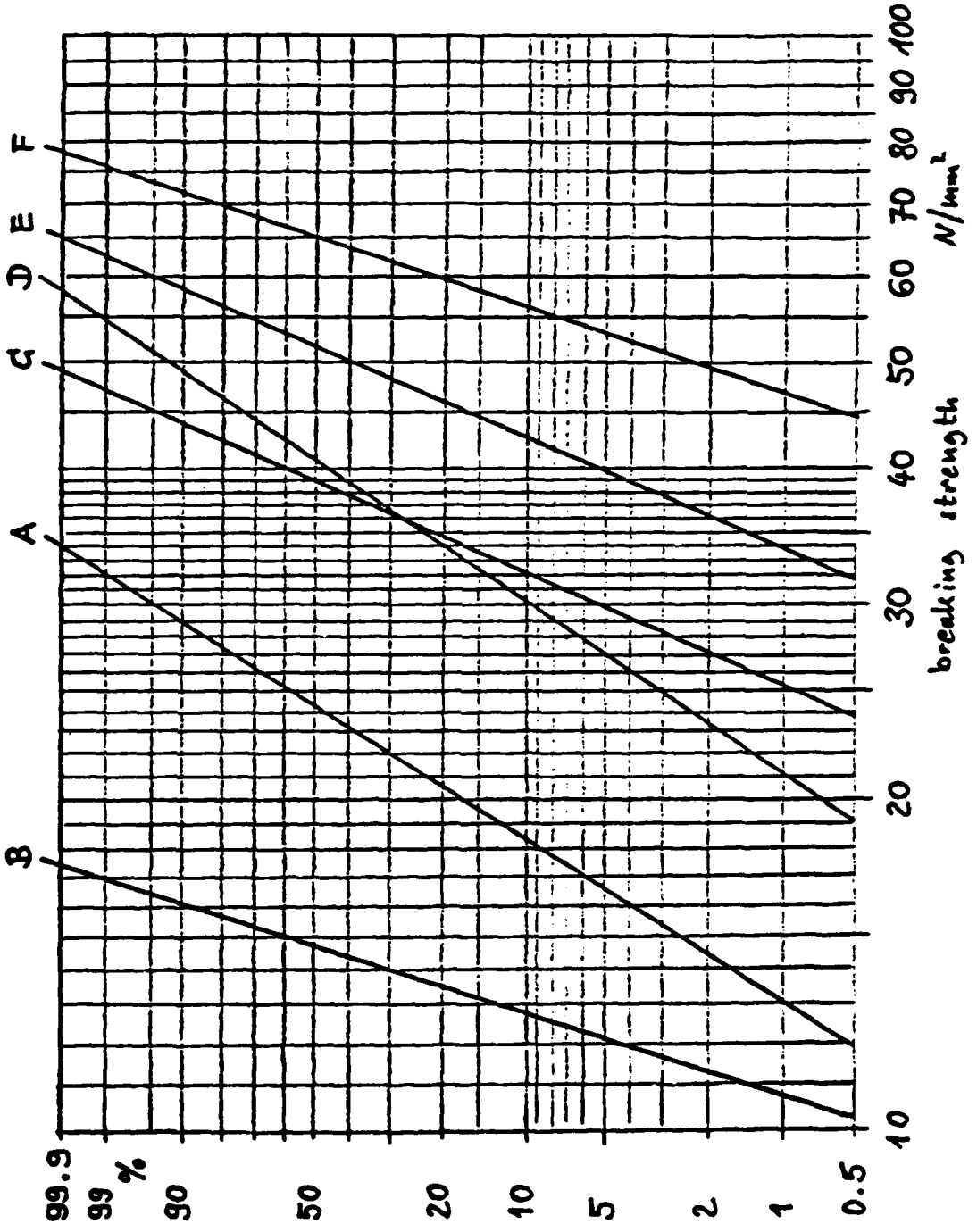
Gerade für die Messuerte Rang :1 bis Rang :15
Sollen andere Messuerte verwendet werden? :

F



B-26

(49)


A
B
C
D
E
F
99.9
99
%
90
50
20
10
5
2
1
0.5
10
20
30
40
50
60
70
80
90
100
breaking strength
N/mm²

APPENDIX C

SCHOTT REPORT

"Production of a Core Section Made by the Welding Process"

Report

on the

production of a core section made by the welding process (referring to paragraphs 3.1.5 of the contract).
A sample was sent to PE at the beginning of April, 1982.

This report describes the production of core sections from Zerodur and the technical glass ceramic Robax by welding bent glassy plates. It contains information about equipment, materials, production of bent plates, welding of cores, and ceramizing of cores.

1. Equipment

1.1. Extension of the available bending machine. so that we were able to bend the glassy plates at both sides in order to receive half of a hexagon.

1.2. Design and construction of the welding machine; design and construction of the required control equipment for an automatic run of the welding process.

1.3. Design and construction of an oven door with an opening in which the welding process runs.

1.4. Setting up the bending plant, consisting of preheating oven, bending machine, annealing oven.

1.5. Setting up the welding plant, consisting of a first preheating oven, a second preheating oven, the welding machine combined with the annealing oven.

2. Materials

2.1. Production of glassy Zerodur plates from cast, quickly annealed blocks (180x180x160 mm) by

sawing
grinding (grain size 320, final dimensions 170x100x4,1mm)
drilling (1 borehole Ø 5 mm in the middle or at the side of the plate)

2.2. Production of glassy Robax plates (technical glass ceramic) from rolled sheets of 4 mm thickness by

sawing
grinding (edges only)

3. Performance of the experiments

3.1. Production of bent plates

3.1.1. Bending was done with the same equipment and under the same conditions of temperature and time as we had for production of the samples for measuring ε and CTE (see earlier report)

3.1.2. Checking of the bent plates concerning the bending angle at both sides (60°) and the right angle (90°) between bending edge and hexagonal base.

3.1.3. Sawing the bent plates to different length of the sides for being able to find out the right length in preexperiments with the welding machine.

3.2 Welding of the core

Maintaining all bent plates required for 1 core at approx. 500°C in the first preheating oven; no nucleation occurs at this temperature.

Maintaining 1 magazine each for 2 and 3 bent plates, respectively in the second preheating oven at approx. 650°C.

Maintaining the oven conveying device of the welding machine within the welding oven at approx. 650°C (oven port closed).

Run:
Opening of welding oven, withdrawing conveying device, and closing port.

Mounting of ceramic cleats and first line of bent plates (3 pieces, room temperature) into the conveying device.

Moving conveying device into oven, closing of port, and awaiting temperature of approx. 650°C (duration approx. 8 min.).

Transferring 2 bent plates (500°C) in magazine (650°) and preheating to approx. 650°C in approx. 4 min.

Withdrawing conveying device with first line of bent plates from welding oven and placing in welding position.

Transferring magazine with 2 bent plates (650°C) into welding machine.

Start of welding process with automatic run:

elevation of burners into welding position and ignition of gas-oxygen-mixture;
melting time approx. 5s;
lowering of burners and turning off;
compressing of plates at the melted-on edges;
lowering the tilting table and withdrawal of empty magazine.
moving conveying device into the welding oven by 1 step, and moving it completely by hand into the oven and closing the port;
transferring of empty magazine into the second preheating oven;
removal of next magazine and placing 3 bent plates into same.

etc.

with 1 line following every 5 min.
welding together maximum of 7 lines
(for 4 closed hexagons 5 lines only);
heating up of welded core in welding oven to 700°C, turning off oven, cooling-off within approx. 15h to room temperature.
dismontage of core.

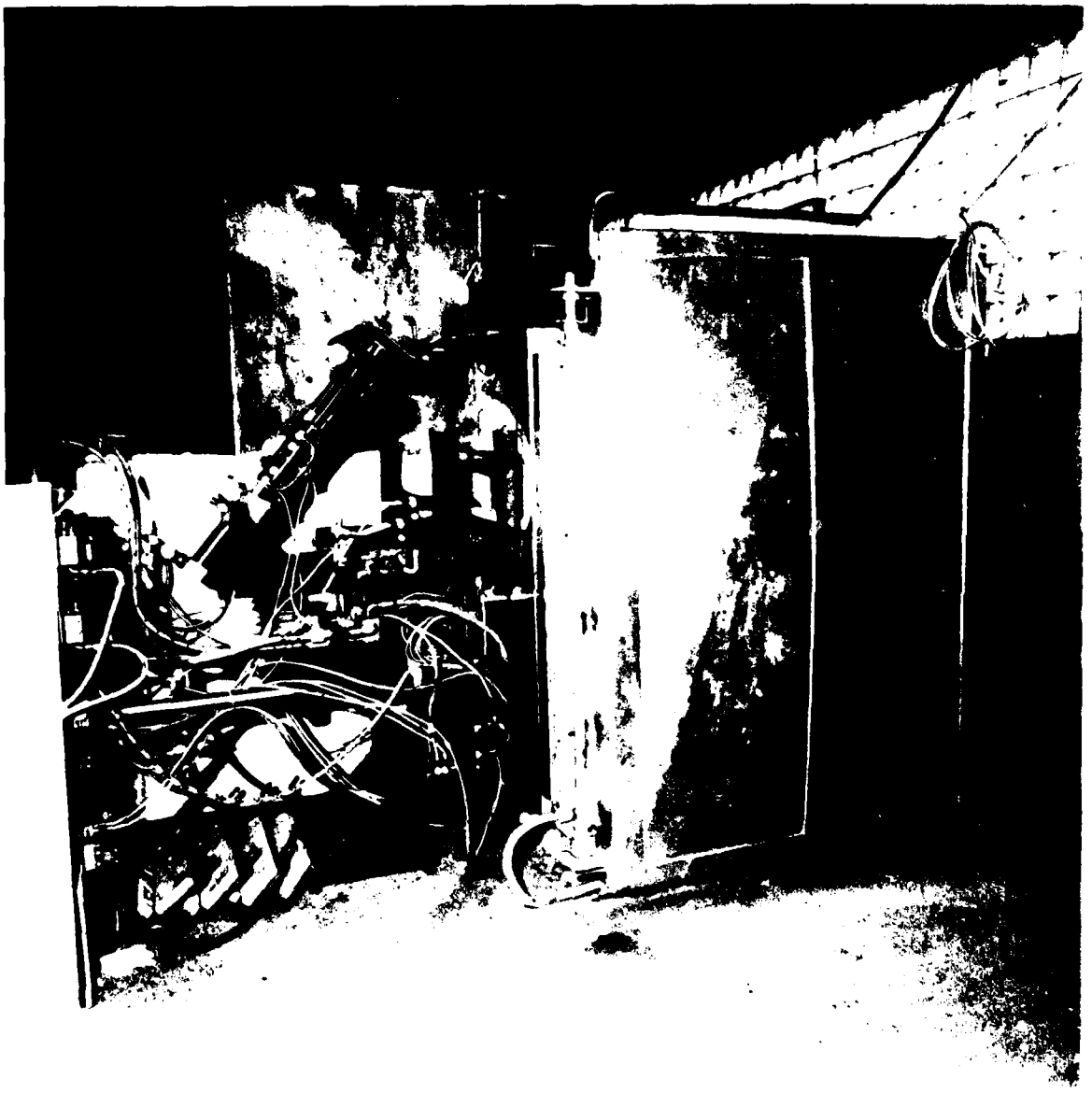
3.3. Ceramization of the core

Sample received by PE was ceramized with nearly the same temperature-time-program as the samples for measuring σ and CTE.

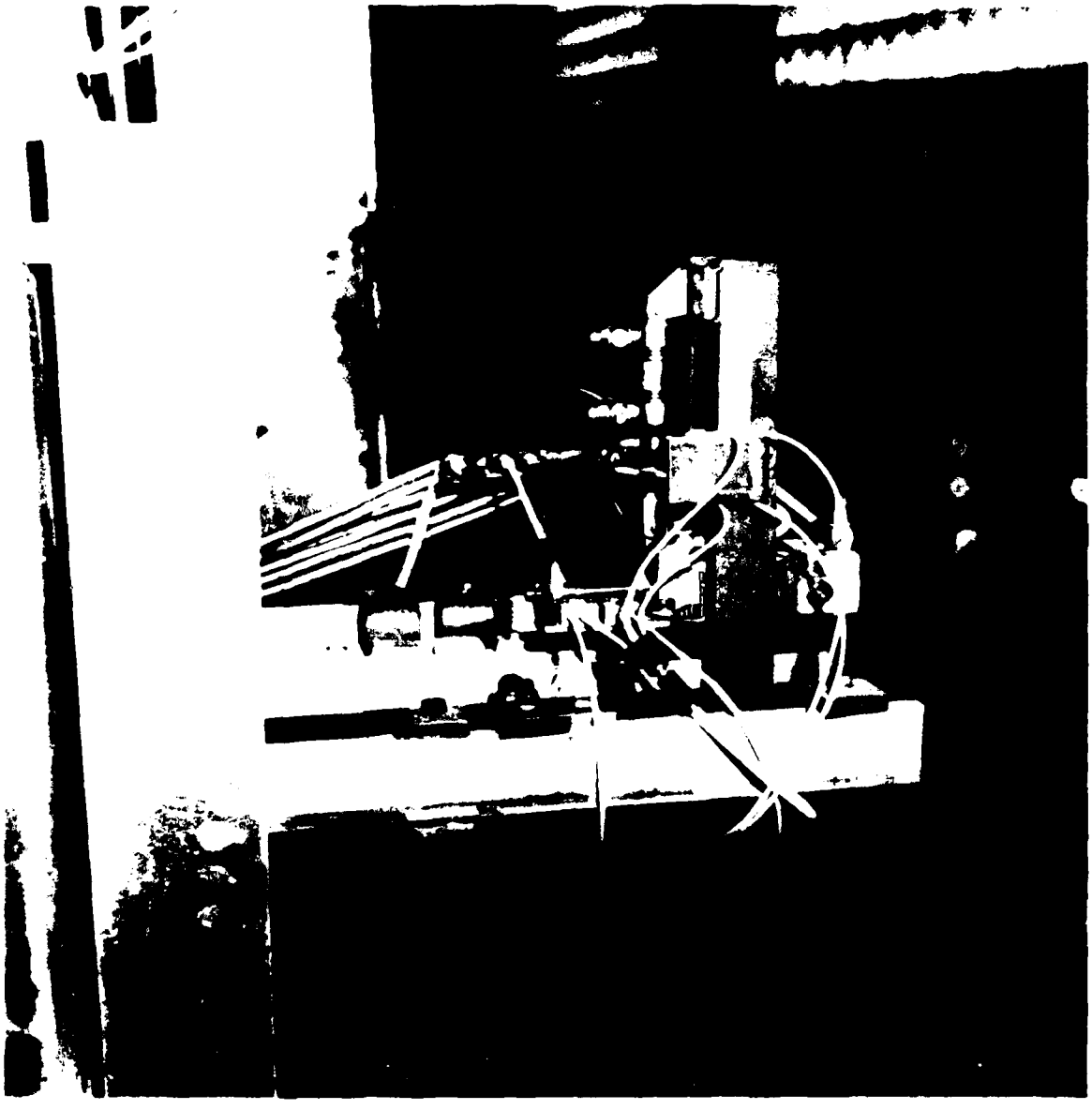
2 additional samples have been ceramized, while 1 sample with 7 closed hexagons still is available in the vitreous state.

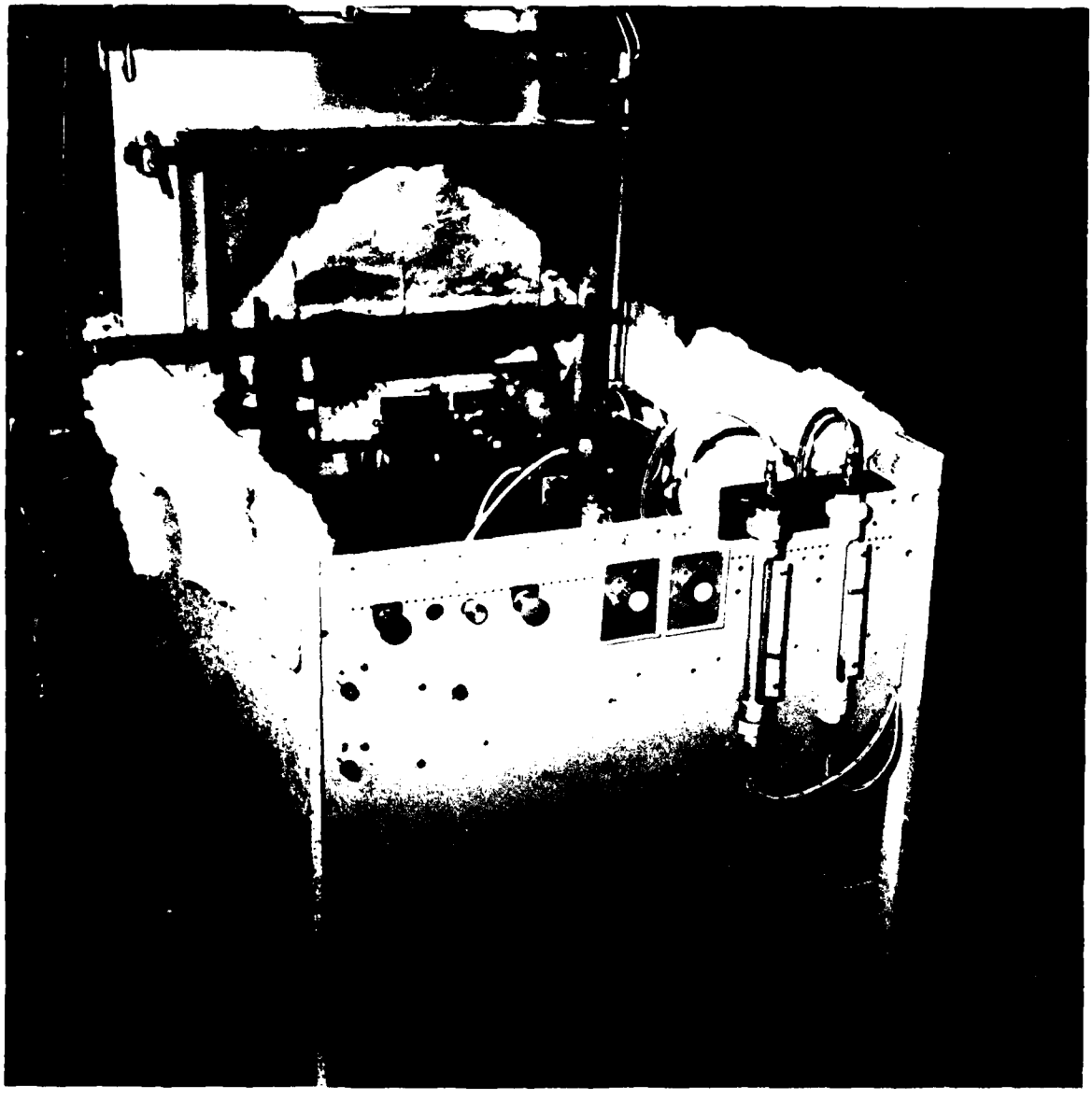
3.4. Conclusion

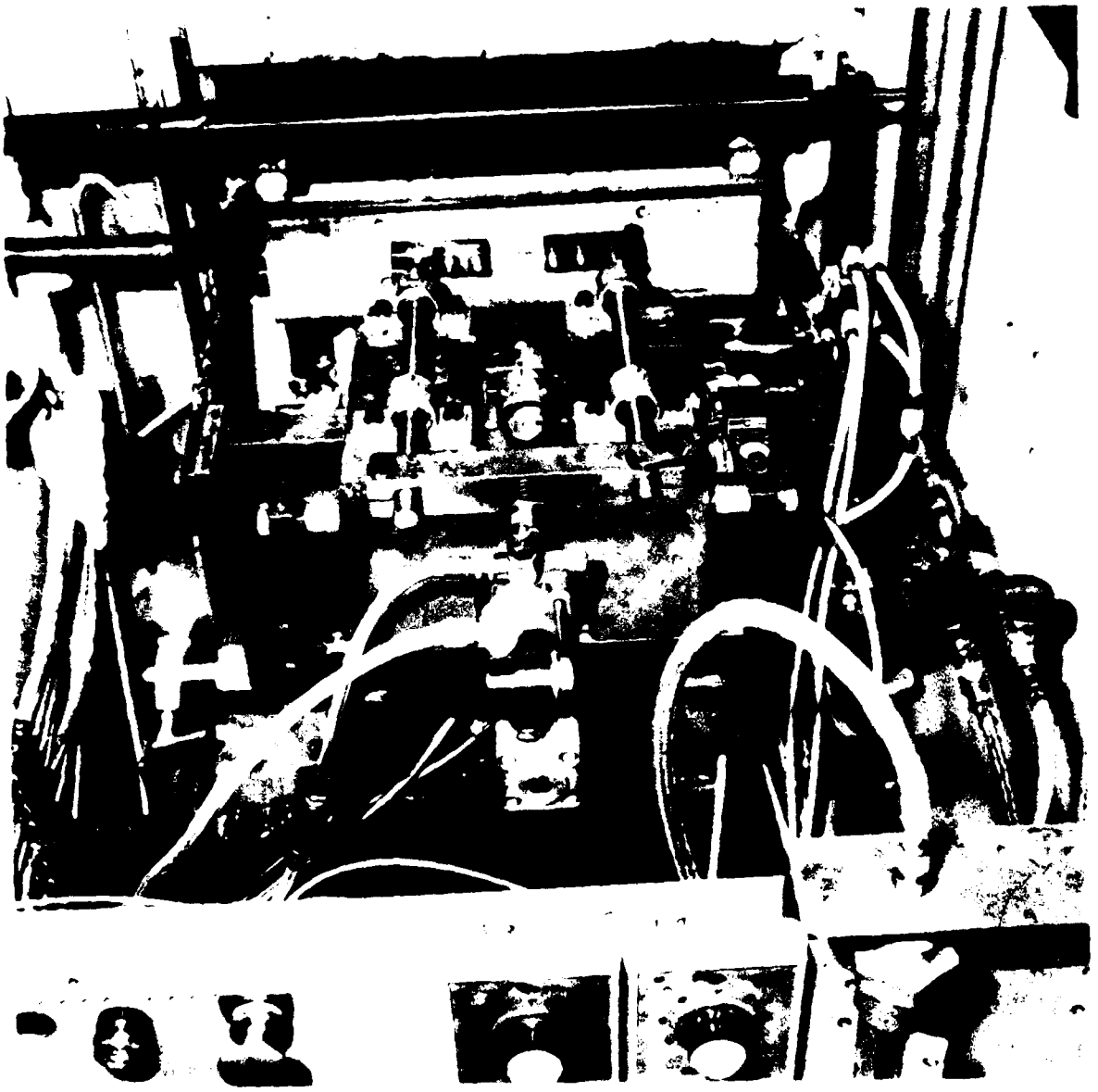
Welding and ceramizing of the core were done essentially under the same conditions as we had for production of the samples for measuring σ and CTE (see earlier report).

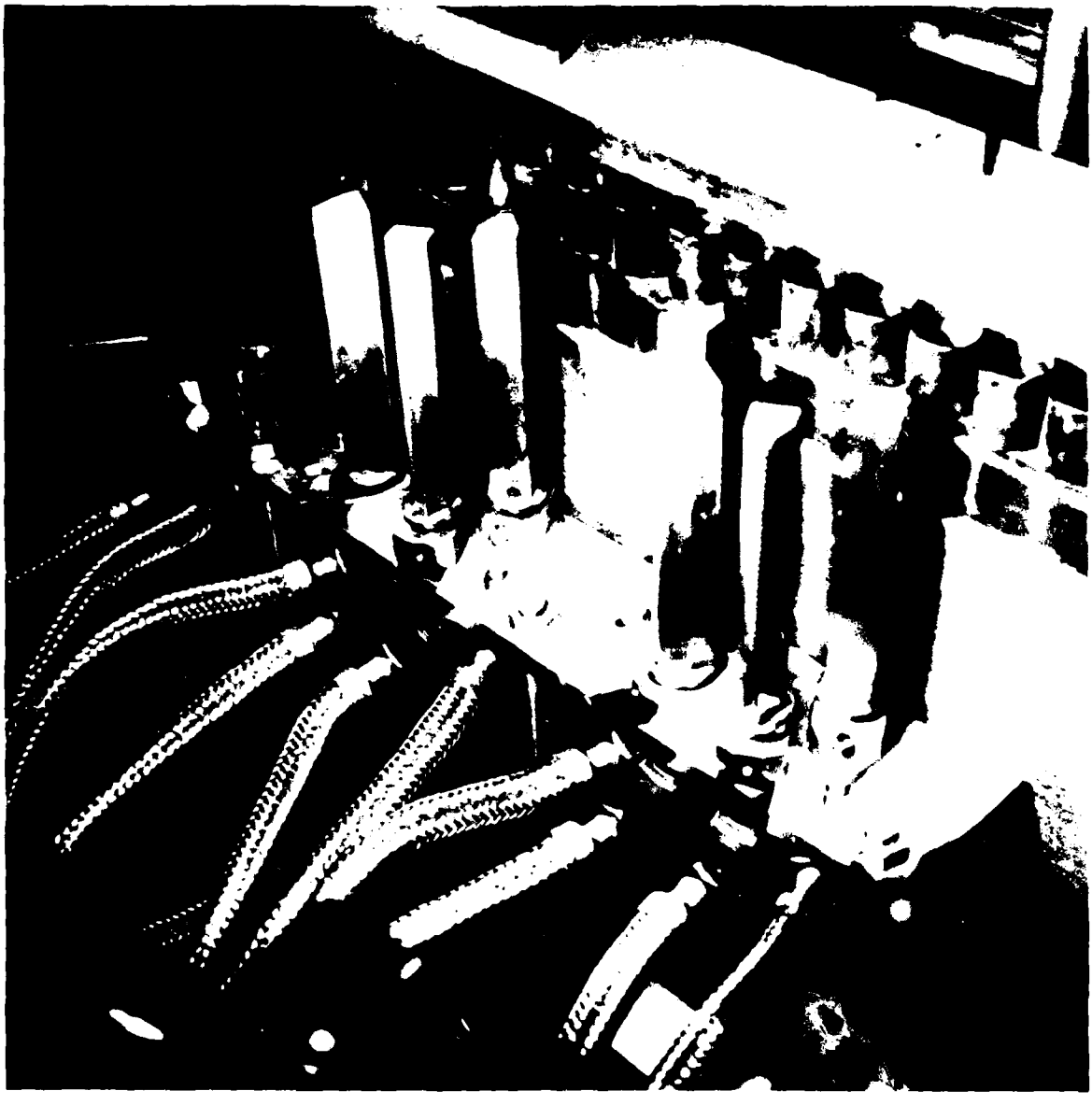


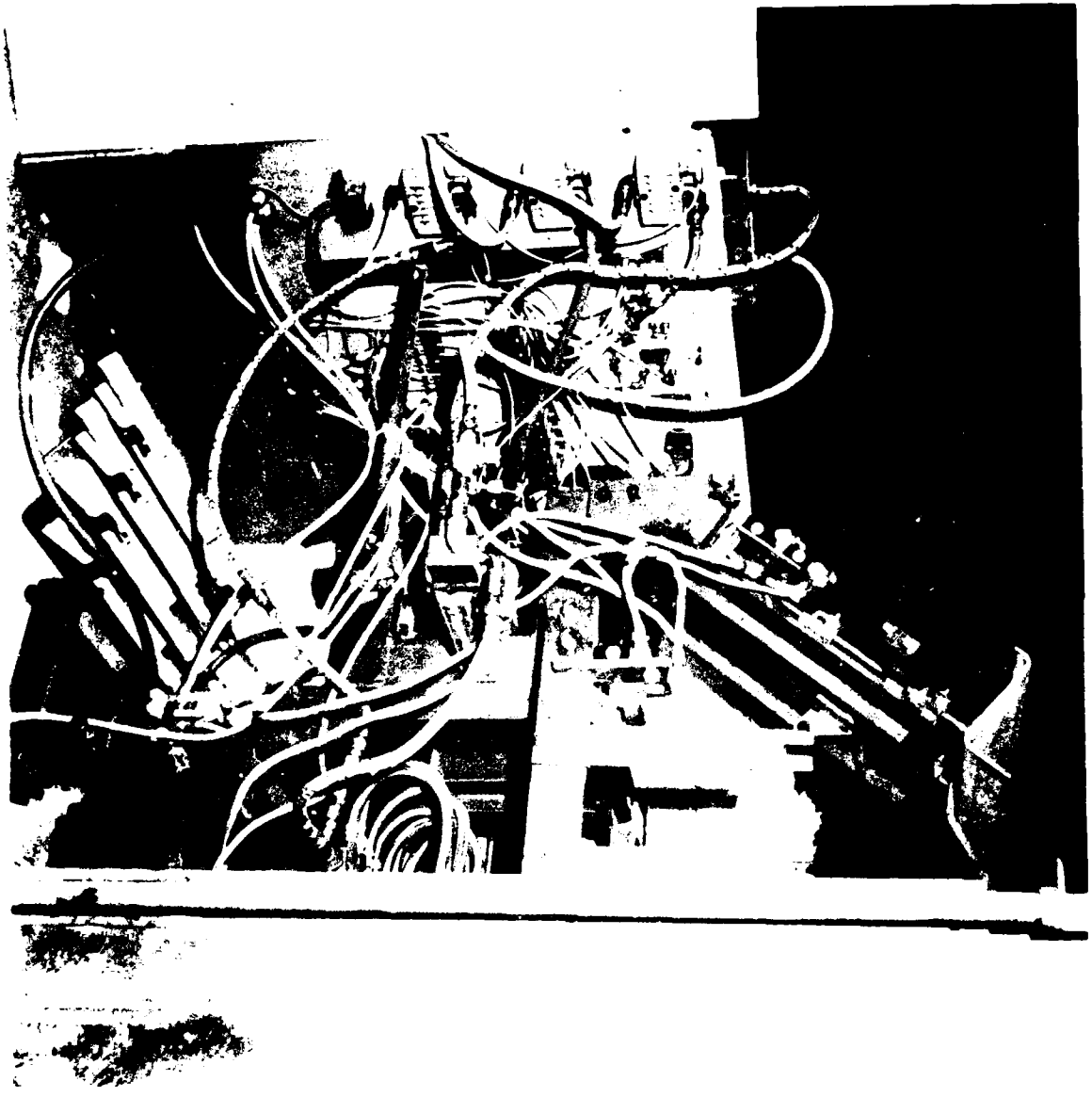


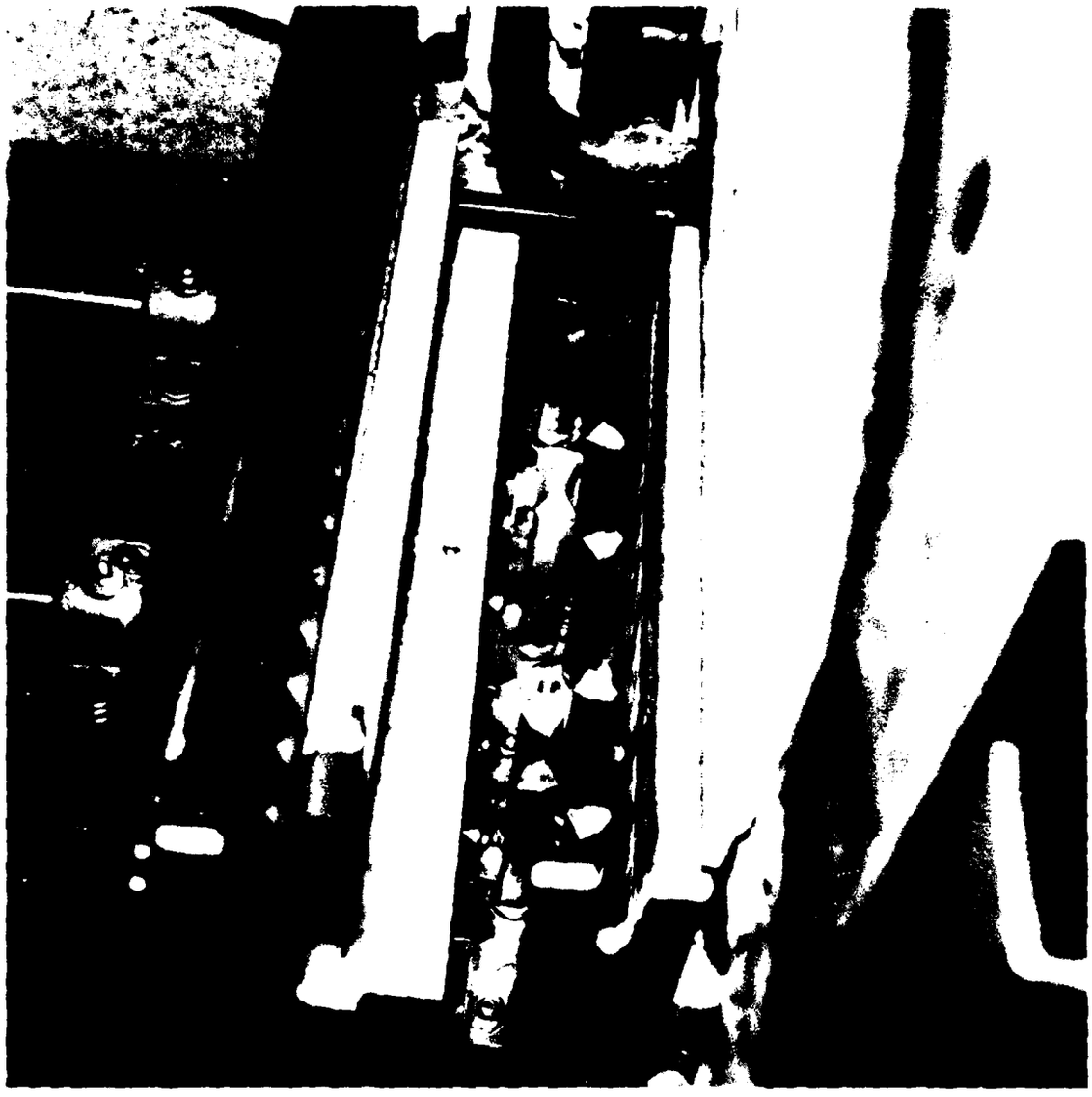












APPENDIX D

SCHOTT REPORT

"Spin Casting"

Mainz, March 22, 1982

Preliminary note on the study of spin casting

The present study does not include the costs for the melting tank.

SCHOTT posses the know-how for building a melting tank capable of yielding the glass quantities needed per unit of time for the spin casting of face and bottom sheets for light-weight mirrors. At the moment, we do not have available a tank of the type described.

Building a melting tank at the site of an already existent tank unit will take some 9 months, which means that less time is needed for the building of a tank than for designing and setting up the spin casting unit.

The costs for building the tank will amount to 555 T$.

Mainz, March 22, 1982

Abstract of the study on spin casting tests

SCHOTT have gained experiences in the spin casting of industrial large-capacity glass vessels. The study describes the application of this known spin casting process to the manufacture of 1.5 m dia. or 2.1 m dia. curved ZERODUR plates. Further development covers the following items:

- Larger diameters, 1.5 and 2.1 ,, resp. (up to 4 m later on),
- Larger radiuses of curvature,
- ZERODUR instead of glass.

The following costs have been calculated for further development:

- Costs for glass and melt		800 T$
- Costs for annealing	(22 T$)	65 T$
- Costs for design and construction of the casting unit		750 T$
- Costs for performing tests		350 T$
		1,965 T$

The costs given in brackets refer to the 1.5 m dia. face plate. Costs covering the melting tank are not included (please cf. preliminary note).

The time to be expended from receipt of order for design and construction of the spin-casting unit is 2 years, while one year will be needed for performing the tests and preparing the sample blank. Some likely and additional postponement of the time schedule due to the construction of the melting tank has not been considered here (please cf. preliminary note).

Mainz, March 22, 1982

Study on the manufacture of curved face and bottom sheets for ZERODUR light-weight mirrors by spin casting

SCHOTT have experiences in the spin casting of industrial large-capacity glass vessels. The present study, starting from the mentioned experiences, is meant to describe the further development of the spin casting process for the manufacture of curved ZERODUR plates, 1.5 m and 2.1 m in dia., respectively. The further development covers the items listed below:

- Larger diameters, 1.5 m - 2.1 m (later on, up to 4 m in dia.).
- Larger curvature radiuses.
- ZERODUR instead of glass.

The following costs are covered by the present study:

- Costs for glass.
- Costs for design, construction and installation of 2.1 m dia. spin casting unit (subgroups of the spin casting unit can be coverted to 4 m dia.).
- Costs for tests.
- Costs for annealing.
- Costs for sample blank.

What is to be determined is the time required from receipt of the order.

Costs and time needed for the melting tank (please cf. preliminary note) have not been taken into account.

1. Theoretical considerations

The present study has been based on the dimensions submitted to us by telex from PERKIN ELMER of February 2, 1982.

1.1. Calculating the spin casting rotational speed

Theoretically, a full-parabolic inside contour is caused during the spin casting.
The contour can be adapted to a sphere at the apex and at the edge.
In the case of flat calottes, contour variations are of the order of a few 1/10 mm only and can be neglected.

Formulae:

$$n = \frac{30}{\pi} \sqrt{\frac{g}{p}}$$

$$p = \frac{D^2}{8h}$$

$$h = S \left(1 - \sqrt{1 - \left(\frac{D}{2S}\right)^2}\right)$$

n = rotational speed in rpm.
g = acceleration due to gravity, g = 9,81 m/s²
p = parabolic opening
D = calotte diameter
h = vertes of calotte (without wall thickness)
S = curvature radius of calotte

In practice, deviations from the theoretical speed of rotations have to be expected:

- Downward; during feed-in.
- Upward; for faster spinning out.

1.2. Compilation of numerical values

The face and the bottom sheets of the varous mirror types are identical as far as their dimensions are concerned. In the case of the 4-m mirror, the curvature data vary from a radius of 6 - 16 m. Since determination is impossible, the two limits will be considered in the design, and so will the more far-reaching consequence in all individual cases.

The preliminary wall thicknesses achievable by means of the spin casting technique are estimated in proportion to D.

The mass (M) is calculated from the mean thickness.

Table 1

Data referring to the geometry of spin-cast plates.

Type No.	1	2	3	4	5	6	7
D (mm)	500	1000	1500	2000	2100	4000	4000
ϱ (mm)	2000	4000	1000	8000	10000	6000	16000
h (mm)	15,7	31,4	28,2	62,7	55,3	343	125,5
p (mm)	1990	3980	9990	7970	9972	5828	15940
d (mm)	12,5	25	37,5	50	52,5	100	100
M (kg)	6,1	49	166	393	455	3142	3142

In accordance with the task set, the present study covers in detail types 3 and 5 (small spin casting unit) and 6 and 7 (large spin casting unit).

In the feed-in of the glass strand into the mold, the feed-in level from outlet lower edge to mold bottom upper edge represents an essential characteristic value, which determines the constructional set-up, and SCHOTT have special know-how about this. Owing to this particular condition, attention must be paid to this item in the development of the process for the 1.5 m mirror. Modification of the height later on must be feasible and will be considered in cost calculation.

2. Description of the units

2.1. Melting tank

Within this study, the melting tank is taken for granted (please cf. preliminary note). The requirements to be met by the melting tank will be as follows:

- Feed-in throughput:	Controllable up to 20 kg/s.
- Temperature:	Approx. 1.450 °C ($\eta = 1 \cdot 10^3$ dPs).
- Height of drop onto mold bottom surface:	2.6 - 2.8 m max.
- Max. output per one casting:	750 kg, small mirror; 5500 kg, large mirror.

The feed-in unit is equipped with shutter, shears and swivel chute.

2.2. Spin casting unit

The small spin casting unit is shown in annex 1 (SK 912), while the large spin casting unit is evident from annex 2 (SK 906). In the drawings covering the small spin casting unit, the largest diameter assumed is that of 2.1 m.

The spin casting unit consists of the following:

- Machine base with displacing frame,
- Mold support,
- Drive with power unit and shaft,
- Control mechanism.

It is envisaged using the same drive components and the same control mechanism for the two spin casting units.

2.2.1. Spin casting mold

The spin casting molds for small and large mirrors of different dimensions are illustrated in annex 3 (SK 907).
The set-up consists of segment units guyed by means of tie rods, the glass-contacting side exhibiting an unworked casting skin.

2.2.2. Suction disk

The suction disk is evident from annex 4 (SK 908) for small and large mirrors of different dimensions.
The envelope of the asbestos cloth unit is adjusted to the calotte contour.

2.2.3. Covering hood and heat maintenance burners for spin casting mold

Both covering hood and heat maintenance burners are dependent on the mirror diameter.

2.2.4. Carrying support for transfer to lehr

A support is shown in annex 5 (SK 909) for conveying large mirrors into the lehrs. Smaller mirrors are carried in transportation boxes.

2.2.5. Preheating hood

The preheating hood is required for preheating the support and the vacuum lifting plate.

2.3. Annealing

The transportation boxes used for transferring small mirrors into the lehrs are moved by means of fork-lift trucks, while the carrying support for large-sized mirrors is moved by means of the lift truck available.

The 1.5 m mirrors are annealed in the hooded annealing lehrs available, while the 2.1 and 4 m dia. mirrors are annealed in 4 round-type annealing lehrs.

3. Process course

- The mold is preheated up to the operating temperature required, using the preheating burners and the screening hood; the optimum temperature should be determined through experiments. At the same time, carrying support and vacuum lifting plate are heated.

- After removing the tap-out block, a purification strand first runs into the swung-on outlet chute.

- To initiate the feed-in process, the shear cut motion is started.
  Prior to this, the spin casting unit has to be operated in a manner as to reach the feed-in rotational speed (no reduced and full rotational speed).
  At the same time the shear cut motion is initiated, the chute is being swung off.
  The new strand now drops, centrally or slightly offset, into the non-moving or rotating mold. The precise conditions will have to be determined by experiments.

- Feed-in is terminated by the shear cut motion and the swinging-in of the chute, and step-up of the rotational speed, if necessary, is started as a function of time.

After reaching the final speed of rotation, same will be maintained until the glass has sufficiently solidified so that the glass will not be able to run back into the interior.
The burners are meant to support the spinning-out and are turned off after molding has been completed. The optimum rotational speed: time course, as well as the wall thickness achievable, are determined within the experimental program.

- As soon as the spin casting unit has been slowed down, it is moved, using a displacement frame, away from the melting tank area to a place far enough to allow the vacuum lift-up disk to be superimposed.

  The following are the subsequent steps:

  - Draw-in and lift-off of blank,
  - Placing the mirror onto the preheated and sand-strewn carrying support and transportation box, respectively, and
  - transfer into the annealing lehr.

4. Development of technology

4.1. Testing the feed-in technique

The feed-in technique can be tested after completion of the melting/feeder system irrespective of the spin casting unit.

- Closure technique, cutting, swivel chute,
- Throughput,
- Stable strand area/feed-in level.

Depending on the test results obtained, modifications may have to be performed, e.g. lifting of spin casting unit etc.

4.2. Mechanical testing of spin casting unit

The mechanical testing of the spin casting unit (with mold) can be performed after completion, irrespective of the feed-in system.

- Range of rotational speed,
- Period of acceleration,
- Running quietness, possibly mechanical defects,
- Familiarization with service,
- Cold-condition testing of handling operations, possible of dummy.

4.3. Testing of mold heat-up

Attaining the temperature desired:

- How fast can it be realizied?
- What is the temperature distribution like?

Certain circumstances might necessitate modifications to the heating-up system.

4.4. First spin casting test series

Clarification of conditions possible in respect of feed-in:

- Feed-in rotational speed,
- Eccentricity (in feed-in into rotating mold),
- Mold temperature.

Spin casting at first takes place at theoretical rotational speed and with mean weight.

4.5. Second spin casting test series

- Variation of spin casting rotational speed and of
- feed-in quantity

in respect of complete spin casting with even contours and a possible minor wall thickness.
After completion of this test series, the conditions will have been laid down.

4.6. Third spin casting test series

This test series' objective is to confirm that the process is able to be controlled. It is conceivable that slight modifications to the conditions may have to be made.

The components for the delivery of samples are also manufactured during that period.

5. Cost calculation

5.1. Tank costs

Tank costs are not included in the present study (please cf. preliminary note).

5.2. Costs for design and construction of the spin casting unit

5.2.1. Small spin casting unit (2.1 m dia.)

- Design and construction of spin casting machine	380 T$
- Control and measuring technique	130 T$
- Design and construction of mold and carrying supports	95 T$
- Design and construction of suction disk, preheating area with hood	20 T$
- Expenditure for modifications (approx. 20 % cost share of design and construction costs)	125 T$
- Total costs	750 T$

The costs calculated refer to the construction of a 2.1 m dia. spin casting unit as those for a 1.5 m dia. spin casting unit are not essentially lower.

5.2.2. Large-type spin casting unit (4 m dia.)

The extra costs for enlarging the spin casting unit to a 4 m diameter can be specified only upon completion of the test series in respect of the small-type spin casting unit. By a first rough estimate, these costs will amount 650 T$ to 870 T$.

5.3. Glass and melting costs

Glass and melting costs for the spin casting tests involving 1.5 m or 2.1 m dia. mirrors will amount to 800 T$.
These costs include those for the samples blank.

5.4. Annealing costs

Annealing costs in regard to the 1.5 m dia. tests will be 22 T$ while the costs referring to the 2.1 m dia. tests amount to 65 T$.

5.5. Personnel costs in relation to tests

The following personnel are needed in relation to the tests:

1 certificated engineer,
2 technicians,
2 auxiliaries.

The activities of the certificated engineer are envisaged to commence as from the beginning of detail planning/design, and to extend onto the delivery of the sample components.
Technicians should start their activities approximately at the time construction of the unit is initiated.

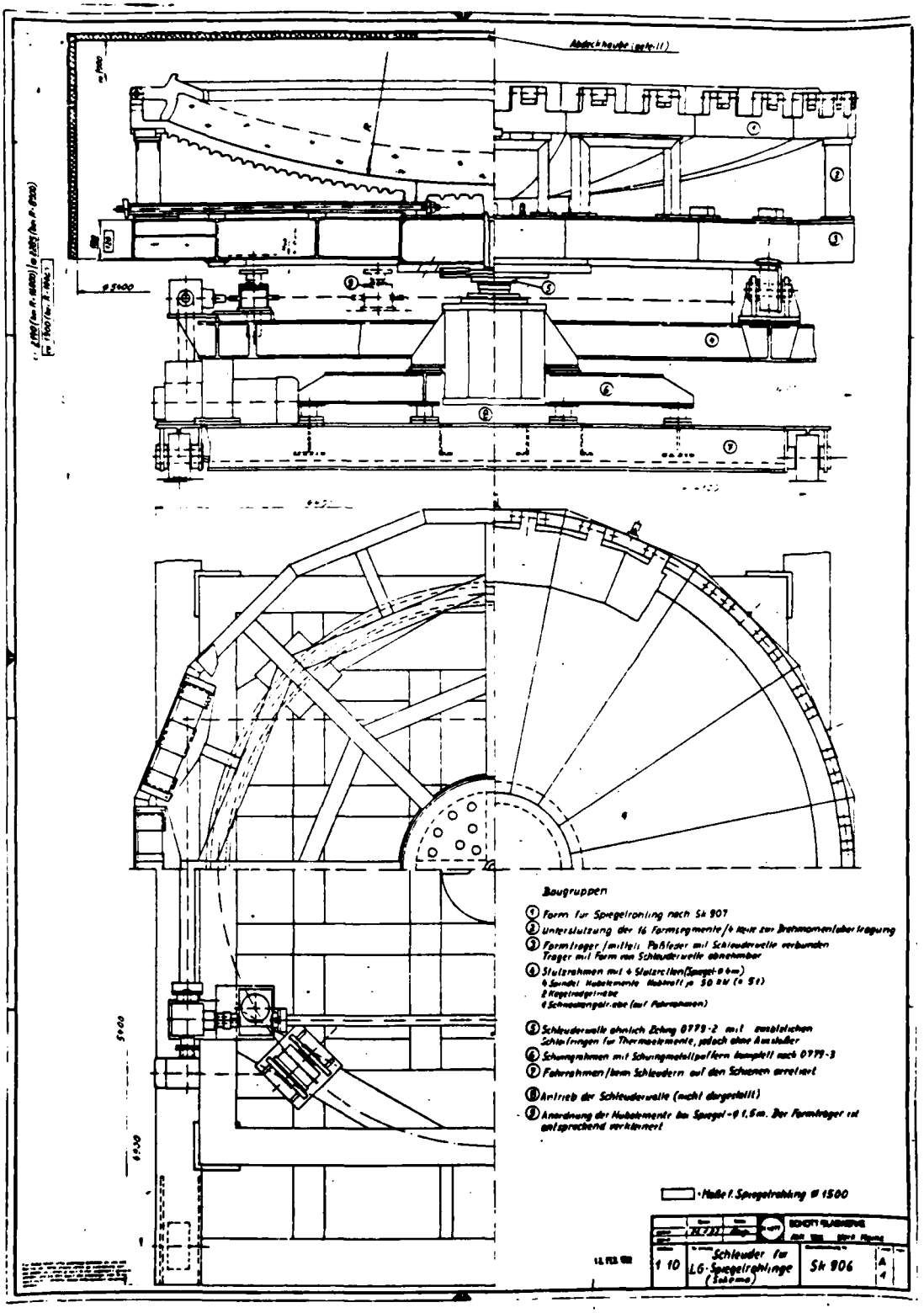
Of the auxiliaries, one will be needed for two weeks each during the experimental phases 1 and 2, while the two will be needed together during the experimental phases 4 to 6 for just 4 weeks each.

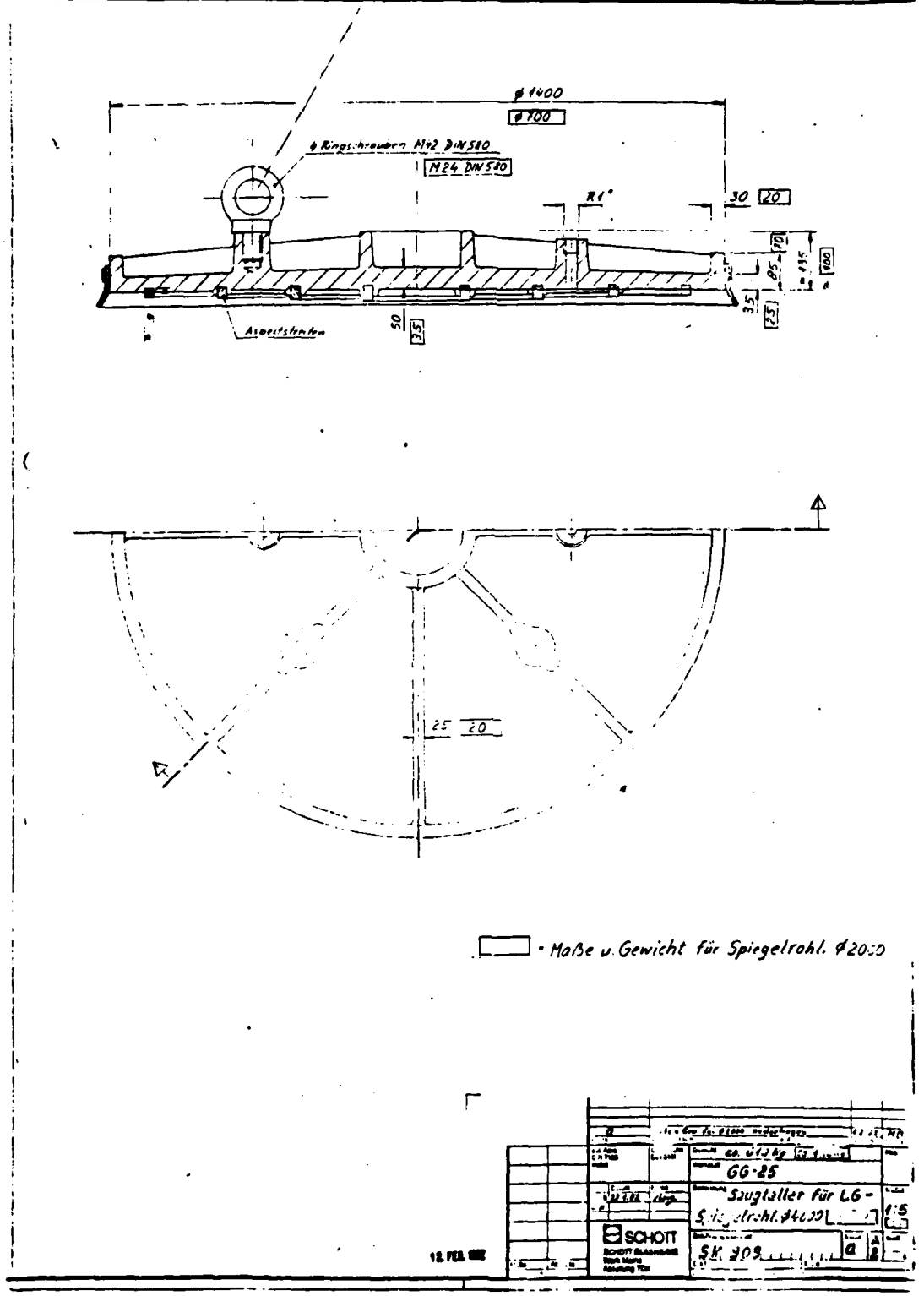
Personnel costs and expenditures:

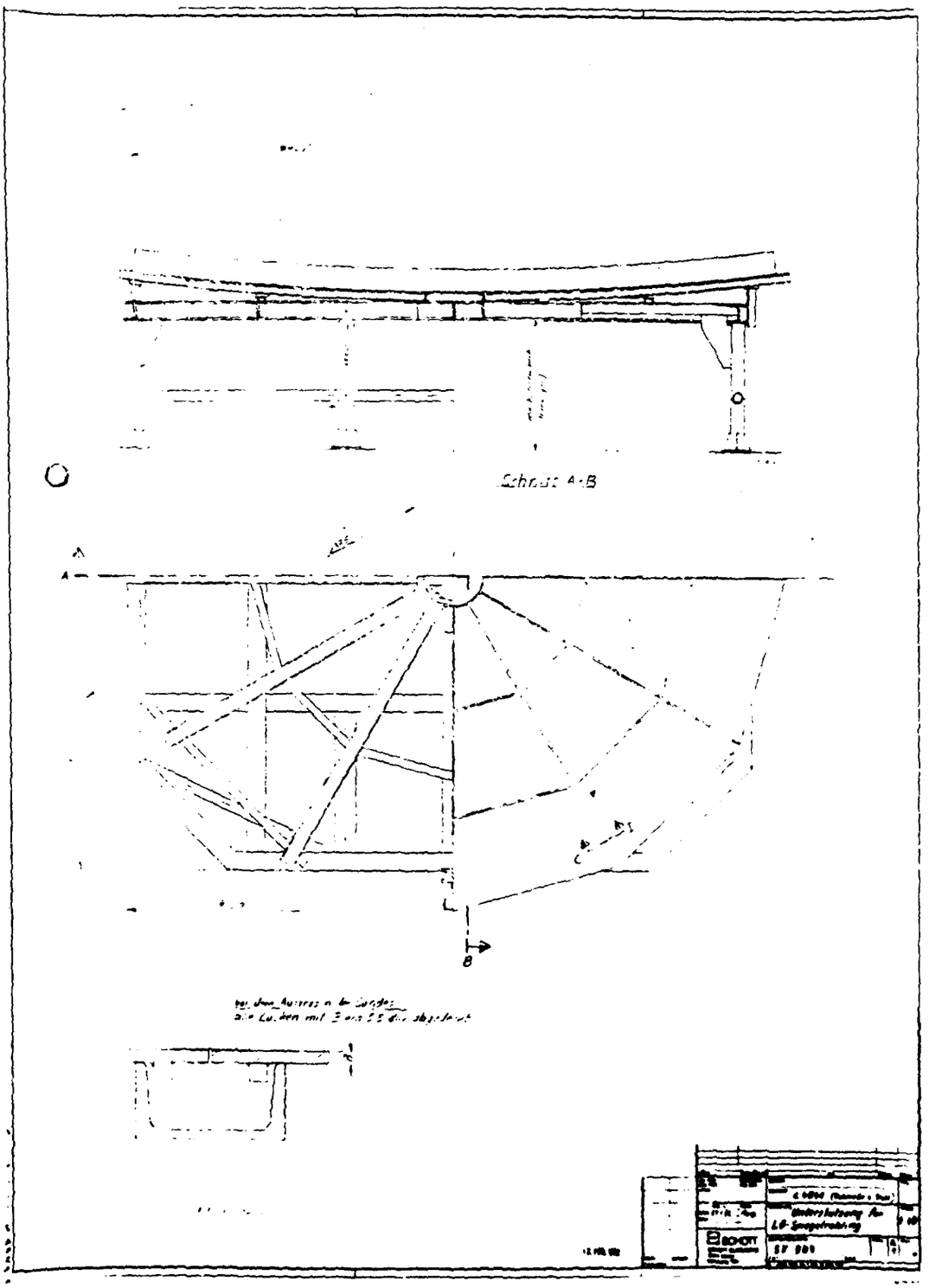
- 36 months, certificated engineer	190 T$
- 42 months, technicians	145 T$
- 7 months auxiliaries	15 T$
- Total personnel expenditures	350 T$

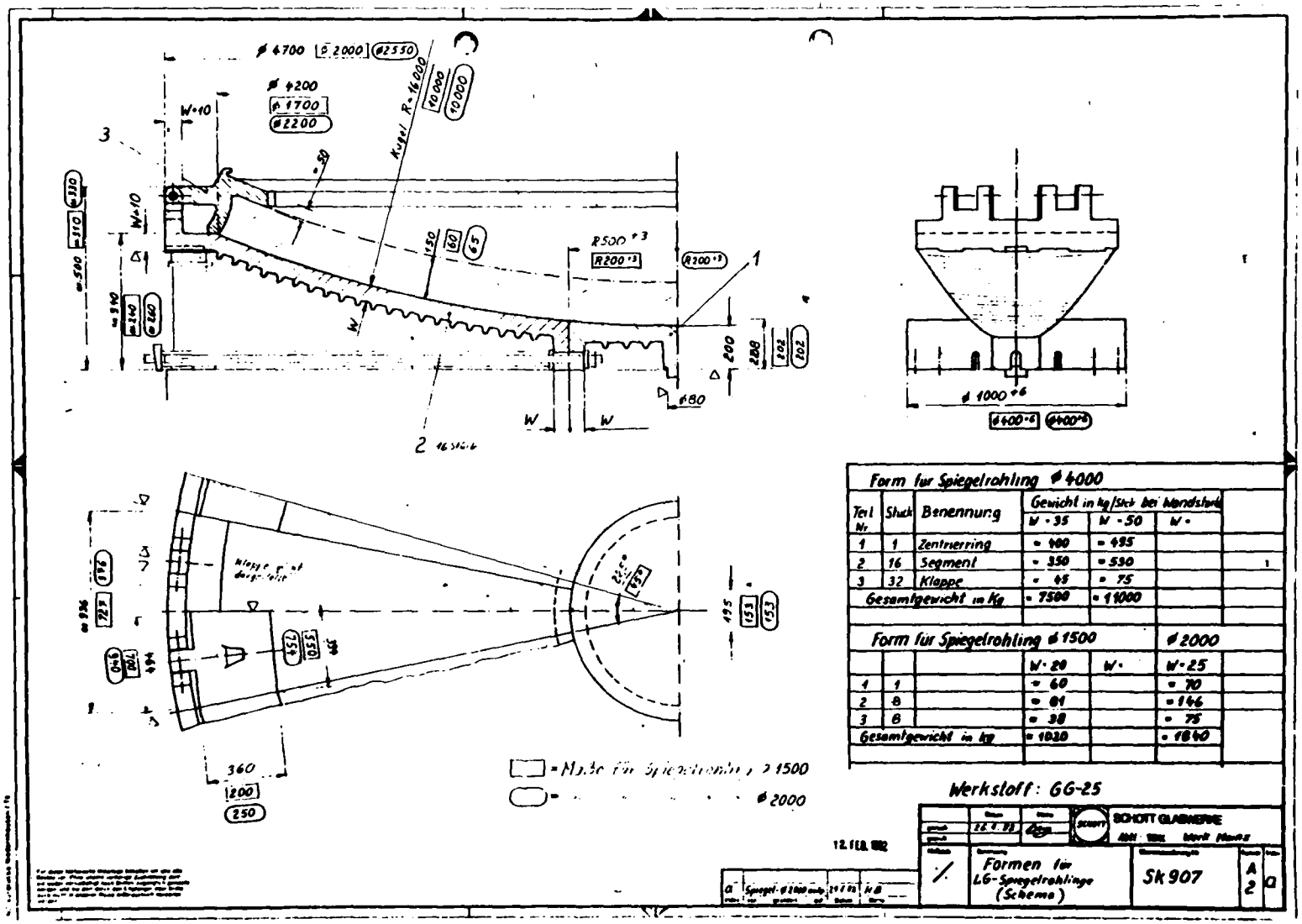
6. Time expenditure

The times indicated will be valid as from receipt of the order. Two years will be needed for design and construction of the spin casting unit (2.1 m dia.). A period of 1 year will have to be fixed for performing spin casting tests.
Costs and time to be expended for the melting tank have not been considered (cf. preliminary note).


Abdeckhaube (siehe 11)
Baugruppen
① Form für Spiegeleisring nach Sk 907
② Unterstützung der 16 Formsegmente/6 Hauptträger zur Drehmomentübertragung
③ Formträger (mittels Paßlager mit Schleuderwelle verbunden
Träger mit Form von Schleuderwelle abnehmbar
④ Stützrahmen mit 4 Stützarmen (Spiegel-Ø 6m)
4 Spindel-Hubelemente Hubkraft je 50 kN (≈ 5 t)
2 Kegelradgetriebe
4 Schwenkgetriebe (auf Fahrrahmen)
⑤ Schleuderwelle ähnlich Zeichnung 0779-2 mit entsprechenden Schleifringen für Thermoelemente, jedoch ohne Auswuchter
⑥ Schutzrahmen mit Schutzmetallpaketform komplett nach 0779-3
⑦ Fahrrahmen (beim Schleudern auf den Schienen arretiert
⑧ Antrieb der Schleuderwelle (nicht dargestellt)
⑨ Anordnung der Hubelemente bei Spiegel-Ø 1,5m. Der Formträger ist entsprechend verkleinert
Hülse f. Spiegeleisring Ø 1500
Schleuder für LG-Spiegeleisringe (1500mm)
Sk 906


ø 1400
ø 700
ø Ringschrauben M42 DIN 580
M24 DIN 580
R1"
30
20
10
85
135
100
35
25
Abgleichstrahlen
50
35
25
20
□ = Maße u. Gewicht für Spiegelrohl. ø2030
GG-25
Sauglaller für LG -
Spiegelrohl. ø4030
1:5
SCHOTT
SK 909
a
18. FEB.


Schnitt A-B
A
B
C



Form für Spiegelrohling Ø 4000						
Teil Nr.	Stück	Benennung	Gewicht in kg/Stck bei Wandstärke W = 35	W = 50	W =	
1	1	Zentrierring	= 400	= 495		
2	16	Segment	= 350	= 530		
3	32	Klappe	= 65	= 75		
Gesamtgewicht in Kg			= 7500	= 11000		

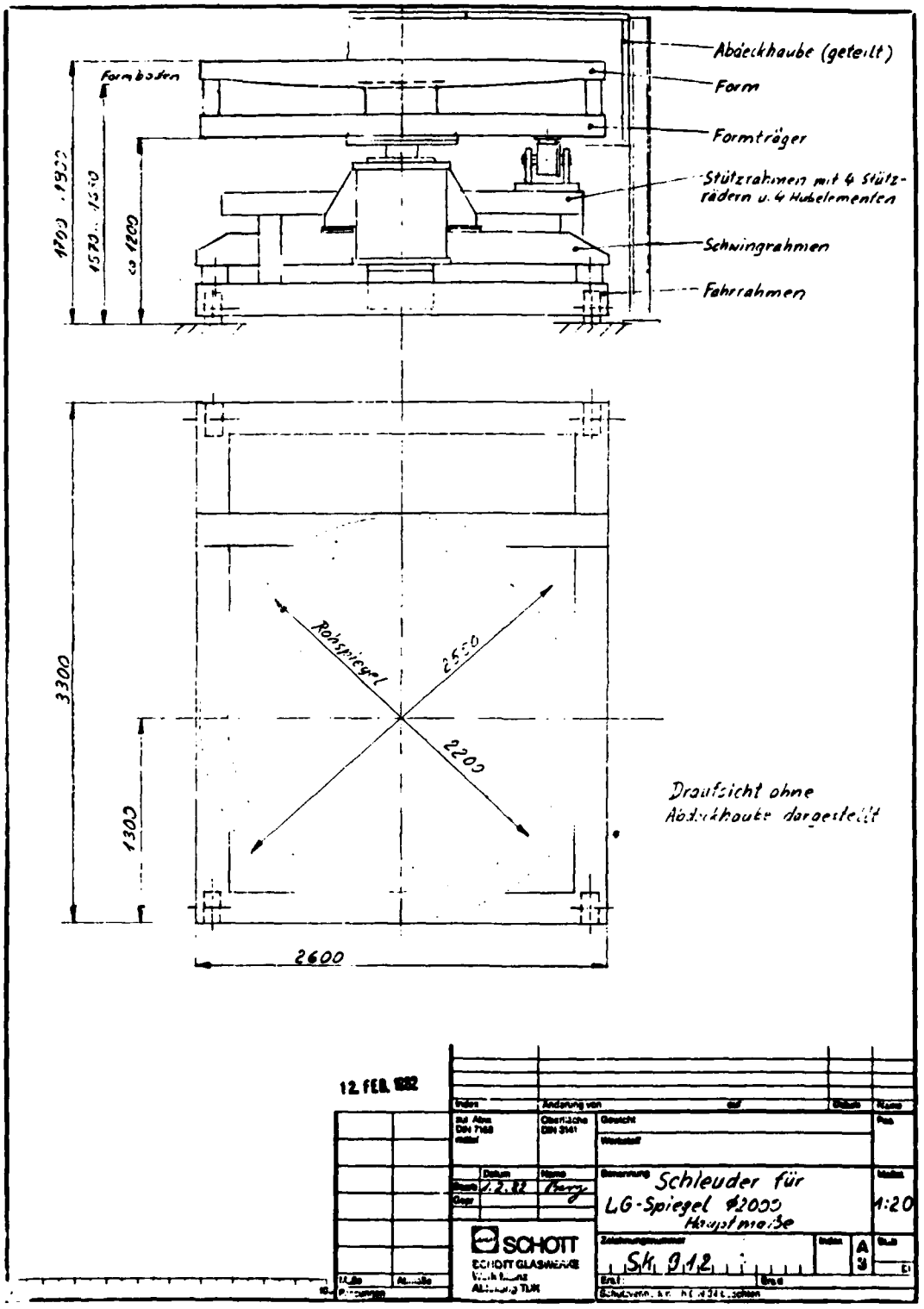
Form für Spiegelrohling Ø 1500					Ø 2000
			W = 20	W =	W = 25
1	1		= 60		= 70
2	8		= 91		= 146
3	8		= 38		= 75
Gesamtgewicht in kg			= 1020		= 1840

Werkstoff: GG-25

	12.1.82		SCHOTT GLASWERKE	
		Formen für LG-Spiegelrohlinge (Schema)	Sk 907	A 2 / a

12. FEB. 1982

D-18


Abdeckhaube (geteilt)
Form
Formträger
Stützrahmen mit 4 Stützrädern u. 4 Hubelementen
Schwingrahmen
Fahrrahmen
Formboden
1700 ... 1900
1570 ... 1550
ca. 1200
Rohspiegel
2650
2200
3300
1300
2600
Draufsicht ohne Abdeckhaube dargestellt
12. FEB. 1992
SCHOTT
SCHOTT GLASWERKE
Schleuder für LG-Spiegel ø2000 Hauptmaße
1:20
SK 912
A3

APPENDIX E

SCHOTT REPORTS

"Report of Frit Data" and "Final Report on the Bonding of Zerodur to Glass Frit"

REPORT OF FRIT DATA

(WEIBULL STATISTIC OF BONDING STRENGTH,

CTE AND ELASTIC MODULUS

This report contains the Weibull statistics of bonding strength, coefficient of thermal expansion and of the elastic moduli of three different frits.

In the present state of frit development we are testing contemporarily three frits: one composite frit (13-51) and two devitrifying frits (GM 31615 and GM 31811), because we are not sure, which of them up to now is the best one.

1. WEIBULL STATISTICS OF BONDING STRENGTH

For the Weibull statistics of bonding strength "L"-samples were prepared and measured as shown in Fig. 1

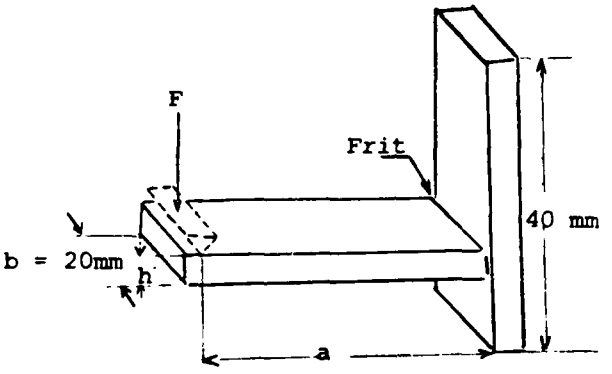


Fig. 1 "L"-samples for the measurement of bonding strength

The bonding strength has been calculated from the following equation:

$$\sigma = \frac{6.F.a}{b.h^2} \quad \left[\frac{N}{mm^2}\right]$$

In table 1 the bonding strength measurements and the Weibull analysis are summarized.

With exeption of frit GM 31615 (No 2), the grain seize of all frits was $<20\mu m$. The layer thickness of the frit was normally between 3 and 4 mm. With the composite frit 13-51 (No 9) we made some additional tests with a layer thickness of < 1 mm - normally about 100 µm. The fritting of all "L"-samples was performed under a pressure of 5 N/mm^2 during tempering.

The Weibull analysis has been calculated by a computer programm. To give you the possibility to make calculations of your own, we listed all the single values too.

There are no characteristic differences in the grain seizes of < 20 µm and < 60 µm (Analysis No 1 and 2).

We have had the possibility of tempering but three "L"-samples together in the pressure-furnace. From the single values of analysis No 4, 5 and 6 you can see, that there are but small differences in the values of one group. There seems to be an influence of the preparation mode of the "L"-samples and of the tempering programm. A comparison of analysis No 8 and 9 shows, that we would have a higher bonding strength with thinner frit layers.

Up to now it seems, that the values of the bonding strength of frit GM 31811 are a little bit better than the values of the other two frits.

The Figures 2 - 10 show the Weibull analysis of No 1 - No 9.

2.COEFFICIENT OF THERMAL EXPANSION

In Fig. 11 the $\Delta l/l$ versus temperature curves are plotted for the three frits: GM 31615, GM 31811 and 13-51. All the samples for these measurements were sintered under the same tempering programm, but without pressure. The grain seize of the frits was < 20 µm.

While the curve of frit GM 31811 lies in the positive part, the frit 13-51 lies in the negative one. Frit GM 31615 lies between them. As evident from Fig. 12, the values of frit GM 31615 are dependent also upon the grain seize.

The deviation of frit 13-51 versus Zerodur is smaller, when the sintering process proceeds under a pressure of 0.5 N/mm^2, as shown in Fig 13.

Up to now we cannot sinter devitrifying frits under pressure because of their too high shrinkage.

3. ELASTIC MODULUS

For the measurement of the elastic modulus, samples of 100 x 7 x 3.4 mm^3 were sintered and grinded. The elastic modulus was measured in a dynamic way, with ultrasonic (transversal) waves of 1 - 10 kHz, and in a static way.

Table 2

ELASTIC MODULI OF FRIT 13-51 and GM 31615

Frit 13-51 (without pressure)	8.4×10^3 N/mm^2
Frit 13-51 (with pressure)	8.8×10^3 N/mm^2
Frit GM 31615 (without pressure)	23.5×10^3 N/mm^2

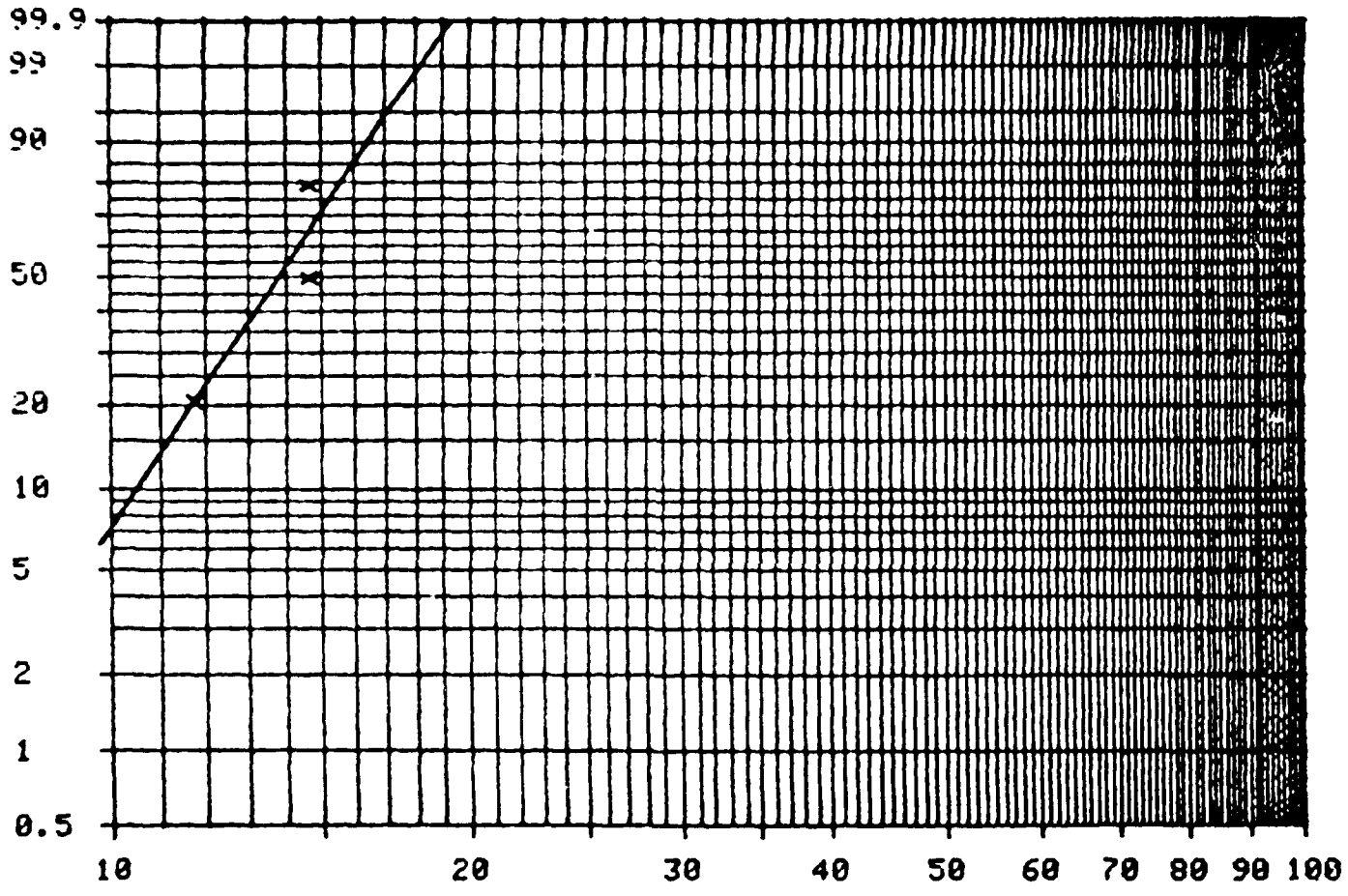
There are no high differences between frits sintered with or without pressure (Frit 13-51), but there are high differences between the two frits 13-51 and GM 31615.

Up to now we have not got enough measurements of the elastic moduli in order to say anything about the influence of different parameters, such as pressure, grain seize and tempering programm on the elastic modulus.

Table 1

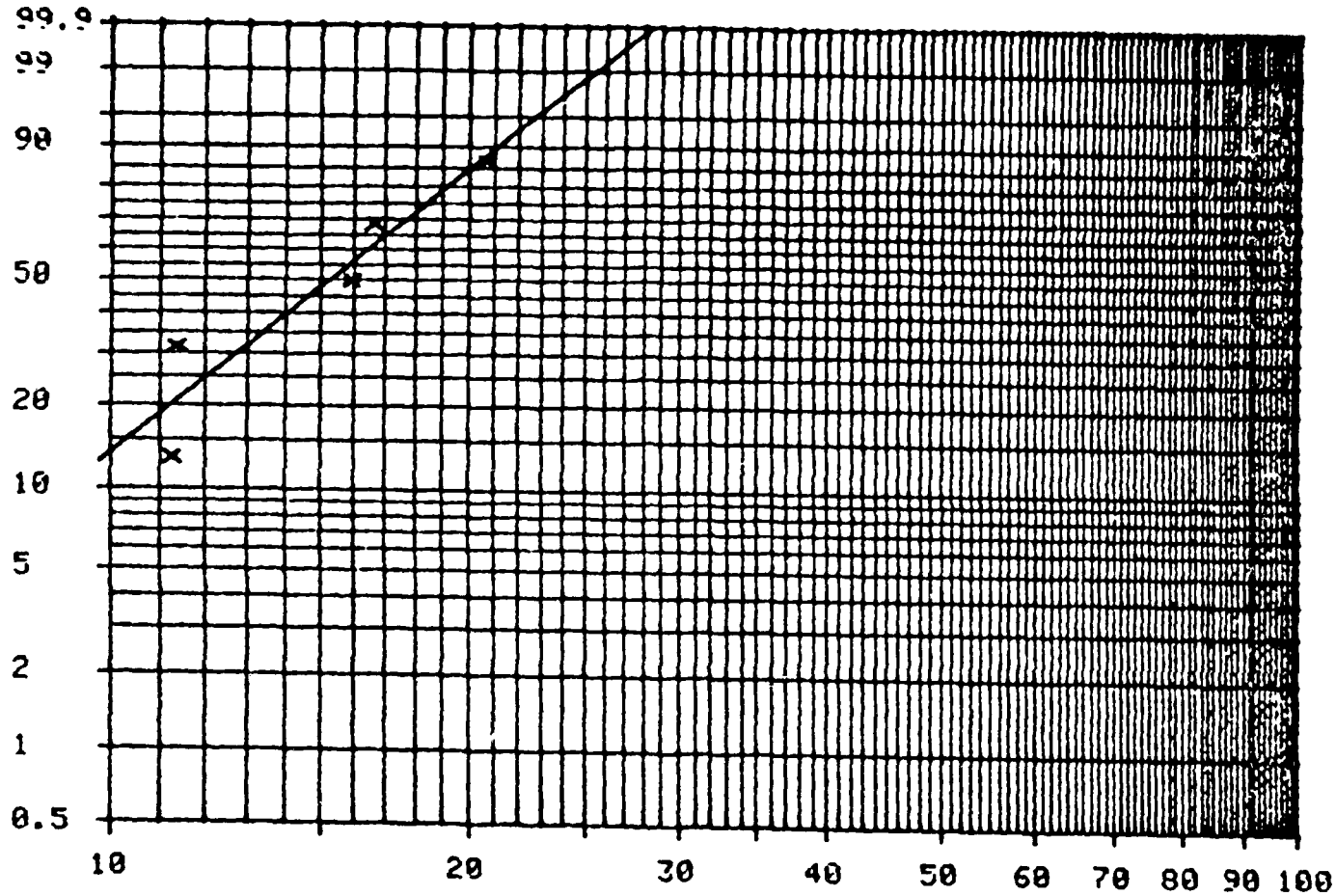
Weibull Statistics of Bonding Strength

No	Frit	Grain Seize	Layer Thick-ness	Pressure [N/mm^2]	Single Measurements [N/mm^2]	Mean Value [N/mm^2]	Standard Deviation	Weibull Factor	Charact. Strength	Smallest Value	Highest Value	Correlation Coefficient
1	GM 31615	<20µm	3-4 mm	5 N/mm^2	11.5; 14.6; 14.6;	14.56	3.22	4.73	15.90	11.20	20,60	0,9298
2	GM 31615	<60µm	3-4 mm	5 N/mm^2	16.5; 11.3; 11.2; 20.6;15.9;	13.63	1.67	6.83	14.50	11.70	14.60	0.9044
3	GM 31615	<20µm <60µm	3-4 mm	5 N/mm^2	11.5; 14.6; 14.6; 16.6; 11.3; 11.2; 20.6; 15.9;	15.12	3.96	3.68	16.80	11.20	20.60	0.9360
4	GM 31811	<20µm	3-4 mm	5 N/mm^2	16.4; 16.8; 16.2	16.47	0.31	50.34	16.62	16.20	16.80	0.9642
5	GM 31811	<20µm	3-4 mm	5 N/mm^2	17.5; 17.2; 18.0	17.56	0.40	41.08	17.76	17.20	18.00	0.9759
6	GM 31811	<20µm	3-4 mm	5 N/mm^2	12.3; 14.2; 14.8	13.77	1.31	9.69	14.39	12.30	14.80	0.9746
7	GM 31811	<20µm	3-4 mm	5 N/mm^2	16.4; 16.8; 16.2; 17.5; 17.2; 18.0; 12.3; 14.2; 14.8;	16.00	1.85	8.70	16.87	12.30	18.00	0.9707
8	13-51	<20µm	3-4 mm	5 N/mm^2	13.7; 14.7; 12.2; 16.5; 13.4; 14.8; 14.3; 16.1;	14.47	1.41	10.97	15.10	12.20	16.50	0.9851
9	13-51	<20µm	<1 mm	5 N/mm^2	24.6; 21.6;26.7; 20.6; 19.6; 22.7; 35.4; 16.7;	23.49	5.70	4.54	25.70	16.70	35.40	0.9392



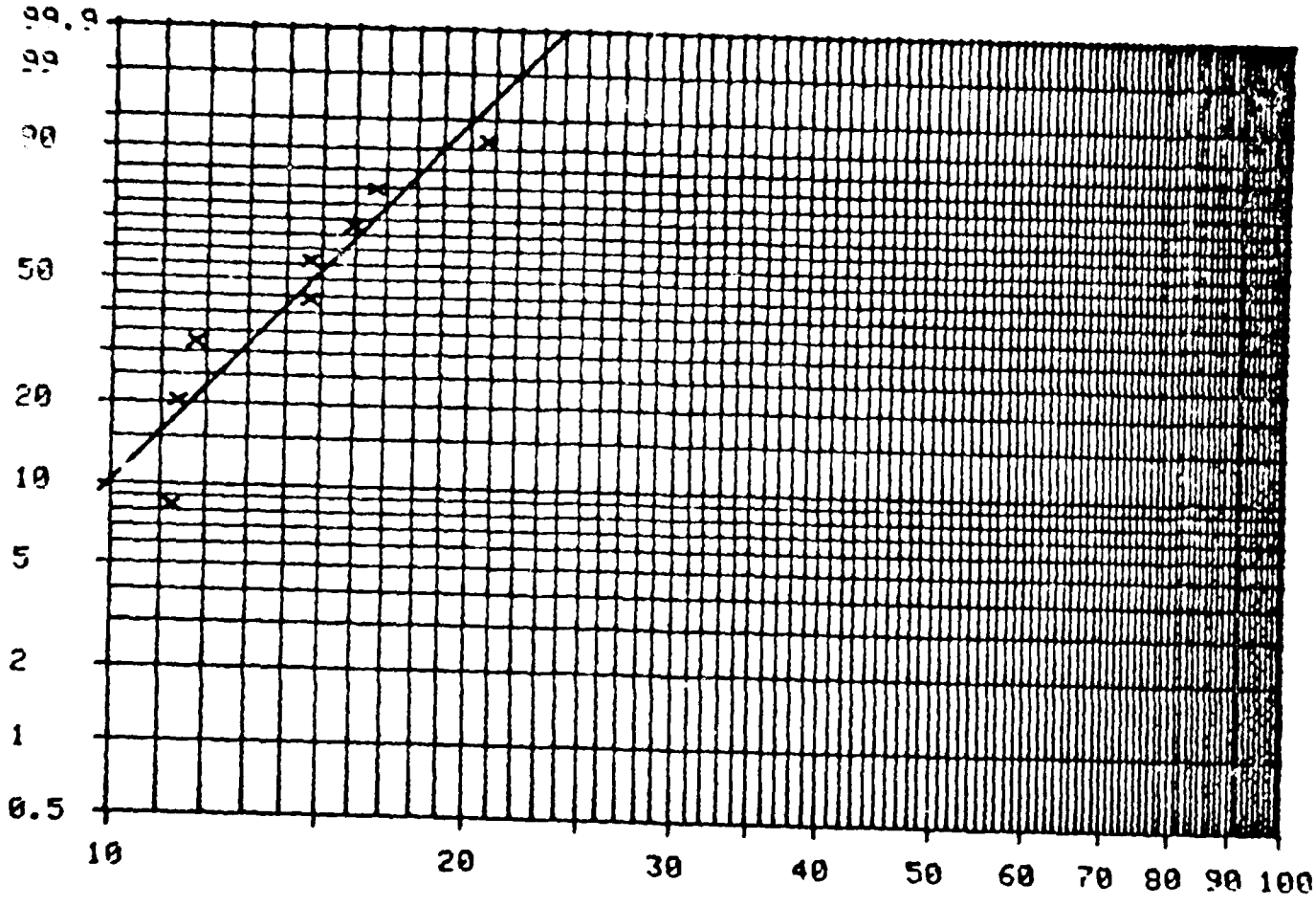
Weibull analysis of frit GM 31615 (Nr 1)

Fig. 2



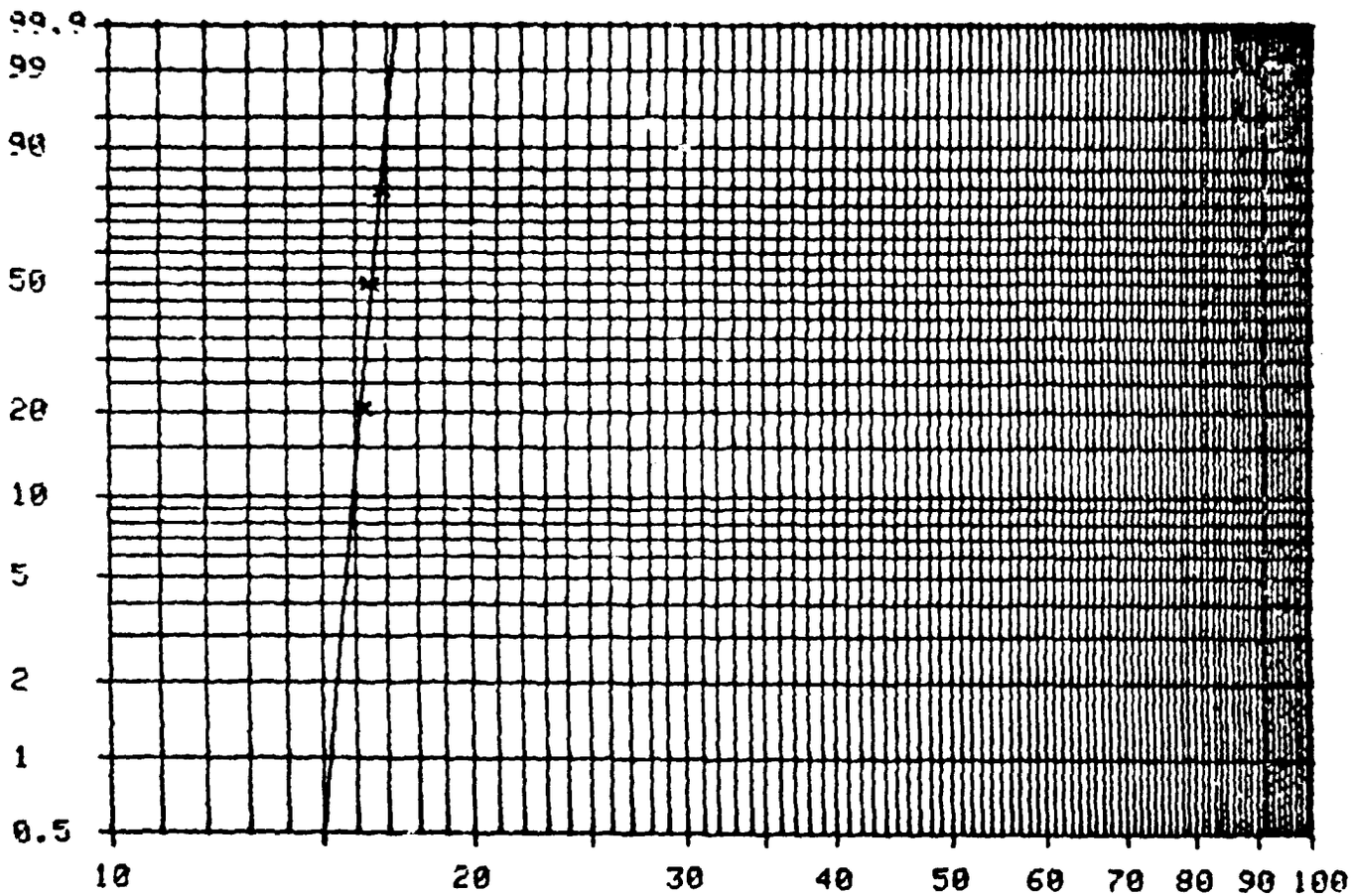
Weibull analysis of frit GM 31615 (Nr. 2)

Fig. 3



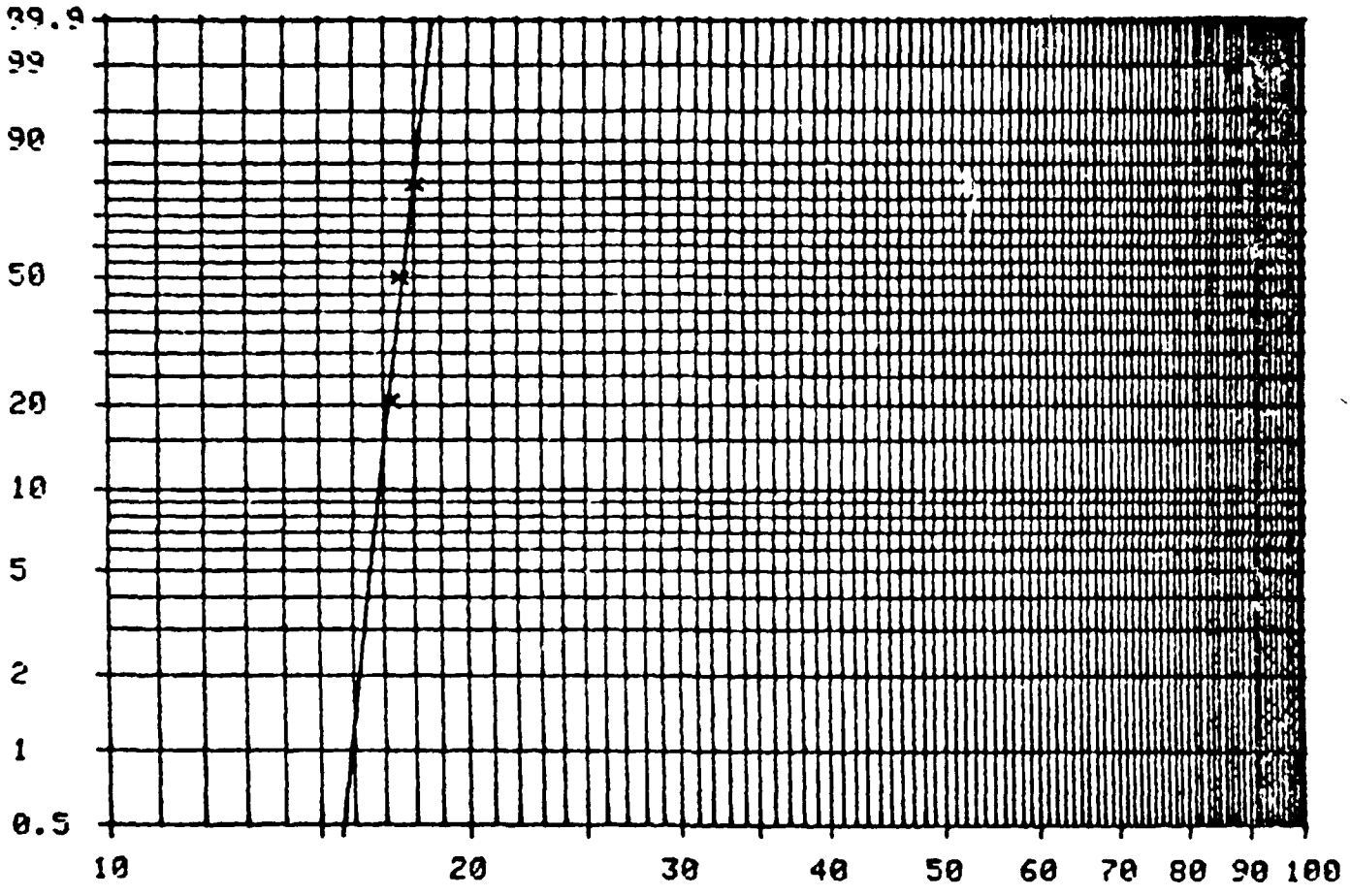
Weibull analysis of frit GM 31615 (Nr 3)

Fig. 4



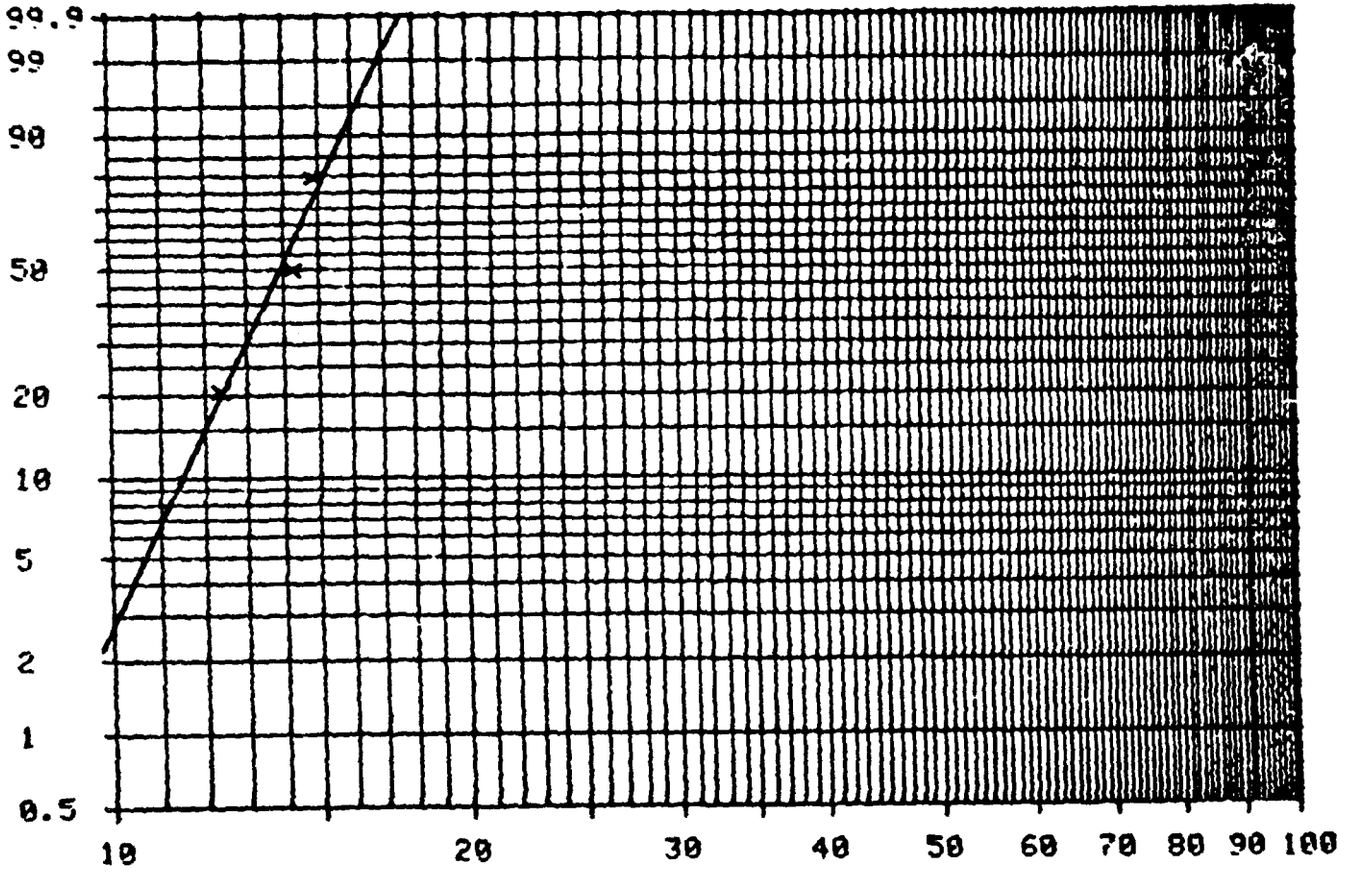
Weibull analysis of frit GM 31811 (Nr. 4)

Fig. 5



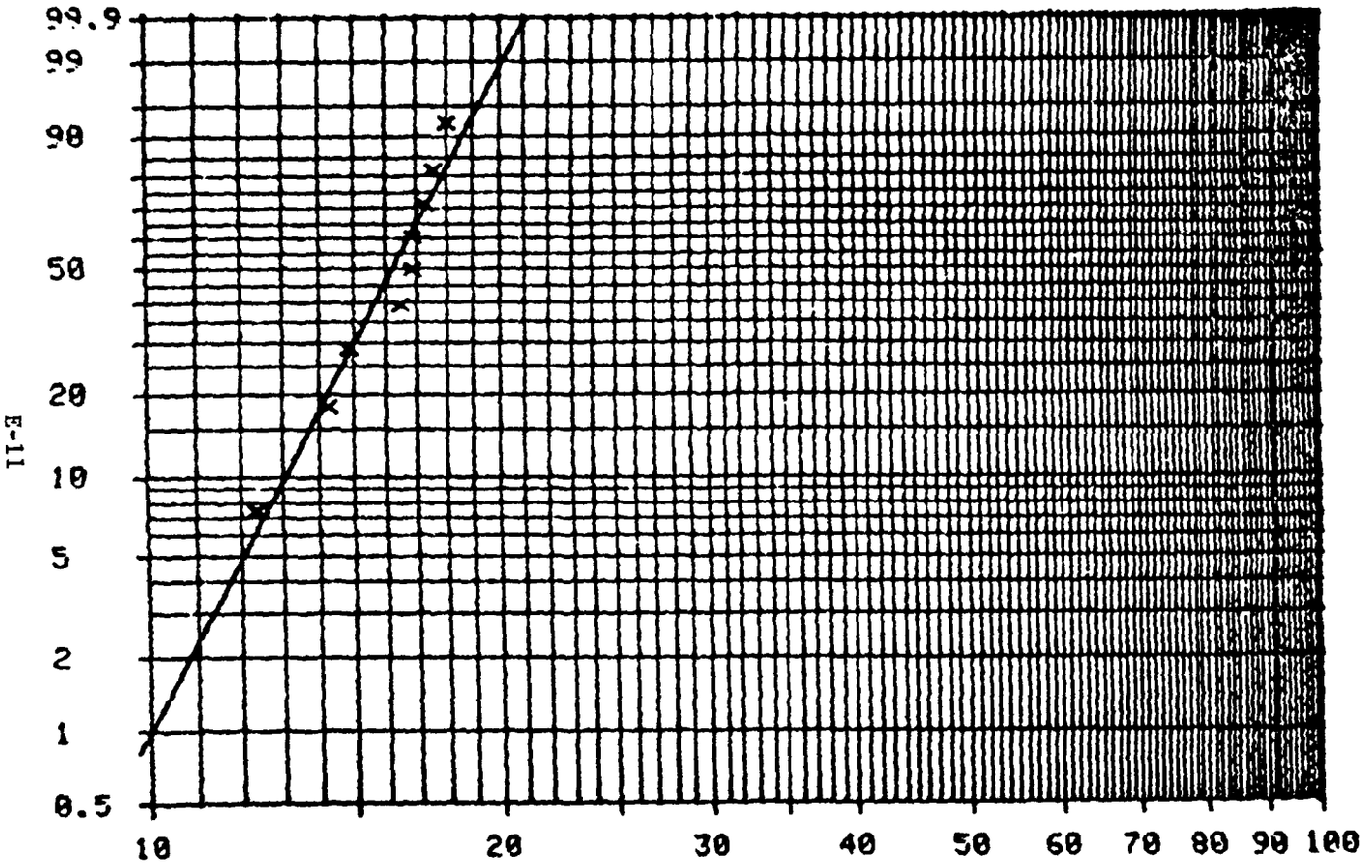
Weibull analysis of frit GM 31811 (Nr.5)

Fig. 6



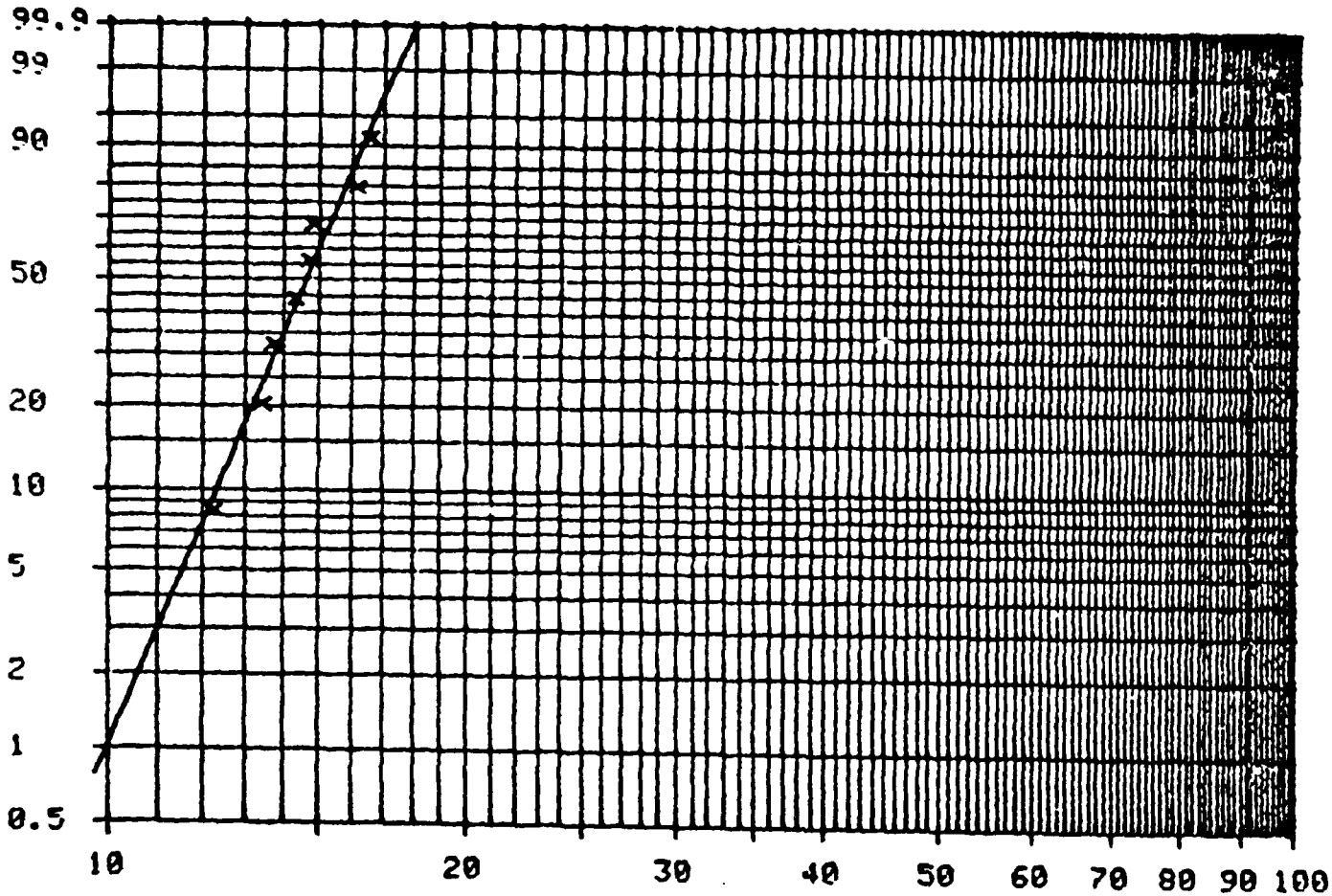
Weibull analysis of frit GM 31811 (Nr. 6)

Fig. 7



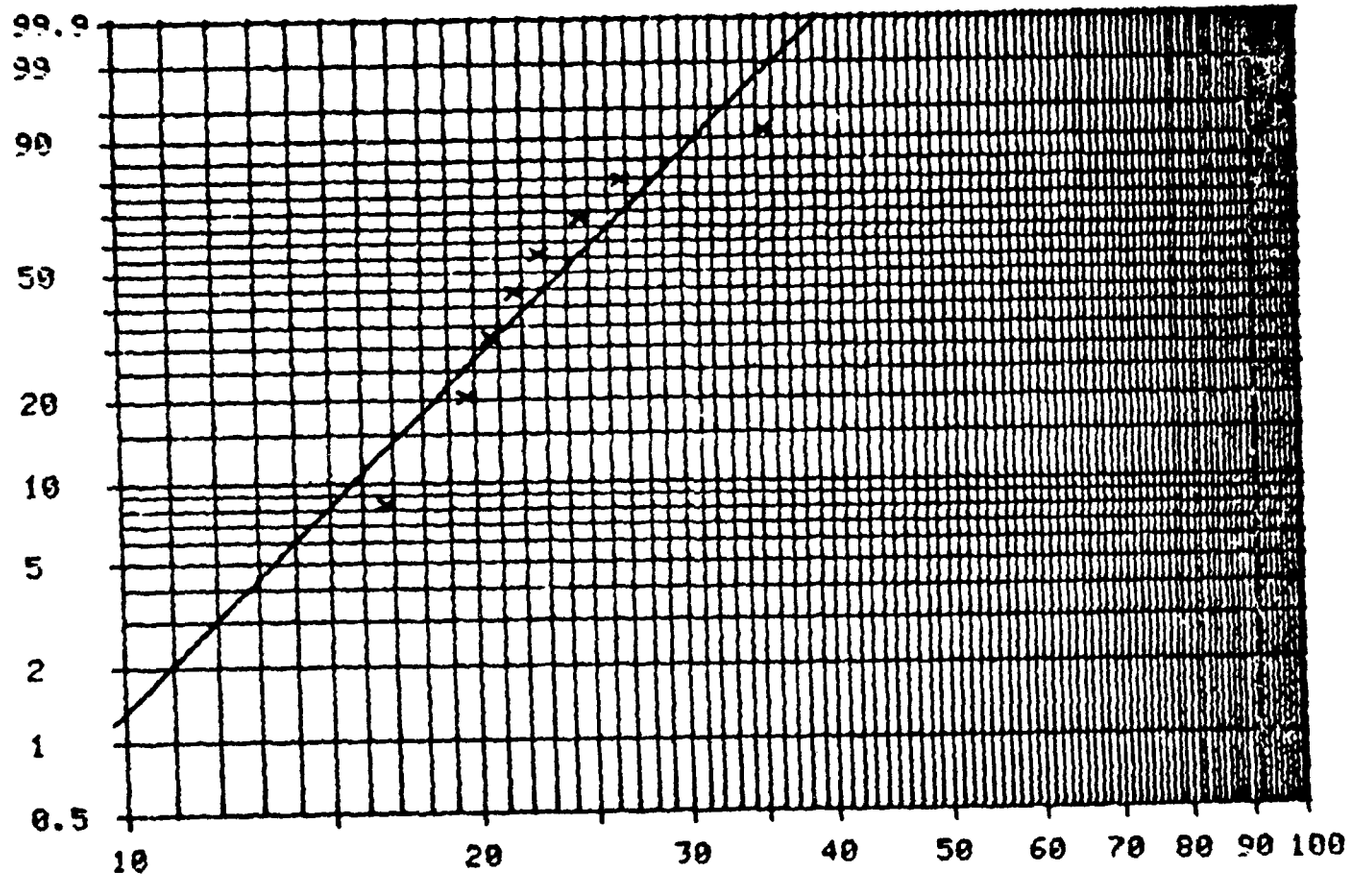
Weibull analysis of frit GM 31811 (Nr. 7)

Fig. 8



Weibull analysis of frit 13-51 (Nr.8)

Fig. 9



Weibull analysis of frit 13-51 (Nr. 9)

Fig. 10

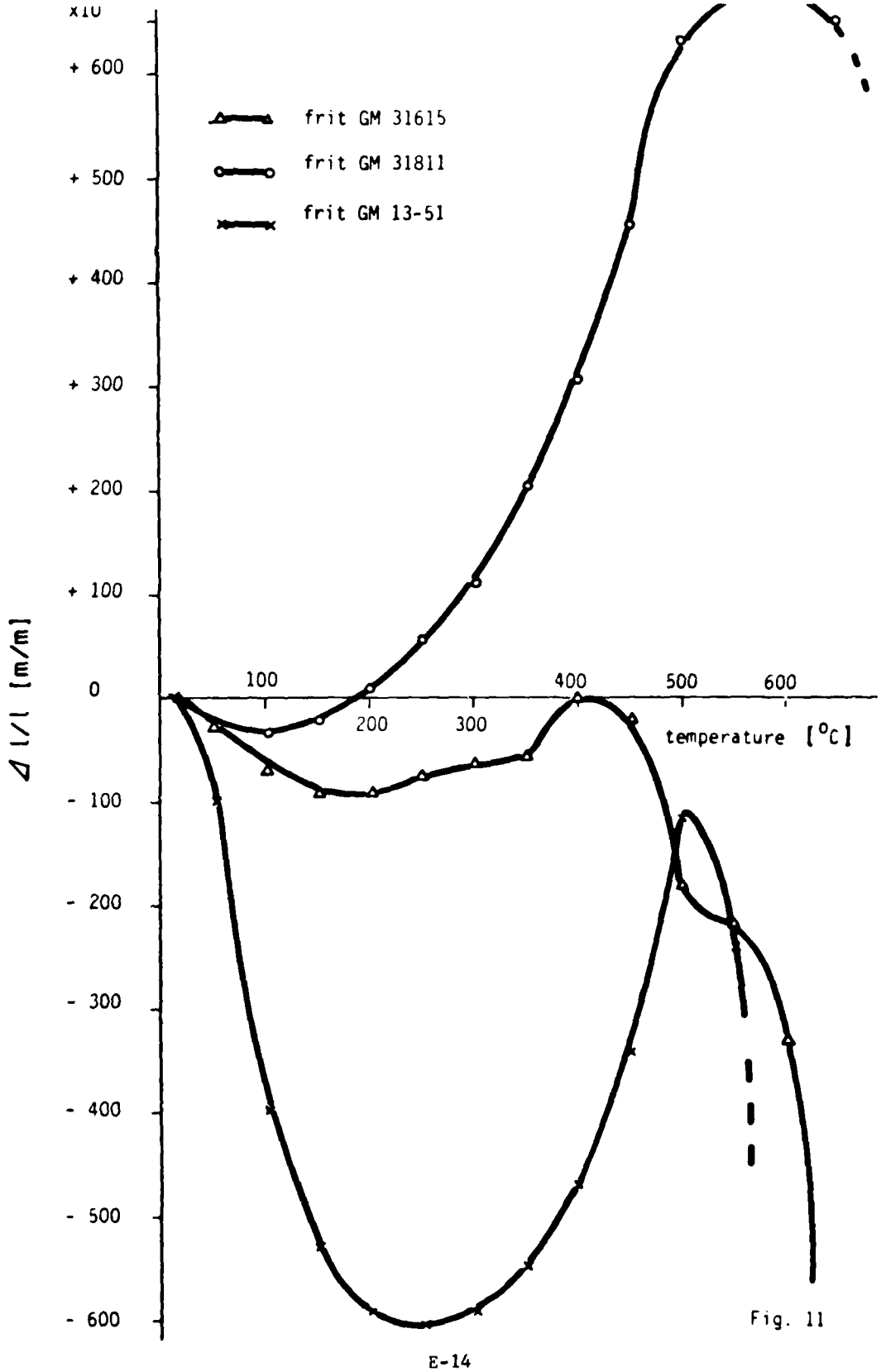
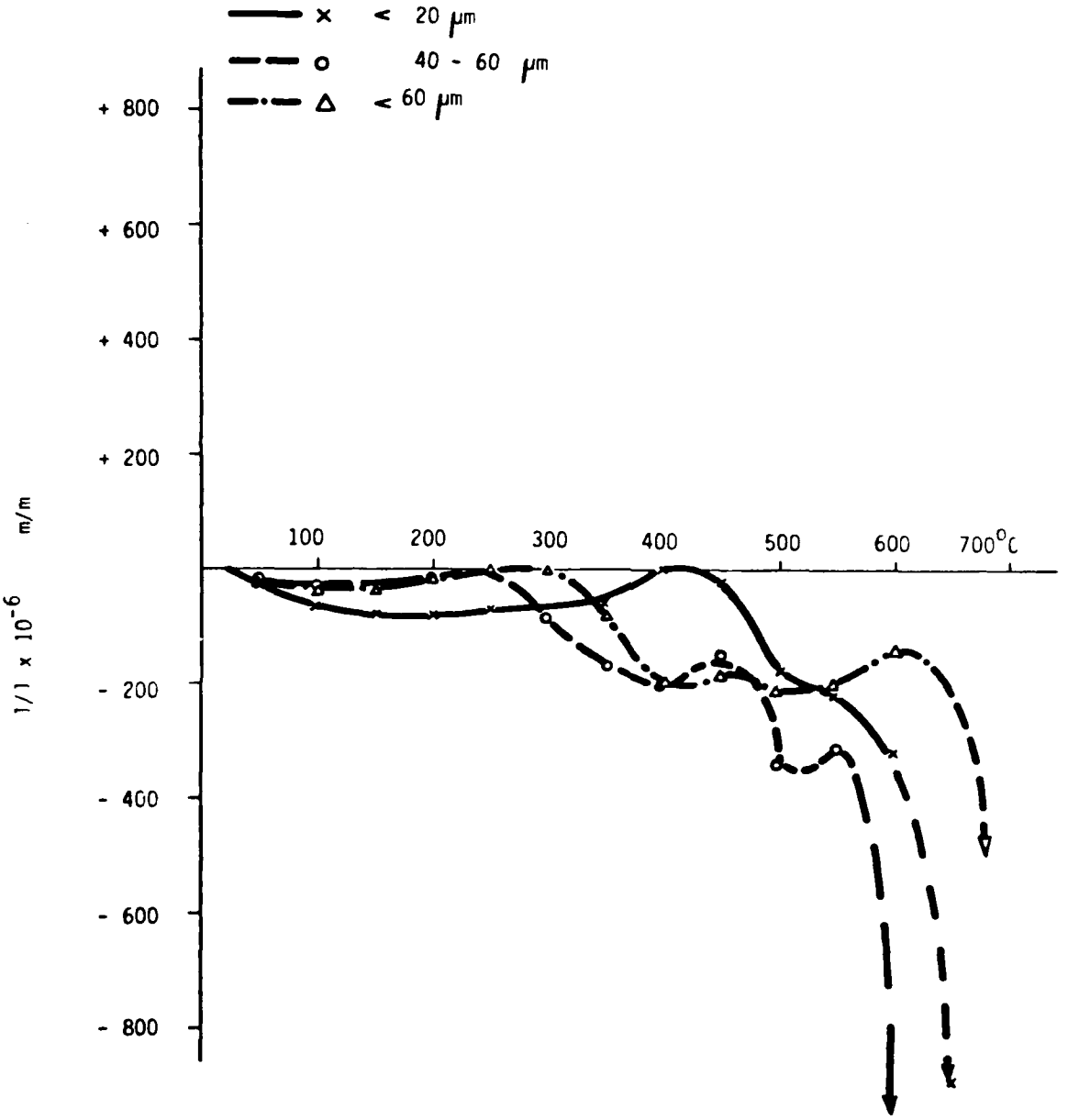
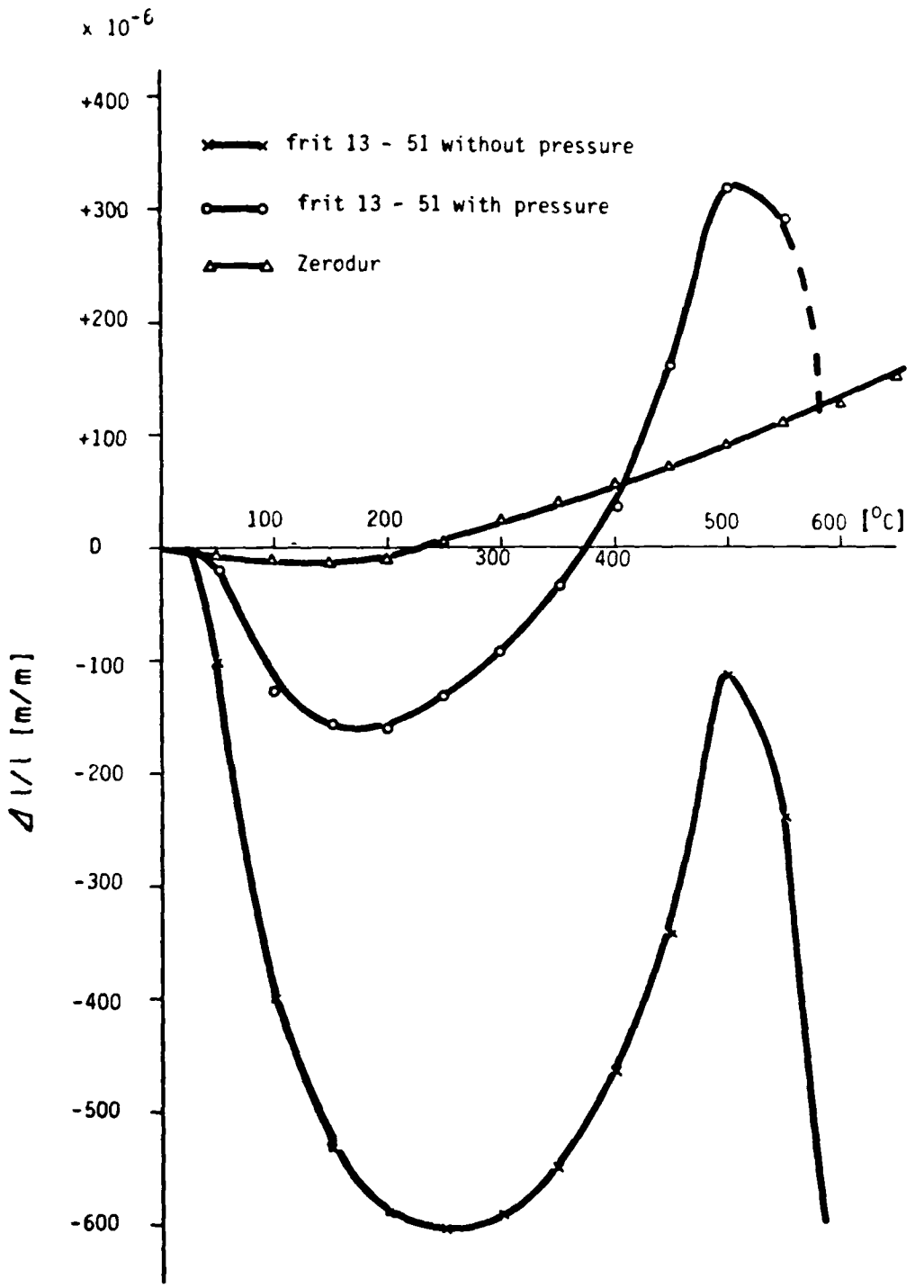

x10
+ 600
+ 500
+ 400
+ 300
+ 200
+ 100
0
- 100
- 200
- 300
- 400
- 500
- 600
Δ l/l [m/m]
frit GM 31615
frit GM 31811
frit GM 13-51
100
200
300
400
500
600
temperature [°C]

Fig. 11



Δl/l - CURVES OF DIVITRIFYING FRIT (GM 31615) OF DIFFERENT GRAINS

Fig 12



Δl/l TO TEMPERATURE OF FRIT 13 - 51 (WITH AND WITHOUT PRESSURE) IN COMPARISON WITH ZERODUR

FIG. 13

April 30, 1982

FINAL REPORT ON THE BONDING OF ZERODUR TO GLASS FRIT

1. Task

By the commencement of the Agreement, SCHOTT had developed glass frits and methods for the preparation of defined frit layers. The properties below listed were to be measured of the best of these glass frits, and samples were to be made of these:

Measurement of properties:

- Weibull statistics of bonding strength,
- E modulus,
- Poisson's ratio,
- CTE-value.

Samples:

- 3 L samples,
- 6 lap-shear samples,
- 1 bonded mirror, 0.30 m in dia. and 0.015 m in thickness.

In addition, the bonding process is designed to be described to the extent necessary for estimating the feasibility of frit-bonding.

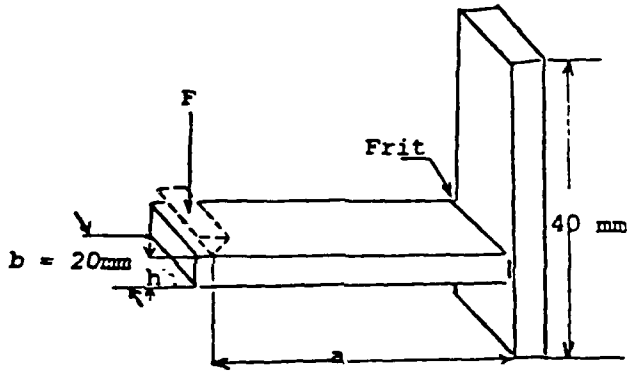
The final report is meant to include the developmental steps necessary yet, as well as the expenditure in terms of time and costs.

2. Selection of a suited glass frit

Three different glass frit types (GM 31613, GM 31811 and 13-51) were used to measure the $\Delta l/l$ curves, the bonding strengths of L samples and the E moduli.

2.1. Weibull statistics on bonding strength

For the Weibull statistics on bonding strength, "L" samples were prepared and measured as shown in fig. 1.



The bonding strength has been calculated from the following equation:

$$\sigma = \frac{6 \cdot F \cdot a}{b \cdot h^2} \qquad [\frac{N}{mm^2}]$$

The bonding strength measurements and the Weibull analysis are summarized in table 1 and fig. 2 - 6.

With the exception of frit GM 31615 (No. 2), the grain size of all frits was < 20 µm. The layer thickness of the frit was between 3 and 4 mm. The fritting of all "L" samples was performed under a pressure of 0.05 N/mm² during the tempering operation (the value of 5 N/mm² in previous reports is wrong).

The Weibull analysis has been calculated, using a computer program. To make it possible for you to make calculations of your own, we have listed all the single values, too.

There do not appear to be great differences in the grain sizes of *< 20 µm and < 60 µm (analyses, No. 1 and 2).*
Out of the three glass frits selected, frit GM 31811 was found to have the greatest strength.

2.2. Δ l/l curves

To perform the measurements of the Δ l/l curves, the glass frit powder, whose grain size was < 20 µm, was tempered in accordance with the same tempering program as the "L" samples, however, without pressure. The Δ l/l vales as a function of the temperature are shown in fig. 7. Glass frit GM 31811 has proved to have the lowest variation of Δ l/l within the temperature range of 20 °C to 200 °C.

Also a measurement sample was prepared under 0.05 N/mm² pressure from glass frit GM 31811. The Δ l/l curve, however, did not change.

2.3. Modulus of elasticity

To measure the modulus of elasticity, samples 100 mm x 7 mm x 3.4 mm, are sintered and ground. The following moduli of elasticity were measured in accordance with the static method:

Frit 13-51 (without pressure) - $8.8 \cdot 10^3$ N/mm²,
Frit 13-51 (with pressure) - $8.4 \cdot 10^3$ N/mm²,
Frit GM 31615 (without pressure) - $23.5 \cdot 10^3$ N/mm²,
Frit GM 31811 (without pressure) - $23.0 \cdot 10^3$ N/mm²,
Frit GM 31811 (with pressure) - $15.0 \cdot 10^3$ N/mm².

2.4. Poisson's ratio

Poisson's ratio has not been able to be measured.

Glass frit GM 31811 was chosen for the performance of further tests and for the samples.

3. Preparation of samples from GM 31811

In order to prepare the following frit-bonding samples, glass frit GM 31811 was melted and ground to ≤ 20 µm.
The glass powder was pasted on with amyl acetate and a deflocculator, and applied as a layer 300 µm thick. To adjust the layer thickness, 300 µm-thick spacers were used. Frit-bonding was performed at 820 °C (2 hours) under a pressure of 0.05 N/mm².

The following frit-bonded samples were supplied to PERKIN ELMER:

- 3 "L" samples,
- 6 "lap-shear" samples,
- one 0.30 m mirror with a round plate provided with 7 drilled holes, approx. 10 cm in dia., bonded to a cover plate.

Out of 5 "L" samples, which had been frit-bonded according to the same method, a Weibull statistics sheet was established (cf. table 1, No. 5 and 6).

4. Further developments of the glass frit and the frit-bonding technology

For the frit-bonding of ZERODUR to ZERODUR in relation to the manufacture of a lightweight mirror, the following developments yet have to be carried out:

- Development of glass frit,
- Development of frit-bonding technology.

The development of the frit-bonding technology is composed of the preparation of the frit and the application of same, as well as of the tempering under pressure for frit-bonding.

4.1. Development of glass frit

Before initiating further development of the glass frit, the frit properties need to be defined precisely, and below are the questions that have to be answered yet in relation to this:

- Allowed stresses in ZERODUR,
  maximum compressive stress in surface,
  maximum temperature-independent stresses,
  maximum temperature-dependent stress;

- Allowed stresses in glass frit;

- Minimum bonding strength;

- Young's modulus;

- Poisson's ratio;

- Heat transfer values;

- Density.

New measuring methods and methods for the preparation of samples need to be developed in respect of the measuring of properties:

- Stress measurement,
  distinction between mismatch stress and chemical ion exchange stress;

- $\Delta l/l$ measurements,
  sandwich samples;

- Bonding strength measurements,
  but-samples;

- "E" modulus,
  sandwich samples,
  measuring method;

- Poisson's ratio,
  sandwich samples,
  measuring method;

- Heat transfer,
  sandwich samples,
  measuring method;

- Chemical ion exchange,
  temperature-dependent, yes or no.

The aspired-to properties can be influenced, and obtained, by the following factors:

- Influence of chemical composition,
- Chemical additives,
- Grain size,
- Frit thickness,
- Tempering program,
- Pressure,
- Barrier layers for ion exchange.

4.2. Frit-bonding technology

The frit-bonding technology for one thing includes the preparation and application of precisely defined frit layers, which requires the following operations to be carried out:

Frit layers of an exact thickness between 10 µm and 300 µm have to be prepared and applied onto the honeycomb system.

- Preexperiments for production of frit layers by spraying, toughening or other direct methods.
- Preexperiments for production of frit layers and subsequent application onto the honeycomb system.
- Decision on the technology of application.
- Equipment for the production of glass powder $\leqslant 5$ µm.
- Development of the technology of application.
- Construction of equipment for the production of thin frit layers and/or application of these onto the honeycomb system.
- Experiments and production of samples.

Apart from the application of the frit layers, it is the frit-bonding operation itself that has be studied. The experiments mentioned below will be needed for this:

- Preexperiments under the pressure of weights.
- Preexperiments under vacuum.
- Decision on the frit-bonding technology.
- Development of the frit-bonding technology.
- Influence of the application technology on the frit-bonding technology,
- Determination of the tempering program.
- Experiments with single ROBAX and ZERODUR honeycomb.
- Experiments with four ROBAX and ZERODUR honeycomb systems.

- Determination of the frit layer tolerance.

- Determination of the admissible surface roughness.

- Determination of the admissible surface waviness.

4.3. Development costs for glass frit and frit-bonding technology

Costs for the glass frit development will amount to

$ 195,000,

while the costs for the frit-bonding technology will amount to

$ 280,000.

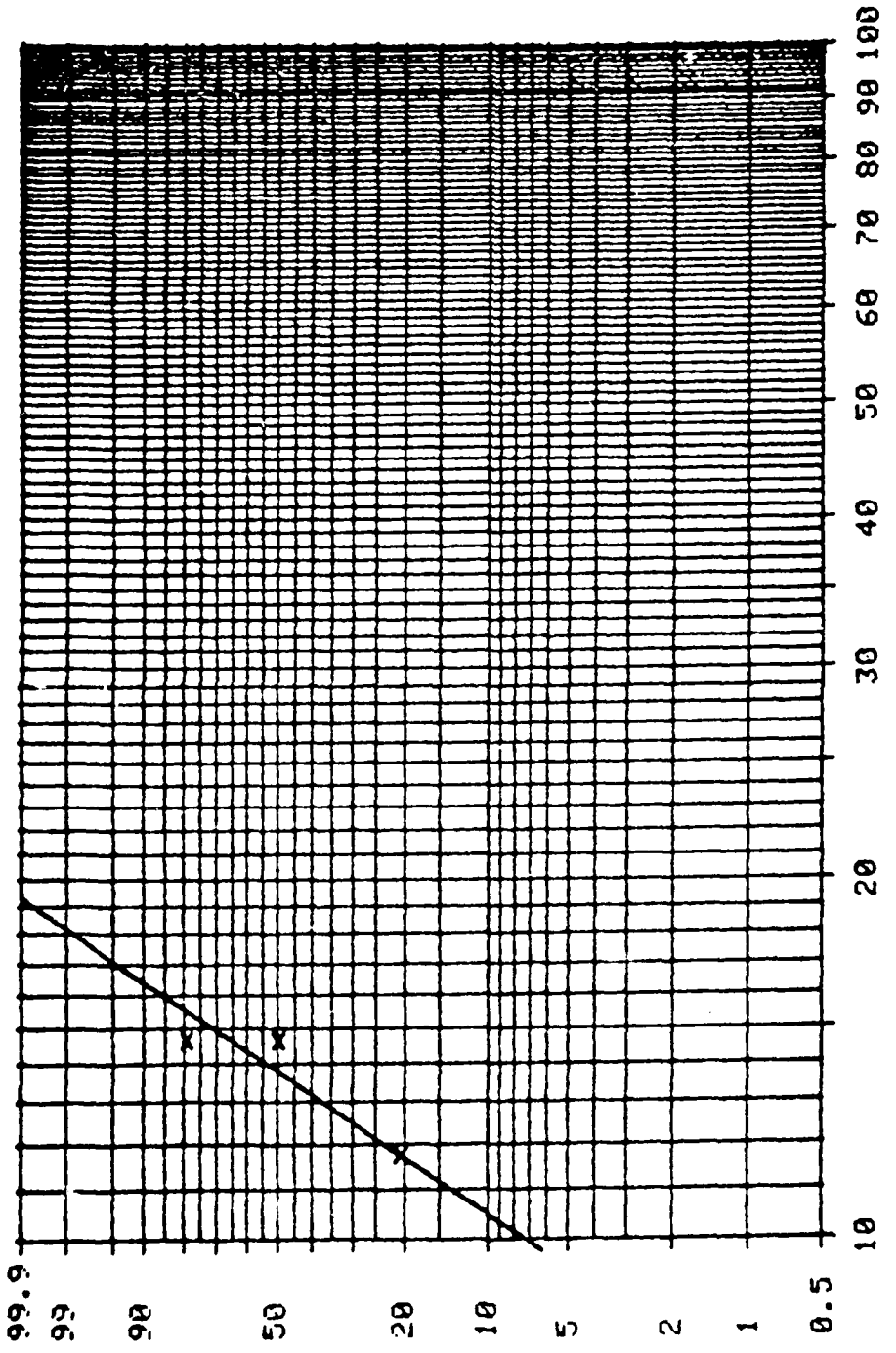
The costs may be given in greater detail if so requested.

4.4. Time required to advance the frit-bonding development

The progress of experiments and, consequently, the required time estimated are shown in fig. 8.

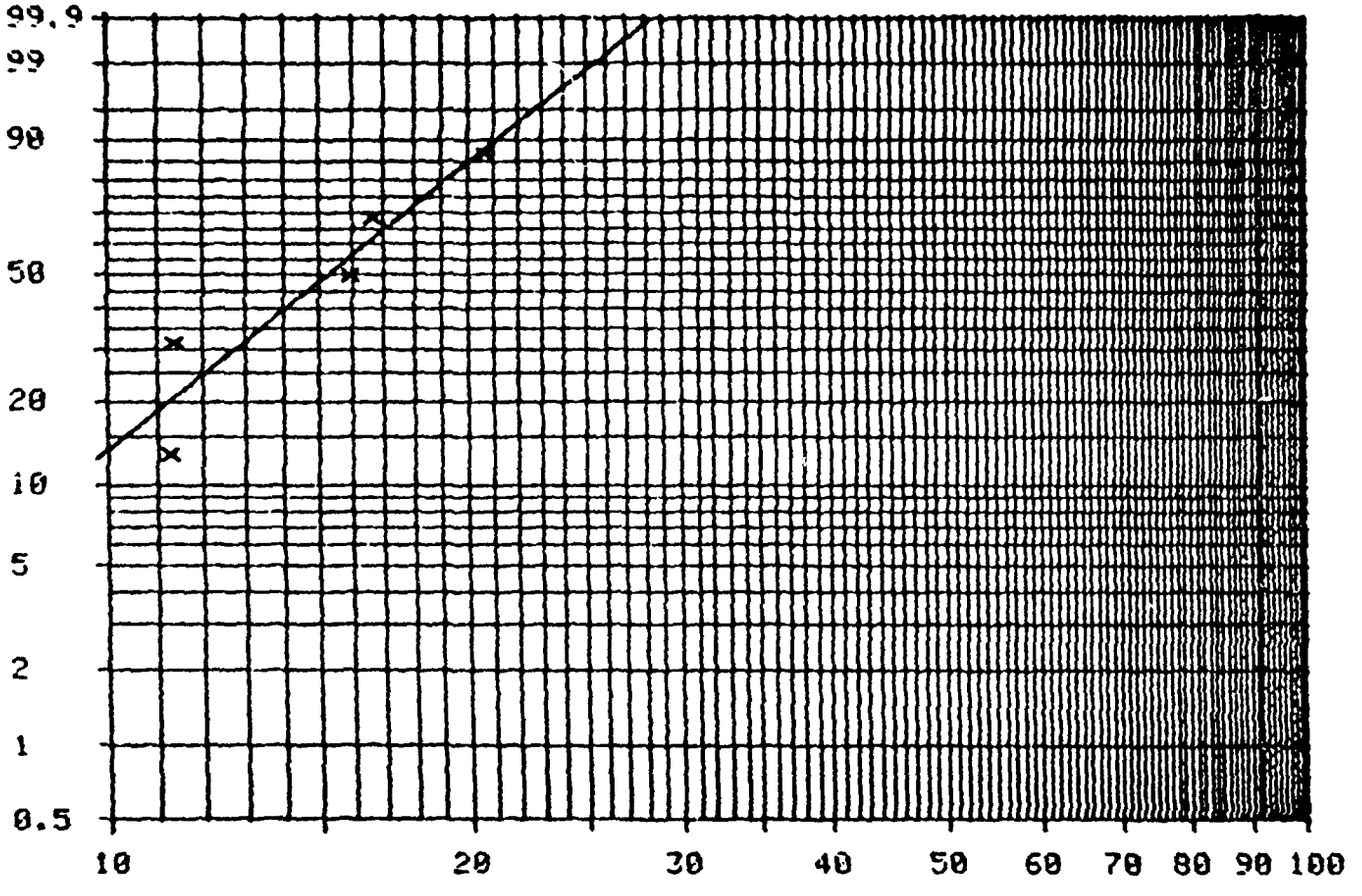
Table 1: Weibull Statistics on Bending Strength

No	Frit	Grain size [µm]	Layer thick-ness [mm]	Pressure [N/mm²]	Single measurements [N/mm²]	Mean value [N/mm²]	Standard devia-tion	Weibull factor	Charact. strength	lowest value	Highest value	Correla-tion coeffi-cient
1	GM 31615	20	3 - 4	0.05	11.5 14.6; 14.6	14.56	3.22	4.73	15.90	11.20	20.60	0.9298
2	GM 31615	60	3 - 4	0.05	16.5; 11.3; 11.2 20.6 15.9	13.63	1.67	6.83	14.50	11.70	14.60	0.9044
3	GM 31811	20	3 - 4	0.05	16.4; 16.8; 16.2 17.5; 17.2; 18.0 12.3 14.2 14.8	16.00	1.85	8.70	16.87	12.30	18.00	0.9707
4	13-51	20	3 - 4	0.05	13.7; 14.7; 12.2; 16.5; 13.4; 14.8 14.3 16.1	14.47	1.41	10.97	15.10	12.20	16.50	0.9851
5	GM 31811	20	0.3	0.05	13.2; 13.9; 16.2 17.0 17.7	15.60	1.96	7.83	16.50	13.20	17.70	0.9678



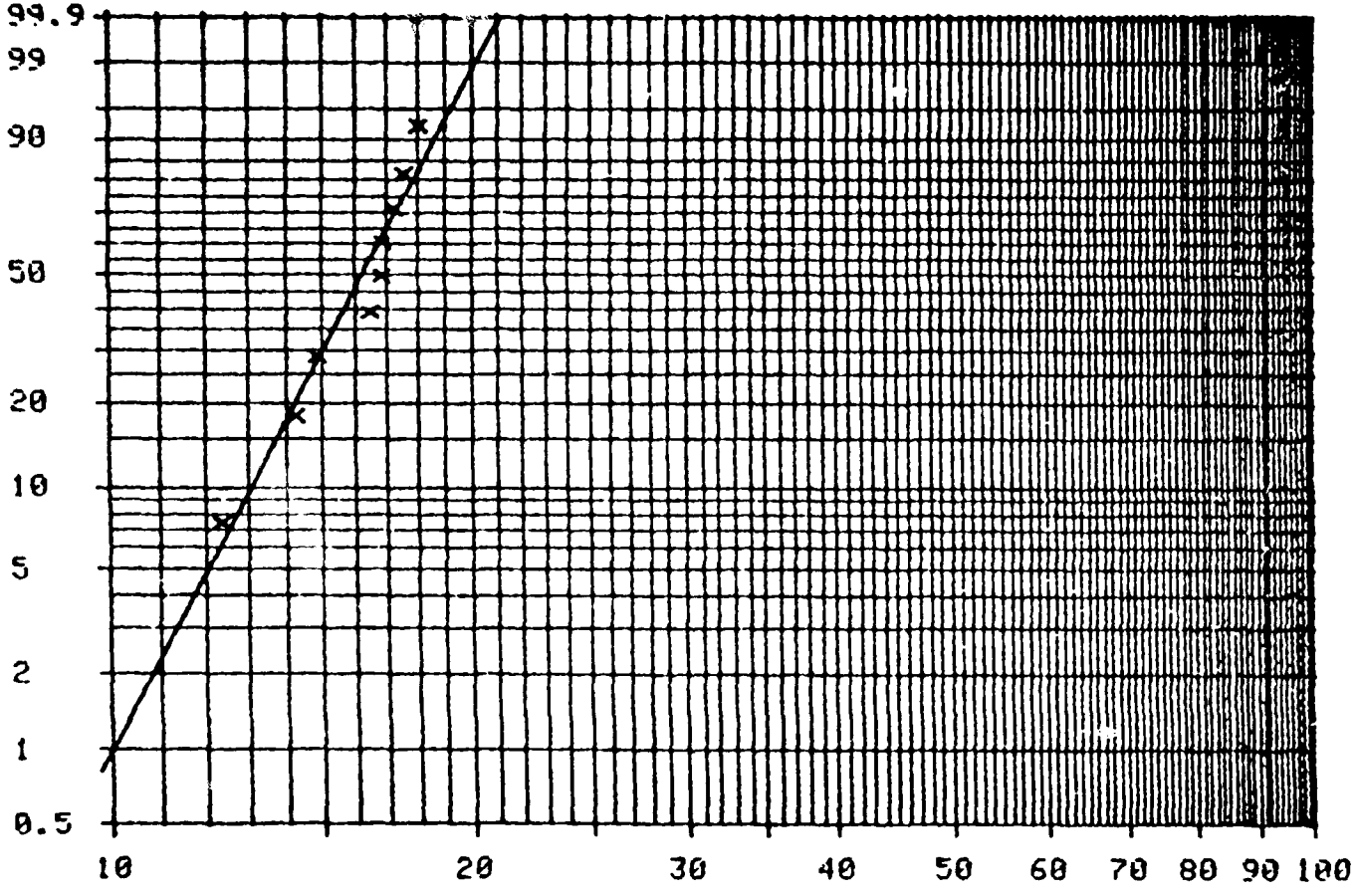
Weibull analysis of frit GM 31615 (No.1)

fig. 2



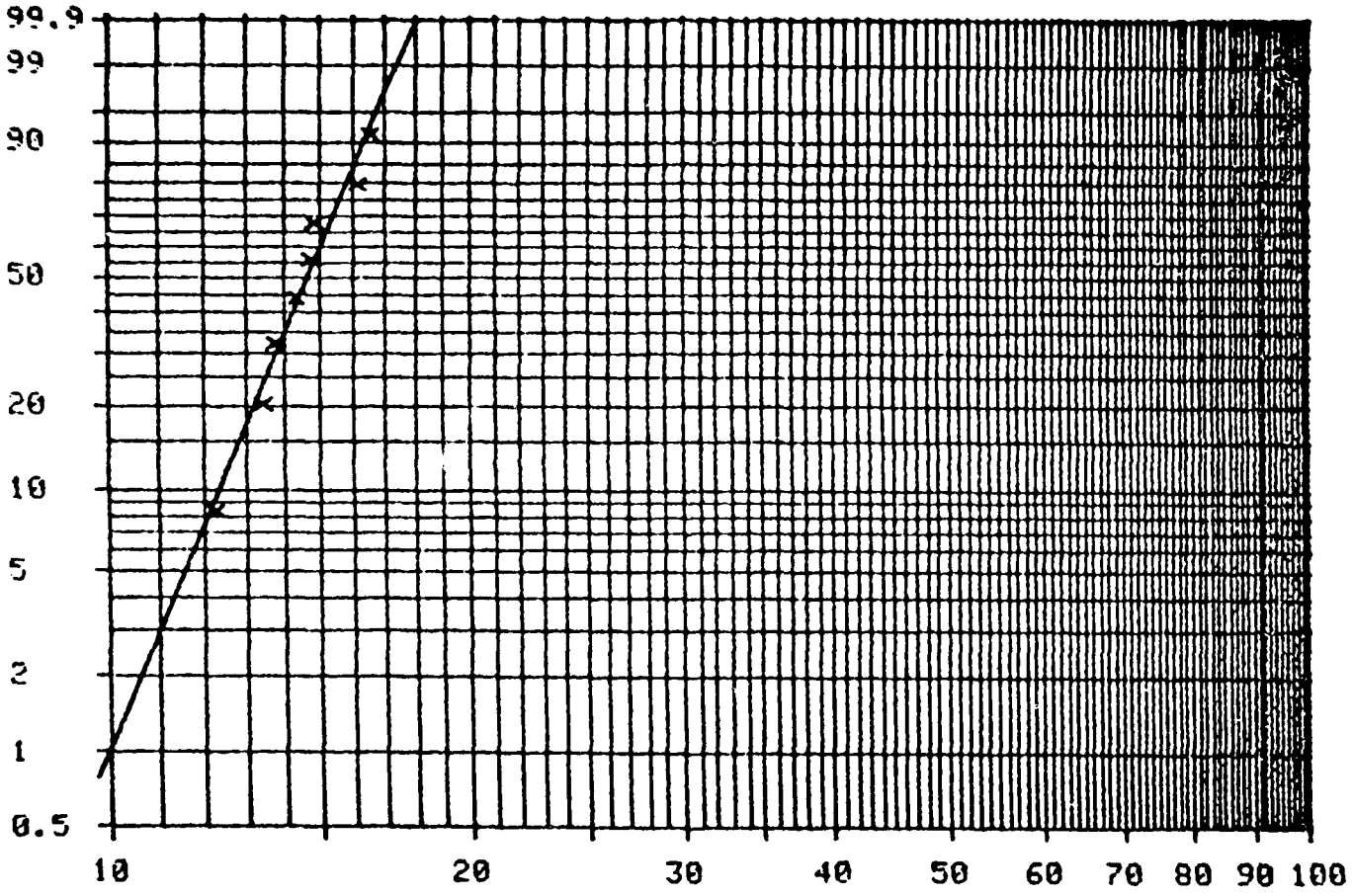
Weibull analysis of frit GM 31615 (No. 2)

fig. 3



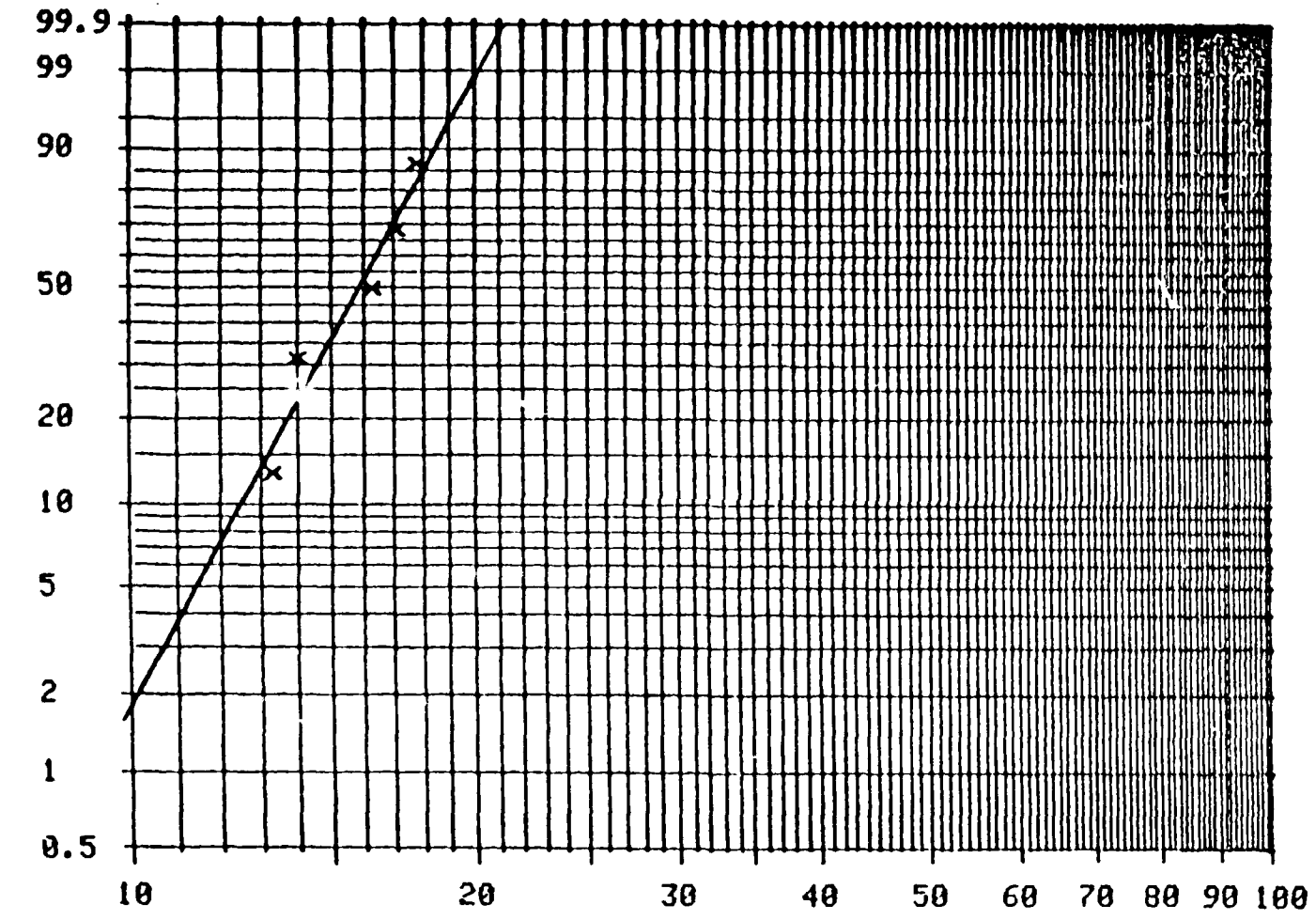
Weibull analysis of frit GM 31811 (No. 3)

fig. 4



Weibull analysis of frit 13-51 (No.4)

fig. 5



Weibull analysis of frit GM 31811 (No. 5)

fig. 6

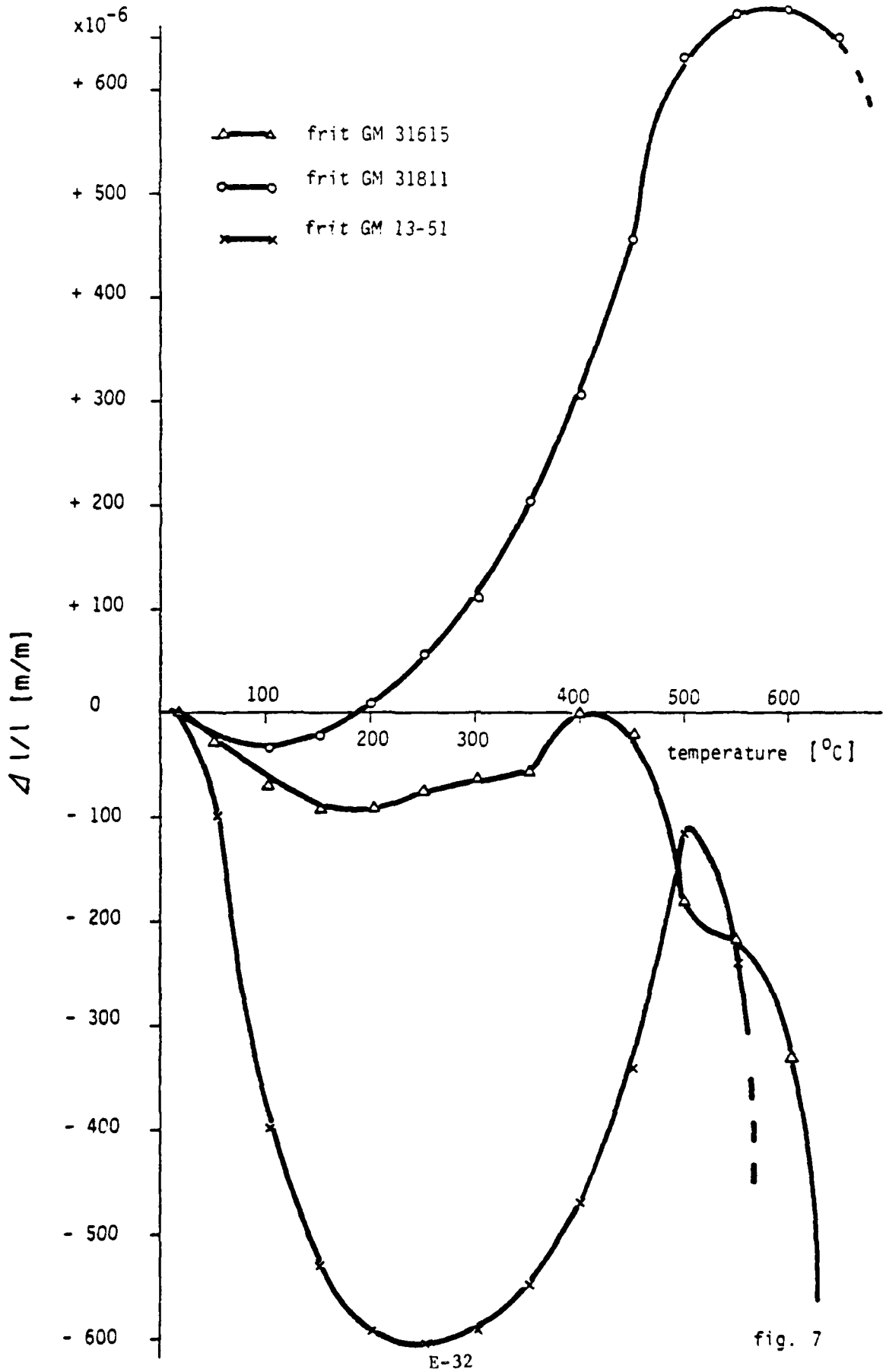

x10⁻⁶
+ 600
+ 500
+ 400
+ 300
+ 200
+ 100
0
- 100
- 200
- 300
- 400
- 500
- 600
Δ l/l [m/m]
frit GM 31615
frit GM 31811
frit GM 13-51
100
200
300
400
500
600
temperature [°C]

fig. 7

TIME SCHEDULE FOR FRIT BONDING TECHNOLOGY

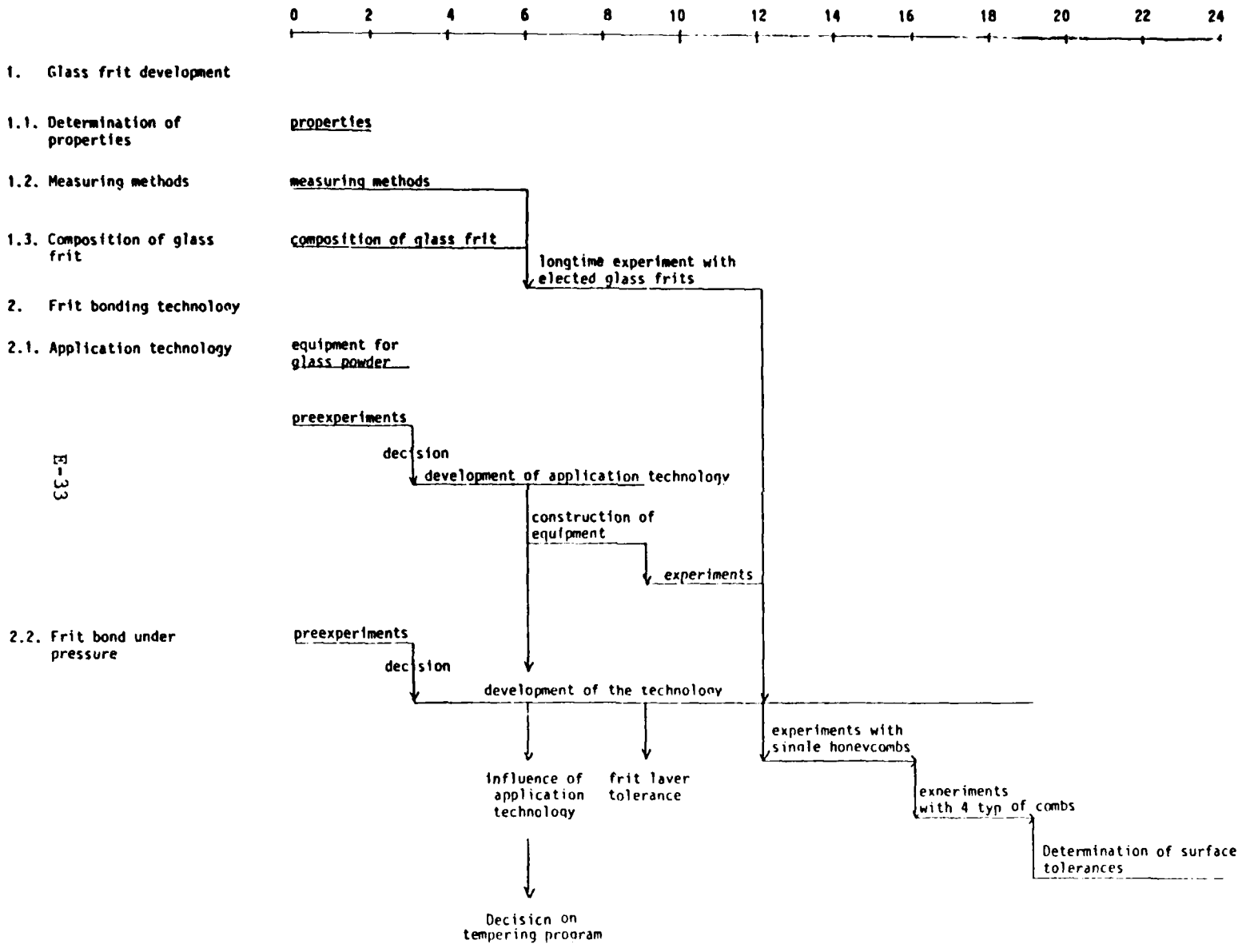


fig. 8

APPENDIX F

SCHOTT REPORT

"Study for the Manufacture of 1.5 Meter Lightweight Mirrors and Scale-up Technology Report"

Preconditions to the "Study for the manufacture of 1.5 m light-weight mirrors"

The costs in the "Study for the manufacture of 1.5 m light-weight mirrors" are only valid under the following preconditions:

1. Costs are based on today prices.
   Prices have to be increased according coming inflation rates.

2. $ to DM conversion rates are based on

   1 $ = 2,30 DM

   any change will be transferred to verdee.

3. All detail costs must be seen in conection to the total project of the manufacture of the two 1.5 m light-weight mirrors. It is not possible to take some detail costs seperate.

STUDY FOR THE MANUFACTURE OF 1.5 M LIGHT-WEIGHT MIRRORS (ENLARGEABLE TO 4 M LIGHT-WEIGHT MIRRORS)

1. Description of task

The manufacture of two light-weight mirrors with the following dimensions is meant to be described in the present study:

Plane mirror: 1.50 m dia,
0.25 m height of honeycomb,
12.70 mm height of the core sheets.

Spherical mirror: 1.50 m dia,
0.25 m height of honeycomb,
12.70 mm height of cover sheets,
10.00 m radius.

The manufacture of the light-weight mirrors may be divided in the manufacture of the honeycomb system, manufacture of the cover and bottom sheets and the soldering of the honeycomb system to the cover and bottom sheets.

The study starts from the assumption that the following development have been positively completed:

- Development of the glass frit,
- Development of the technology to bring up the glass frit,
- Development of the soldering technique up to diameters of 0.46 m,
- Manufacture of a plane and a spheric light-weight mirror up to a diameter of 0.46 m,
- Slumping of ZERODUR disks to a 1.3 m diameter.

An additional assumption is that both the rolling of ZERODUR sheets for the honeycomb system and the casting of round ZERODUR blanks for the cover sheets can be performed, using existent tanks already employed in production.

The 1.5 m light-weight mirrors have to be considered a preceding step on the road to the 4 m light-weight mirrors, i.e. all manufacturing steps required for 4 m light-weight mirrors have to be developed and tested in relation to the 1.5 m mirrors.

After manufacture of the 1.5 m light-weight mirrors has been successfully completed, the 4 m light-weight mirrors are destimed to be manufactured in the shortest period of time and with the optimum security possible. Total investment for the 1.5 m and 4 m light-weight mirrors are to be kept at as low a level as possible.

The present study is to specify the ideal course of the manufacturing process and the equipment needed, as well as the tests envisaged with the time history and personnel required.

Apart from this, the study is to offer alternative solutions in case the ideal process of manufacturing steps cannot be performed for technological reasons.

2. Preparation of the honeycomb system

Plane and vitreous ZERODUR sheets are preformed to semi-honeycombs by means of a bending fixture and are welded to a honeycomb system, using a welding apparatus. Onces welding has been completed the vitreous honeycomb system is ceramised and subsequently,subjected to rough and fine grinding processes.

2.1. Manufacture of the vitreous ZERODUR sheets

The plane and vitreous ZERODUR sheets are rolled from the glass available at an existent tank. SCHOTT master the technology of the rolling of glass ceramics and have continuous production of rolled industrial glass ceramic plates with thicknesses ranging from 3 to 7 mm. As is evident from the report "Manufacture of rolled glass for the honeycomb system of ZERODUR light-weight mirrors", the ZERODUR sheets for the honeycomb system can be rolled at a number of tanks. Which of the tanks will be used in the respective cases, will depend on the quantity of sheets required.

The rolled and plane ZERODUR sheets have yet to be cut to the dimensions required, by machines that we have available here, and have to be provided with a hole before they are bent into semi-honeycombs within the bending machine.

2.2. Preforming of semi-honeycombs

The vitreous ZERODUR sheets cut to dimensions are placed by band on to a conveyor, on which they travel discontinuously (step-by-step control) through a preheating furnace (drawing No. Pr. 1). The plates are heated up to 600 to 700 °C in the preheating furnace. The sheets, which are delivered out of the furnace in fixed-cycle operation, are received at the free delivery end - without precise positioning - by an automatic transfer device (drawing No. 1) and placed into the bending machine. The bent hot pieces are then removed from the bending machine by an automatic transfer device and then placed either on some support or directly onto a belt at the lehr charging end (drawing Pr. 2). After completing the travel cycle through the annealing lehr, the bent pieces are removed by hand, classified and stacked.

2.3. Reworking of the semi-honeycombs

In order to compensate for inaccuracies in regard to dimensions and those attributable to the mold, the prebent semi-honeycomb need to be worked on a grinding machine (drawing SK 913, sheets 1 and 2). The semi-honeycombs, in order to be ground, are placed on a feed belt, while the retaining force needed for the working is applied by a counter pressure tape. The two longitudinal edges are first milled and bevelled in a continuous-process operation, which is followed by the transfer of the semi-honeycomb from the feed belt to a faster positioning belt. As soon as the honeycomb element has touched a stop, it is pneumatically gripped and worked, and it is removed by hand when working has ended.

2.4. Welding to honeycomb system

Before the semi-honeycombs can be welded to a honeycomb system within the welding machine, they need to be preheated in a preheating furnace. Such preheating furnaces (drawing Pr. 3) are provided, one at each side, at the sealing furnace's lefthand and righthand side. The two preheating furnaces are equipped for automatic operation.

The conveying magazines are designed such that they can be charged by hand with a maximum of 12 semi-honeycombs. After conveyance into the first furnace chamber, the semi-honeycombs are preheated and subsequently heated up in the second furnace chamber to the preheating temperature required for the welding process. The preheated semi-honeycombs are automatically transferred into the welding machine.

In-line with the task set of the study, the welding machine is designed in a manner as to enable at first a 1.5 m dia. honeycomb system to be prepared, and then to allow reequipment later on for the preparation of 4 m dia. honeycomb systems. A welding machine exclusively suited for the preparation of 1.5 m dia. honeycomb systems, would not be essentially cheaper in regard to design and construction costs and would not be able to be reequipped later on for 4 m honeycomb systems.

The welding machine is designed to suit just one height of the honeycomb system. If the honeycomb system's height is changed by more than 5 mm (maximum height envisaged is 750 mm), an additional conversion kit will be needed.
The honeycomb system is illustrated on the drawings 1182-SK 1 and 1182-SK 2 the profile cross section for all honeycomb systems being equal.

Drawing No. 1182-SK 12 permits a general view of the entire welding installation with preheating furnaces. After the preheating, the bent semi-honeycombs are automatically transferred to the receiving device of the welding machine (drawing 1182-SK 6). The first line of semi-honeycomb elements feeding device (drawing 1182-SK 9) carrying the growing honeycomb system through the furnace. The functions required for the gripping device of the first line (drawing 1182-SK 13) are started manually, the subsequent steps being automatic. Drawing No. 1182-SK 10 shows the receiving device by means of which the additional lines are attached to the growing honeycomb system. The positions to be welded of the preheated semi-honeycomb elements are very rapidly heated by special-type burners and the semi-honeycomb elements welded to the honeycomb system. In accordance with drawing No. 1182-SK 7, platforms are provided to support the honeycomb system, the said platforms being guided by five rails inside the furnace and being dragged by the feeding device. During the entire welding operation, the welded portion of the honeycomb system is placed inside a ceramisation furnace at a temperatur between 600 and 700 °C. After welding has been terminated, the honeycomb system is adjusted to the furnace center and automatically unlocked.

Before ceramisation starts, the welding burners and the conveying equipment have to be removed from the ceramisation furnace (drawing Pr. 4). To achieve good furnace insulation, the slots and openings provided have to be carefully made tight by means of prepared elements. After completing ceramisation, the second furnace port opposite the welding machine is opened in order to allow the honeycomb piece to be transferred by means of a special-type pneumatic hoisting device (drawing Mz 43-8-001) onto a transfer car.

2.5. Rough and fine grinding of the honeycomb system

After ceramisation has been completed, the semi-honeycomb's protruding parts are first cut off.
In order to enable the honeycomb system to be rough- and fine-worked, same has to be provided with a ZERODUR clamping and retaining ring, whose thickness has to be at least 10 mm. To this end, single plates of rolled ZERODUR are cold-cemented to the prerounded honeycomb system and subsequently rounded to form a ring.

Rough working of the plane and spheric honeycomb systems is carried out at SCHOTT's domicile, while the fine working is performed at ZEISS.
Judging by the present state of development of the glass frit, a frit layer thickness of between 10 µm and 20 µm is to be taken into account. The demand resulting from this is that the peak-to-valley heights and unevennesses on the cover and bottom sheets and at the honeycomb system front sides, respectively, shall be < 10 µm. The honeycomb system-to-cover sheet distance is permitted to be only as large as to cause the cover sheets to be pressed all over onto the honeycomb system as a result of the pressure applied.
After fine grinding has been completed, the honeycomb system is transported back to Mainz for soldering.

3. Manufacture of cover and bottom sheets

Both cover and bottom sheets have the same radius of curvature. To manufacture curved cover and bottom sheets, there are three alternatives:

- Elaboration from a ceramised ZERODUR plate,

- Spin-casting of curved ZERODUR plates and separate ceramisation,

- Slumping of vitreous ZERODUR plate with subsequent ceramisation.

The elaboration of cover and bottom sheets from ceramised thick ZERODUR plates is a non-productive operation if a larger number of pieces is involved. It is therefore listed under the alternative manufacturing operations.

The spin casting of curved ZERODUR plates entails high costs for the experiments performed, as is evident from the study about the spin casting of cover sheets. The spin-casting of cover and bottom sheets is, consequently, listed under the alternative solutions for the manufacture.

The most advantageous method at present offered and considered for the manufacture of bottom and cover sheets is the slumping of vitreous ZERODUR plates.

3.1. Slumping of vitreous ZERODUR plates

The manufacture of spheric cover and bottom sheets can be achived by the slumping of plane vitreous ZERODUR plates into or above a mold.

The ceramised ZERODUR is virtually no longer able to be slumped since the viscosity of ZERODUR is too high. Therefore, the slumping has to be carried out prior to the ceramisation process, and the sagging process, thus, competes with the ceramisation process. In the case of large ZERODUR blocks of the type used here, already during the annealing in the manufacturing process partial crystallization occurs, which may obstruct the slumping ensuing. The slumping, therefore, of the vitreous ZERODUR plates is a function of the ZERODUR's thermal prehistory, the geometric dimensions, the temperature run and the pressure during the slumping process.

The present study starts from the assumption that plane, round, vitreous ZERODUR plates can be slumped by the application of vacuum below the temperature of crystallization. To achieve this end, the vitreous ZERODUR plate is placed into a mold exhibiting the desired radius of curvature, which can be connected to a vacuum pump. The mold, along with the ZERODUR plate, is transferred into a furnace provided and heated up to the desired slumping temperature after applying the vacuum. After the slumping operation has been completed, the ZERODUR plate still proves to be largely vitreous and will have to be ceramised in a second heating-up run, which may be performed again in the furnace available.
Crystallization following directly after slumping is possible, but is not strived for at the moment.

A final statement on the slumping of ZERODUR plates can be made only after the laboratory tests planned and the manufacture of the samples of 0.5 m and 1.3 m, respectively (cf. PERKIN ELMER RFP 8182-RZ). These experiments are also meant to demonstrate that the slumping of vitreous ZERODUR plates is feasible up to a diameter of 4 m.

Under the alternative solutions, the rapid heating-up and slumping in a special-type twin-chamber furnace is discussed.

3.2. Rough and fine working of plane and curved cover and bottom sheets

In regard to peak-to-valley heights and the unevennesses, the same applies to the cover and bottom sheets as to the honeycomb systems. It is envisaged to perform the rough working of cover and bottom sheets at SCHOTT and the fine working at ZEISS.

4. Soldering of cover and bottom sheets to the honeycomb system

The joining of the cover and bottom sheets to the honeycomb system is meant to be performed by means of a glass frit. In order to guarantee a success of the project, a positive completion of the following developments is an absolutely necessary pre-condition for the present study:

- Development of the glass frit,
- Development of the technology related to the application of the glass frit,
- Development of the soldering technology up to 0.46 m diameter.

The experimental program required for this and the pertinent costs will be compiled in a separate report.

4.1. Development of the glass frit

SCHOTT have developed a glass frit at their own expense. The present state of this development has been made known to PERKIN ELMER. The glass frit available is considered to be insufficient, and development will have to be continued in order that the requirements listed below be met:

- High degree of bonding strength,
- a possible low Δ (Δ 1/1) between ZERODUR and the glass frit,
- a possible low variation of the tension between -50 °C and +150 °C,
- soldering temperatur $\leqslant$ 800 °C.

In the present study, the glass frit with its required properties is considered as being available.

4.2. Development of the technology for applying the glass frit

The glass frit has to be applied to the webs of the honeycomb system and/or to the interior side of the cover and bottom sheets as evenly as possible, the layer thickness tolerance being low. The layer thickness will be between 10 µm and 20 µm. Starting from certain conceptions on the manufacture and application of such thin glass frit layers, we have to develop the respective processes and test them in the laboratory.
Application of the glass frit has to be performed in an ambient where impurities are < 10 µm.

4.3. Development of the soldering technique

For the soldering of ZERODUR to ZERODUR, pressure has to be applied for intensifying the sintering process in accordance with the present state of development.
Such pressure can be caused either by weights or by the application of vacuum. In both cases it is important that the pressure is caused to act uniformly all over. This, for instance, makes it a necessity that both the weights put on the curved mirror and the calotte supporting the mirror have to be precisely ground. The advantage attached to the vacuum technique is that higher pressures can be used; the problems of sealing and deformation during the sintering process, however, first need to be tested on a laboratory scale, then with a 0,46 m light-weight mirror, before a final statement can be made on the soldering technique.

The present study starts from the assumption that pressure is caused through weights.

Judging by the present state of the development, the soldering process might proceed as follows hereafter. The fine-worked mirror components (cover sheet, honeycomb system, bottom sheet) are cleaned and placed on mounting appliance, whereafter the glass frit is applied to the lower side of the honeycomb system and/or to the interior side of the bottom sheet. Within an assembly stand, the bottom sheet is placed on top of the honeycomb system's lower side, which is turned upside-down, and fixed. Following this, the honeycomb system with bottom sheet is turned in a roll-over frame and fixed in a receiving appliance. The glass frit is now applied to the honeycomb system upper side and/or to the cover sheet interior side, and the cover sheet is then fixed onto the honeycomb system by means of the assembly stand. The assembly stand has to be designed in a way as to make possible the precise fixing of both cover and bottom sheet, and as to prevent the two sheets from becoming displaced while the weights are being put on and the vacuum is being applied, respectively, and during the transfer into the ceramisation furnace.

Transport from the purified ambient into the ceramisation furnace will be by means of a transfer car running on rails. Charging of the ceramisation furnace will be through the port situated at the furnace side showing away from the sealing machine. The light-weight mirror, together with receiving device and weights, is put on a stand inside the ceramisation furnace and soldered.

5. Realization of the project

Realization of the entire project can be devided in 8 sections which are marked in the diagram from I to VIII.

I: Planning, design and construction of required buildings and installations (buildings, furnaces for bending, furnaces for welding/ceramisation/soldering, bending machine, welding unit, soldering installations, transfer and turing devices, slumping installation, data acquisition and data processing unit).

II: Continued development of soldering technique for 1.5 m dia., in relation with which we assume that the solder and the soldering technique for the 0.46 m dia. have been developed in full. The tests required are to be performed with small honeycomb systems (height 100 mm, 0.46 mm dia.) made of ZERODUR and ROBAX 8568 that have been prepared on the welding machine available. The cold-working processes can, as far as this is deemed to be necessary, be further developed with these honeycomb systems. In the present study, 20 of such honeycomb systems have been considered. The required cover sheets are planned to be made of ROBAX 8568 (ROBAX 8568 is an industrial glass ceramic).

Essentially, I and II run parallel in time.

III: Testing of all installations needed for bending and welding. As far as the employment of glass will be necessary, we will use ROBAX 8568 (manufacture of ROBAX sheets from available rolled raw material, testing of bending furnaces, bending machine, welding furnaces, welding unit, manufacture of 4 large honeycomb systems up to 1.7 m dia. from ROBAX 8568).

IV: Manufacture (rolling included) of parts to be bent from ZERODUR for testing purposes (cf. V), and for the production of the honeycomb systems (cf. VII).

III and IV run essentially parallel in time.

V: Practicing of the technolgies WELDING, COLD-WORKING and SOLDERING together with large honeycomb systems and 2 large cover sheets; initially, this is done with ROBAX 8568, while at the end ZERODUR is used.

VI: Manufacture (sawing, slumping, ceramising, rough-working) of cover sheets for the two 1.5 m dia. mirrors to be delivered. The number of pieces to be manufactured essentially depends on how many failures occur in soldering. Within the framework of the present study, 7 plane and 13 spheric cover sheets are planned to be made.

VII: Manufacture of honeycomb systems for the two 1.5 m dia. mirrors to be delivered, inclusive of the manufacture of the components to be bent (without rolling). The number of pieces to be manufactured essentially depends on how many failures occur in soldering. 6 plane and 8,5 spheric honeycomb systems are planned to be made.

VI and VII run essentially parallel in time.

VIII: Manufacture of two mirrors, 1.5 m in dia. (fine-working of honeycomb systems together with 2 cover sheets each, soldering of the honeycomb systems with 2 cover sheets each, finishing, delivery). The number of parts subjected to fine-working essentially depends on how many failures occur on soldering. The present study assumes that 3 plane and 6 spheric systems (cover sheet, honeycomb system and bottom sheet) will have to be fine-worked.

VIII in part runs parallel in time with VII:

The precise timely progress is evident from the diagrams of the network plan prepared for the 1.5 m mirror.

6. Cost calculation

In the following cost calculation starts from the assumption that after successful manufacture of the two 1.5 m lightweight mirrors is to ensure within a possibly short period of time, the total investments for the 1.5 m and the 4 m lightweight mirrors being as low as possible. Additionally, the assumption is made that both rolling of the ZERODUR plates for the honeycomb system and the casting of ZERODUR blocks for the cover sheets will be able to be realized, using tanks already available in production.

In line with the task set, costs for the developments preceding the manufacture of the two 1.5 m mirrors will be listed separately.

6.1. Costs for the developments preceding the manufacture of 1.5 m lightweight mirrors

In order to provide a better general view of the costs, we are compiling again hereafter the costs already depanded separately for developments preceding the present study.

Development costs for soldering: (in thsd. dollars)

- Development of glass frit	195
- Development of the technology related to the application of the glass frit and the soldering technology	280
	475

Development costs for two 0.46 m lightweight mirrors (assuming that development of soldering will be successful): (in thsd. dolla

- 1 plane and 1 spheric mirror	220

Costs for slumping experiments: (in thsd. dollars)

- Laboratory development	125
- Manufacture of a 0.5 m plate	30
- Manufacture of a 1.3 m plate	75
	230

Total costs for the developments assumed by the present study amount to: (in thsd. dollars)

925

6.2. Costs for buildings and general-type installations

The building meant to be used in regard to the manufacture of honeycomb systems and the soldering of honeycomb systems to cover and bottom sheets is designed for the manufacture of 4 m lightweight mirrors. The costs for the two factory buildings and the three-storey office and laboratory building (drwg. MZ 43-2-001) are composed of the following: (in thsd. dollars)

- Preparation of the building site	83
- Development costs	113
- Erection of the buildings with fuel and electricity installations and cranes	1635
- Outside installations	30
- Incidental building costs	140
- Equipment of offices, laboratories and 4 staff facilities	56
- Centre of controls	322
- General transportation means	177
	2556

6.3. Investment costs for the manufacturing facilities

6.3.1. Investment for the manufacture of the honeycomb systems

The manufacturing facilities for the manufacture of the honeycomb systems are designed in part as to allow the manufacture of 4 m honeycomb systems, too. This particularly applies to the bending of the semi-honeycombs and the ceramisation furnace. The welding machine can likewise be modified to suit 4 m honeycomb systems by attaching additional welding burners.

The present study starts from the assumption that the ZERODUR plates serving for the manufacture of the semi-honeycombs can be produced, using a melting tank with rolling unit already employed in production. For the preparation of the honeycomb systems, the following production and control installations will be needed:

ZERODUR plates: (in thsd. dollars)

- Reworking tools for ZERODUR plates	40

Transformation into semi-honeycombs: (in thsd. dollars)

- Preheating furnace	60
- Bending machine	60
- Handling machine	57
- Annealing lehr	211

Reworking of semi-honeycombs: (in thsd. dollars)

- Grinding machine	220

Welding to form honeycomb system: (in thsd. dollars)

- Two preheating furnaces	329
- Welding machine	910
- Controlling unit	94
- Ceramisation furnace	437

Rough working of honeycomb systems

- Working tools	274

Total investment costs for honeycomb system: (in thsd. dollars)

2692

The conversion of the welding machine to a different honeycomb height will entail costs in the amount of 260,000 $. A ceramisation furnace for honeycomb systems of a 1.5 m maximum would amount to only 284,000 $ instead of 437.000 $. But the 437,000 $ would have to be defrayed later on in addition to the 284,000 $ for a 4 m honeycomb system.

6.3.2. Investments for the manufacture of cover sheets

We start from the assumption that slumping of the ZERODUR plates for spherical cover and bottom sheets can be realized under pressure within a provided furnace with slumping device: (in thsd. dollars)

- Slumping device	124
- Grinding tools and mounting support	38
	162

6.3.3. Investments for soldering

Investments for soldering cannot be specified exactly as the soldering technique has not yet been finally established.

Estimated costs: (in thsd. dollars)

- Purification unit	30
- Installation for the preparation of thin solder layers	15
- Installation for application of solder layers	40
- Adjusting device	25
- Assembly appliances	15
- Ceramisation molds	150
- Weights, ground	50
	325

6.4. Costs for material and rough working

Material costs include the costs for melting the glasses and the batch costs. Rough-working costs only take into consideration the work performed by SCHOTT.

6.4.1. Material and rough-working costs for honeycomb system (in thsd. dollars)

Glass: 193

- 3000 ROBAX plates for preliminary tests
- 200 ZERODUR plates for preliminary
- 2850 ZERODUR plates for plane honeycombs
- 4080 ZERODUR plates for curved honeycombs

Rough-working for plates: 198

- 3000 ROBAX plates for preliminary tests
- 200 ZERODUR plates for preliminary
- 2430 ZERODUR plates for plane honeycombs
- 3480 ZERODUR plates for curved honeycombs

Working for honeycomb systems: 988

- 10 plane honeycombs for preliminary tests (small type)
- 4 plane honeycombs for preliminary tests (large type)
- 4 plane honeycomb systems, 1.5 m in dia
- 6 curved honeycomb systems, 1.5 m in dia.

Total costs for material and rough-working of honeycomb systems:

1379

6.4.2. Material costs and rough-working costs for cover sheets (in thsd. dollars)

Glass: 170

- 40 cover sheets for preliminary tests
- 7 plane cover sheets, 1.5 m dia.
- 13 spherical cover sheets, 1.5 m in dia.

Rough-working: 299

- Plane cover sheets for preliminary tests
- Spherical cover sheets for preliminary tests
- 7 plane cover sheets, 1.5 m in dia.
- 13 spherical cover sheets, 1.5 m in dia.

Total costs for material and rough-working of cover sheets:

469

6.4.3. Rough-working costs for soldered lightweight mirror

Costs include only one rough-working operation of completely soldered lightweight mirrors before these are supplied to PERKIN ELMER.

Rough-working: (in thsd. dollars) 188

- 1 plane mirror system
- 1 spherical mirror system

6.5. Personnel costs and fuel and electricity costs for tests and manufacture of samples

In the calculation of fuel and electricity costs we have started from the assumption that tests and production might take up to 8 years and that all 12 mirrors must be produced.

Fuel and electricity costs: (in thsd. dollars)

- Electricity, gas and water	335
- Heating	209
Total fuel and electricity costs	544

Maintennance costs: (in thsd. dollars)

- Building	75
- Furnaces	120
- Equipements	240
	435

Personnel costs: (in thsd. dollars)

- Academics 77 man/months	690
- Engineers 75 man/months	385
- Laboratory assistants 95 man/months	328
- Auxiliaries 100 man/months	370
- Secretary 48 man/months	184
Total personnel costs	1957

6.6. Compilation of investment and manufacturing costs

Investment costs: (in thsd. dollars)

- Building and general installations	2556
- Manufacturing facilities:	
for honeycomb system	2692
for cover sheets (sagging)	162
for soldering	325
Total of investment cost	5735

Material costs and rough-working costs: (in thsd. dollars)

- for honeycomb system	1379
- for cover sheets	469
- for mirror	188
Total of material costs and working-costs	2036

Personnel and fuel and electricity costs: (in thsd. dollars)

- Fuel and electricity costs	544
- Maintennance costs	435
- Personnel costs	1975
Total of personnel and fuel and electrocity costs	2936

Total costs for two 1.5 m lightweight mirrors: (in thsd. dollars)

10707

Preliminary development costs for commencing 1.5 m lightweight mirror project: (in thsd. dollars)

- Development of glass frit and soldering	475
- Manufacture of two 0.46 m dia. mirrors	220
- Slumping tests with ZERODUR plates	230
	925

Costs for predevelopment and 1.5 m mirror: (in thsd. dollars)

- Predevelopments	925
- Manufacture of two 1.5 m mirrors	10707
	11632

7. Alternative solutions

In preparing the present study on the manufacture of 1.5 m lightweight mirrors some assumptions have been made the coming true of which is not certain. It is for this reason that we are showing some alternative solutions.

7.1. Melting tank and rolling unit for ZERODUR plates

This study has assumed that during the time in which the ZERODUR plates are planned to be rolled a ZERODUR tank will be in operation, where the plates would be rolled.

In the event that no agreement with the melting schedule can be reached, an extra tank will have to be set up for rolling tests. This would entail additional costs of the order of

550000 $.

7.2. Additional slump furnace for cover sheets

The assumption has been made in the present study that the slumping tests can be realized in the furnaces provided. A final statement can be made only after laboratory tests and the 0.5 m sample plate.

It cannot be precluded, therefore, that a special-type two-chamber furnace (drwg. No. 2) will be required for the slumping tests which allows rapid heat-up of the vitreous ZERODUR plate. Costs for this two-chamber furnace will amount to 167000 $. But this two-chamber furnace would necessitate an enlargement of the planned building, which would entail investment costs of the order of 215000 $.Thus, the additional investment costs for the slumping of the cover and bottom sheets would total 382000 $.
If the slumping of the cover and bottom sheets is not to be realized within the framework the production of the 1.5 m light-weight mirror, but independently, a new building will be needed for the two-chamber furnace instead of an enlargement. In such case, investment costs for the building will amount to 700000 $ instead of 215000 $.Along with the costs for the two-chamber furnace, investment costs, then, will rise to a total of 867000 $.

7.3. Working-out of spherical cover sheets from solid ZERODUR plates

In the case of large curvature radiuses and small numbers of pieces, the working out of spherical cover sheets from solid ZERODUR plates is possible, too.

SCHOTT cope with the manufacture and ceramisation of ZERODUR blocks up to a diameter of 4 m. From 1.5 m dia. ZERODUR blocks available, 60 mm plates can be cut off, while the 12,7 mm thick curved cover and bottom sheets can be mechanically worked out from these.

7.4. Spin-casting of curved cover sheets

SCHOTT have managed to gain experiences with the spin-casting of industrial large-size glass vessels. These experiences, however, need to be transferred to the manufacture of curved ZERODUR plates, 1.5 m (and 2.1 m, respectively) in diameter. The testing equipment required to this end (drawings SK 909 and SK 912) and the tests are to be gathered from the "Study on the Manufacture of curved Cover and Bottom Sheets for Lightweight ZERODUR Mirrors by Spin-casting".

Once these spin-casting tests can be considered to have been successful, the curved cover and bottom sheets can be directly manufactured. A tank with special-type feeder will be needed for the spin-casting tests and the manufacture of spin-cast cover and bottom sheets. This tank may be set up at an already existent tank installation.

Costs for spin-casting tests (cf. study on spin-casting tests):
(in thsd. dollars)

- Tank costs	555
- Glass and melting costs	800
- Annealing costs	65
- Design and construction of spin-casting unit (up to 2.1 m dia.)	750
- Costs for testing	350
Costs for spin-casting tests	2520

What has to be added to these test costs are the manufacturing costs in relation to the 1.5 m dia. cover and bottom sheets needed for the 1.5 m lightweight mirrors. The following costs are valid, if the spherical sheets are produced immediately after the spin-casting tests, that means in the same tank.

Investment costs: (in thsd. dollars) 38

- Grinding tools and mounting support

Material and working costs: 502
(in thsd. dollars)

- Glass costs for 14 spherical cover sheets, 1.5 m dia.
- Working costs for 14 spherical cover sheets, 1.5 m dia.

Manufacture of the cover and bottom sheets in accordance with the spin-casting process initially required extremely high testing and investment costs in relation to the spin-casting tests. But also for the subsequent manufacture of cover and bottom sheets, using the tank and spin-casting unit provided for, the material and working costs reach high. For spherical cover and bottom sheets, 1.5 m dia. and > 10 m curvature radius, the spin-casting process is more expensive than the slump process or the working-out from a solid ZERODUR-plate.

Spin-casting is only of interest in relation to small-curvature-radius cover sheets not able to be manufactured in accordance with the slump process.

8. Fine-working costs

Within the framework of the present study, fine-working of cover sheets, honeycomb systems and bottom sheets is to be realized at ZEISS. Costs, however, will be specified sparately as PERKIN ELMER might very well intend to perform these jobs themselves.

Investment costs: (in thsd. dollars) 1005

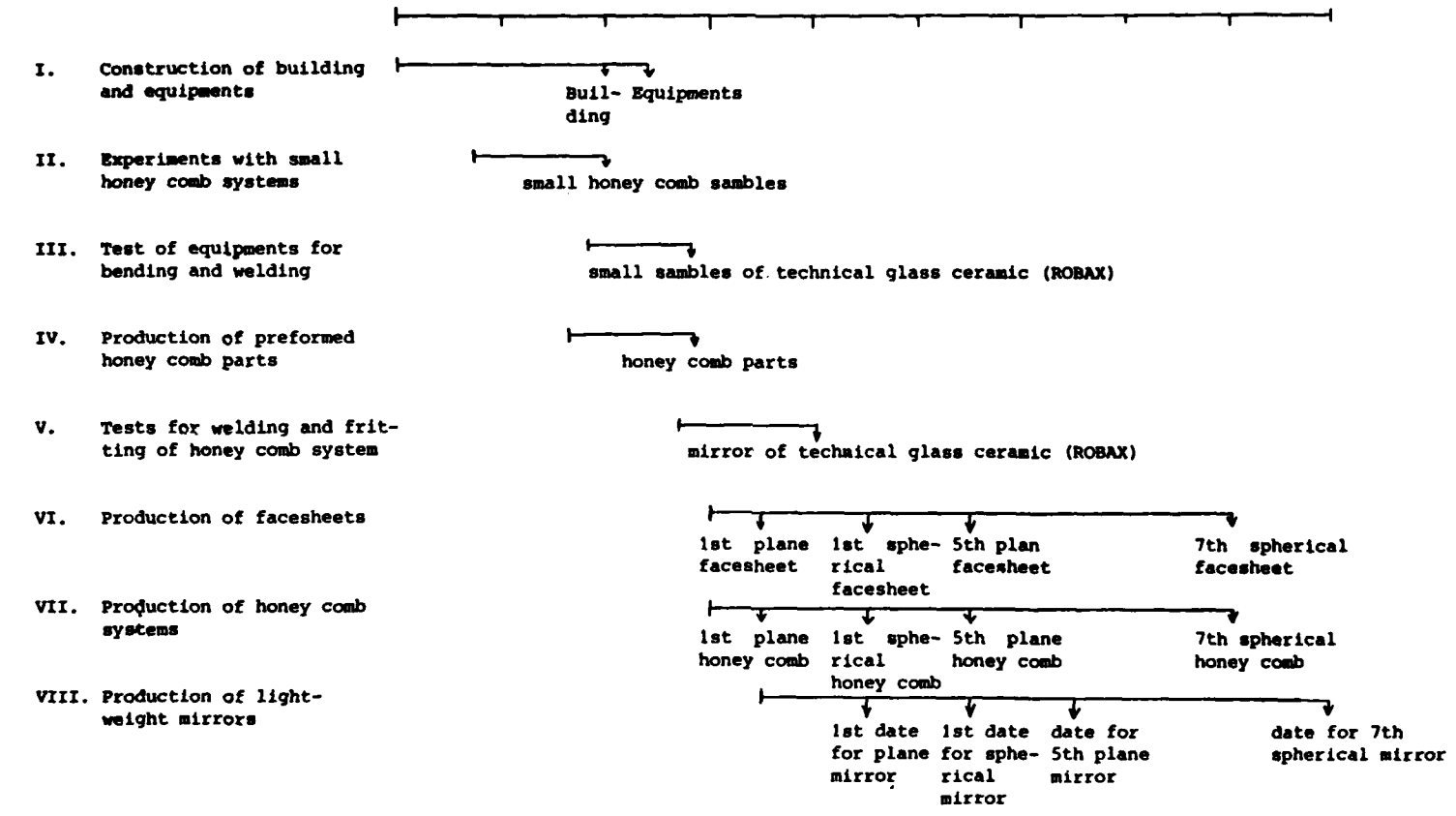
- Tool costs for plane 1.5 m mirrors
- Tool costs for spherical 1.5 m mirrors

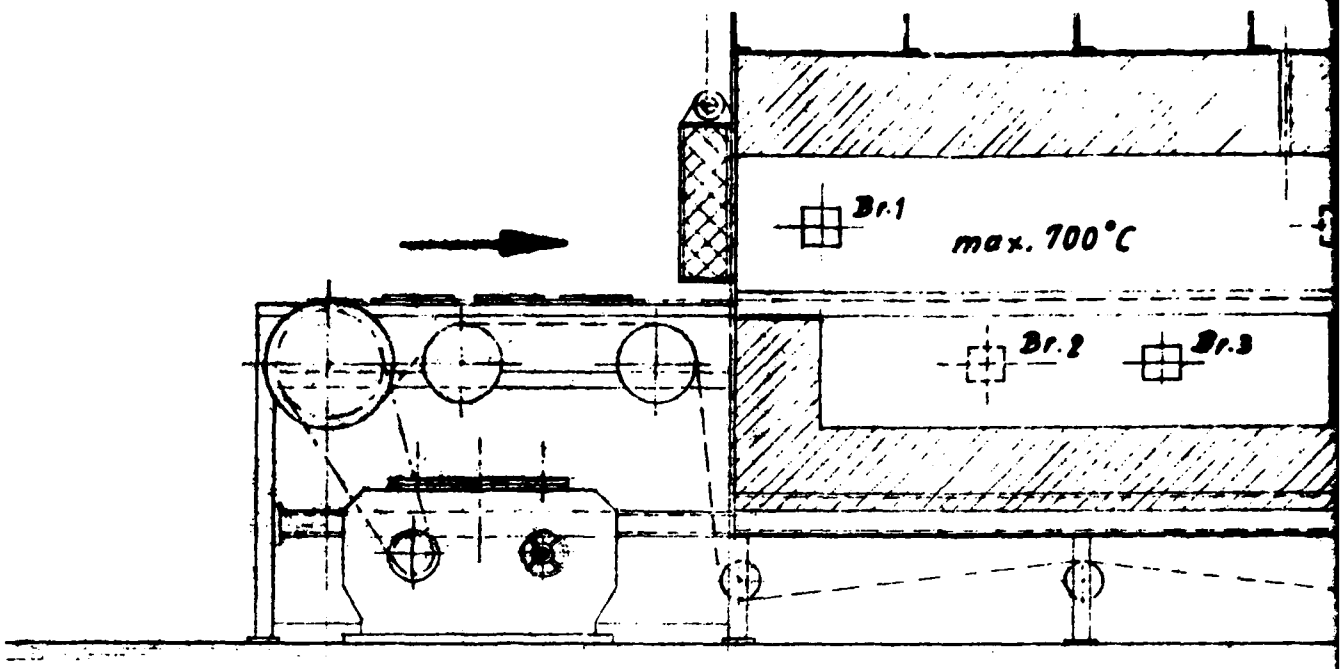
Fine-working costs: (in thsd. dollars)

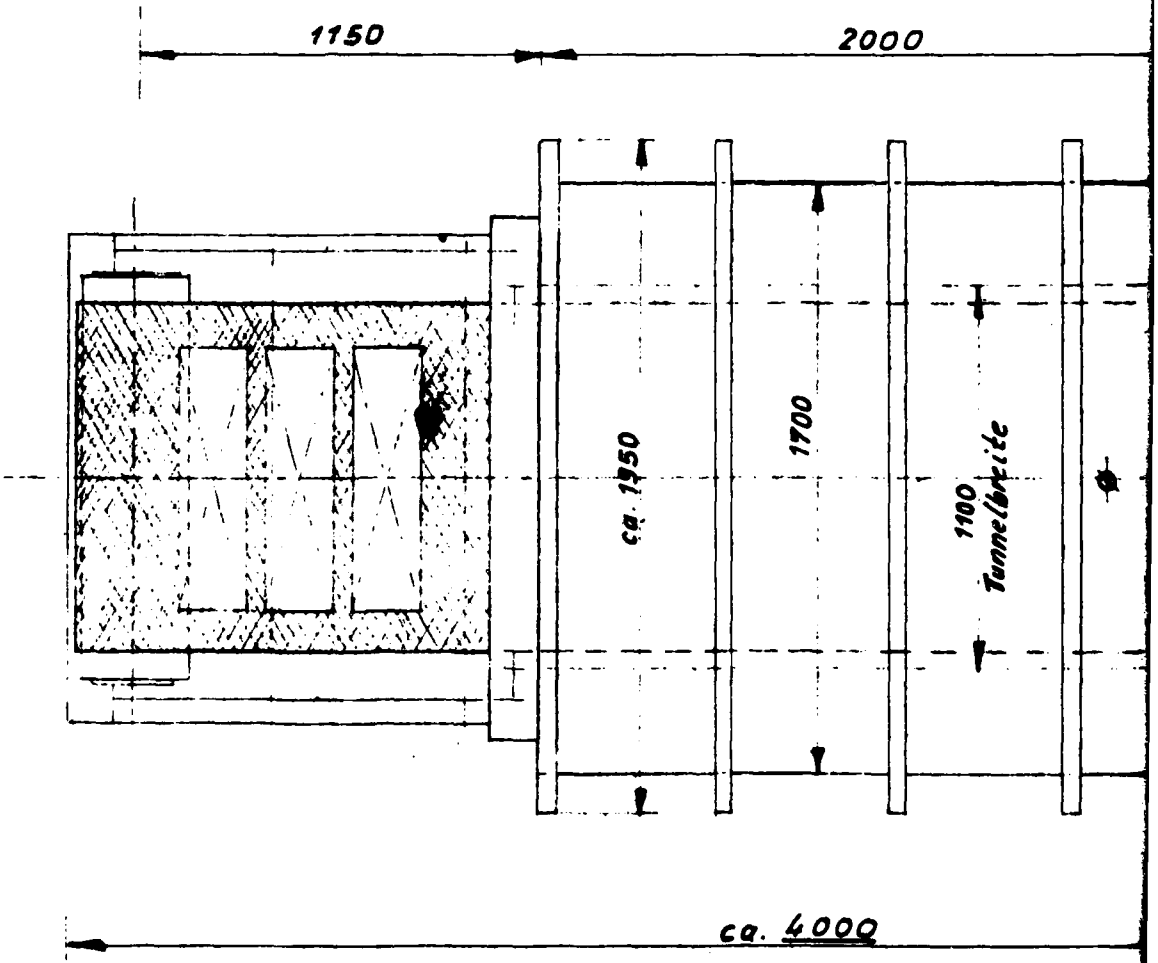
- 10 honeycomb systems with cover sheet for preliminary tests 55
- 1 honeycomb system with cover sheet, 1.5 m in dia., for preliminary tests 95

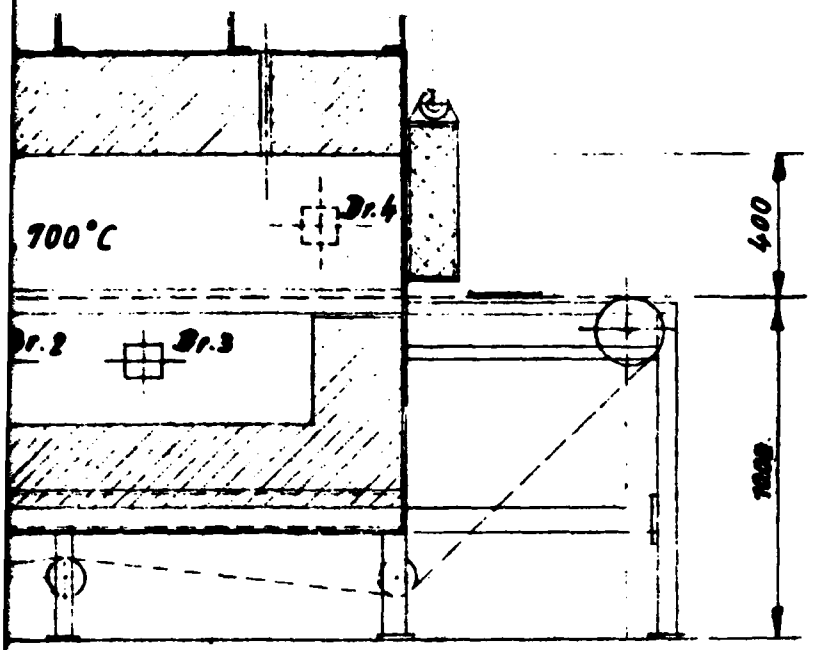
- 3 plane honeycomb systems, 1.5 m in dia., with cover sheets for tests and samples	290
- 6 spherical honeycomb systems, 1.5 m in dia., with cover sheets for tests and samples	580
	1020

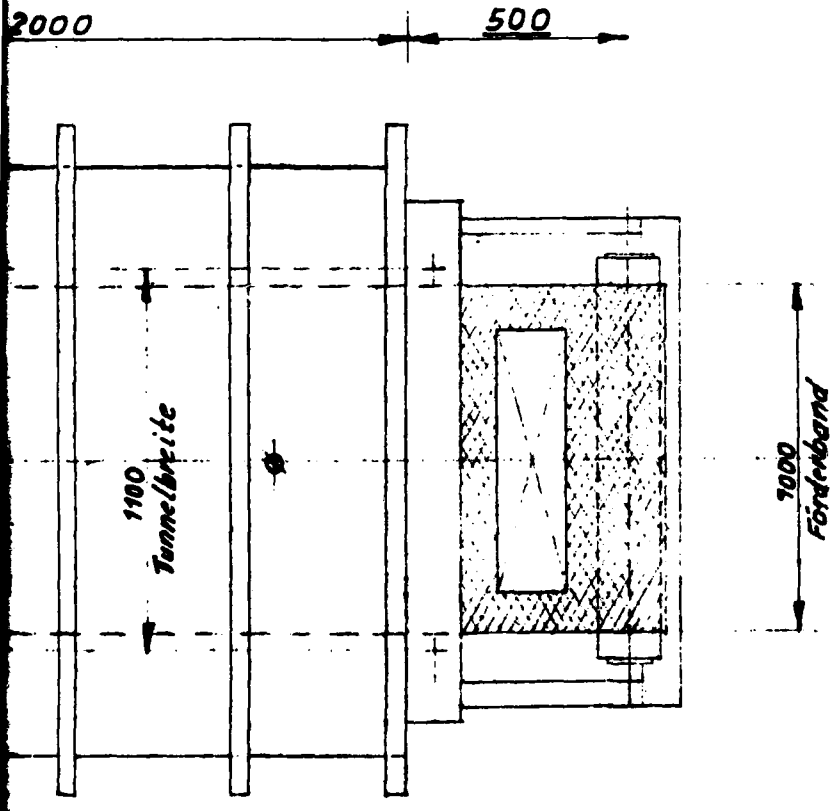
Time schedule for the production of a plane and a spherical 1,5 m light-weight mirror




Br.1
max. 700°C
Br.2
Br.3


1150
2000
ca. 1950
1700
1100
Tunnelbreite
ca. 4000





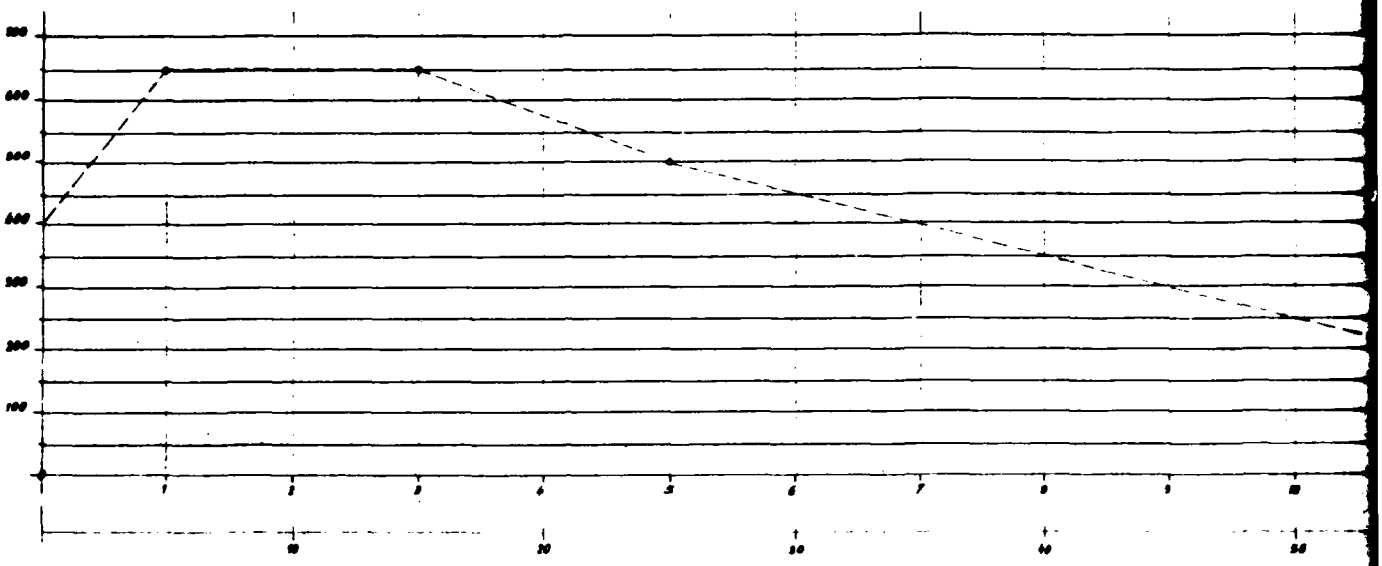
	gez.	7.1.82	
	gepr.	Bo	
Maßstab 1:20	Vorwärmofen für plane Zerodurglas-Platten		Pr. 1

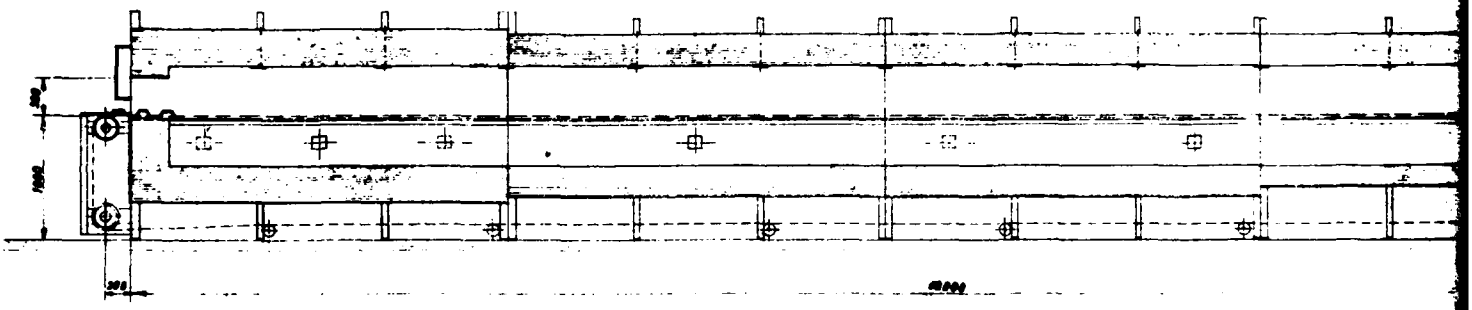
F-33

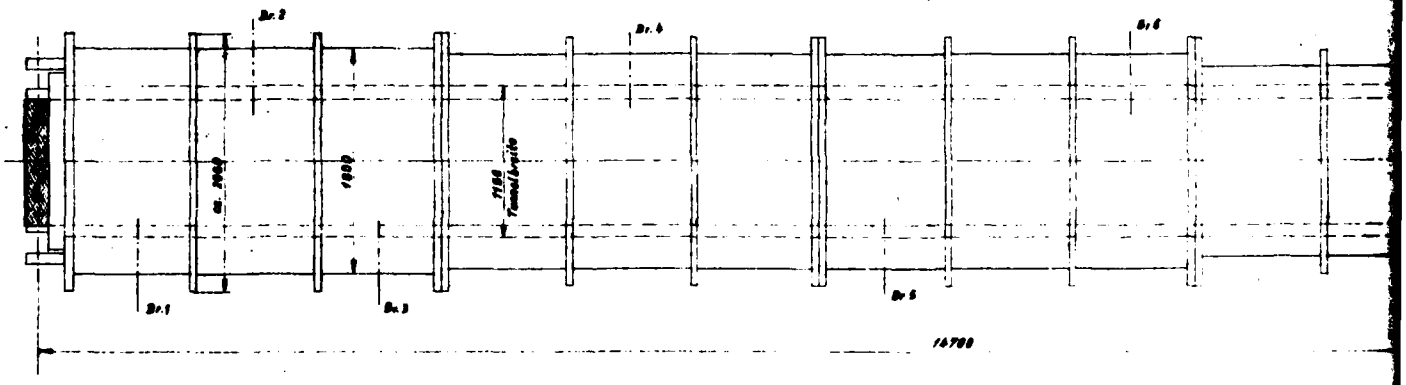
SCHOTT

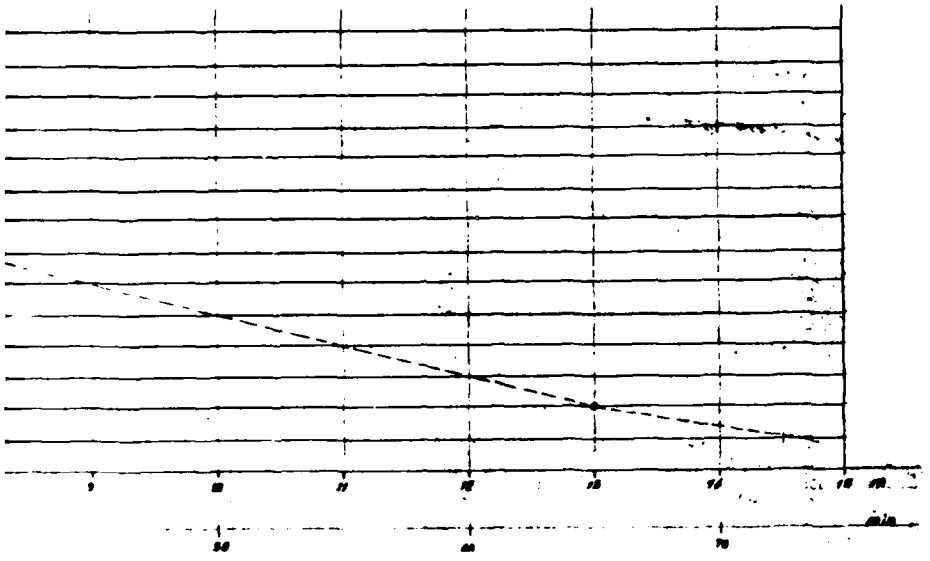
fen
irglas-Platten

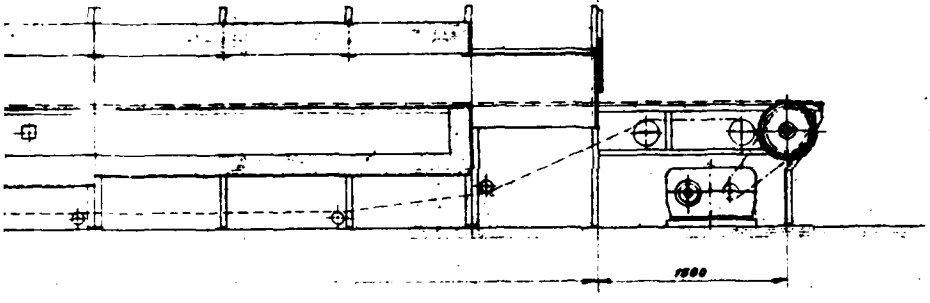
Pr. 1

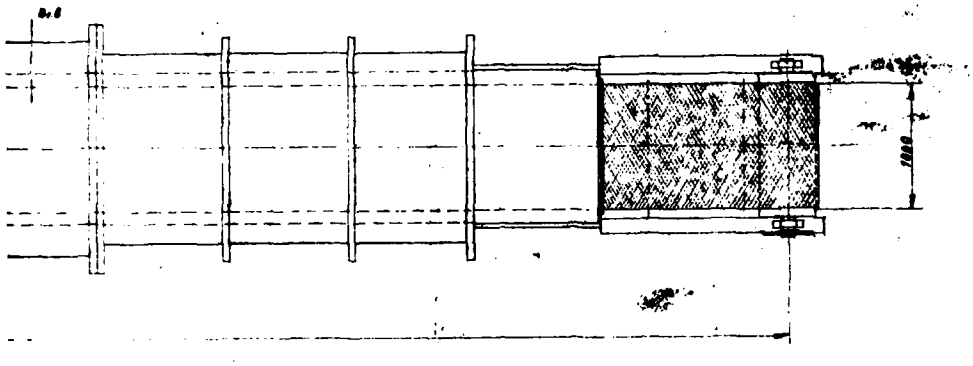












Zust. stell	Bezeichnung	Teil	Zeichnung Nr.	Werkstoff	Gewicht
Änderungsvermerke:					

Diese technische Unterlage ist unser Eigentum. Sie darf nur zu dem vereinbarten Zweck verwendet werden. Jede unbefugte gewerbliche Benutzung, Vervielfältigung oder Weitergabe an Dritte ist ohne unsere vorherige Zustimmung strafbar. Zuwiderhandlungen verpflichten zum Schadenersatz.

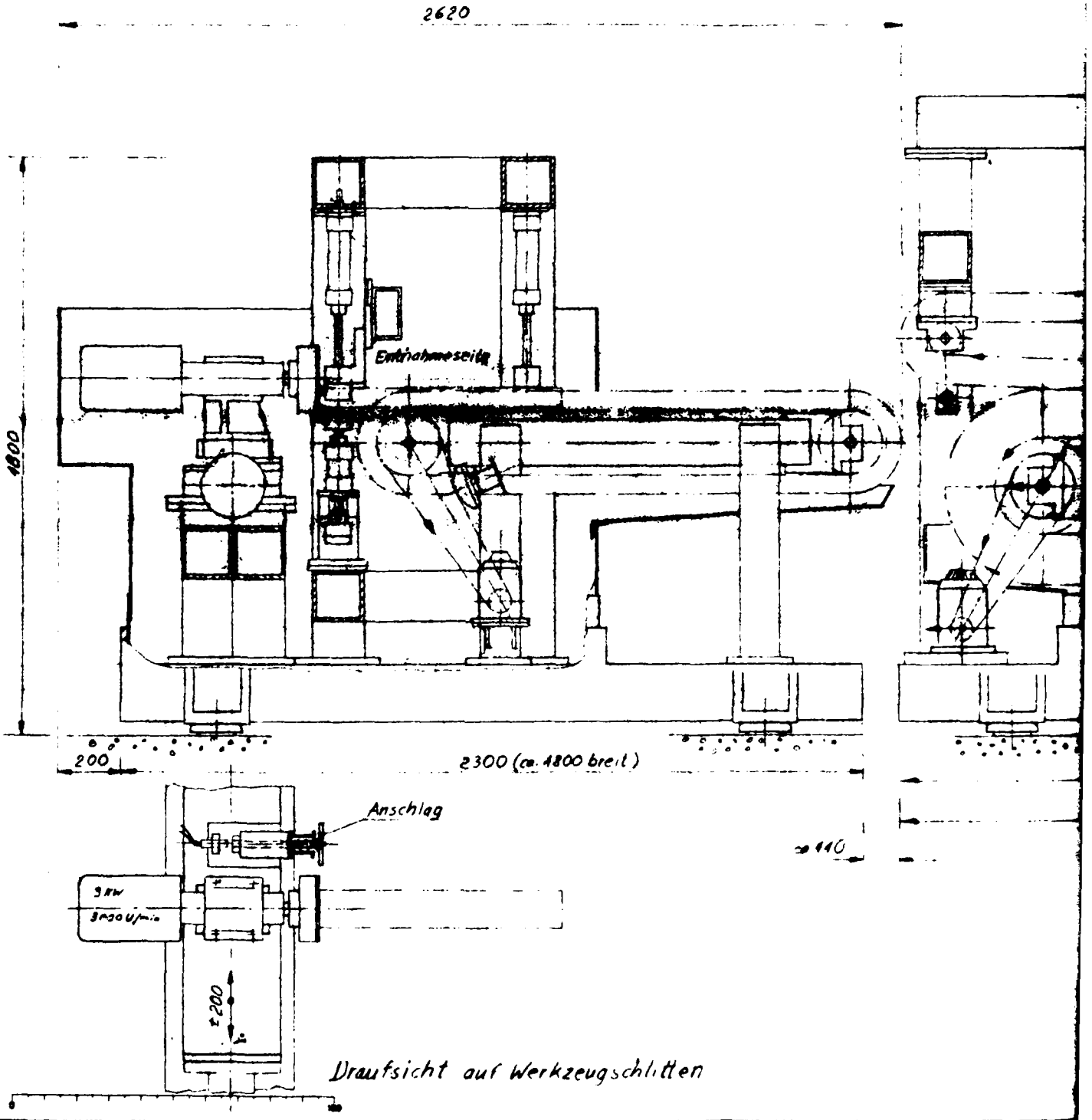
	Tag	Name	
gezeichnet	6.1.82	Bo	SCHOTT
geprüft			

Maßstab 1:25	Bandkühlofen für gebogene Zerodurglas-Platten	Glasbau-Bibl. Nr. Pr. 2 45%
		Ersatz für
		Ersatz durch

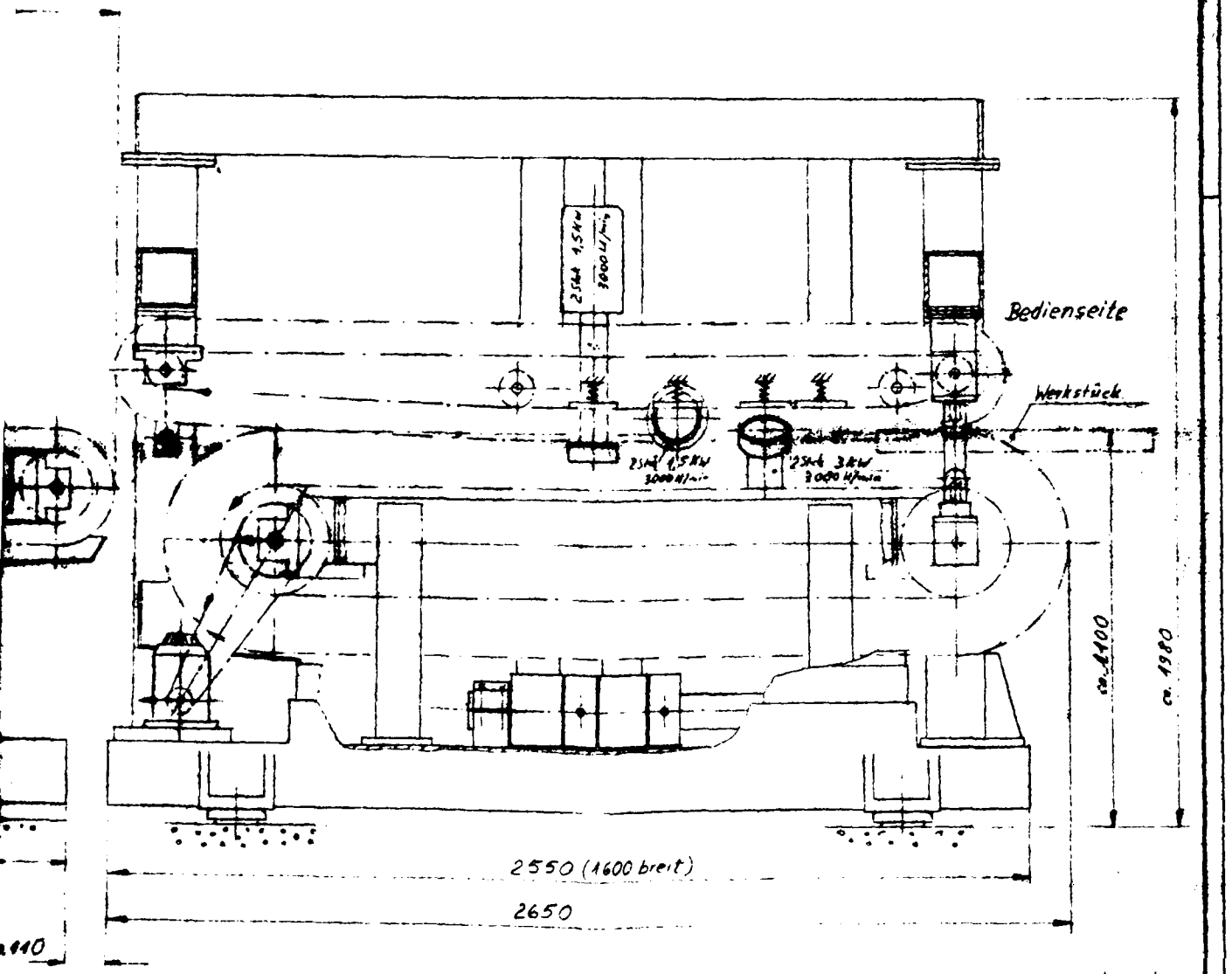
1 2

II. Bearbeitung der Stirnseite

I. Bearb

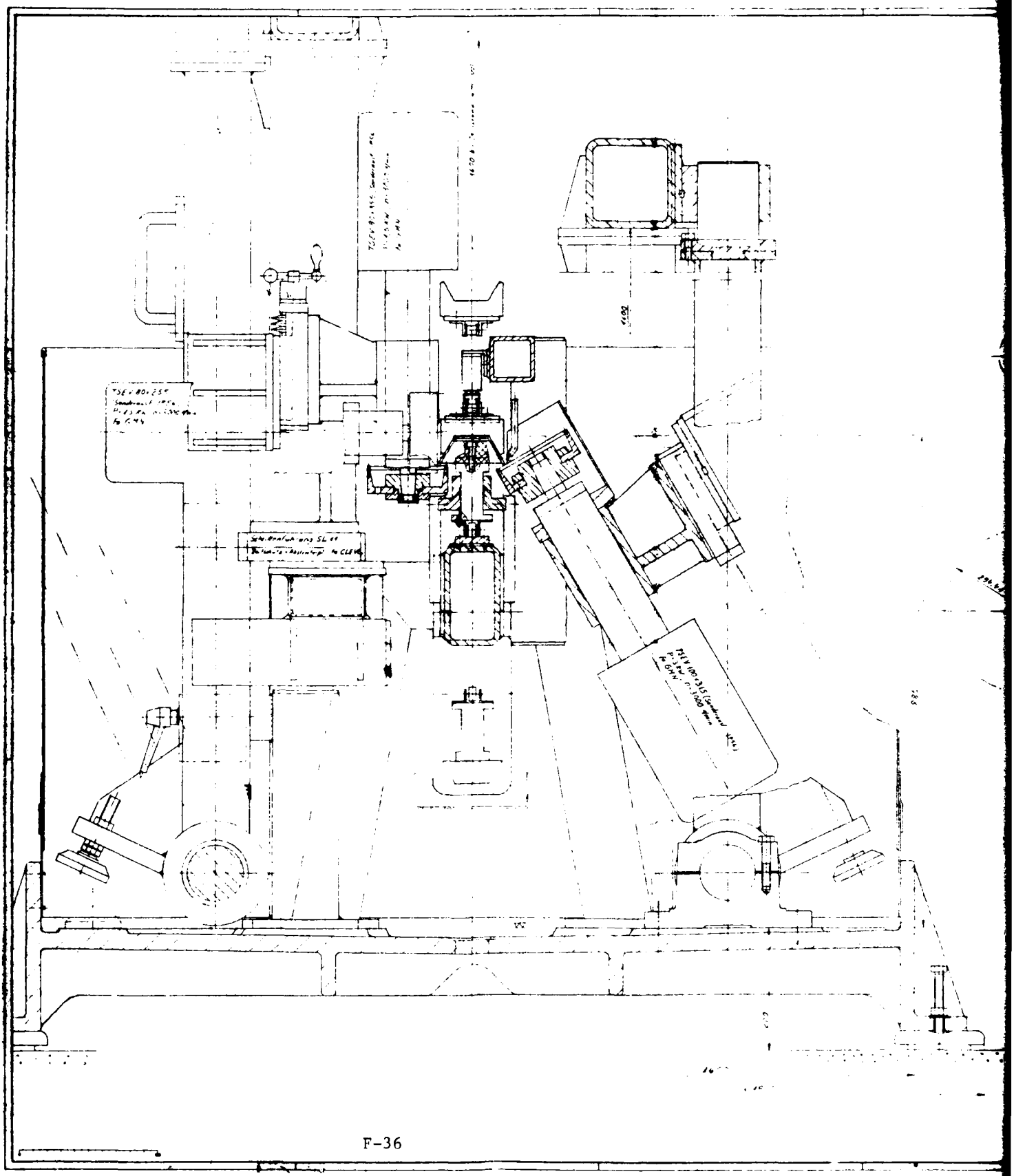


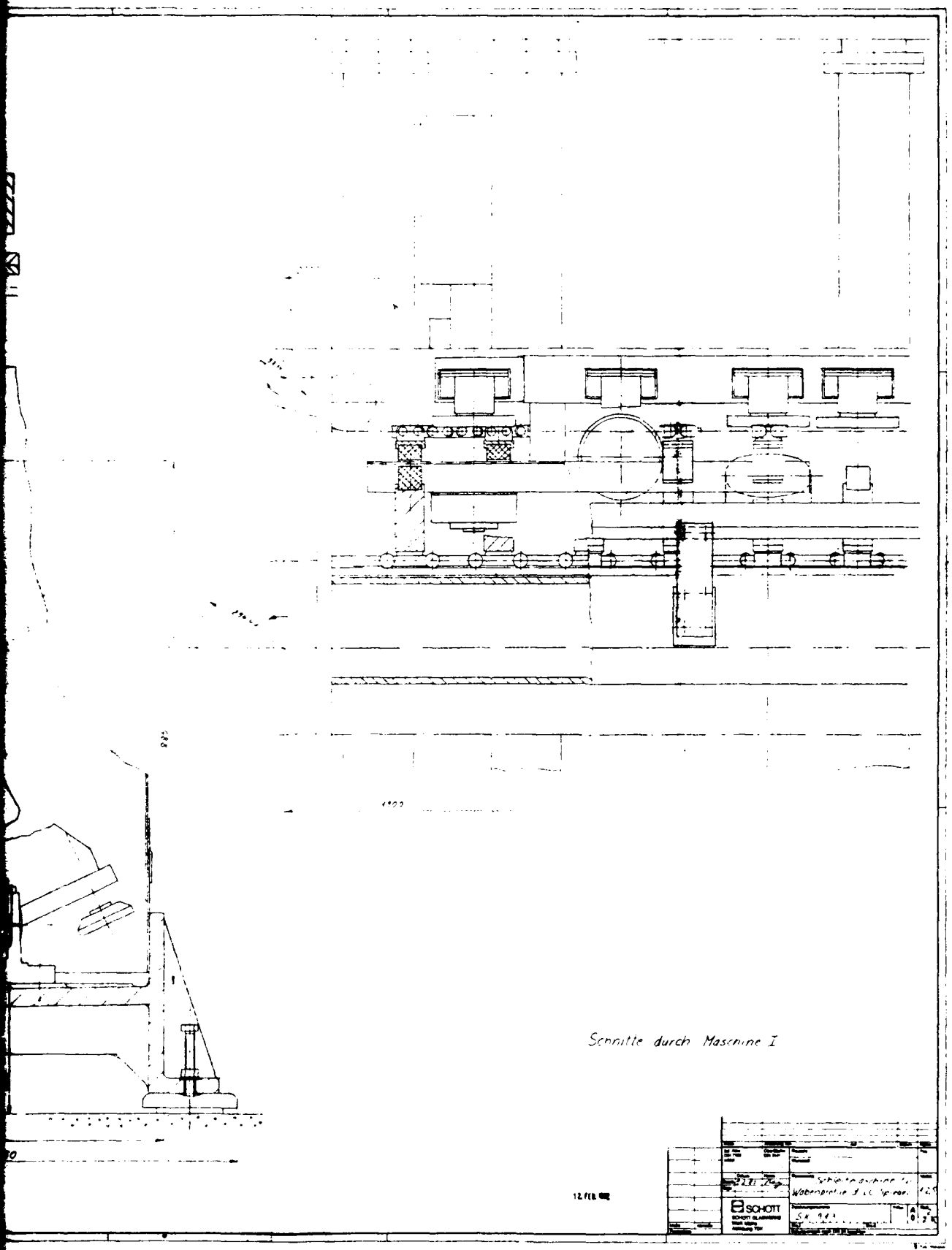
I. Bearbeitung der Schweißkanten u. Fasen



Index	Änderung von	auf	Datum / Name
Gezeichnet	MI ca. 3500	4E ca.	Pos.
Benennung	Schleifmaschine für Wabenprofile d. LG ...gel		Maßst. 1:10
Datum / Name	11.1.82		
SCHOTT GLASWERKE Werk Mainz Abteilung TDK	Zeichnungsnummer SK 913	Index	A2

12. FEB. 1982

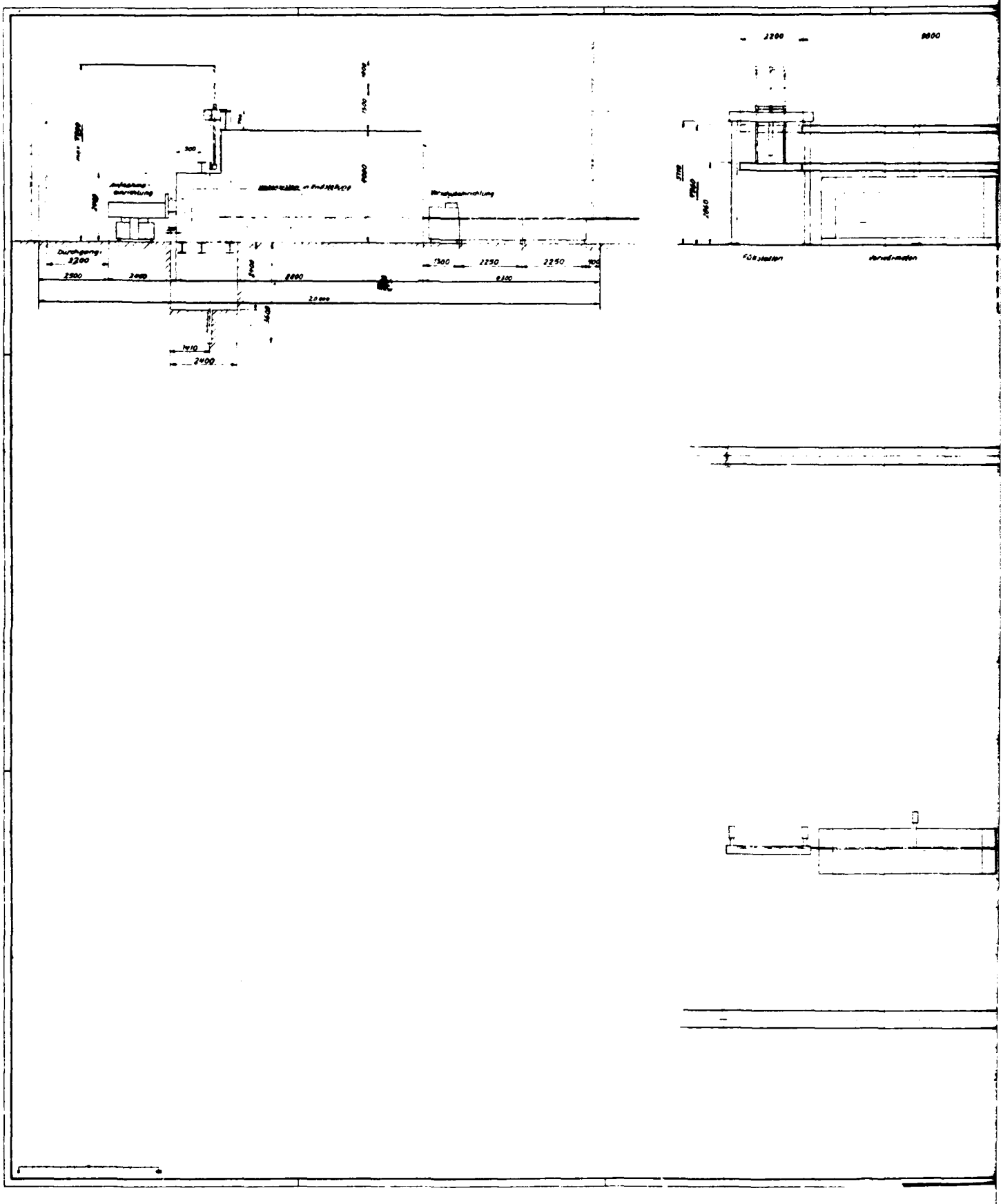


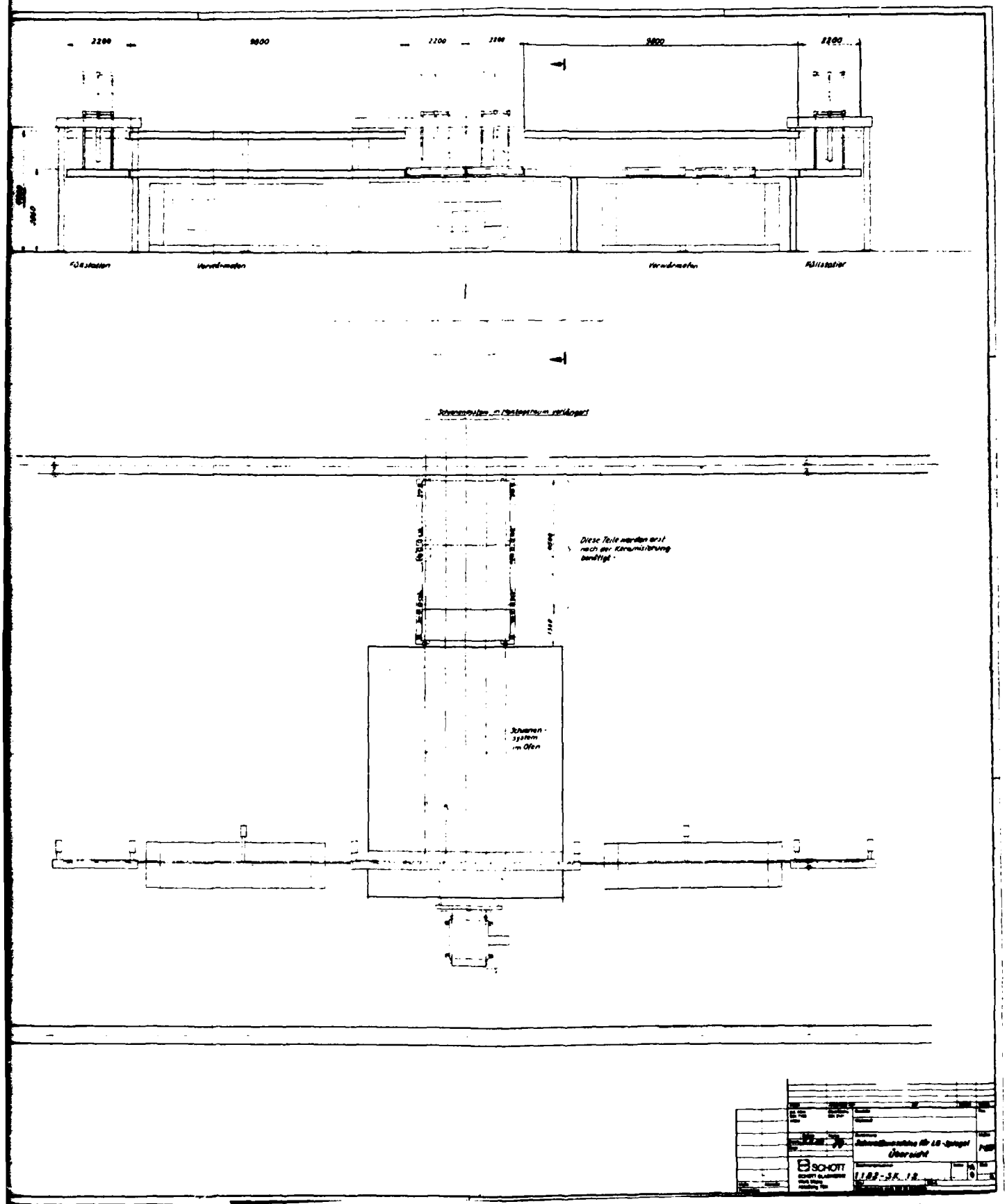


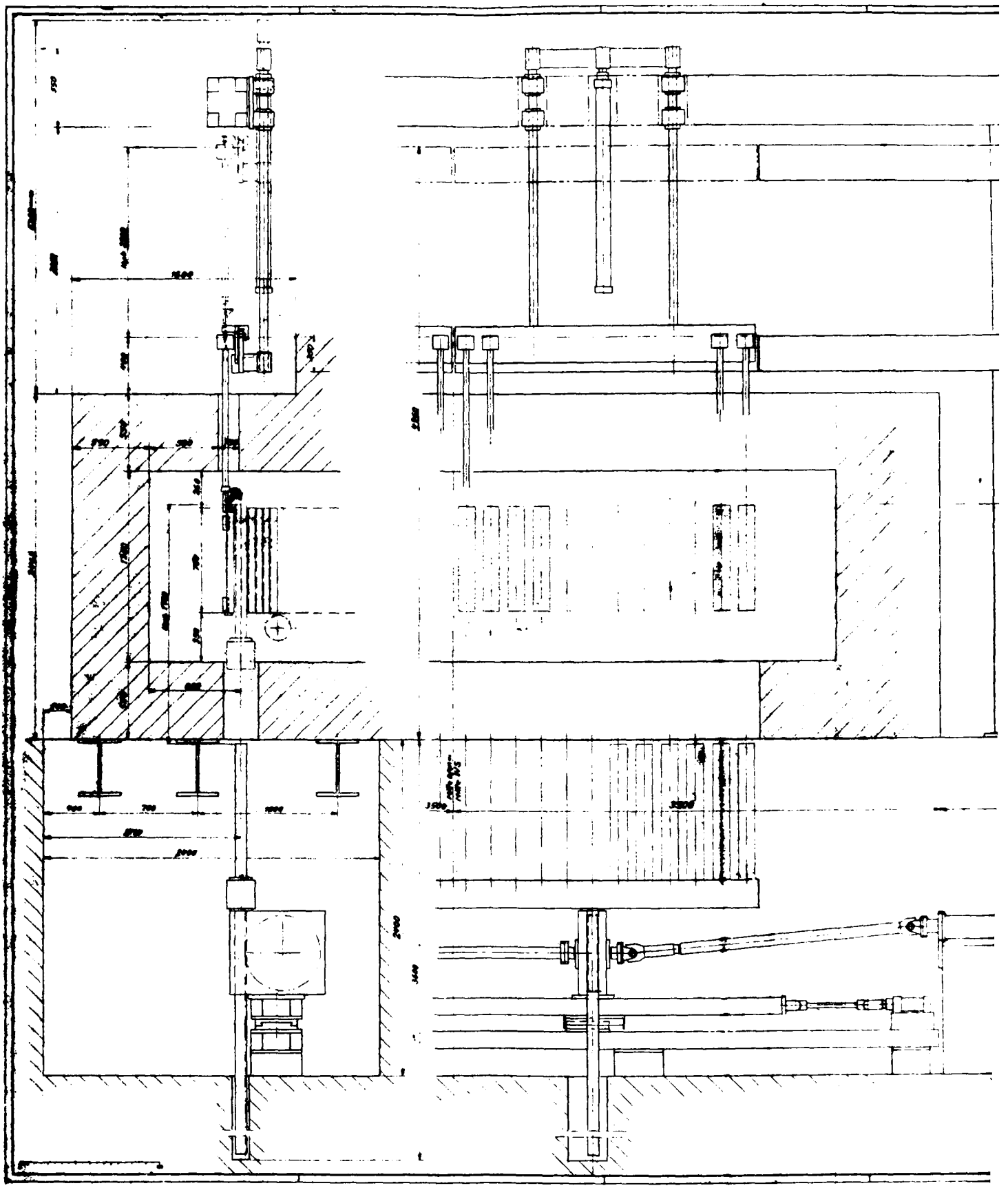
Schnitte durch Maschine I

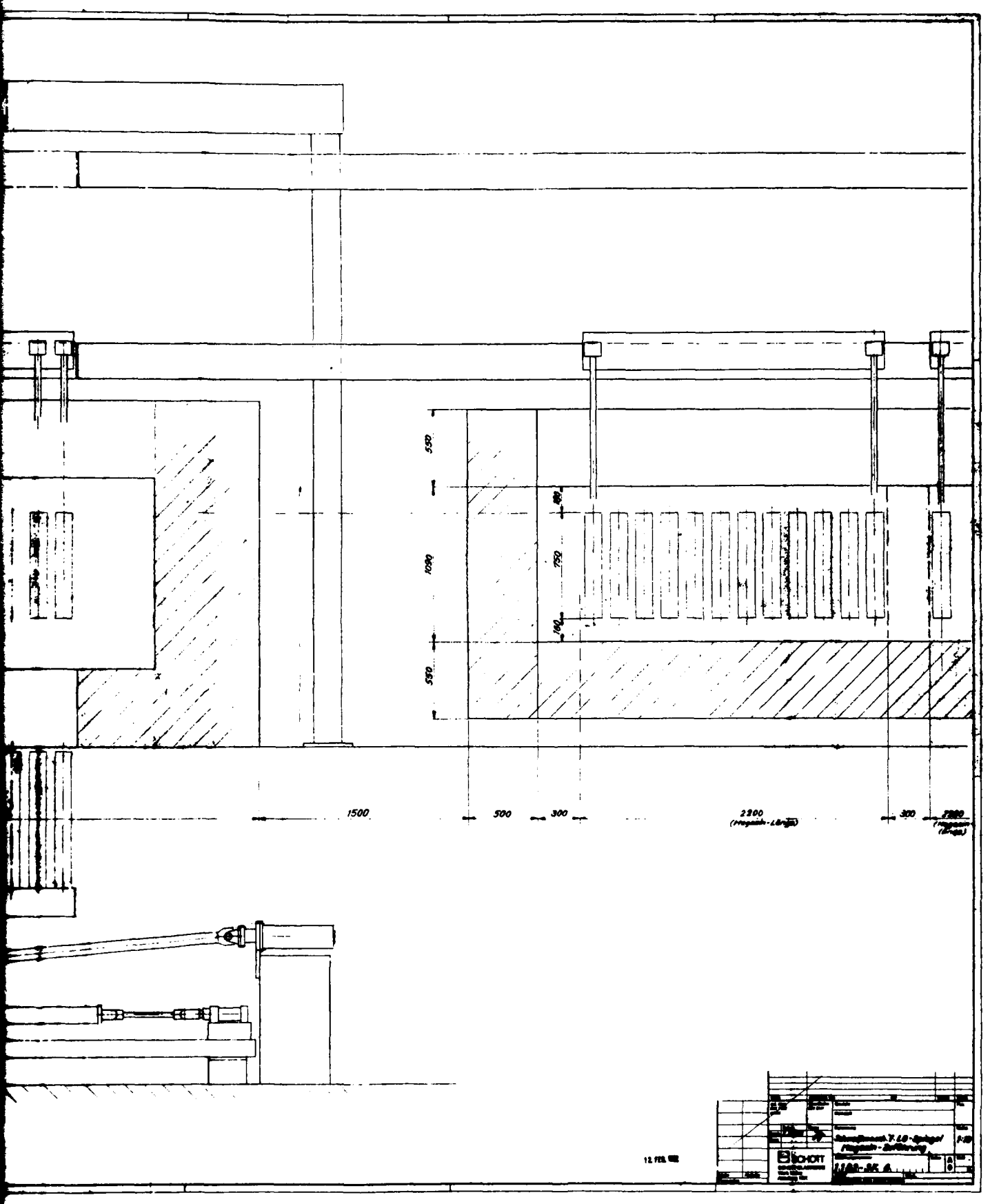
SCHOTT

12. FEB

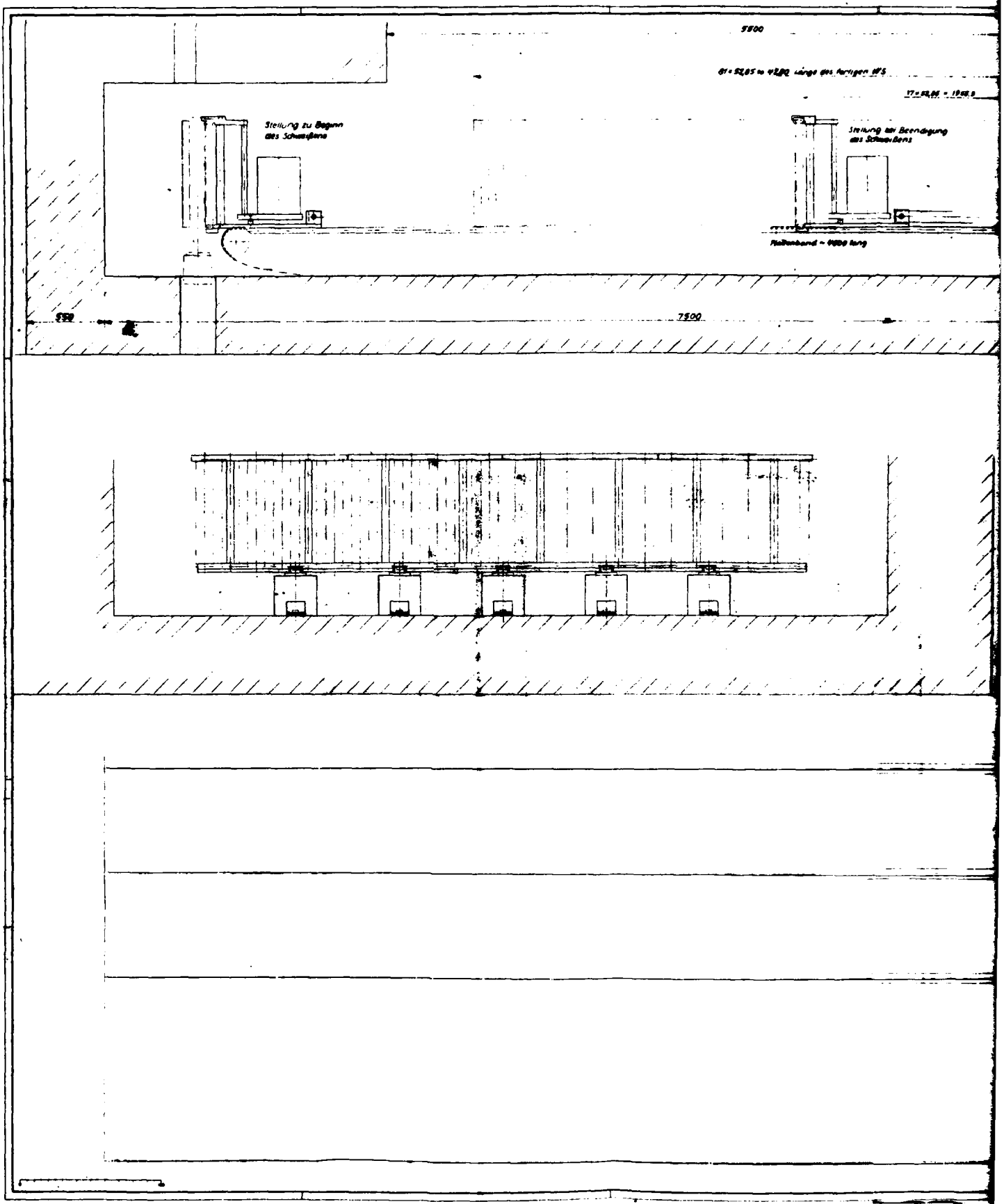

2200
9900
Durchgang
2200
2900
3400
8800
9100
1500
2250
2250
20 000
1410
2400

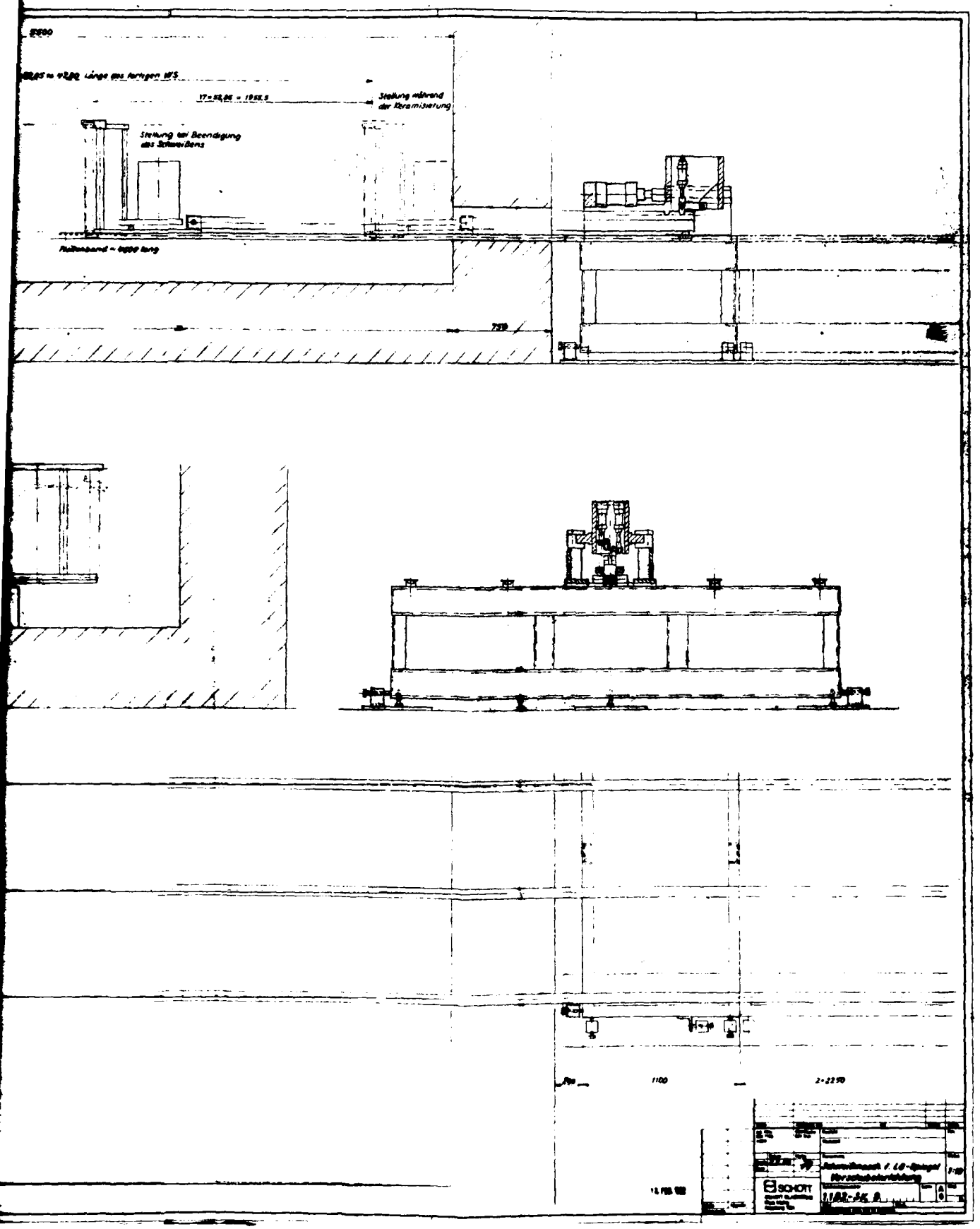

2200
9800
2200
2100
9800
8200
Diese Teile werden erst nach der Kanalmontage benötigt.
Schwanensystem im Ofen

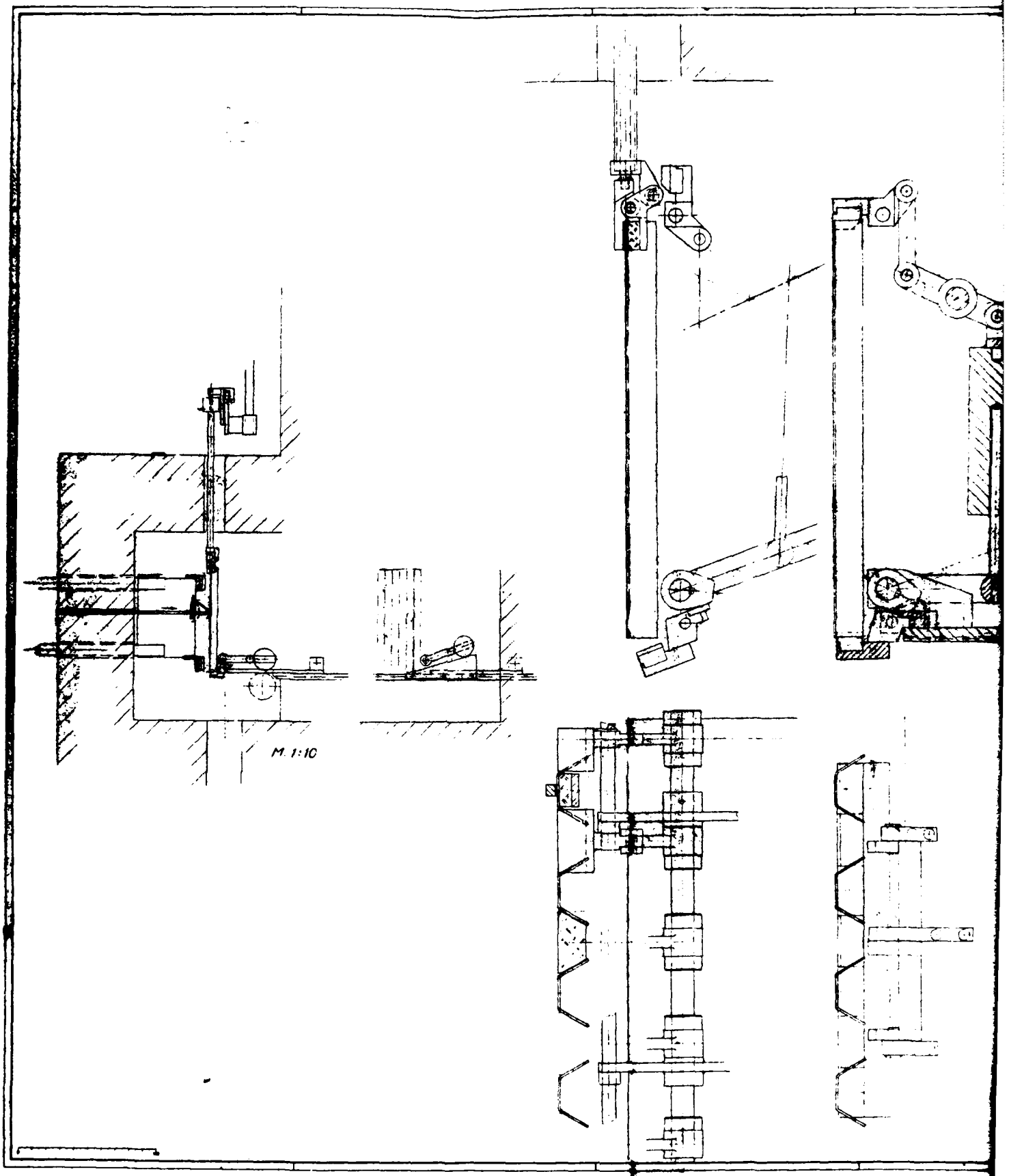


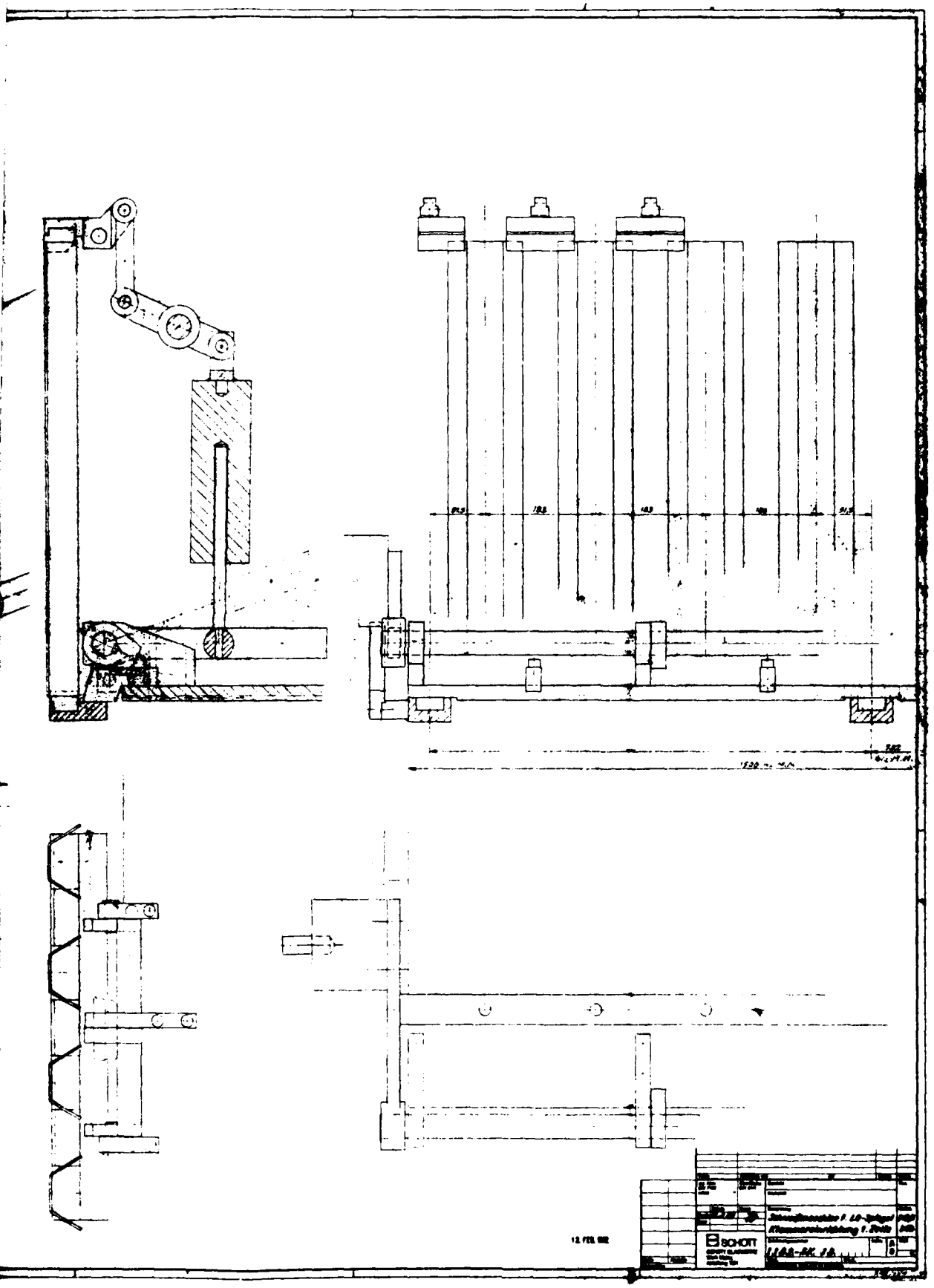


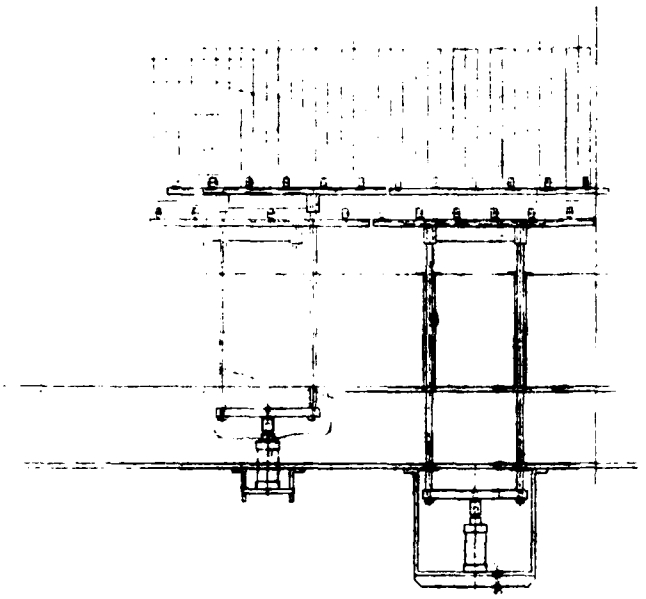
2

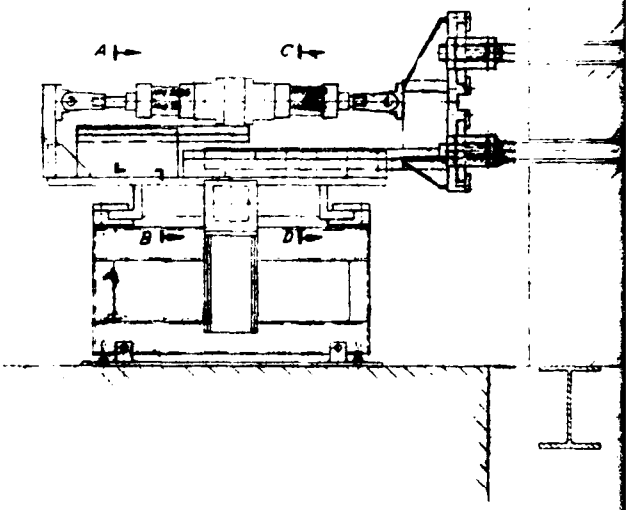

9800
Stellung zu Beginn des Schweißens
Stellung bei Beendigung des Schweißens
Rollenbahn = 9800 lang
500
7500

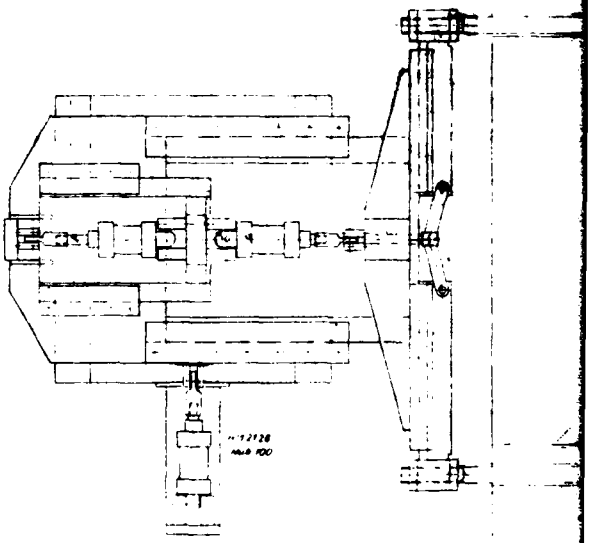

Stellung während der Keramisierung
Stellung bei Beendigung des Schweißens
Rollensand = 6000 lang
SCHOTT

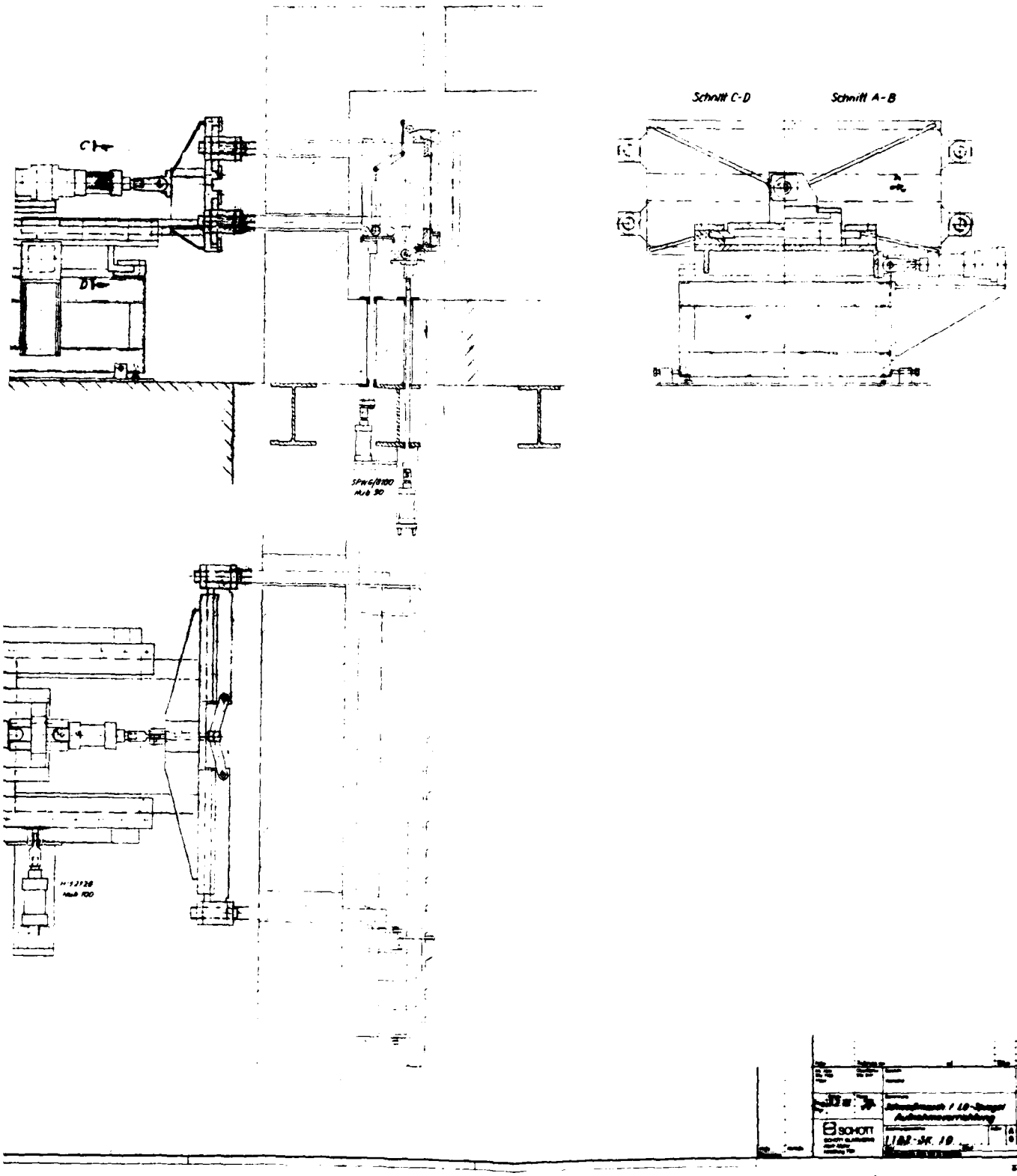

M. 1:10

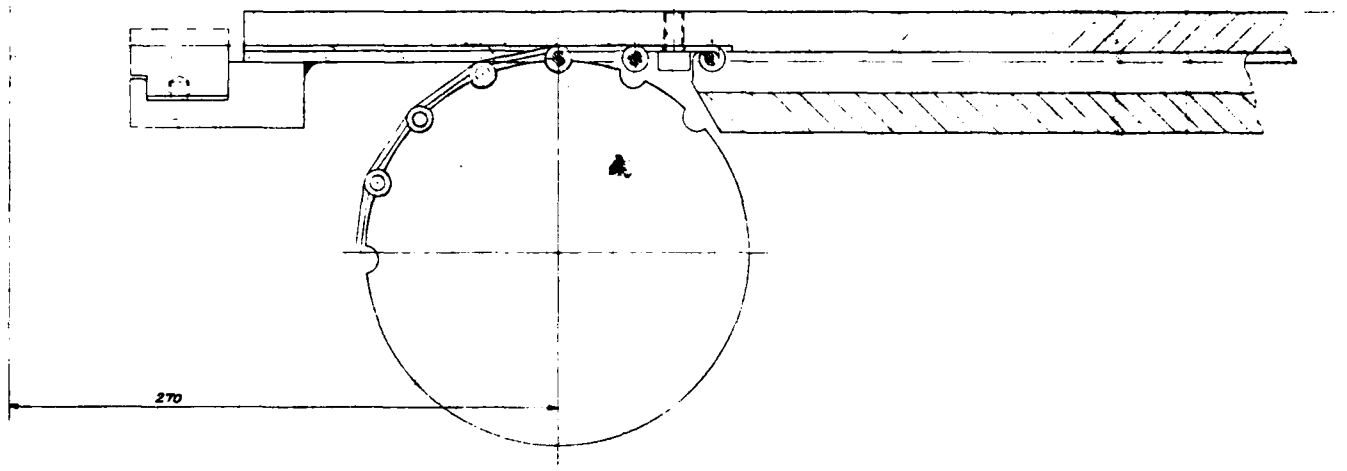

SCHOTT

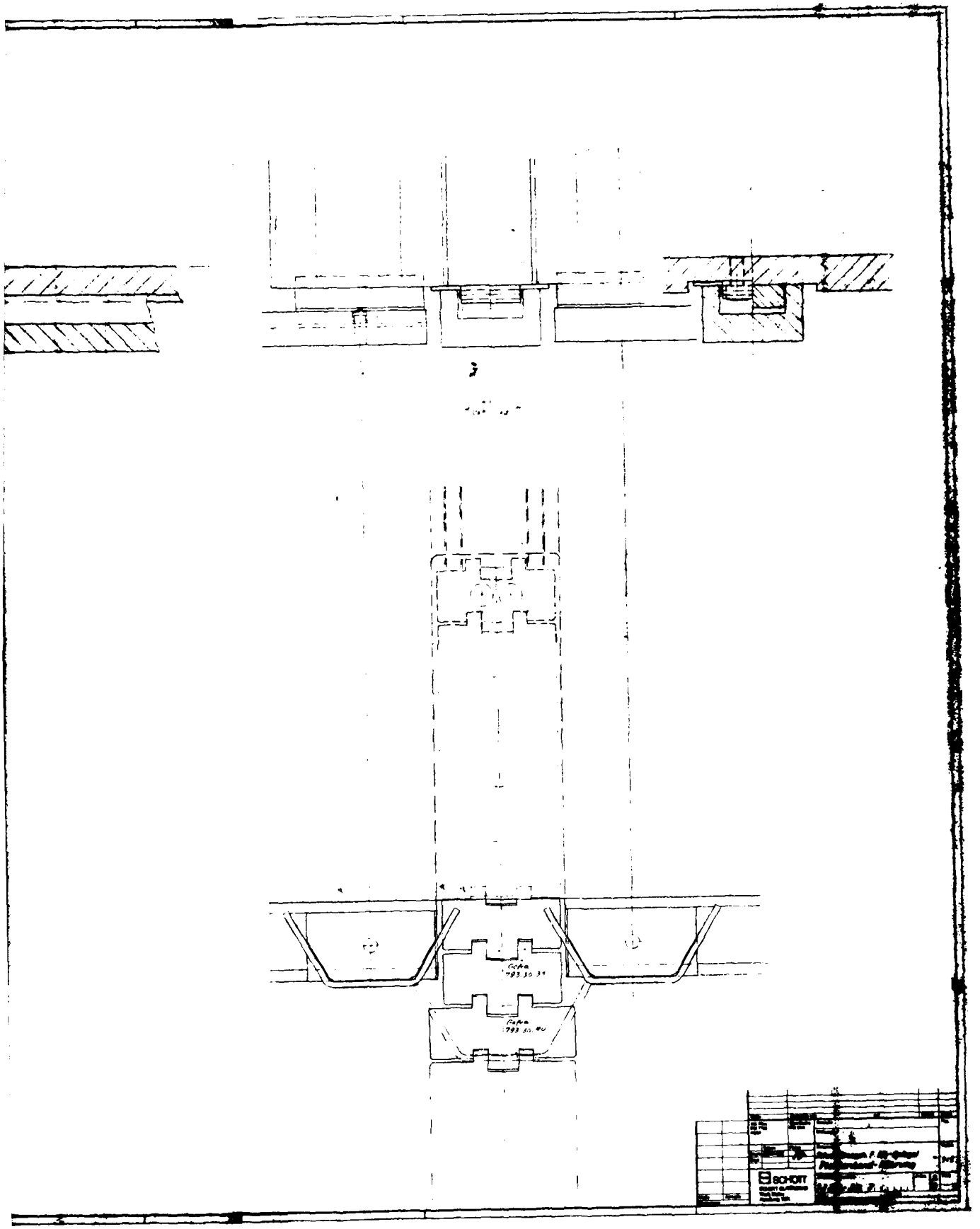


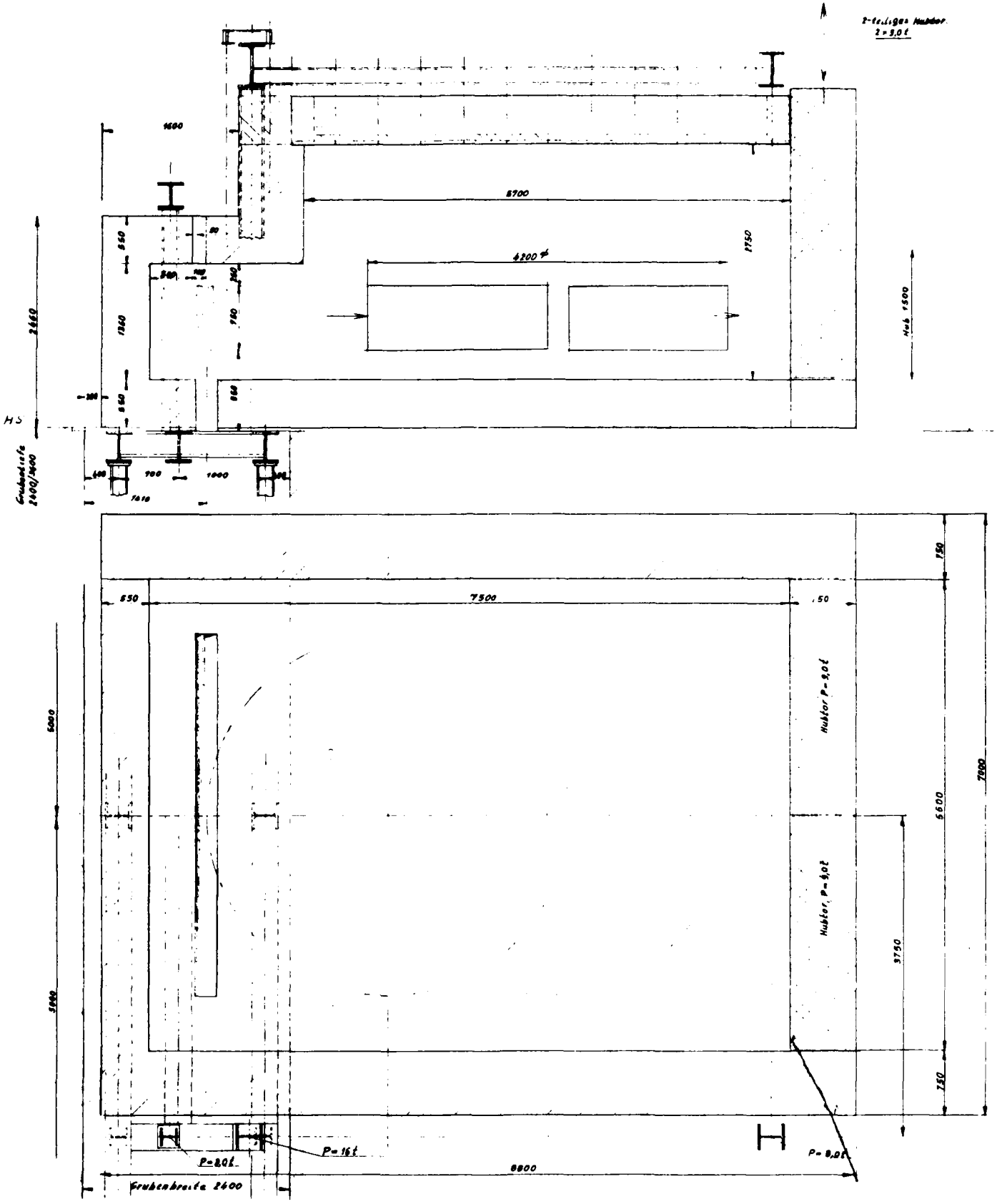

A
C
B
D

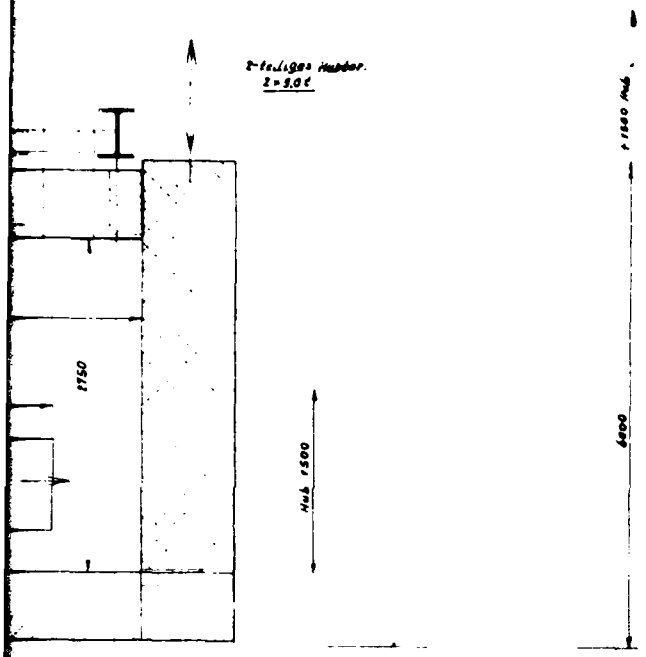


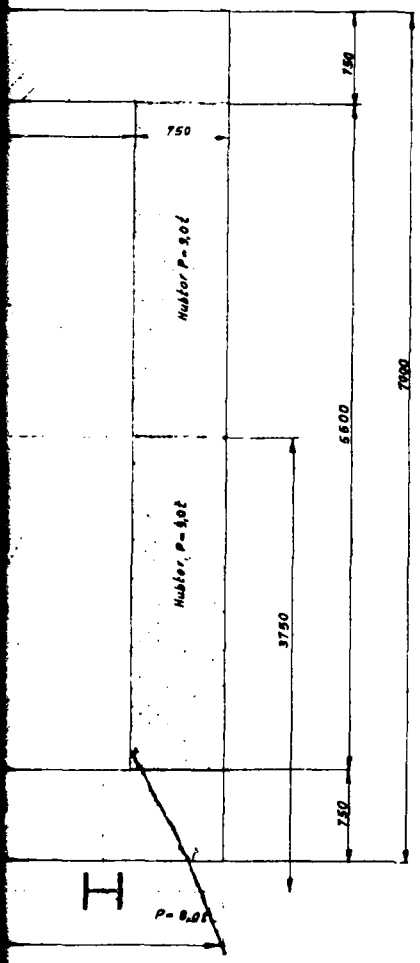

Schnitt C-D
Schnitt A-B
C
D
SPNG/8100
M16 30
SCHOTT


270


SCHOTT


2-fa.Lüga. Hubtor
2 x 5,0 t
1600
5700
4200
1750
Hub 1500
2660
1360
550
150
HS
Grubenbreite
2400/3400
700
1000
7500
150
Hubtor P = 5,0t
6600
7800
5000
3750
P = 2,0t
P = 16t
P = 5,0t
8800
Grubenbreite 2400





Ofenmaucerung: ca. 150,0 t
Ofen-Verspannung: ca. 22,0 t

Bleistift	Benennung	Teil	Zeichnung Nr.	Werkstoff	Gewicht
Änderungsvermerke:					
Diese technische Unterlage ist unser Eigentum. Sie darf nur zu dem vereinbarten Zweck verwendet werden. Jede widerrechtliche gewerbliche Benutzung, Vervielfältigung oder Weitergabe an Dritte ist ohne unsere vorherige Zustimmung unzulässig. Zuwiderhandlungen verpflichten zum Schadenersatz.					
gezeichnet	Tag 1.2.82	Name Bo	SCHOTT		
geprüft					
Maßstab 1:26	Verschweiß- und Kreuzisierungs- - Ofen für Lochkegelrichtspiegel		Glashütte - Zeichn. Nr. Pr. 4.6		
			Ersatz für:		
			Ersatz durch:		

APPENDIX G

SCHOTT REPORT

"Cost and Time Required for the Manufacture of Two Li htweight Mirrors, 0.46 Meter Diameter"

Costs and Time required for the Manufacture of 2 lightweight Mirrors, 0.46 m ø (Task No. 3.1.8.)

1. Objective

The manufacture of two lightweight mirrors with a diameter of 0.46 m ø. One of the mirrors is plane-parallel and the other has a radius on both top and bottom.

The mirrors consist of a central piece of a honeycomb system and a top and base plate. The honeycomb piece is welded. The top and base plates are fritted to the central honeycomb piece by means of a glass frit..

2. Prerequisites

It was assumed in the calculation of costs and time required for the mirrors with 0.46 m ø that the glass frit and frit bonding technology has been developed. The calculation of the costs and time required for these two developments were detailed separately (Report Task No. 3.1.6.). That means, that the 0.46 m ø mirrors cannot be made without the frit and frit bonding technology developments.

3. Manufacturing Process

The costs and time required are based on the following manufacturing processes.

3.1. Manufacture of the honeycomb central Piece

Plates are produced from Zerodur glass blocks by means of sawing, grinding and boring. The plates are then bent to form half of the honeycomb and then welded together to form a honeycomb unit. The honeycomb unit is crystallized and then ground.

3.2. Manufacture of top and base Plate

The top and base plates are manufactured from a Zerodur glass block, which has already been crystallized, by means of sawing and grinding.

3.3. Fritting top and base Plates to honeycomb Unit

The top and base plates are fritted to honeycomb unit under pressure.

4. Remarks on Method of Calculation

Two calculations of costs and time required were compared. The first calculation assumes that the grinding of the honeycomb unit and the top and base plates will be carried out by Zeiss. In the case of the second calculation, this grinding would be carried out by Perkin Elmer.

Grinding has been calculated for the following:

	parallel	radius
Top plate	1	2
Base plate	1	2
Honeycomb unit	1	2

It has been assumed that one mirror with radius will be damaged during the fritting process.

5. Calculation of Costs

In accordance with calculation No. 1 (grinding at Zeiss) the costs for both mirrors amount to:

$ 220,000.-,

in accordance with calculation No. 2 (grinding at P.E.)

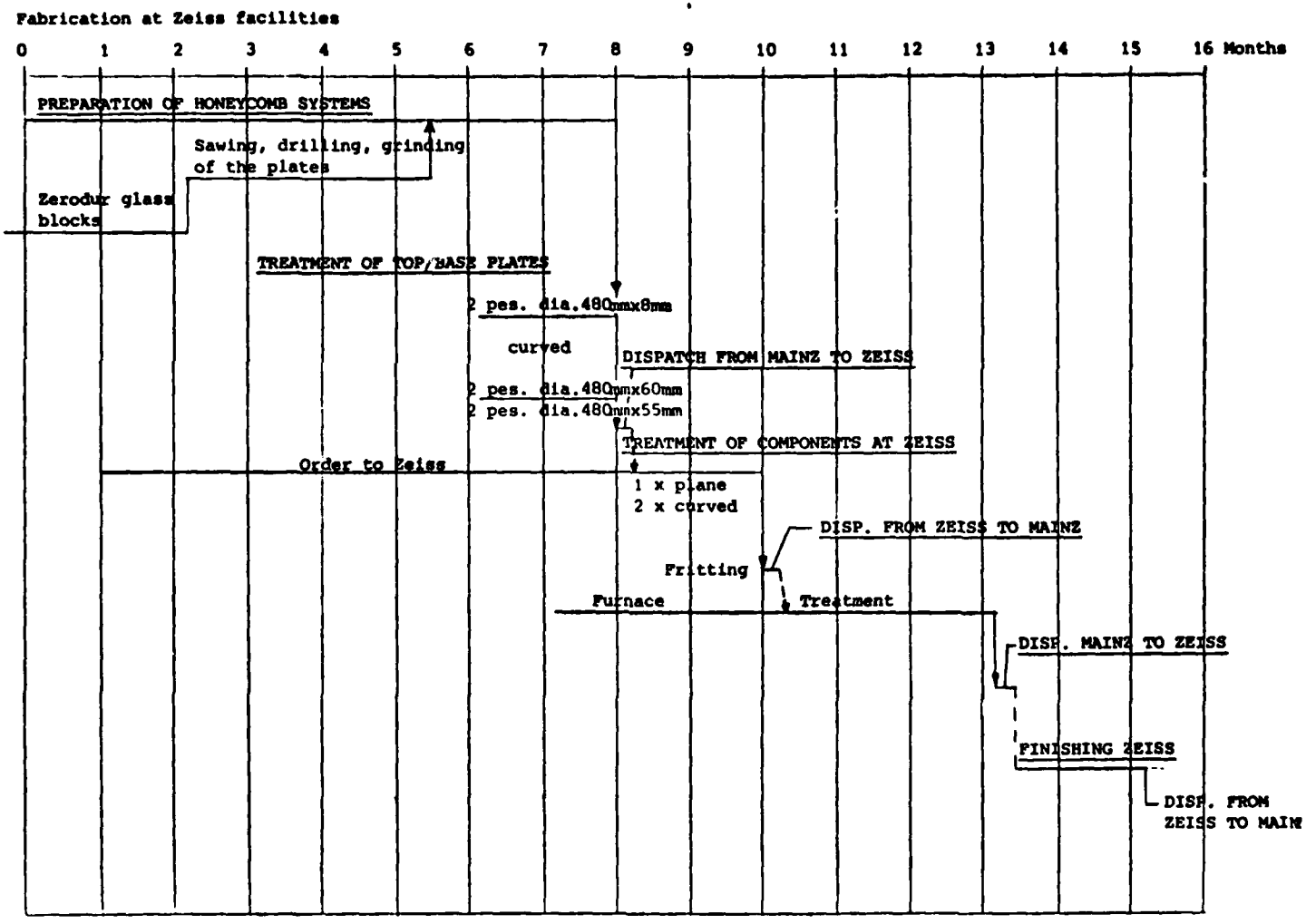
$ 197,000.-.

6. Time required

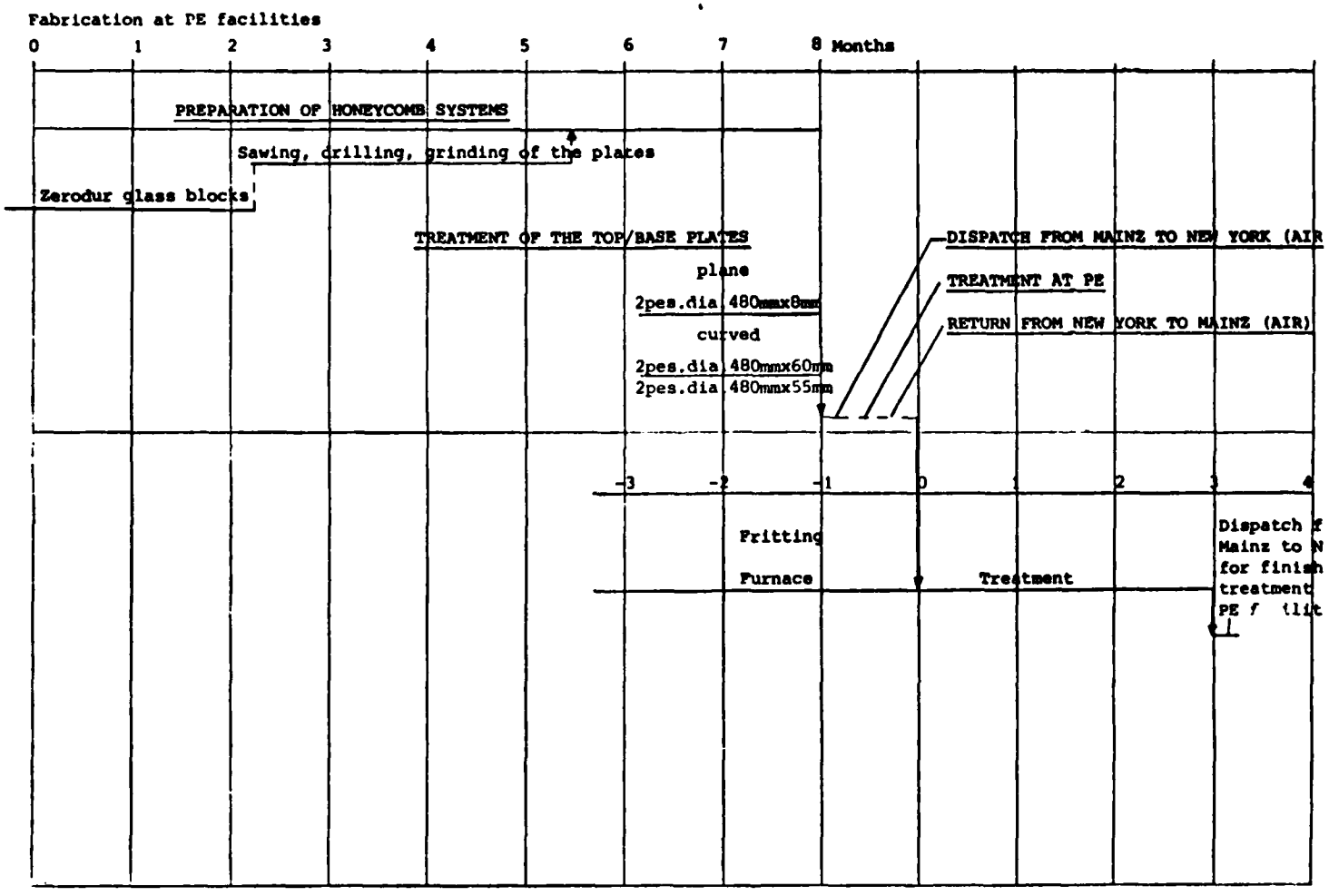
The time required can be seen from the time graphs. It should be noted again at this point, that in the calculation of the time required it has been assumed that the developments of the fritting compound and the frit bonding technology have been completed by the time of fritting.



SCHEDULE FOR THE MANUFACTURE OF THE 0,46 M MIRRORS (TREATMENT AT ZEISS)



SCHEDULE FOR MANUFACTURE OF 0,46 M MIRRORS (TREATMENT AT PERKIN ELMER)



APPENDIX H

THERMAL MODELING

OBJECT

Documentation of the thermo/math modeling used to investigate the transient thermal behavior of lightweight mirrors is presented. The mathematical model is a basic derivative of the well known SINDA codes and employs the classical finite-differencing routine for transient numerical analysis. The model is capable of analyzing a host of mirrors ranging from solid to hollow-core to rib-reinforced configurations.

SUMMARY

Algorithms were developed to model the thermal analysis of mirrors being temporally exposed to thermal loads. Such mirrors may exist in either a vacuum or non-vacuum environment with exposure to radiation and/or front and rear faceplate blowing conditions.

For hollow-core mirrors, the internal heatflow is transferred from the front to the rear faceplate by radiation as well as conduction and optional convection routines. Radiative exchanges between variously configured surfaces have been reduced to algorithmic forms that are capable of handling all three types of mirror geometries.

The transient temperature gradients generated by the model are used to determine the thermal bending moments necessary to calculate mirror thermo/mechanical distortions. Consequently, the model serves as a valuable tool which forms one of a series of subroutines in a powerful, mechanical distortion and material stress program that is capable of evaluating optimum mirror geometries for applications involving transient thermal loadings.

RESULTS

The analytical model is composed of a composite system of nodes ranging from six to twelve depending upon the mirror geometric configuration. A two-dimensional, heatflow network was setup using the classical finite-differencing technique to determine the transient, thermal behavior of the nodal system. Cross-checking and model verification was performed for a variety of cases encompassing the spectrum of interest by using SINDA codes.

1.0 Model Flow Logic

Nodal temperature distributions are calculated over minute time-step increments which are influenced by the geometric breakup characteristics employed by the model in generating its nodal network. This network is generated by subroutine "breakup" which accommodates any system input geometry to the pre-specified nodal count as shown in Figure 1. The finite-differencing time step to be used in the numerical analysis is then determined from knowledge of the smallest nodal time constant in the network. Each nodal time constant is an involved relationship dependent upon nodal mass, thermal properties, and its conductance relationship to neighboring nodes which is a function of both local temperatures and nodal time history.

Figure 2 is a flow diagram of the calculational procedure showing the various subroutines that make up the thermo/math model. Provisions have been made to update the nodal thermal properties of specific heat (C_p), thermal conductivity (K), and density (ρ) with variations in temperature during each time step increment.

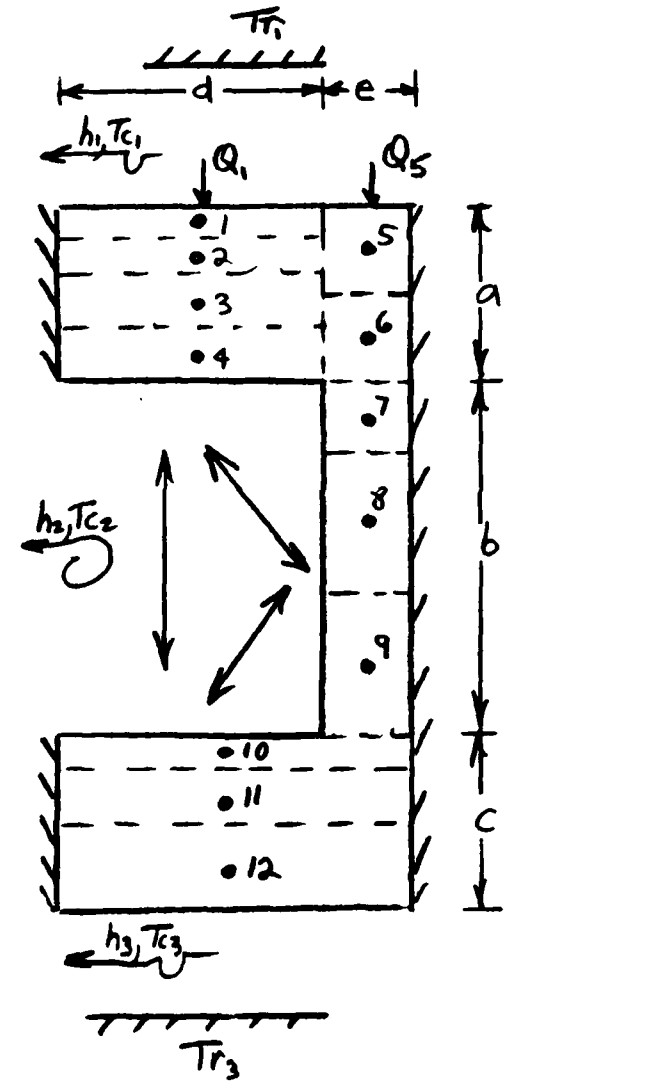


Figure 1. Model Nodal Breakup Configuration

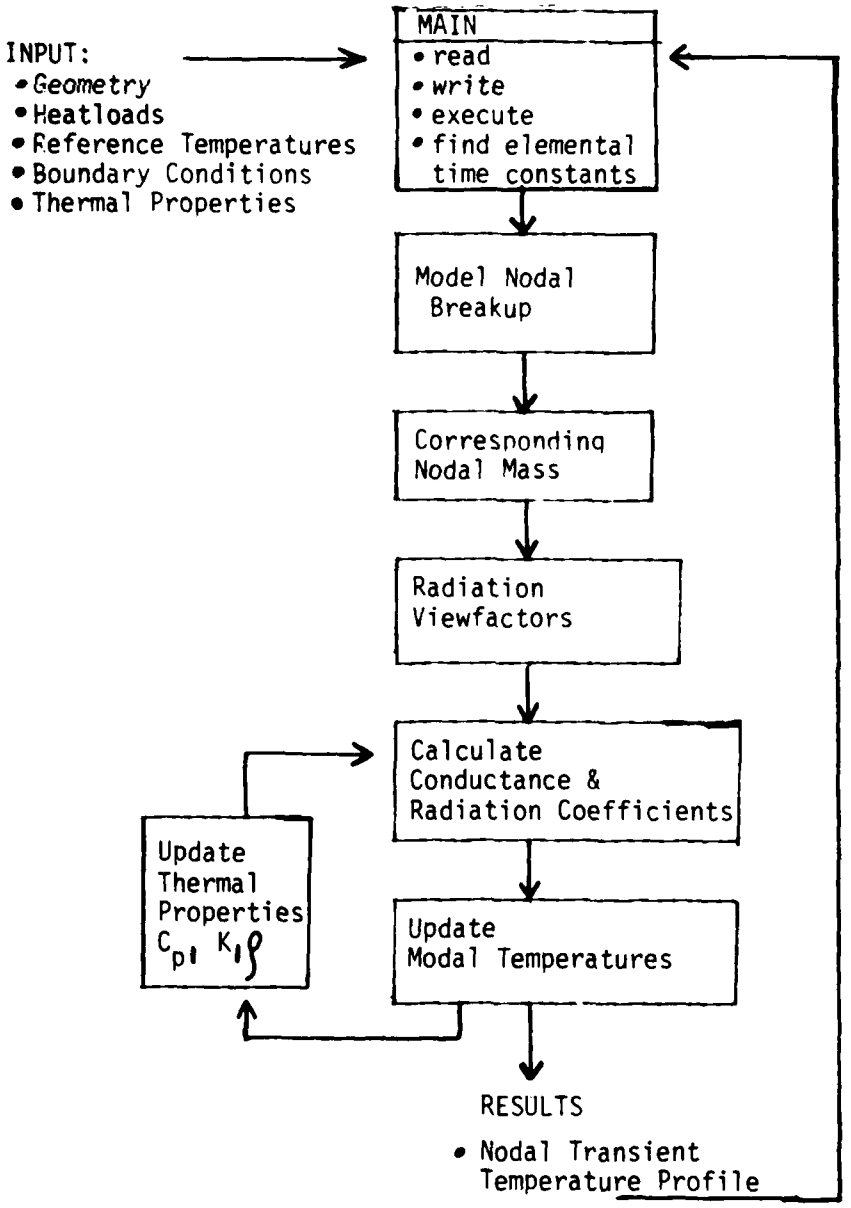


Figure 2. Flow Diagram of Thermo/Math Model Transient Thermal Analyzes

1.1 2-D Network

Nodal breakup of the model is designed to accommodate local variations in irradiance levels over the mirror surface. This added convenience required the introduction of a two-dimensional heatflow network whose third dimension is unity.

1.2 Radiation Viewfactors

Radiation viewfactors are calculated using algorithms developed from the traditional NASA tables of:

1) Finite parallel plates

2) Parallel plates enclosed by sidewalls which re-radiate but do not conduct.

3) Plates facing at right angles with a common side either touching or removed from each other.

2.0 Transient Thermal Algorithm

The first law of thermodynamics is employed to determine the temperature rate of change of an "open" nodal system which exchanges heat with its environment (other nodes or boundary conditions). Equation #1 is the most general relationship to define the rate of temperature change for node "i" in a network of "n" nodes:

$$T_{i_{t+1}} = \left[\frac{\Delta t}{M_i C_{pi}}\right]\left[\Sigma I_j + \Sigma U_j T_j\right] + T_{i_t}\left[1 - \left(\frac{\Delta t \Sigma U_j}{M_i C_{pi}}\right)\right] \qquad (1)$$

Where, T_{it} = Initial temperature of node "i"

T_{it+1} = Final temperature of node "i"

Δt = Time increment elapsed

mi = Mass of node "i"

C_{pi} = Specific heat of node "i"

I_j = Irradiant heat absorbed by node "i" from "j"

U_j = Conductance between node "i" and other network nodes "j"

T_j = Temperature of network nodes "j"

This equation is solved for each node of the network, at time steps of Δt, until the total desired elapsed time is achieved. Conductance values are a function of network geometry and nodal conductivity. The thermal properties of both conductivity and specific heat are continually updated, during each time step Δt, throughout the finite-differencing procedure.

APPENDIX I

SCHOTT REPORT

ZERODUR FRIT DEVELOPMENT OUTLINE OF WORK AND SCHEDULE

Mainz, April 16, 1982

Development of glass frit and frit bonding technology

1. Glass frit development

1.1. Definition of properties

- allowed stresses in ZERODUR
  maximum compressive stress in surface,
  maximum temperatur independent stresses,
  maximum temperatur dependent stress,
- allowed stresses in glass frit,
- allowed chemical stress
  maximum temperature dependent stress,
  maximum temperatureindependent stress,
- minimum of bonding strength,
- youngth modulus,
- poisson's ratio,
- heat transfer values,
- density.

1.2. Methods for property measurements

New methods for sample preparation must be developed.

- Stress measurement
  distinguish between stress of mismatch and stress of chemical ion exchange,
- $\Delta l/l$ measurements
  sandwich samples,
- bonding strength measurements
  but-samples,
- E-Modulus
  sandwich samples,
- poisson's ratio
  sandwich samples,
- heat transfer
  sandwich samples,
- chemical ion exchange
  temperature dependent yes or no.

1.3. Composition of glass frit

- influence of chemical composition,
- influence of chemical additives,
- influence of grain seize,
- influence of frit thickness,
- influence of temper program,
- influence of pressure,
- influence of barrier layers for ion exchange.

2. Frit bond technology

2.1. Production and bring-up of frit layers

Frit layers of exact thicknesses between 10 µm and 300 µm must be produced and bring-up to the honeycomb system.

- Preexperiments for production of frit layers by spraying, toughening or other direct methods,
- preexperiments for production of frit layers and then bring-up to honeycomb system,
- decision of the bring-up technology,
- equipment for the production of glass powder $\leqslant$ 5 µm,
- development of the bring-up technology,

- construction of equipments for the production of thin frit layer and/or bring-up them to the honeycomb system,

- experiments and production of samples.

2.2. Frit bonding under pressure

- Preexperiments under pressure of weights,

- preexperiments under vacuum,

- decision of the frit bond technology,

- development of the frit bond technology,

- influence of the bring-up technology to the frit bond technology,

- determination of the temper program,

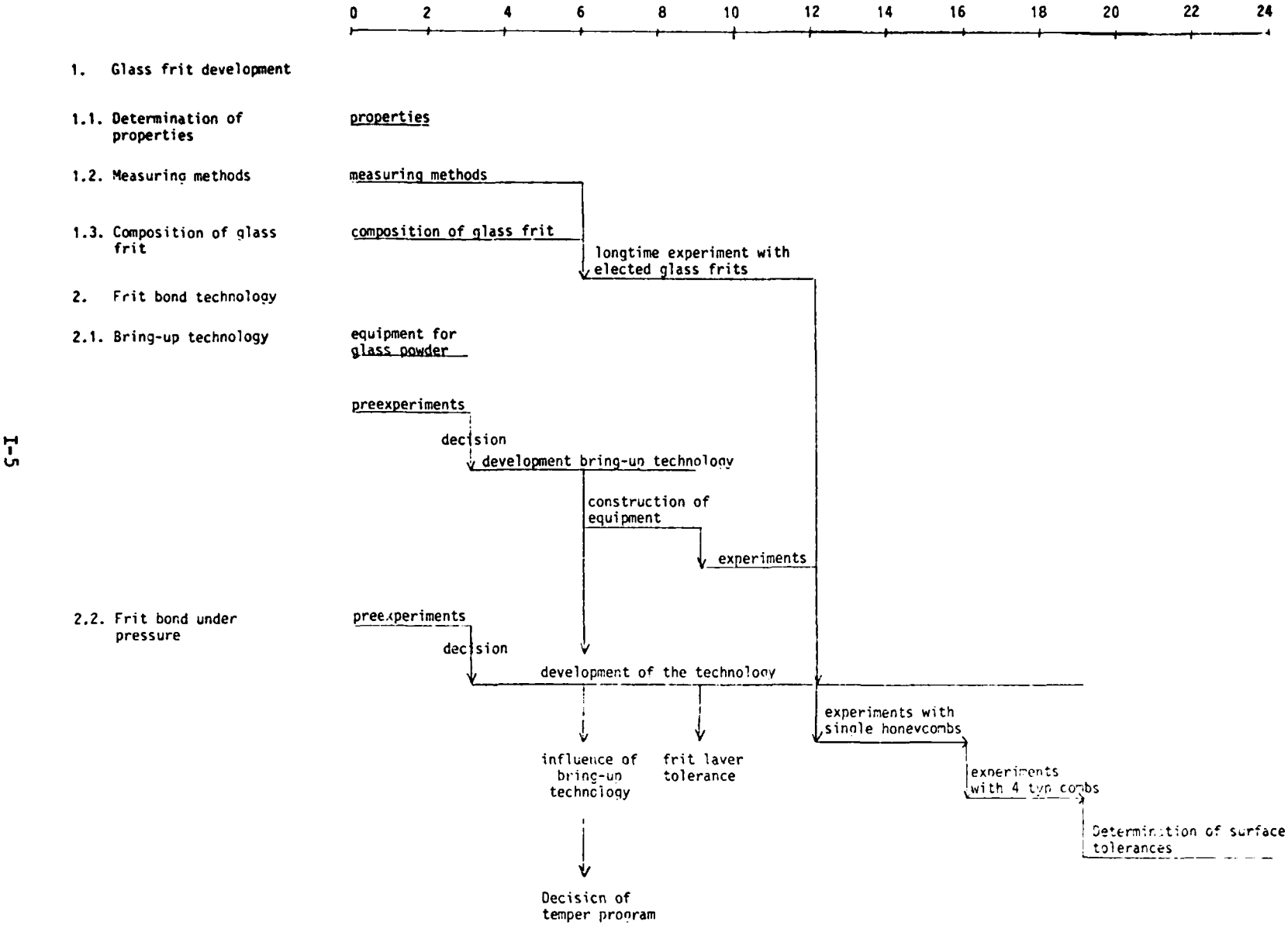
- experiments with single honeycomb of ROBAX and ZERODUR,

- experiments with four honeycomb systems of ROBAX and ZERODUR,

- determination of the frit layer tolerance,

- determination of the allowed surface roughness,

- determination of the allowed surface wavyness.


0
2
4
6
8
10
12
14
16
18
20
22
24
1. Glass frit development
1.1. Determination of properties
properties
1.2. Measuring methods
measuring methods
1.3. Composition of glass frit
composition of glass frit
longtime experiment with elected glass frits
2. Frit bond technology
2.1. Bring-up technology
equipment for glass powder
preexperiments
decision
development bring-up technology
construction of equipment
experiments
2.2. Frit bond under pressure
preexperiments
decision
development of the technology
experiments with single honeycombs
experiments with 4 typ combs
Determination of surface tolerances
influence of bring-up technology
frit layer tolerance
Decision of temper program

DISTRIBUTION LIST

Capt Doris Hamill RADC/OCSE	5	
RADC/TSLD GRIFFISS AFB NY 13441	1	2
RADC/DAP GRIFFISS AFB NY 13441	2	3
ADMINISTRATOR DEF TECH INF CTR ATTN: DTIC-DDA CAMERON STA BG 5 ALEXANDRIA VA 22314	12	5
Perkin-Elmer Corp Attn: George Gardopee MS 955 100 Wooster Heights Rd Danbuty, CT 06810	5	3
AFWL/ALAO Attn: Dr. William Lowrey Kirtland AFB, NM 87117	1	4
AFWL/ARAA Attn: Dr. J. Fender Kirtland AFB, NM 87117	1	5
AFWL/ARAA Attn: Dr. L. Skulnyk Kirtland AFB, NM 87117	1	6
The Aerospace Corp Attn: Dr. E.W. Silvertooth Bldg 110 MS 2339 PO Box 92957 Los Angeles, CA 90009	1	7
The Aerospace Corp Attn: T. Taylor Bldg 115 Room 1334C PO Box 92957 Los Angeles, CA 90009	1	8

Analytic Decisions Inc Attn: Emmanuel Goldstein 1401 Wilson Blvd Arlington, VA 22209	1	9
BDM Corp Attn: Ed Brunson 1820 Randolph Rd Albuqurque, NM 87106	1	10
BMD/ATC Attn: A. Carmichael PO Box 1500 Huntsville, AL 35807	1	11
Boeing Aerospace Co. Attn: B. Allasina PO Box 3999 Seattle, WA 98124 Cambridge, MA 02139	1	12
Charles Starke Draper Labs Attn: Dr. Keto Soosar 555 Technology Dr MS 95 Cambridge, MA 02139	1	14
DARPA/DEO Attn: Col Ronald Prater Arlington, VA 22209	2	15
Eastman Kodak Attn: Robert Keim Kodak Aparatus Division 121 Lincoln Ave. Rochester, NY 14650	1	16
Eastman Kodak Attn: Richard Price KAD-Lincoln Park 901 Elmgrove RD Rochester, NY 14650	1	17
GRC Attn: G. Gurski 7655 Old Springhouse RD McLean, VA 22102	1	18

Itek Corp Attn: Roland Plante Optical Systems Division 10 Maguire Rd. Lexington, MA 02173	1	19
Lockheed Palo Alto Research Lab Attn: Richard Feaster 0/52-03, B201 3251 Hanover St. Palo Alto, CA 94304	1	20
Lockheed Space and Missile Co. Attn: Dennis Aspinwall Dept 5203 Bldg. 201 3251 Hanover St. Palo Alto, CA 94304	1	21
Lockheed Space and Missile Co. Attn: Dick Wallner Dept 5203 Bldg 201 3251 Hanover St. Palo Alto, CA 94304	1	22
Martin Marietta Aerospace Attn: C.W. Spieth Denver Division PO Box 179 Denver, CO 80201	1	23
MIT/Lincoln Laboratory Attn: Alex Parker PO Box 73 Lexington, MA 02173	1	24
MRJ Corp Attn: Dr. Kenneth Robinson 71 Blake St. Needham, MA 02192	1	25
NASA Ames Attn: James Murphy MS 244-7 Moffett Field, CA 94035	1	26
NASA Marshall Space Flight Center Attn: Charles O. Jones Mail Code EC32 Huntsville, AL 35812	1	27

Naval Sea Systems Command Attn: Dr. Sadeg Siahatgar PMS-405 NC 1 Room 11N08 Washington, DC 20742	1	28
Naval Weapons Center Attn: Dr. H. Bennett Code 6018 China Lake , CA 93555	1	29
Perkin Elmer Attn: Dr. David Dean MS 241 Main Ave Norwalk, CT 06856	1	30
Perkin Elmer Attn: Conrade Neufeld 100 Wooster Heights Rd. Danbury, CT 06810	1	31
Rockwell International Attn: R. Brandenie Rocketdyne Division 6633 Canoga Ave Canoga Park, CA 91304	1	32
Rockwell International Attn: J. Murphy Space Division 12214 Lakewood Blvd Downey, CA 90241	1	33
Rockwell International Attn: R. Greenberg Space Division 12214 Lakewood Blvd Downey, CA 90241	1	34
Riverside Research Institute Attn: Dr. Robert Kappesser 1701 N Fort Myer Dr. Suite 711 Arlington, VA 22209	1	35
SD/YNS Attn: Col H.A. Shelton PO Box 92960 Worldway Postal Center Los Angeles, CA 90009	1	36

United Technologies Research Center Attn: Dr. J. Pearson Optics & Applied Technology Lab PO Box 2691 West Palm Beach, FL 33402	1	37
University of Arizona Attn: Prof Robert Shannon %Charles Peyton Administration Bldg Tuscon, AZ 85721	1	38
W.J. Schaffer Assoc. Inc. Attn: Edward Borsare 10 Lakeside Office Park Wakefield, MA 01880	1	39

MISSION
of
Rome Air Development Center

RADC plans and executes research, development, test and selected acquisition programs in support of Command, Control Communications and Intelligence (C^3I) activities. Technical and engineering support within areas of technical competence is provided to ESD Program Offices (POs) and other ESD elements. The principal technical mission areas are communications, electromagnetic guidance and control, surveillance of ground and aerospace objects, intelligence data collection and handling, information system technology, ionospheric propagation, solid state sciences, microwave physics and electronic reliability, maintainability and compatibility.